VELOCITY AND TURBULENCE CHARACTERISTICS IN FLOWS THROUGH RIGID VEGETATION

By
Jonathan D. Fairbanks

Thesis submitted to the faculty of Virginia Polytechnic Institute & State University in partial fulfillment of the requirements for the degree of

Master of Science
In
Civil Engineering

Dr. Panayiotis Diplas, Chairman
Dr. G.V. Loganathan
Dr. Tamim Younos

16 September 1998
Blacksburg, Virginia

Keywords: Wetlands, Vegetation, Velocity, Turbulence, Flow

VELOCITY AND TURBULENCE CHARACTERISTICS IN FLOWS THROUGH RIGID VEGETATION

Jonathan D. Fairbanks

Abstract

Laboratory experiments were conducted to investigate the velocity and turbulence characteristics in flows through rigid vegetation. The vegetation was simulated by an array of acrylic dowels mounted to the bed of a recirculating hydraulic flume. Velocity measurements were taken in both the longitudinal and vertical directions using a one-dimensional laser doppler velocimeter (LDV). Experiments were conducted under partially submerged, fully submerged and double layer flow conditions. The term double layer flow is used to describe flows that contain two different heights of vegetation. In each experiment, velocity and turbulence intensity profiles were taken at several different locations within the array.

Additional experiments were conducted to examine how bed and vegetative skin roughness influence the velocity and turbulence characteristics. Belt sander strips were glued to the bed of the flume to simulate bed roughness and adhesive sandpaper was attached to the dowels to simulate vegetative skin roughness. Finally, experiments were conducted to study sediment transport and deposition in flows containing vegetation.

Dedication

I dedicate this work to my wife and best friend, Kristie, who supports me in all of my endeavors.

Acknowledgements

I would like to thank my thesis advisor, Dr. Panos Diplas, for his guidance throughout my graduate studies and his many contributions to this research. I would also like to thank the other two members of my graduate committee, Dr. G.V. Loganathan & Dr. Tamim Younos, for reviewing this thesis and providing helpful comments. Of the many people who deserve mention, the most credit goes to my wife, Kristie, whose encouragement and support motivated me throughout this project. Finally, I want to thank my parents, Richard and Barbara Fairbanks, who taught me to work hard and set high goals for myself.

This research was supported in part by the Virginia Water Resources Research Center at Virginia Polytechnic Institute and State University.

Table of Contents

List of Figures

List of Tables

Definition of Symbols

A = Area of bed within control section
A_f = Cross-sectional flow area
b = Channel width
C_d = Drag coefficient
$C_d(z)$ = Height-dependent drag coefficient
$C_R(h)$ = Height-dependent drag coefficient for an isolated surface mounted cylinder
$C_S(h)$ = Unobstructed height-dependent drag coefficient for the bed
d = Diameter of roughness element
d_h = Displaced height
D_g = Geometric mean diameter
F = Drag force
F_o = Unobstructed drag force on furthest upstream element
g = Acceleration of gravity
h = Height of roughness element
h_s = Height of short dowels
h_t = Height of tall dowels
K = von Karman's constant (0.4)
k_s = Nikuradse's equivalent sand grain roughness
K = Conveyance
l = Mixing length
M = Stability limit of viscous sublayer (11.4)
n = Manning's roughness coefficient
n_S = Manning's roughness coefficient for the bed
N_s = Number of velocity samples
Q = Flow rate
R = Reynolds number
s = Mean separation between roughness elements
S = Energy gradient
u_o = Depth-averaged upstream approach velocity
u_* = Friction velocity
($\mathbf{u}$,$\mathbf{v}$,$\mathbf{w}$) = Instantaneous velocity vector (longitudinal, lateral, vertical)
(u, v, w) = Mean velocity vector (longitudinal, lateral, vertical)
(u', v', w') = Instantaneous velocity fluctuation about the mean (long., lateral, vertical)
U = Bulk longitudinal velocity
w = Fall velocity
Z = Flow depth
z = Distance above channel bed
z = Rouse #
z_o = Roughness length
z_w = Height of roughness sublayer
ν = Kinematic viscosity
ω = Lateral vorticity
σ_g = Geometric standard deviation
ρ = Density of the fluid

τ_o = Total surface shear stress
τ_R = Shear stress on the vegetation
τ_S = Shear stress on the underlying surface
τ^* = Dimensionless shear stress
τ_c^* = Critical dimensionless shear stress
λ = Vegetation density (frontal area per unit ground area)
$\beta = C_R(h)/C_S(h)$
γ = specific weight of water
γ_s = specific weight of sediment
η = eddy viscosity
δ' = thickness of viscous sublayer
α_1, α_2, α_3, α, ξ = empirical constants
λ_m = Density at the point of maximum roughness
u_{rms},v_{rms},w_{rms} = Turbulence intensities in the x, y, and z directions

Chapter 1

State of the Art

Fluid flow through vegetation has been analyzed within a number of disciplines. Meteorologists have studied turbulent flow through vegetation to better understand the structure of the atmospheric boundary layer. Agricultural engineers have researched wind profiles through crops to develop wind erosion models. Hydraulic engineers have studied water flow through vegetation to better model sediment and contaminant transport. Since air and water are both fluids that exhibit many of the same properties, we can study them in conjunction with one another to develop a better overall understanding of turbulent flow through vegetation.

Turbulent flow of water through vegetation is a very complex phenomenon. Until the 1960's, it was believed that a single resistance coefficient such as Manning's n could adequately describe the resistance effects caused by vegetation. Empirical curves were developed that related n to the product of the average velocity (V) and the hydraulic radius $\left(R_h\right)$ (Palmer,1945). It is widely accepted today that a single resistance coefficient cannot adequately describe either shallow flow over vegetation or partially submerged flow through vegetation. To effectively model flows containing vegetation, we must understand how the length scales that characterize the vegetation affect the mean velocity profile, the turbulence structure, and the drag characteristics of the roughness elements.

1.1 Mean Velocity

The study of velocity in turbulent flow can be broken down into two parts. The mean velocity vector, (u, v, w), can be analyzed to determine the basic direction of flow and the magnitude of the mean velocity. The mean velocities (u, v, w) correspond to flow in the streamwise, lateral and vertical directions. We also can study the instantaneous velocity fluctuations, (u', v', w'), about the mean velocity vector due to the turbulence structure. Therefore, the instantaneous velocity vector equals the sum of the mean velocity vector and the instantaneous fluctuation:

$$(\mathbf{u},\mathbf{v},\mathbf{w}) = (u, v, w) + (u', v', w') \qquad \text{(Eqn.1.1)}$$

Mean velocity will be the focus of this Section, while turbulence will be the focus of Section 1.3. In each Section, the discussion will pertain to both the partially submerged and fully submerged flow conditions.

1.1.1 Fully Submerged Flow

When vegetation is fully submerged, the mean velocity vector can be analyzed in two basic regions (See Figure 1.1). The *roughness sublayer* is the region between z=0 and $z=z_w$ where the mean velocity is dynamically influenced by the surface length scales of the vegetative elements.

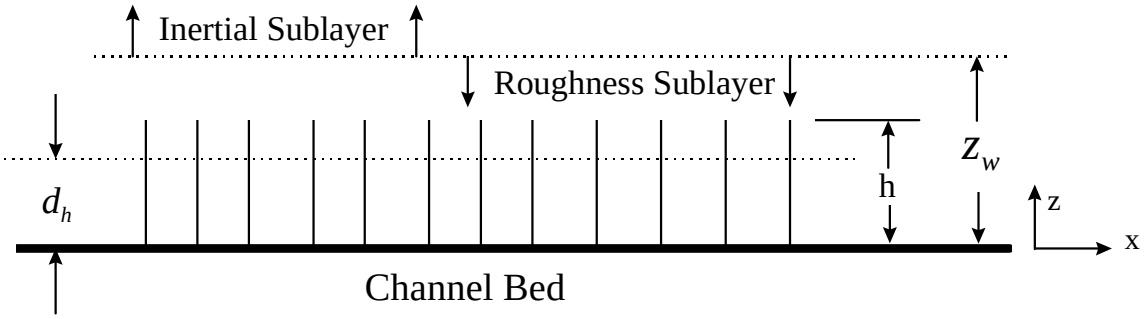

Figure 1.1 - Fully Submerged Flow Through Vegetation

The roughness sublayer is analogous to the viscous sublayer that exists above a smooth wall. Above the roughness sublayer lies the *inertial sublayer* where the mean velocity profile can be described by the logarithmic law(Raupach et al. 1991):

$$\frac{u(z)}{u_*} = \frac{1}{\mathrm{K}} \ln\left(\frac{z - d_h}{z_o}\right) \qquad \text{(Eqn. 1.2)}$$

where z_o = the roughness length, K = von Karman's constant (0.4) and d_h = the displaced height defined as the centroid of the drag profile within the roughness. The displaced height also represents the distance above the bed at which the velocity in the logarithmic profile equals zero (See Figure 4.2). The mean longitudinal velocity in Eqn. 1.2 is normalized by the friction velocity (u_*). The friction velocity is defined by:

$$u_* = \sqrt{gZS} \qquad \text{(Eqn. 1.3)}$$

where g = the acceleration of gravity, Z = the flow depth, and S = the channel bed slope. As the density increases, both z_w, and d_h tend to approach the top of the vegetation, h. The roughness length, z_o, is an alternate way to specify the drag on a rough surface in fully developed turbulent flow. It can also be seen as a measure of the capacity of the rough surface to absorb momentum. Kouwen et al.(1969) modified the logarithmic law to model the mean velocity above fully submerged flexible vegetation. When the vegetation is partially submerged or only slightly submerged , the logarithmic law cannot be used since the roughness sublayer extends throughout the entire flow depth.

The mean velocity profile in fully submerged flow has been researched extensively in the field of meteorology as canopy flow. Cup anemometers have been

placed in vertical arrays within a variety of different vegetation canopies to determine the mean velocity characteristics. An unpublished study was conducted by Bradley to determine the mean velocity profile in a uniform Ponderosa Pine canopy(Raupach and Thom 1981). Figure 1.2 shows the mean wind velocity, normalized by the velocity at z = h, as a function of the normalized height, z/h:

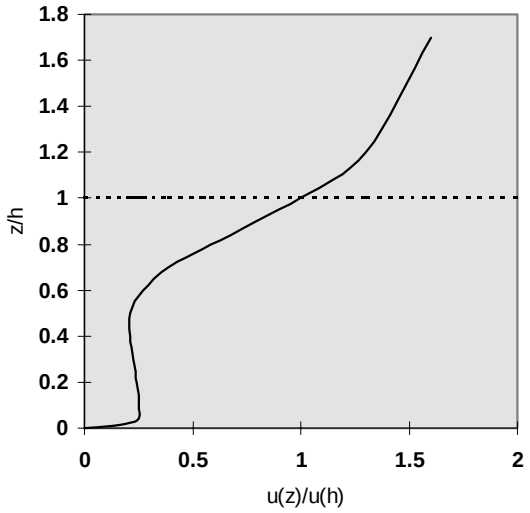

Figure 1.2 - Longitudinal Velocity Profile Measured in a Ponderosa Pine Canopy (Taken from Raupach et al. 1981)

The wind shear, $d\bar{u}/dz$, increases dramatically in the upper 40% of the canopy and reaches a maximum near the top of the trees. In the central portion of the canopy, between 0.05 < z/h < 0.6, the wind shear is quite low. The lower 5% of the forest is another region of high wind shear due to the surface boundary layer. There is a region between 0.1<z/h<0.5 where the wind shear is slightly negative resulting in a secondary maximum near z/h = 0.1. Similar behavior has been observed in other forest and agricultural canopies (Shaw 1977). Raupach and Thom(1981) suggest that counter-gradient momentum transport occurs in the region where the wind shear is negative.

Researchers have found that the mean velocity profile in vegetation canopies is strongly influenced by the prevailing meteorological conditions. In an unpublished study, Denmead measured the mean velocity profile within a corn canopy (Raupach and Thom 1981). He compiled mean velocity profiles for periods of light wind $(u(h) = 0.88m/s)$ and periods of strong wind $(u(h) = 2.66m/s)$ (See Figure 1.3).

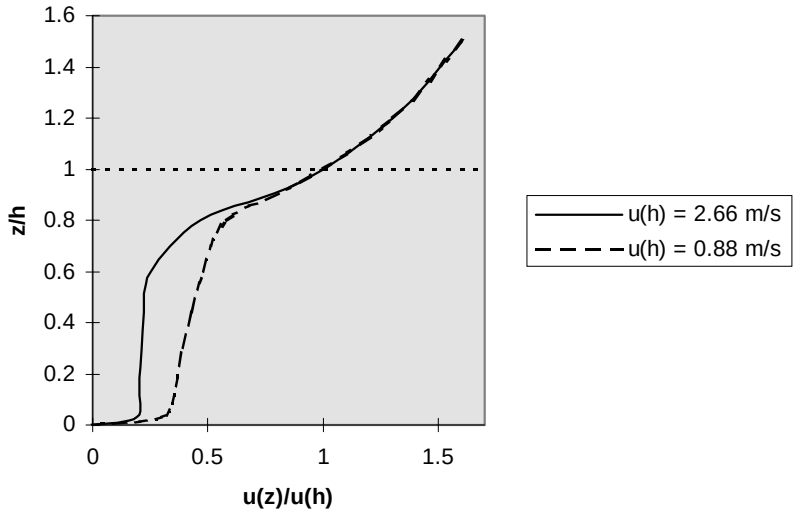

Figure 1.3 - Longitudinal Velocity Profiles for Different Flow Conditions (Taken from Raupach et al., 1981)

As seen in Figure 1.3, the normalized velocity in the lower 80% of the canopy was substantially higher during the light wind period. In actual velocity terms, the mean velocity above z=h is over three times higher during the strong wind period; below z=h, the mean velocity is only slightly higher during the strong wind period. Gao et. al.(1989) also measured the mean velocity within a forest canopy at different wind speeds. They also found that the normalized velocity (u(z)/u(h)) was substantially higher in the lower portion of the canopy during lighter wind. This indicates that as the overall air flow rate increases, a higher portion of the air flows above the canopy where there is less flow resistance.

Local diffusion models have been developed to describe the mean velocity profile within the canopy. In such models, a relationship needs to be developed that relates the eddy viscosity, η, to the other variables in the one dimensional momentum transport equation. One method is the mixing-length approach which assumes that the eddy viscosity is proportional to the wind shear:

$$\eta = \rho\, l^2 \frac{\partial u}{\partial z} \qquad \text{(Eqn. 1.4)}$$

where l is the mixing length and is assumed to remain constant within the canopy. From this assumption results the exponential wind profile:

$$\frac{u(z)}{u(h)} = \exp\left[\alpha_1 (z/h - 1)\right] \qquad \text{(Eqn. 1.5)}$$

where α_1 = a constant that tends to increase as the vegetation density increases. This equation is widely used to describe the mean velocity profile in the upper portion of the canopy. Similar equations for the mean velocity profile can be developed by making different assumptions concerning η. Cowan(1968) suggested that $\eta \propto u$ while Thom(1971) assumed that η remains constant within the canopy. From these assumptions, each derived an equation that describes u as a function of z/h and a constant:

Cowan

$$\frac{u(z)}{u(h)} = \left(\frac{\sinh \frac{\alpha_2 z}{h}}{\sinh \alpha_2} \right)^{0.5} \qquad \text{(Eqn. 1.6)}$$

Thom

$$\frac{u(z)}{u(h)} = \left[1 + \alpha_3 \left(1 - \frac{z}{h} \right) \right]^{-2} \qquad \text{(Eqn. 1.7)}$$

where α_2 and α_3 are constants. All three of the above equations give similar mean velocity profiles within the canopy providing an appropriate constant is chosen. This indicates that $u(z)$ is only a very weak function of η.

Local diffusion models give a good approximation of the mean wind profile in the upper portion of the vegetation but fail to give an accurate description towards to base of the canopy. Cowan's equation is the only diffusion model of those presented above that satisfies the no-slip boundary condition at z = 0. Another drawback of diffusion models is their inability to describe the counter-gradient momentum transfer that appears to occur in the lower part of vegetation canopies. As Raupach and Thom(1981) conclude, there are too many assumptions made when modeling the mean velocity profile with a diffusion model for them to be regarded as anything more than a single-parameter empirical fit.

Thompson and Roberson(1976) developed a theoretical model for submerged water flow over vegetation using the mixing-length theory. They suggested that a viscous sublayer extends above the channel bed a distance δ'. The thickness of the viscous sublayer, δ', is a function of the fluid viscosity, the surface shear stress and the density:

$$\delta' = \frac{M\upsilon}{\sqrt{\tau_o / \rho}} \qquad \text{(Eqn. 1.8)}$$

where M is the stability limit of the viscous sublayer (M=11.6) and τ_o = surface shear stress. Within the viscous sublayer, the velocity distribution can be approximated by the linear relationship:

$$\frac{u(z)}{u_*} = \frac{u_* z}{\upsilon} \qquad \text{(Eqn. 1.9)}$$

In the region between the viscous sublayer and the top of the vegetation Thompson and Roberson (1976) assumed that the mixing length is linearly proportional to the distance from the boundary $(l = kz)$. By assuming that Eqn. 1.4 is valid and $\tau(z) = \eta du/dz$, they were able to solve for the finite difference relationship given in Eqn. 1.10:

$$\frac{\Delta u}{u_*} = \frac{\Delta z}{kh}\sqrt{\frac{\tau(z)}{\tau_o}} \qquad \text{(Eqn. 1.10)}$$

The mean velocity at the top of the viscous sublayer (calculated using Eqn. 1.9) is used as a starting point for the finite difference solution to ensure a continuous profile within the vegetation. Above the vegetation, the velocity profile was assumed to follow the logarithmic law.

Tsujimoto et al.(1992) studied the mean velocity profile and turbulence characteristics in shallow water flow through rigid vegetation. They arranged cylinders in a parallel pattern and took measurements at the center of four model plants. Using experimental data, they developed an empirical model for the mean velocity within vegetation under fully submerged conditions:

$$\frac{u(z) - u_s}{u(h) - u_s} = \exp \xi z \qquad \text{(Eqn 1.11)}$$

where

$$u_s = \sqrt{\frac{2gS}{C_d \lambda}} \qquad \text{(Eqn. 1.12)}$$

In the above equations, S = the slope of the energy grade line, C_d = the total boundary drag coefficient, ξ = an empirical constant that represents the turbulent flow structure in the vegetation, and λ = the vegetation density (See Eqn. 1.15. The velocity measurements were taken at a position where the mean velocity was probably higher than elsewhere in the flow (at the center of four model plants). Therefore, this empirical model may not adequately describe the mean velocity at other locations in the flow where the stem wakes have more of an influence.

1.1.2 Partially Submerged Flow

Much of the time, the vegetation in floodplains and wetland environments is not fully submerged. As the flow conditions change from fully submerged to partially submerged, the mean velocity profile changes significantly (See Figure 1.4).

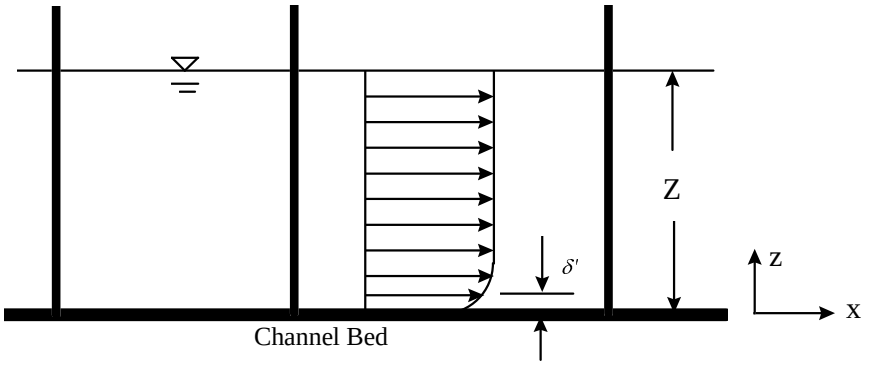

Figure 1.4 - Longitudinal Velocity Profile in Partially Submerged Vegetation

Research indicates that the mean velocity profile consists of two basic regions - A surface boundary layer in which the flow is dominated by bed generated shear and an upper region in which the mean velocity remains fairly constant with height. The mean velocity in the viscous sublayer can be approximated by Eqn. 1.9. Just above the viscous sublayer, the mean velocity profile is influenced by both bed generated turbulence and wake generated turbulence. Zavistoski (1994) tested arrays of cylinders under partially submerged conditions. As the plant density increased, the wake generated turbulence became more dominant, causing the surface boundary layer to be compressed toward the bed.

Zavistoski (1994) also showed that the mean velocity profile can change dramatically depending on the measurement location with respect to the dowels. Just behind dowels, there was a 40% reduction in longitudinal velocity due to wake turbulence; between wakes, the flow was accelerated to a maximum of 140% of the mean velocity.

1.2 Flow Resistance

When analyzing flow resistance through vegetation, many factors must be taken into consideration. Flow resistance is a function of vegetation characteristics such as height, shape, density and flexural rigidity. Channel roughness and flow regime must also be taken into account. In this paper, only flow in the turbulent, subcritical range will be analyzed.

1.2.1 Drag Characteristics

Vegetation has been modeled using arrays of rigid cylinders that are arranged in various patterns. The total drag force on a single cylinder is the sum of the form drag caused by pressure differences on either side of the cylinder and friction drag caused by

shearing stresses. Generally, one is only interested in determining the total drag on the body. The drag force on a single cylinder in idealized two-dimensional flow is given by:

$$F = \frac{C_d d h u_o^{\ 2}}{2} \qquad \text{(Eqn. 1.13)}$$

where C_d = drag coefficient, d = diameter of cylinder, h = height of cylinder and u_o = the upstream approach velocity. The drag coefficient for a cylinder is dependent on the flow regime around that cylinder and the cylinder Reynolds number, which is defined by :

$$R = \frac{d u_o}{\upsilon} \qquad \text{(Eqn. 1.14)}$$

where υ = kinematic viscosity of the fluid. The structure of the boundary layer around the cylinder determines where the point of separation will occur. When $R < 2 \times 10^5$, the boundary layer is usually laminar and the point of separation occurs between 72^o and 90^o from the stagnation point (See Figure 1.5). This creates a wide wake with a relatively high drag force.

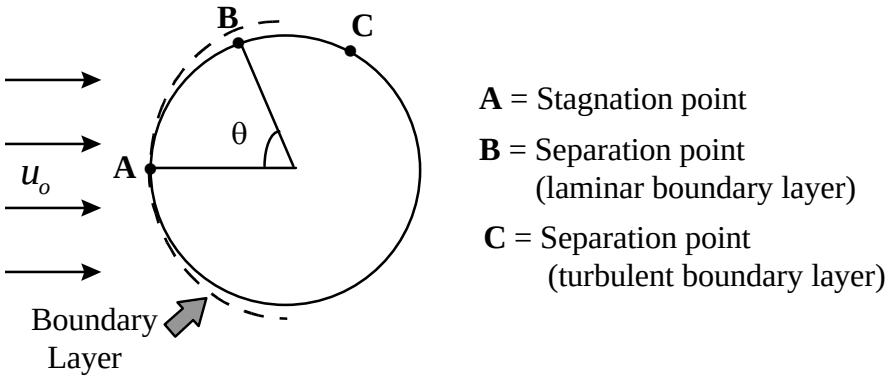

Figure 1.5 - Flow around a Cylinder

For $R > 2 \times 10^5$, the boundary layer is usually turbulent. The high momentum transfer in the turbulent boundary layer delays the separation from the cylinder. The separation point occurs at approximately 110^o from the stagnation point when the boundary layer is turbulent. As a result, the size of the wake and the drag force are both greatly reduced. Generally, as the angle θ increases, the size of the wake and the total drag decrease. A turbulent boundary layer can also be induced at $R < 2 \times 10^5$ by roughening the surface of the cylinder. The additional friction drag caused by the surface roughness is insignificant compared to the large decrease in the form drag. Schlichting (1968) found that a turbulent boundary layer could be induced at a Reynolds number as low as 3×10^4.

As would be expected, a cylinder within an array has different resistance characteristics than a single cylinder in idealized 2-dimensional flow. Under turbulent flow conditions, the drag on a cylinder within an array is primarily a function of both the density and the arrangement pattern of the elements. The *vegetation density,* λ, is defined as the frontal area of an element per unit ground area that the element occupies:

$$\lambda = \frac{dh}{s^2} \qquad \text{(Eqn. 1.15)}$$

where s = the mean separation between elements. Another way to quantify the number of elements on a surface is through the *spacing*, s/d. The spacing does not take into account the height of the roughness elements. The vegetation density and the spacing (s/d) are inversely related; as the vegetation density increases, the spacing decreases.

The arrangement pattern of the elements can significantly change the drag on an element, particularly at high density. The two most commonly studied patterns are the *staggered pattern* and the *parallel pattern* (See Figure 1.6).

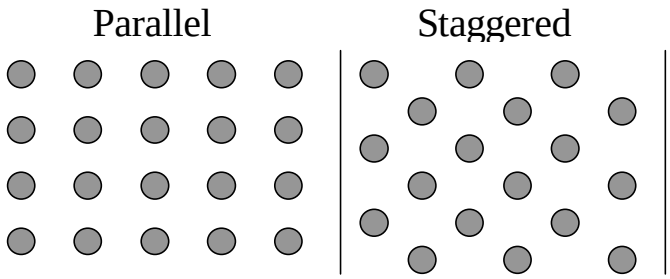

Figure 1.6 - Commonly Studied Arrangement Patterns

Petryk (1969) developed a mathematical model to determine the velocity at any point within an array of partially submerged cylinders. This model is only applicable when the flow is uniform and the spacing is at least 6 diameters in the downstream direction and 3 diameters in transverse direction. Petryk (1969) found a close agreement between results obtained using the mathematical model and comparative experiments conducted in the lab. Li and Shen (1973) used Petryk's model to predict how spacing and arrangement affect the drag force on elements within a partially submerged array under fully developed flow conditions (See Figure 1.7).

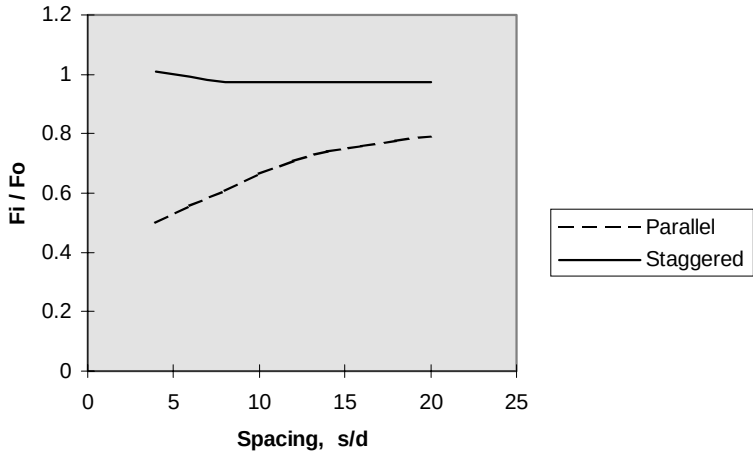

Figure 1.7 - Dimensionless Drag Force for Different Arrangement Patterns (Adapted from Li & Shen 1973)

In the above figure, F_i = the force on an element after the flow has become fully developed, and F_o = the unobstructed drag force on the furthest upstream element in the array(remains constant). For each configuration, the longitudinal and lateral separation were equal. The drag force on cylinders in a staggered array remains nearly constant as the spacing changes. For parallel arrays, the drag force on the elements falls sharply as the spacing decreases. This decrease in drag force can be attributed to a sheltering effect caused by upstream elements. In the wake region downstream of an element, turbulent eddies form which greatly reduce the mean longitudinal velocity. Since the drag force is proportional to the velocity squared, a fairly small decrease in the depth-averaged approach velocity can significantly decrease the drag force on an element. As the spacing decreases in a parallel array, the elements become more sheltered by upstream elements causing a higher reduction in the drag force on the element.

In partially submerged flow, the drag force on a cylinder may be calculated using a depth-averaged approach velocity. This is acceptable because the velocity remains fairly constant with height above the surface boundary layer (See Figure 1.4). When the vegetation is fully submerged, the velocity profile is not nearly as uniform with depth (See Figure 1.2). It is common to define a height-dependent drag coefficient for fully submerged turbulent flow:

$$C_d(z) = \frac{2u_*^2}{\lambda\rho\, u(z)^2} = \frac{2\tau_o}{\lambda u(z)^2} \qquad \text{(Eqn. 1.16)}$$

where τ_o = the total boundary shear stress, ρ = the density of the fluid, and $u(z)$ = the time-mean velocity at height z above the surface. The drag coefficient, $C_d(z)$, is dependent on the chosen reference velocity, $u(z)$. Typically, the velocity at the top of the

canopy, $u(h)$, is selected as the reference velocity. When u(h) is the reference velocity in Eqn. 1.16, the height-dependent drag coefficient is defined as $C_d(h)$.

Marshall (1971) experimented in a wind tunnel with parallel arrays of cylinders. For widely separated cylinders (low density), the height dependent drag coefficient, $C_d(h)$, approaches the height dependent drag coefficient of an isolated element, $C_R(h)$ (See Figure 1.8). The unobstructed drag coefficient tends to increase as the diameter to height aspect ratio, d/h, decreases. This indicates that the drag on an element in fully submerged flow is dependent on the d/h aspect ratio as well as the frontal area, d*h. The dependence of $C_R(h)$ on d/h was also confirmed in a theoretical study by Raupach (1992).

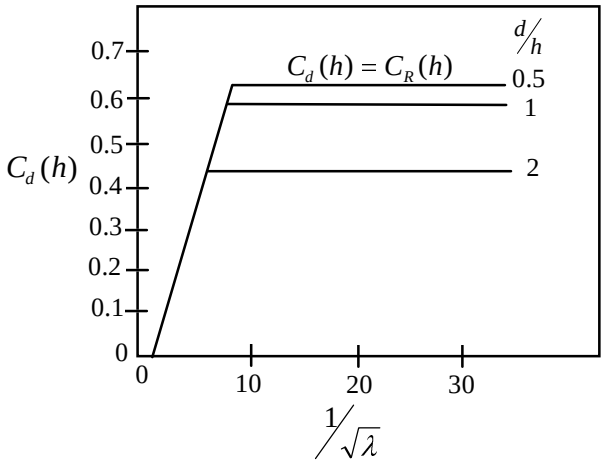

Figure 1.8 - Height Dependent Drag Coefficient as a Function of Density and Aspect Ratio in Fully Submerged Flow (Taken from Marshall, 1971)

When the density is high (low values of $1/\sqrt{\lambda}$), $C_d(h)$ varies linearly with $1/\sqrt{\lambda}$ and is independent of d/h. The point at which $C_R(h)$ intersects the line relating $C_d(h)$ to $1/\sqrt{\lambda}$ gives an approximate indication of the density at which sheltering becomes negligible. Marshall's (1971) results, shown in Figure 1.8, are consistent with the study by Li and Shen (1973); both studies demonstrate that elements in parallel arrays experience a sharp decrease in drag as the density increases.

An alternative way to characterize the roughness of a surface under fully submerged flow conditions is through the roughness length, z_o. The roughness length is an integration constant in the logarithmic law for the mean velocity in the inertial sublayer (See Figure1.1). It is a measure of the capacity of a surface to absorb momentum(Raupach et al.,1991). Unlike the height dependent drag coefficient, z_o depends only on physical properties of the roughness such as the height, diameter and density, provided that the flow is fully rough. If the flow is not fully rough, z_o also depends on the viscosity of the fluid. It will be assumed in this paper that the flow is fully rough.

Studies have been conducted to determine the relationship between the roughness length (z_o) and the density (λ). Raupach et al(1980) analyzed roughness data from three-dimensional arrays of cylinders, cubes and spheres. They found that certain trends occur as the density changes (See Figure 1.9).

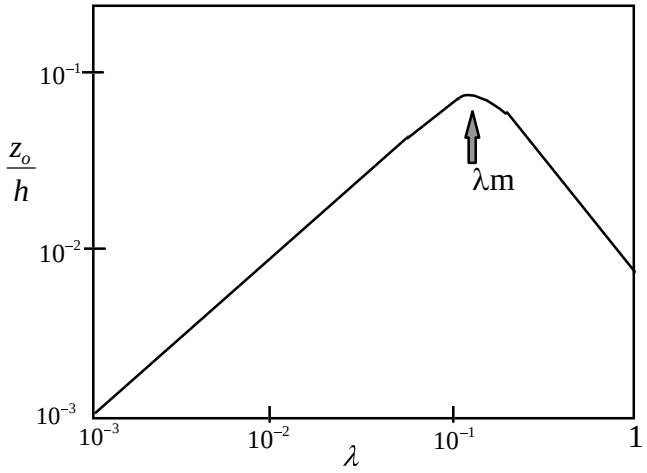

Figure 1.9 - Normalized Roughness Length as a Function of Density

In the above figure, the roughness length is normalized by the vegetation height, h. The normalized roughness length tends to increase linearly when $0 < \lambda < \lambda_m$ where λ_m = the density at the point of maximum roughness. In this range of density, an increase in the number of cylinders will increase the total drag on the array. At the point $\lambda = \lambda_m$, the increased drag force on an additional element balances the decrease in drag force caused by sheltering. Raupach et al.(1980) concluded that λ_m occurs between 0.1 and 0.3 depending on the roughness geometry. As the density increases above λ_m, the normalized roughness decreases. This behavior can be explained by the sheltering effect; the closer the elements are packed together, the more sheltered they are by upstream elements. Eventually, as the density approaches one, a skimming flow develops above the elements and the top of the array will act much like a smooth surface.

According to the theoretical results obtained by Li and Shen(1973) in Figure 1.7, the arrangement of elements would also affect z_o. When the spacing is low, a staggered array would tend to have a higher overall drag and absorb more momentum than a parallel array of equal density. Liu et al(1966) experimented with two-dimensional square bar roughness at varying densities. They found that $\lambda_m = 0.2$, which is similar to the three-dimensional results obtained by Raupach et al.(1980). Flow visualization revealed that permanent vortices occupied the cavity between elements when $\lambda > \lambda_m$. When $\lambda < \lambda_m$, the flow becomes reattached before the next downstream bar. The studies presented above indicate that the drag force on an element and the total drag on an array are strongly dependent on the density and arrangement pattern of the array, as well as the d/h aspect ratio.

1.2.2 Drag Partition

Li and Shen assumed that the resistance in the channel is due entirely to vegetative drag and that shear stress caused by bed resistance is negligible. It is important to determine if this assumption is valid. Raupach(1992) suggested that the total shear stress on a vegetated surface can be separated into two components:

$$\tau_o = \rho u_* = \tau_R + \tau_S \qquad \text{(Eqn. 1.17)}$$

where τ_R = the stress on the vegetation and τ_S = the stress on the underlying surface. Raupach(1992) developed a theoretical model to determine the relative weight of each stress component in fully submerged flow. He concluded that the stress partition relationships for cylindrical roughness are only a function of density:

$$\frac{\tau_S}{\tau_o} = \frac{1}{1+\beta\lambda} \qquad \text{(Eqn. 1.18)}$$

$$\frac{\tau_R}{\tau_o} = \frac{\beta\lambda}{1+\beta\lambda} \qquad \text{(Eqn. 1.19)}$$

where $\beta = C_R(h)/C_S(h)$ and $C_R(h)$ = the height-dependent drag coefficient for an isolated, surface mounted cylinder and $C_S(h)$ = the unobstructed height-dependent drag coefficient for the channel bed. The arrangement of elements on the surface is not taken into account in this model. Raupach(1992) found that data generated using the model compares closely with Marshall's(1971) experimental data when the density is low. The main limitation of the model occurs at high roughness densities, when element wakes interact and are no longer separately identifiable. Raupach concluded that the total shear stress is completely dominated by the cylindrical roughness (τ_R) when λ exceeds a value in the range of 0.03 to 0.1.

Marshall(1971) measured τ_o and τ_R separately for cylindrical roughness ranging in density from 0.0002 to 0.2. He used the equation $\tau_S = \tau_o - \tau_R$ to determine the stress generated by the bed. Figure 1.10 indicates that the amount of stress contributed by the bed decreases exponentially as the density increases.

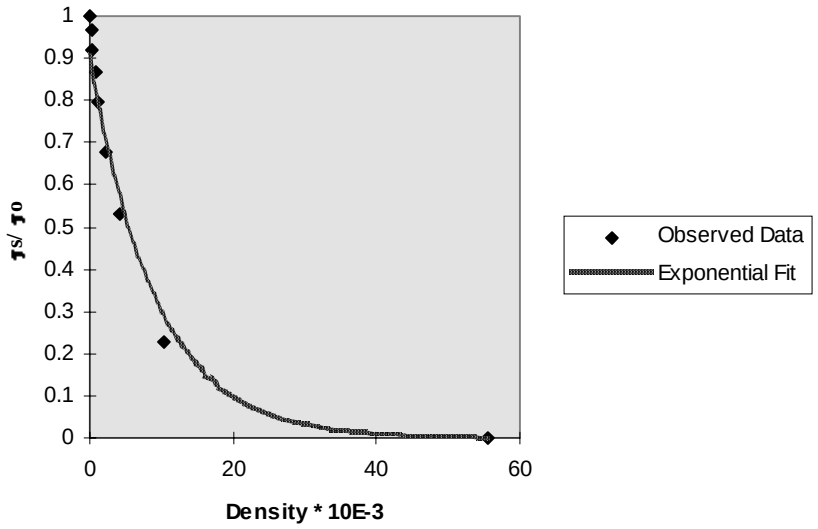

Figure 1.10 - Stress Partition as a Function of Density (Adapted from Marshall 1971)

The density at which surface generated shear becomes insignificant is a weak function of the aspect ratio d/h. Marshall(1971) suggested that the point at which $C_D(h)$ no longer depends on $1/\sqrt{\lambda}$ provides an approximate indication of where the surface generated shear becomes insignificant(See Figure 1.8). For cylindrical roughness in parallel patterns, Marshall(1971) found that surface generated shear stress can be neglected when λ exceeds 0.02 to 0.05. Both Raupach(1992) and Marshall(1971) suggest that it is an acceptable approximation to assume that $\tau_S \approx 0$ when $\lambda > 0.03$.

1.2.3 Resistance Models for Partially Submerged Flow

Although the flow of water through vegetation under partially submerged conditions is very complex, assumptions can be made which lead to simplification. If we assume that the flow is both steady and uniform within the control volume, the sum of the forces in the direction of flow must equal zero. Then the sum of the shear forces on the boundary and the drag forces on the vegetation must equal the force of gravity on the control volume (See Fig. 1.11).

$$\gamma\ AZS = \sum F_i + \tau_S A \qquad \text{(Eqn. 1.20)}$$

where S = the channel slope, A = the total bed area within the control section, and Z = the depth of flow. The drag force on each individual element, F_i, can be solved using Eq. 1.13, provided a suitable depth-averaged approach velocity is used.

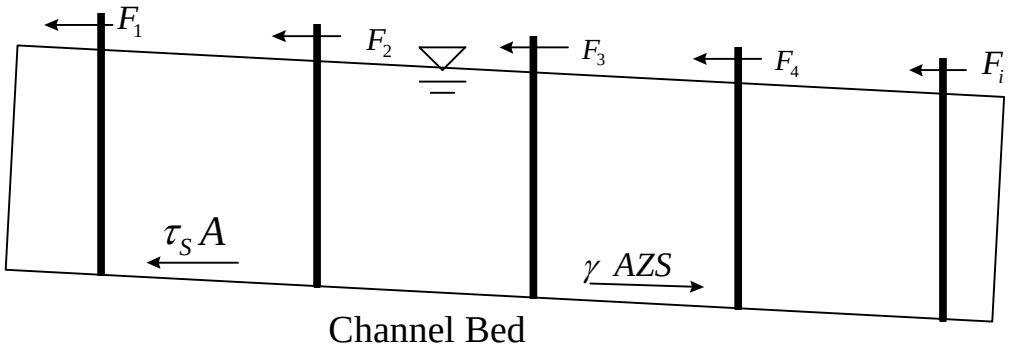

Fig. 1.11 - Control Section for Partially Submerged Resistance Model (Adapted from Petryk and Bosmajian, 1975)

Petryk and Bosmajian(1975) used this basic approach to develop a flow resistance model to determine the total resistance in terms of Manning's n. This model is only appropriate for the English system of units.

$$n = n_S \sqrt{1 + \frac{C_d \sum d_i h_i}{2gAZ} \left(\frac{1.49}{n_S} \right)^2 Z^{\frac{4}{3}}} \qquad \text{(Eqn. 1.21)}$$

where n_S = Manning's roughness coefficient for the bed. This equation would only be valid in a wide channel or floodplain where the hydraulic radius is approximately equal to the depth of flow. As the flow depth increases, it is assumed that the vegetation density remains constant with height. This would probably not be an appropriate model for an environment with varying heights of vegetation.

When the vegetation is dense, Eqn. 1.21 reduces to:

$$n = 1.49 Z^{\frac{2}{3}} \sqrt{\frac{C_d \sum d_i h_i}{2gAZ}} \qquad \text{(Eqn. 1.22)}$$

In this case, the surface roughness parameter drops out of the equation showing that the resistance is completely dominated by the vegetation. The total Manning roughness coefficient obtained from Eqn. 1.22 can be substituted into Manning's equation to determine the mean velocity:

$$u = \sqrt{\frac{2gAZ}{C_D \sum d_i h_i}} \qquad \text{(Eqn. 1.23)}$$

This is very simplified model in which the mean velocity is assumed to be constant throughout the entire depth. Hartly(1980) describes a similar resistance model for

partially submerged flow in which an analytical approach can be used to solve for the total Darcy friction factor.

1.3 Turbulence Characteristics

1.3.1 Fully Submerged Vegetation

When the vegetation is submerged, the interaction between the faster flow over the vegetation and the slower flow inside the vegetation generates turbulence. Using different probabilistic techniques, one can analyze the velocity fluctuations to develop a better understanding of the turbulence structure. Turbulence intensity will be defined in this paper as the root mean squared (RMS) of the turbulent velocity fluctuations about the mean:

$$u_{rms} = \sqrt{\frac{(u')^2}{N_s - 1}} \qquad \text{(Eqn. 1.24)}$$

where N_s = the number of velocity samples. With this definition, the turbulence intensity is the same as the standard deviation of the turbulent velocity fluctuations about the mean. Cionco(1972) found that the turbulence intensity generally increases with vegetation density.

Tsujimoto et al.(1992) analyzed the longitudinal turbulence intensity in both fully submerged and partially submerged flows (See Figure 1.12). They used both a micro-propeller and a hot film anemometer to measure the turbulent velocity fluctuations. All of measurements were taken at the center of four model plants.

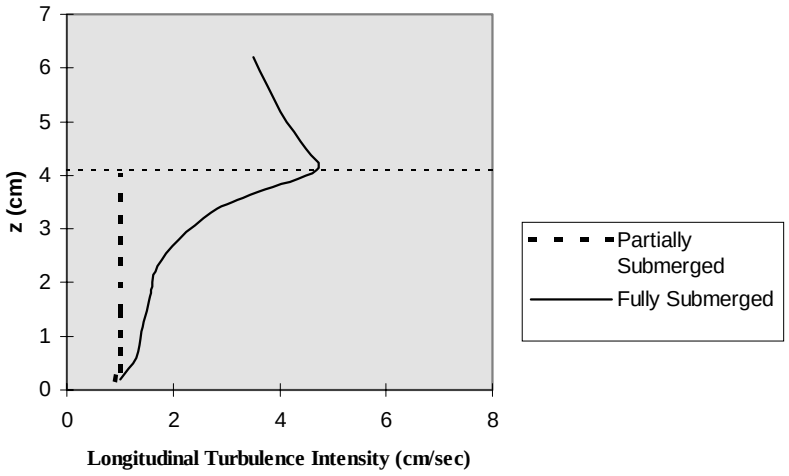

Figure 1.12 - Longitudinal Turbulence Intensity in Partially and Fully Submerged Flows (Taken from Tsujimoto et al. 1992)

When the vegetation is fully submerged, the maximum value of u_{rms} occurs at the top of the canopy and decreases within and above the canopy. A recent study by Ikeda and Kanazawa(1996) confirms that u_{rms} has a maxima at z = h and decreases toward the free surface and the bed. In open channel flows without vegetation, the longitudinal turbulence intensity has a maxima slightly above the bed and decreases toward the free-surface (Grass 1971, Nezu & Nakagawa 1993). Raupach et al. (1991) showed that u_{rms} and w_{rms} remain constant with height above z=h in an atmospheric boundary layer in which no free surface is present.

Turbulent shear stress, also called Reynolds stress, is a direct result of turbulent velocity fluctuations:

$$\tau = -\rho \overline{u'w'} \qquad \text{(Eqn. 1.25)}$$

Tsujimoto et al.(1992) measured the Reynolds stress in fully submerged and partially submerged flows at the center of four model plants. When the vegetation is fully submerged, the Reynolds stress distribution shown in Figure 1.13 has approximately the same shape as the turbulence intensity shown in Figure 1.12.

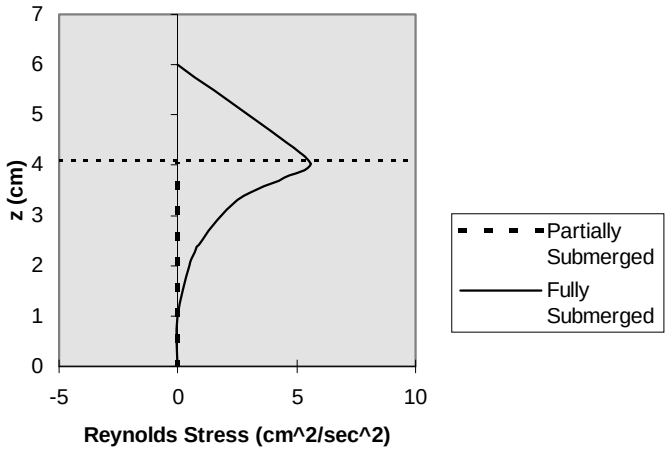

Figure 1.13 - Reynolds Stress Distribution in Partially and Fully Submerged Flows (Taken From Tsujimoto et al. 1992)

The maximum Reynolds stress occurs at the top of the vegetation and decreases linearly to zero at the free surface. The linear distribution above the vegetation is very similar to the stress distribution one would expect in open channel flow when no vegetation is present. The Reynolds stress attenuates rapidly within the vegetation and becomes negligible below z/h = 0.25. Raupach et al.(1991) found that Reynolds stress remains constant in the atmospheric boundary layer above z = h. Within the canopy, they found that the stress distribution is similar to the fully submerged distribution shown in Figure 1.13.

Tsujimoto et al.(1992) developed a model to describe the Reynolds stress in fully submerged flow through vegetation:

$$\tau(z) = \tau(h) \ \exp \alpha \ z \quad (0<z<h) \qquad \text{(Eqn. 1.26)}$$

$$\tau(z) = \tau(h)\left(1 - \frac{Z}{h}\right) \quad (h<z<Z) \qquad \text{(Eqn. 1.27)}$$

where: $$\tau(h) = \rho g(Z - h)S \qquad \text{(Eqn. 1.28)}$$

and α = a constant representing the turbulence structure in the vegetation. Within the vegetation, the shear stress follows an exponential distribution; above the vegetation, the shear stress distribution is linear. Tsujimoto et al.(1992) outlines a method that adjusts the energy slope to create a continuous curve at the free surface. A wind tunnel study by Seigner et al.(1976) using an array of cylindrical rods confirms the exponential shape of the shear stress distribution below z=h.

Raupach et al.(1991) plotted the normalized skewness (third moment about the mean) of the velocity fluctuations in the x and z directions for various vegetation canopies. Within and just above each canopy, he found that the skew of u is strongly positive, and the skew of w is strongly negative. This indicates that there are strong intermittent downward gusts into the vegetation canopy when the flow is fully submerged. Inoue(1955) observed downward sweeps of the air over wheat fields and termed the phenomenon honami.

It is now recognized that turbulence in the roughness sublayer is not random. Raupach et al.(1996) suggests that the high turbulence and instability at the top of the canopy is similar to a mixing layer formed between two coflowing streams with different velocities. Organized turbulent motion has recently been studied in the field of hydraulics by Ikeda and Kanazawa(1996). They experimented with fully submerged flexible vegetation using a 2-D laser-Doppler velocimeter in conjunction with flow visualization. Their tests indicate that the sheared region at the top of the vegetation creates instability, causing discrete vortices to form at a specific frequency. The vortices have an elliptical shape and are inclined downward in the direction of motion. They migrate downstream just above the vegetation at a velocity slightly larger than u(h). An upward flow was observed in front of the vortices. Gao et al.(1989) observed that the organized turbulence at the top of a forest canopy consists of a weak upward motion followed by a strong downward gust toward the inside of the canopy. They found that over 75% of all momentum transport within the canopy results from these organized structures.

1.3.2 Turbulent Kinetic Energy

Rigid vegetation interacts with the flow of water in three basic ways(Wilson&Shaw,1977):

1) Momentum is extracted from the flow due to form drag and skin friction.
2) Large scale turbulent motions are broken down into smaller scale turbulent motions in the wakes behind the elements.

3) The mean kinetic energy (MKE) of the flow is converted into turbulent kinetic energy (TKE) in the wake regions.

Local diffusion models, such as those discussed in Section 1.1.1, have been used to relate the Reynolds stress to the mean wind velocity in the upper portion of the canopy. In such models, it is uncertain how to describe the eddy viscosity as a function of height. Local diffusion models have trouble predicting the flow characteristics in the lower portion of the canopy and provide little information about the turbulent exchange processes. Researchers have recently developed higher order canopy flow models that predict how the TKE is generated, dissipated, and transported within and above the canopy. Figure 1.14 indicates the relative magnitude of the terms in the TKE budget for fully submerged boundary-layer flow.

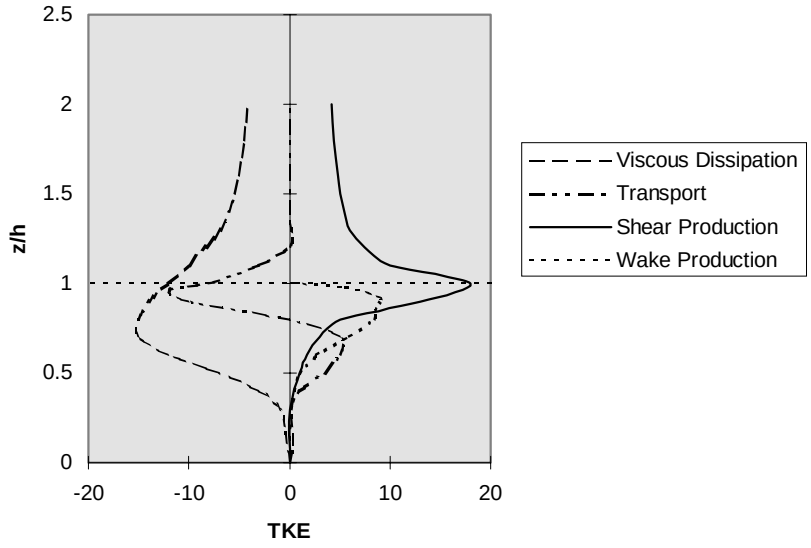

Figure 1.14 - Turbulent Kinetic Energy Budget (Taken From Wilson & Shaw 1977)

As expected, the shear production term is a maximum at the top of the canopy where the wind shear is greatest. In the upper 15% of the canopy, shear production dominates the generation of turbulence. According to the model, a substantial portion of the turbulence in the upper 50% of the canopy is due to wake production behind the individual elements. Raupach et al.(1996) cautions that the model may be misleading. Since the length scale of wake generated turbulence is small, it dissipates quickly and does not contribute significantly to the overall TKE.

The model predicts that turbulent transport extracts TKE from the upper portion of the canopy and increases the TKE in the lower portion of the canopy. Turbulent transport is the dominant source of TKE production in the lower 60% of the canopy. This implies that most of the turbulence in the lower layers of vegetation is not locally generated.

1.3.3 Partially Submerged Vegetation

When the vegetation is only partially submerged, the turbulence structure changes dramatically. The longitudinal turbulence intensity is very small and remains constant with depth (See Figure 1.12). The Reynolds stress is negligible throughout the entire depth (See Figure 1.13). Zavistoski (1994) found that the dominant source of turbulence in the surface boundary layer is surface generated shear. Above this layer, the turbulence is dominated by wake turbulence. The height of the surface boundary layer tends to decrease as the density increases. At high density, it can be assumed that the dowels dominate the turbulence over the entire flow depth.

The profiles in Figures 1.12 & 1.13 were taken in the middle of four plants, and therefore do not reflect the local changes in turbulence that occur within the stem wakes. Zavistoski (1994) found that three diameters behind each dowel, the turbulence intensity was increased by a factor of two due to wake generated turbulence. In addition, the longitudinal and vertical turbulence intensities increased linearly as the density increased.

Using flow visualization, Zavistoski (1994) was able to study the turbulent motion that occurs within the proximity of each dowel. A vortex street formed behind each dowel starting at a certain height above the bed, and a horseshoe vortex formed at the base of each dowel. They suggest that the horseshoe vortex inhibits the formation of a vortex street near the bed.

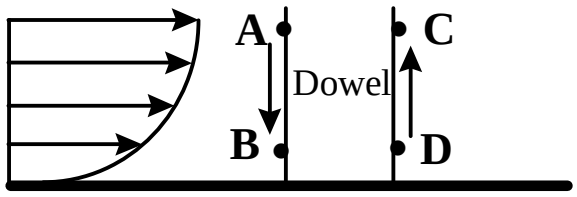

Figure 1.15 - Vertical Motion at the Base of the Dowel

Zavistoski (1994) also observed that upward motion occurs on the downstream side of the dowels and downward motion occurs on the upstream side of the dowels (See Figure 1.15).Since u(A) > u(B), the stagnation pressure at A is greater than the stagnation pressure at B. This causes a downward motion from A to B. Increased approach velocity causes decreased pressure on the downstream side of the dowel. Therefore, the pressure at C is lower than the pressure at D, causing vertical motion in the positive direction. Zavistoski (1994) found that the magnitude of the vertical velocity decreases as the density increases. At higher densities, the mean velocity becomes more uniform with depth and the surface boundary layer compresses towards the bed. Zavistoski (1994) also observed that a region of backflow (negative u) exists behind each dowel. The magnitude of the backflow increased significantly as the density increased.

1.4 Scope and Objective of This Research

This chapter provides a summary of the literature that was reviewed pertaining to fluid flows through vegetation. Many researchers have studied the mean velocity profile, the turbulence structure, and the resistance characteristics in flows through both fully submerged and partially submerged vegetation. Some of the more recent studies have sought to model flows through vegetation using a velocity or turbulence intensity profile from a single location in the flow. Research by Zavistoski (1994) and Hodges (1997) indicates that a single profile may not be representative of the conditions at all locations in the flow. It is therefore necessary to examine the flow characteristics at several different locations in the vegetation. A better understanding of the mean velocity and turbulence characteristics will improve our ability to model sediment movement and turbulent transport processes.

As seen in this chapter, fully submerged flow behaves quite differently from partially submerged flow. While fully submerged flow has been studied extensively in the field of meteorology, much less research is available regarding fully submerged water flow and the effects caused by the free-surface. In addition, almost no research is available for flows containing two different heights of vegetation (double layer flows). Double layer flows commonly occur in floodplains and wetland environments where trees and other tall vegetation grow among denser low-lying shrubs and grasses. The research described in the following chapters was undertaken to examine the mean velocity and turbulence characteristics at several different locations within partially submerged, fully submerged and double layer flows.

Additional experiments were conducted to examine how bed and vegetative skin roughness influence the flow characteristics. In nature, the surfaces of the bed and the vegetation are not always smooth. For example, grass on the bed and bark on vegetation provide roughness that can increase the flow resistance. Researchers, however, have typically used smooth materials to model the bed and the vegetation. Finally, experiments were conducted to study sediment transport and deposition in flows containing vegetation.

Chapter 2

Experiments & Procedures

The research discussed in this paper was undertaken to study the velocity and turbulence characteristics in flows through rigid vegetation. Experiments were conducted under partially submerged, fully submerged, and double layer flow conditions. In each of the experiments, measurements were taken at several locations within the vegetation array. The term double layer flow is used to describe flows that contain two different heights of vegetation. Experiments were also conducted to study how bed and vegetative skin roughness influence the flow characteristics.

While sediment movement has been studied extensively in open channel flow, much less research is available for flows containing vegetation. Experiments were conducted to examine the transport and deposition of sediment in flows containing vegetation. Sediment experiments were conducted under partially submerged, fully submerged and double layer flow conditions.

2.1 Equipment and Facilities

This Section gives a general description of the equipment and materials used in the experiments. The following Sections provide more detailed information about the individual experiments. All of the experiments described in this paper were performed in the Hydraulics Laboratory at Virginia Polytechnic Institute & State University. A recirculating hydraulic flume with a length of 4.3 m and a width of 0.3 m was used in each of the experiments (See Figure 2.1). The slope of the flume remained at 0.3% throughout this research. Prior to each experiment, the slope of the flume was checked using an electronic level.

Figure 2.1 - Recirculating Hydraulic Flume

The vegetation was simulated by a uniform array of rigid 6.35mm-diameter acrylic dowels. The dowels were smooth and varied in height depending on the experiment. They were mounted in holes on a 1.3 cm-thick sheet of smooth plexiglass. The plexiglass base was then bolted to the bed of the hydraulic flume. The model vegetation test section was approximately 3.0 m long and 0.3 m wide. To establish nearly uniform flow and to minimize backwater effects, stoplogs were placed at the end of the flume (See Figure 2.2). The stoplogs consisted of 0.3 m long acrylic dowels. Prior to each experiment, the flow depth was measured 0.5 m from each end of the model to ensure that the flow was nearly uniform. These depth measurements are included in Tables 2.1, 2.2, 2.3 & 2.4.

Figure 2.2 - Stoplogs Used to Establish Uniform Flow

In some of the experiments, roughness was attached to the bed and the dowels. Bed roughness was simulated by 35 grit belt sander strips that covered the entire bed. The belt sander strips were attached to the bed using a waterproof adhesive. The mean grain size diameter (D_{50}) for the bed roughness was approximately 0.7mm. Holes were drilled in each of the belt sander strips allowing the dowels to be mounted in the plexiglass base. Vegetative skin roughness was simulated by adhesive sandpaper that was wrapped around each of the dowels. Fine and coarse sandpaper (100 & 40 grit) were tested to see how different degrees of dowels roughness influence the flow characteristics. The mean grain size diameters for the fine and coarse roughness were 0.2mm and 0.45 mm respectively.

Instantaneous velocity measurements were taken using a Dantec one-dimensional Laser Doppler Velocimeter (LDV). All of the measurements were taken approximately 2.25m downstream from the start of the wetland model to ensure that the flow was fully developed. At each measurement point, 1500 velocity measurements were taken over a duration of approximately 20 seconds. A profile consists of a series of measurement points along a vertical plane. The scope of the LDV was fastened to a traverse. The traverse was used to ensure that the measurement points were the proper distance apart in each of the profiles. An operating nut was used to control the traverse. For every 360° turn of the operating nut, the scope moved vertically 2.31 mm. Vertical velocity was measured by flipping the scope of the LDV 90°. In the vertical velocity experiments, the bed of the flume partially obstructed the laser beams, preventing any measurements from being taken within 5 mm of the bed. All of the data was collected and stored on a 486 computer that was connected to the LDV. Software provided by Dantec was used to compute the mean velocity, turbulence intensity, and skew at each measurement point. This data is included in the Appendix.

In each of the sediment experiments, an auger mounted on top of the flume was used to introduce sediment to the flume at a constant feeding rate (See Figure 2.3). The auger was positioned to discharge sediment approximately 0.5 m upstream of the model test section. An inverted cone mounted below the auger discharge pipe distributed the sediment evenly between the two sides of the flume. In each of the sediment experiments, sediment was introduced to the flume at a rate of 140.89 g/min. over a duration of 15 minutes.

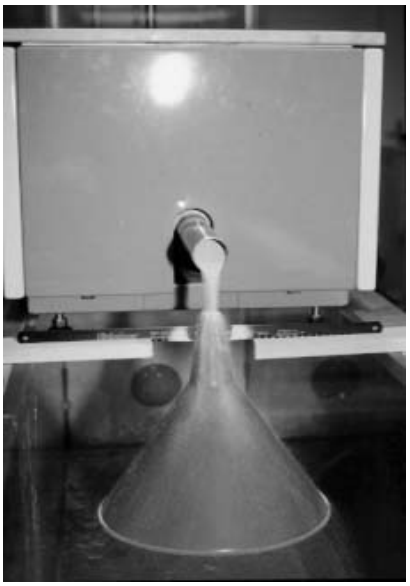

Figure 2.3 - Sediment Auger Mounted on Top of Flume

Sediment not deposited within the array was captured in a sediment trap at the end of the flume. The sediment trap consisted of a pillow case secured to a circular wooden frame (See Figure 2.4). The frame was then clamped to the circular outfall orifice at the end of the flume. This setup forced all of the sediment laden water flowing in the flume to pass through the pillow case before recirculating. The fibers in the pillow case were fine enough to capture the sediment and allow the water to pass freely.

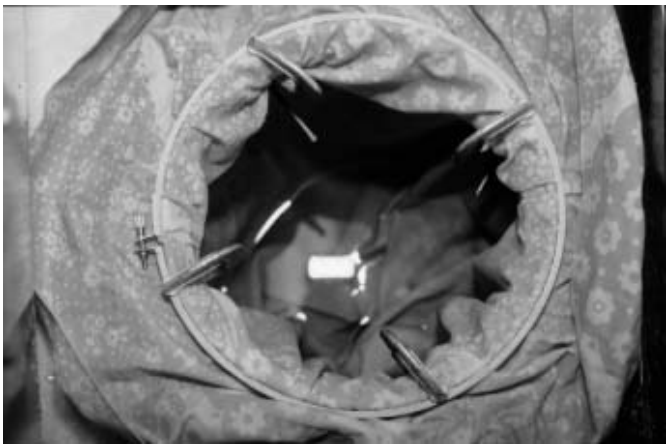

Figure 2.4 - Sediment Trap

2.2 Partially Submerged Experiments

Six experiments were conducted under partially submerged flow conditions. In each of the experiments, the flow rate in the flume was kept constant at 0.0044 m^3/s. All

of the dowels used in the partially submerged experiments were 7.62 cm tall. The dowels were arranged in the staggered pattern shown in Figure 2.5. In each partially submerged experiment, vertical profiles were taken at the each of the six measurement locations shown in this figure.

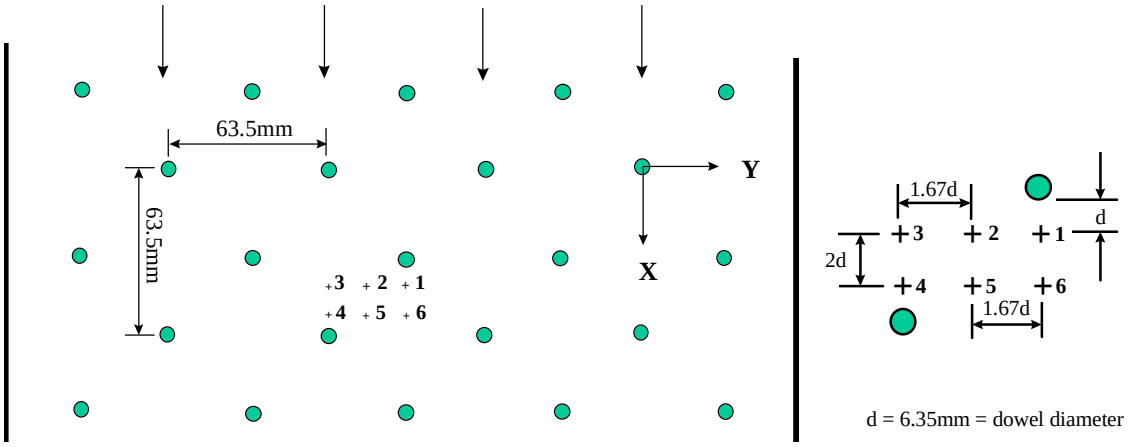

Figure 2.5 - Staggered Dowel Arrangement Showing Measurement Locations

Table 2.1 summarizes the six partially submerged experiments. The first two experiments were conducted to study the longitudinal and vertical velocities when the bed and dowels were smooth. In the four remaining experiments, different combinations of bed and dowel roughness were tested. The results from the partially submerged experiments are presented in Chapter 3.

Table 2.1 - Partially Submerged Experiments

Exp. #	Description	Upstream Depth (m)	Downstream Depth (m)
PS#1	No Roughness; Longitudinal Velocity	0.0649	0.0649
PS#2	No Roughness; Vertical Velocity	0.0649	0.0649
PS#3	Bed Roughness and Fine Dowel Roughness; Longitudinal Velocity	0.0697	0.0672
PS#4	Bed Roughness and Coarse Dowel Roughness; Longitudinal Velocity	0.0762	0.0722
PS#5	Bed Roughness and Coarse Dowel Roughness; Vertical Velocity	0.0762	0.0722
PS#6	Bed Roughness and No Dowel Roughness; Longitudinal Velocity	0.0664	0.0657

2.3 Fully Submerged Experiments

Six experiments were conducted under fully submerged flow conditions. The dowels in the fully submerged experiments had the same height, density and

configuration as the dowels in the partially submerged experiments. In each of the fully submerged experiments, vertical profiles were taken at the same six measurement locations shown in Figure 6.5. To achieve fully submerged flow conditions, the flow rate in the flume (Q) was increased to 0.0114 m^3/sec. This flow rate is approximately 2.5 times higher than the flow rate in the partially submerged experiments.

As seen in Table 2.2, the fully submerged experiments followed the same sequence as the partially submerged experiments. The first two experiments were conducted to study the longitudinal and vertical velocities when the bed and dowels were smooth. In the four remaining experiments, different combinations of bed and dowel roughness were tested. The results from the fully submerged experiments are presented in Chapter 4.

Table 2.2 - Fully Submerged Experiments

Exp. #	Description	Upstream Depth (m)	Downstream Depth (m)
FS#1	No Roughness; Longitudinal Velocity	0.1141	0.1141
FS#2	No Roughness; Vertical Velocity	0.1141	0.1141
FS#3	Bed Roughness and Fine Dowel Roughness; Longitudinal Velocity	0.1192	0.1169
FS#4	Bed Roughness and Coarse Dowel Roughness; Longitudinal Velocity	0.1215	0.1173
FS#5	Bed Roughness and Coarse Dowel Roughness; Vertical Velocity	0.1215	0.1173
FS#6	Bed Roughness and No Dowel Roughness; Longitudinal Velocity	0.1156	0.1136

2.4 Double Layer Experiments

Three experiments were conducted under double layer flow conditions. The flow rate in each of the double layer experiments was 0.0114 m3/s, which is the same flow rate used in the fully submerged experiments. The dowels were arranged in the pattern shown in Figure 2.6. In each double layer experiment, vertical profiles were taken at the each of the ten measurement locations shown in this figure.

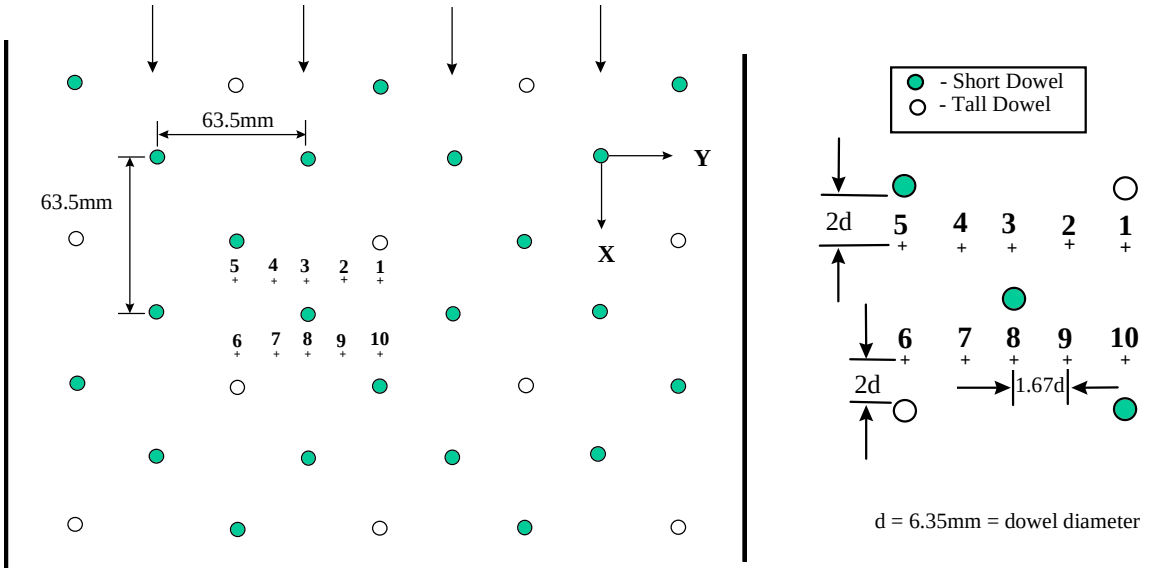

Figure 2.6 - Double Layer Dowel Arrangement Showing Measurement Locations

Table 2.3 summarizes the three double layer experiments. Velocity measurements were only taken in the longitudinal direction. Three different heights of dowels were used in the double layer experiments - 15.2 cm, 7.6 cm and 5.1 cm. The height of the tall and short dowels (h_s & h_t) varied depending on the experiment. In experiments DL#1 & DL#2, the tall dowels were partially submerged while the short dowels were fully submerged. Both the tall and the short dowels were submerged in experiment DL#3. The results from the double layer experiments are presented in Chapter 5.

Table 2.3 - Double Layer Experiments

Exp. #	Description	Upstream Depth (m)	Downstream Depth (m)
DL#1	h_t = 15.2cm (Partially Submerged) h_s = 7.6 cm (Fully Submerged); Longitudinal Velocity	0.1278	0.1253
DL#2	h_t = 15.2 cm (Partially Submerged) h_s = 5.1 cm (Fully Submerged); Longitudinal Velocity	0.1224	0.1199
DL#3	h_t = 7.6 cm (Fully Submerged) h_s = 5.1 cm (Fully Submerged); Longitudinal Velocity	0.1095	0.1090

2.5 Sediment Experiments

All of the material used in the sediment experiments was fine sand ranging in size from 0.075mm to 0.25 mm. The grain size distribution for the sediment is shown in Figure 6.7. The sediment tends to follow a log-normal distribution, which is consistent with most natural sediment distributions. Typically, sediment is classified as well sorted when σ_g<1.3 and poorly sorted when σ_g>1.3. Since σ_g=1.3 in this experiment, the sediment cannot be classified as either poorly sorted or well sorted.

As discussed previously, sediment was introduced to the flume at a constant rate of 140.89 g/min. over a period of 15 minutes. The total mass of material added to the flume in each experiment was slightly more than 2 kg. After each experiment, the sediment captured in the sediment trap was baked to remove all moisture. The baked sediment was weighed and then placed in a mechanical shaker to determine the grain size distribution. Prior to each experiment, the flume was cleaned to remove all sediment deposited from the previous experiment.

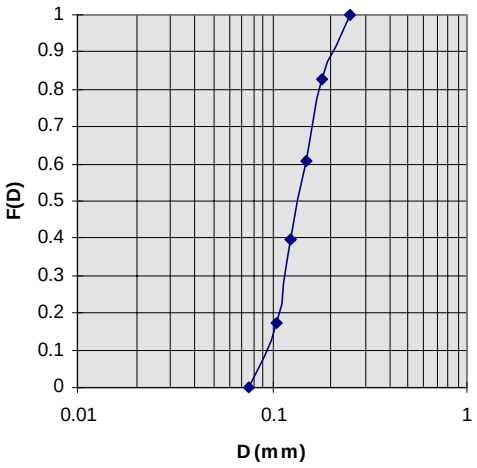

D_{84}=0.180
D_{16}=0.106

D_g=Geometric Mean Diameter
$= \sqrt{D_{16} D_{84}}$ = 0.138mm

σ_g =Geometric Standard Deviation
$= \sqrt{D_{84} / D_{16}}$ = 1.3

Figure 2.7 - Sediment Grain Size Distribution

Sediment experiments were conducted under six different flow conditions (See Table 2.4). Experiments S#1 & S#2 were conducted as control experiments to determine how much sediment would fall out of suspension in the absence of dowels. Two experiments were conducted under partially submerged conditions - one with the dowels smooth and one with the dowels rough. Finally, experiments were conducted under fully submerged and double layer flow conditions. In the double layer experiment, the tall dowels (h_t=15.2cm) were partially submerged and the short dowels (h_s=7.6cm) were fully submerged. The results from the sediment experiments are presented in Chapter 6.

Table 2.4 - Sediment Experiments

Exp.#	Description	Flow Rate (m^3/s)	Upstream Depth (m)	Downstream Depth (m)
S#1	No Dowels	0.0044	0.0239	0.0223
S#2	No Dowels	0.0114	0.0435	0.0423
S#3	Partially Submerged; No Roughness; h=7.6cm	0.0044	0.0679	0.0660
S#4	Partially Submerged; Coarse Dowel Roughness and no Bed Roughness; h=7.6cm	0.0044	0.0761	0.0715
S#5	Fully Submerged; No Roughness; h=7.6 cm	0.0114	0.1160	0.1145
S#6	Double Layer; h_s=7.6cm and h_t=15.2cm; No Roughness	0.0114	0.1287	0.1270

2.6 Summary Flow Characteristics

Table 2.5 summarizes the flow characteristics for each of the experiments discussed in this chapter. The average depth was calculated by taking the average of the upstream and downstream depth measurements. As seen in this table, Manning's n ranges from 0.0313-0.0381 in the partially submerged experiments, 0.0271-0.0289 in the fully submerged experiments, and 0.0255-0.0312 in the double layer experiments. The Froude number indicates that the flow was subcritical in each of the experiments.

Table 2.5 - Summary Flow Characteristics

Exp.	Channel Slope (m/m)	Flow Rate (m^3/s)	Average Depth (m)	Average Velocity (m/s)	Flow Area (m^2)	Wetted Perimeter (m)	Hydraulic Radius (m)	Manning's n	Friction Velocity (m/s)	Froude #
PS#1	0.0030	0.0044	0.0649	0.2228	0.0198	0.4346	0.0455	0.0313	0.0437	0.2792
PS#2	0.0030	0.0044	0.0649	0.2228	0.0198	0.4346	0.0455	0.0313	0.0437	0.2792
PS#3	0.0030	0.0044	0.0685	0.2112	0.0209	0.4417	0.0472	0.0339	0.0449	0.2577
PS#4	0.0030	0.0044	0.0742	0.1948	0.0226	0.4532	0.0499	0.0381	0.0467	0.2284
PS#5	0.0030	0.0044	0.0742	0.1948	0.0226	0.4532	0.0499	0.0381	0.0467	0.2284
PS#6	0.0030	0.0044	0.0661	0.2189	0.0201	0.4369	0.0461	0.0321	0.0441	0.2719
FS#1	0.0030	0.0114	0.1141	0.3272	0.0348	0.5330	0.0652	0.0271	0.0579	0.3093
FS#2	0.0030	0.0114	0.1141	0.3272	0.0348	0.5330	0.0652	0.0271	0.0579	0.3093
FS#3	0.0030	0.0114	0.1181	0.3162	0.0360	0.5409	0.0665	0.0284	0.0589	0.2939
FS#4	0.0030	0.0114	0.1194	0.3127	0.0364	0.5436	0.0669	0.0289	0.0593	0.2889
FS#5	0.0030	0.0114	0.1194	0.3127	0.0364	0.5436	0.0669	0.0289	0.0593	0.2889
FS#6	0.0030	0.0114	0.1146	0.3258	0.0349	0.5340	0.0654	0.0273	0.0581	0.3072
DL#1	0.0030	0.0114	0.1266	0.2950	0.0386	0.5579	0.0691	0.0312	0.0610	0.2648
DL#2	0.0030	0.0114	0.1212	0.3082	0.0369	0.5471	0.0675	0.0294	0.0597	0.2827
DL#3	0.0030	0.0114	0.1093	0.3417	0.0333	0.5233	0.0636	0.0255	0.0567	0.3301
S#1	0.0030	0.0044	0.0231	0.6249	0.0070	0.3510	0.0201	0.0065	0.0261	1.3128
S#2	0.0030	0.0114	0.0429	0.8718	0.0131	0.3906	0.0335	0.0065	0.0355	1.3439
S#3	0.0030	0.0044	0.0670	0.2156	0.0204	0.4387	0.0465	0.0328	0.0444	0.2661
S#4	0.0030	0.0044	0.0738	0.1956	0.0225	0.4524	0.0497	0.0378	0.0466	0.2299
S#5	0.0030	0.0114	0.1153	0.3244	0.0351	0.5354	0.0656	0.0275	0.0583	0.3050
S#6	0.0030	0.0114	0.1279	0.2925	0.0390	0.5605	0.0695	0.0316	0.0613	0.2612

Chapter 3

Partially Submerged Flow

This section will examine the velocity and turbulence characteristics in partially submerged flow. Experiments were initially conducted when both the bed and the dowels were smooth. Further experiments studied how bed roughness and dowel roughness influence the flow characteristics. Each experiment consists of six vertical profiles taken at the six *measurement locations* shown in Figure 2.5. Four of the measurement locations are positioned in-line with dowels while two are in the unobstructed flow region between dowels. The channel slope, dowel arrangement, dowel spacing, and the flow rate all remained constant in each of the partially submerged experiments.

3.1 Experiments with a Smooth Bed and Smooth Dowels

3.1.1 Longitudinal Mean Velocity

As seen in Figure 3.1, the longitudinal mean velocity varies considerably depending on the measurement location. One-diameter downstream of a dowel (Location #1), the longitudinal mean velocity is significantly lower than elsewhere in the flow. At this location, a portion of the turbulent fluctuations were negative at each measurement position along the vertical profile, indicating that some of the fluid moves in the upstream direction. Hodges (1997) and Zavistoski (1994) also measured reversed flows in the region immediately downstream of a dowel. This phenomenon can be explained by the low pressure in the wake of a dowel. When separation occurs at the sides of a cylinder, a region of low pressure forms on the downstream side of the cylinder (Janna 1987, Schlichting 1979). This low pressure region creates considerable suction, forcing a portion of the fluid to reverse direction (Schlichting 1979).

As seen in Figure 3.1, the longitudinal velocity increases rapidly with distance downstream of a dowel. At Location #6, just two diameters downstream of Location #1, the depth-averaged velocity is nearly 2.5 times greater than the depth-averaged velocity at Location #1. Locations #2 & #5 in the unobstructed flow region are less influenced by the dowel wakes, and therefore, have the highest mean velocities.

Although the longitudinal velocity profiles vary with measurement location, each of the profiles have certain features in common. The velocity profiles can be divided into three distinct regions. The upper 30% of the flow depth (above $z \approx 45\,\text{mm}$) will be referred to as the **free-surface region**. The flow in this region is influenced by shear stress resulting from the interaction of the free-surface and the dowels. Overall, the mean velocity is slightly higher in the free-surface region than elsewhere in the flow. The **intermediate region** is located directly below the free-surface region (17mm<z<45mm). The flow in this region tends to be dominated primarily by wake generated turbulence,

rather than influences from the bed or the free-surface. The mean velocity remains nearly constant with height in the intermediate region.

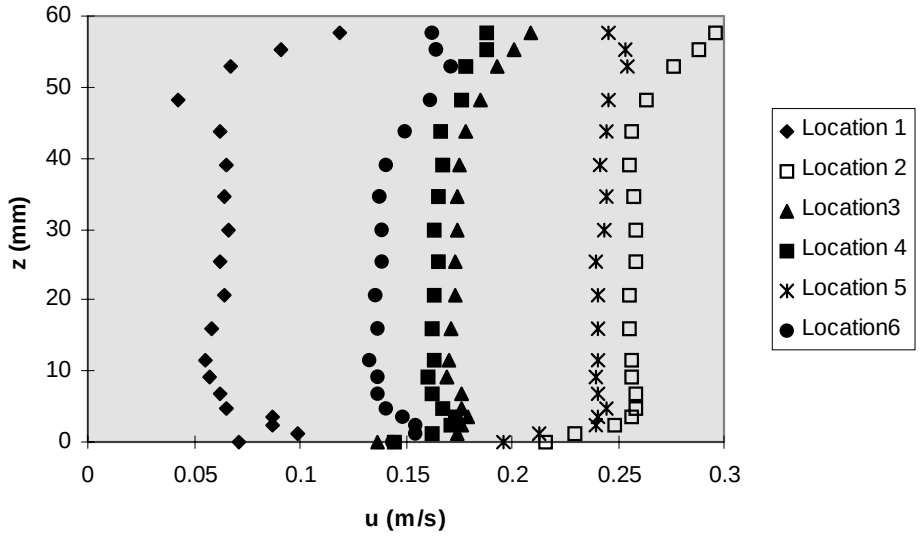

Figure 3.1 - Longitudinal Velocity Profiles in Partially Submerged Flow

The **bed region** is located below the intermediate region(0<z<17mm) and tends to be dominated by surface generated shear stress and horseshoe vortices that form at the base of each dowel. At measurement locations in-line with dowels (Locations #1,3,4&6), the longitudinal velocity profiles in the bed region are characterized by a *high-velocity spike* very close to the bed. The high-velocity spike is far more pronounced directly behind a dowel and becomes less pronounced further downstream of a dowel. A high-velocity spike was also observed by Hodges (1997) in a partially submerged dowel array under similar flow conditions. The secondary maximum observed near the base of a forest canopy (See Figure 1.2) is similar to the high velocity spike shown in Figure 3.1.

The high-velocity spike appears to be generated by the horseshoe vortex that forms at the base of each dowel. A horseshoe vortex is caused by lateral vorticity in the boundary layer upstream of a dowel (Sumer et al. 1997). Researchers have found that the clockwise rotation of a horseshoe vortex tends to draw higher momentum fluid downward on the upstream face of a cylinder toward the bed (Sumer et al. 1997, Simpson et al. 1990). As the horseshoe vortex wraps around the cylinder, the lateral vorticity in the boundary layer is transformed into longitudinal vorticity on each of the counter-rotating limbs. Research indicates that the longitudinal rotation in each of the limbs also draws higher momentum fluid near the sides of the dowel downward toward the bed (Simpson, 1990). The downward flow at the front and sides of a dowel tends to energize the mean flow near the bed (Simpson, 1990). The same phenomenon occurs when small appendages, called vortex-generators, are attached to the wings of jet aircraft; higher velocity fluid is drawn downward toward the surface of the wing, forestalling large-scale separation (Vennard & Street 1982).

The downward momentum transport associated with the horseshoe vortex may cause the high-velocity spike to form in the wake of a dowel. As seen in Figure 3.1, the mean velocity on the upstream side of a dowel (Location #4) is significantly higher than

the mean velocity on the lee side of a dowel (Location #1). As discussed in the preceding paragraph, the higher momentum fluid from the upstream side of a dowel is drawn downward into the horseshoe vortex. It is believed that this higher momentum fluid is transported by the horseshoe vortex around the sides of a dowel to the wake region, causing a high-velocity spike to form. In addition, Raupach et al. (1980) found that the direction of rotation in the two horseshoe limbs is such that higher velocity fluid is drawn into the central wake region behind a surface mounted body. The horseshoe vortex may also draw higher velocity fluid from the adjacent unobstructed flow region into the central wake region. No additional research was found concerning the high-velocity spike to confirm these hypotheses.

The separation point on the surface of a dowel may also be influenced by the horseshoe vortex. Dargahi (1989) found that increased turbulence generated by the horseshoe vortex shifts the separation point further downstream in the vicinity of the bed. Such a shift would cause the size of the wake to decrease and may increase the mean velocity within the wake. This is another possible explanation for the presence of a high-velocity spike.

Just above the high-velocity spike, the velocity is reduced to a secondary minimum at approximately z=10mm. The high-velocity spike and the secondary minimum seem to be related in some way; both are most pronounced one diameter downstream of a dowel (Location #1) and become less evident further downstream. At measurement locations in the unobstructed flow region (Locations #2&#5), there is little evidence of either a high-velocity spike or a secondary minimum. The flow in this region tends to be influenced more by surface generated shear stress than the horseshoe vortices.

The high-velocity spike and the associated secondary minimum exhibit many properties that are characteristic of a wall jet in quiescent fluid. The flow at the base of a sluice gate is an example of a wall jet. The high velocity flow in a wall jet tends to expand vertically with distance downstream of the nozzle, causing momentum to be transported vertically away from the wall (Launder & Rodi 1983). As seen in Figure 3.1, the point of maximum velocity in the spike becomes higher above the bed with distance downstream of a dowel, indicating that momentum is transported vertically in this region. Figure 3.3 confirms that upward motion occurs near the bed at measurement locations downstream of a dowel. Launder & Rodi (1983) explain that a secondary minimum forms above the high-velocity jet in the 'developing flow region' immediately downstream of the nozzle. They attribute this phenomenon to a clockwise rotating vortex that forms above the high-velocity jet.

3.1.2 Turbulence Intensity

Turbulence intensity is defined by Eqn. 1.24. The longitudinal and vertical turbulence intensity profiles are plotted in Figure 3.2. Each of the profiles has approximately the same shape; the turbulence intensities remain nearly constant throughout the entire flow depth. Research conducted by Tsujimoto et al. (1992) supports this observation.

Although the turbulence intensity profiles have roughly the same shape at the different measurement locations, they vary considerably in magnitude. Turbulence

intensity tends to vary with position in an array in the opposite trend as the mean velocity; the highest turbulence intensities were measured at positions where the mean velocity was lowest, and vice-versa.

Immediately downstream of a dowel, both the longitudinal and vertical turbulence intensities are significantly higher than elsewhere in the flow due to the wake-generated turbulence. When the fluid separates from a cylinder, small-scale eddies are shed from either side of the cylinder in what is known as a *von Karman vortex street* (Daugherty et al. 1985). These eddies are generated by the rotation in the boundary layer over the surface of the dowel (Sumer et al., 1997). A vortex street forms when the cylinder Reynolds number, R, is between $60 < R < 5000$ (Schlichting 1979). The cylinder Reynolds number is defined by:

$$R = \frac{U_d d}{\nu} \qquad \text{(Eqn. 3.1)}$$

where U_d = the depth-averaged approach velocity, d = the cylinder diameter, and ν = the fluid kinematic viscosity. In each of the partially submerged experiments, $R \approx 1000$ indicating that a vortex street is expected to form behind each dowel. The small-scale eddies in the vortex street dramatically increase both the longitudinal and vertical turbulence intensities immediately downstream of a dowel.

As seen in Figure 3.2, the turbulence intensities decrease with distance downstream of a dowel. Since the eddies in a vortex street have a small length scale when compared to the shear generated turbulence, they are dissipated fairly quickly (Raupach et al. 1981). The two measurement locations in the unobstructed flow region (Locations #2&#5) are less affected by the vortex shedding and, therefore, have the lowest turbulence intensities. Notice that the longitudinal turbulence intensity at the two locations in the unobstructed flow region increases near the bed due to the shear generated turbulence. This phenomenon is typical in open channel flows in the absence of dowels (Grass 1971; Nezu and Nakagawa 1993).

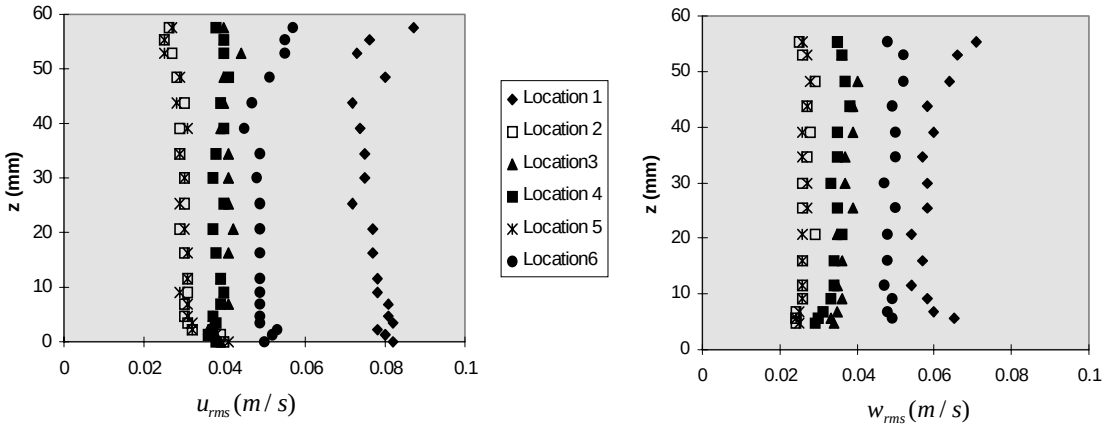

Figure 3.2 - Longitudinal & Vertical Turbulence Intensities in Partially Submerged Flow

The longitudinal and the vertical turbulence intensities have approximately the same magnitude at Locations #2-5, indicating that the turbulence may be nearly isotropic at these locations. At Location #1, however, the longitudinal turbulence intensity is approximately 30% higher than the vertical turbulence intensity, indicating that the small-scale eddies in the vortex street increase the longitudinal turbulence more than the vertical turbulence.

3.1.3 Vertical Velocity

Profiles of the mean vertical velocity were taken at each of the six measurement locations under partially submerged flow conditions. Due to limitations in the measuring apparatus, vertical velocity measurements could not be taken between $0<z<5$mm. Figure 3.3 shows the vertical velocity profiles at the four locations in-line with dowels. The horizontal scale is greatly exaggerated in this figure to show more detail; the arrows beneath the bed show the position of the measurement locations.

A region of relatively high upward flow was observed near the bed at Locations #1, #6, & #3. The upward flow becomes less pronounced and extends further from the bed with distance downstream of a dowel. It is believed that the upward motion near the bed is caused by the vertical growth of the high-velocity spike (jet) that forms behind a dowel. As discussed in Section 3.1.1, a wall jet (which is similar to the high-velocity spike) expands vertically with distance downstream of the nozzle, causing momentum to be transported upward away from the bed (Launder & Rodi 1983).

In the intermediate region, weak upward flow occurs downstream of a dowel and weak downward flow occurs upstream of a dowel. Others have observed similar secondary flows on the upstream and downstream sides of surface mounted cylinders (Vogel 1994, Zavistoski 1994). Zavistoski (1994) suggests that the upward and downward flows are driven by vertical pressure gradients that form on either side of a surface mounted cylinder (See Section 1.1.3).

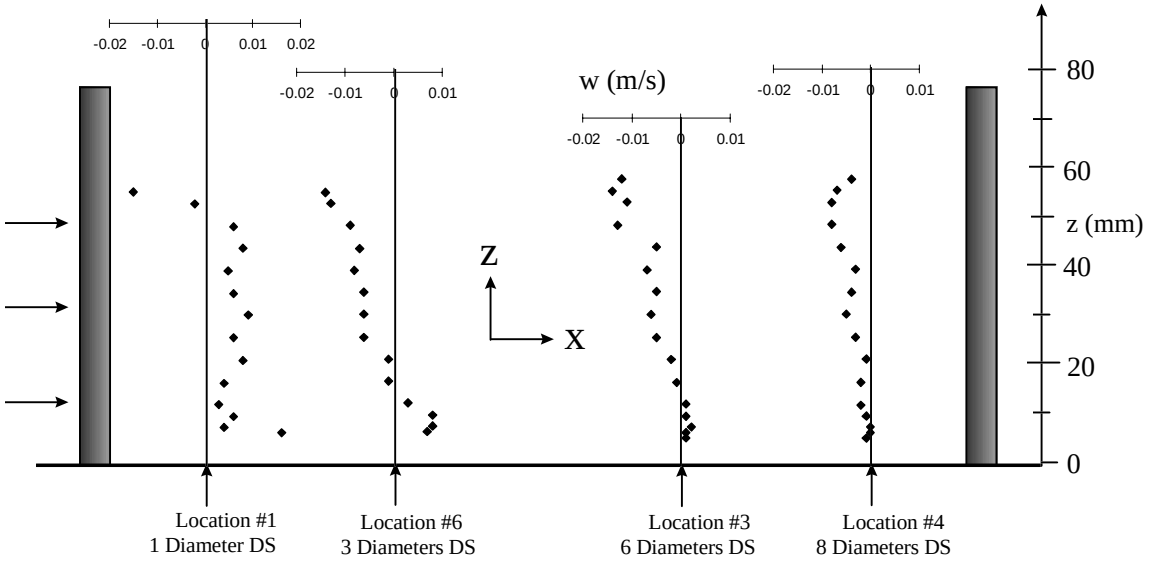

Figure 3.3 - Vertical Velocity Profiles at Locations In-Line with Dowels

Downward flow was observed in the vicinity of the free-surface at each of the measurement locations in-line with dowels. This downward motion is most pronounced directly behind a dowel and becomes slightly less pronounced further downstream of a dowel.

All of the mean vertical velocity data from the six measurement locations was input into SURFER (Surface Mapping Software) to generate the shaded contour images shown in Figure 3.4. The three contour images represent different vertical cross-sectional views of the mean vertical velocity within the array. The plan views beneath each image show the location of each cross-section. As seen in the legend, darker regions indicate downward (negative) velocity and lighter regions indicate upward (positive) velocity. The dashed line in each image represents the zero-velocity contour. Image (c) is a graphical representation of the four velocity profiles shown in Figure 3.3.

At Locations #1 & #6, the upward flows near the bed and the downward flows near the free-surface are very localized (See Images (a)&(b)); they only occur directly behind a dowel. In the adjacent unobstructed flow regions, the vertical motion tends to be in the opposite direction. Downward flow occurs near the bed adjacent to the upward flow at Locations #1 & #6; similarly, upward flow occurs near the free surface adjacent to the downward flow at Locations #1 & #6.

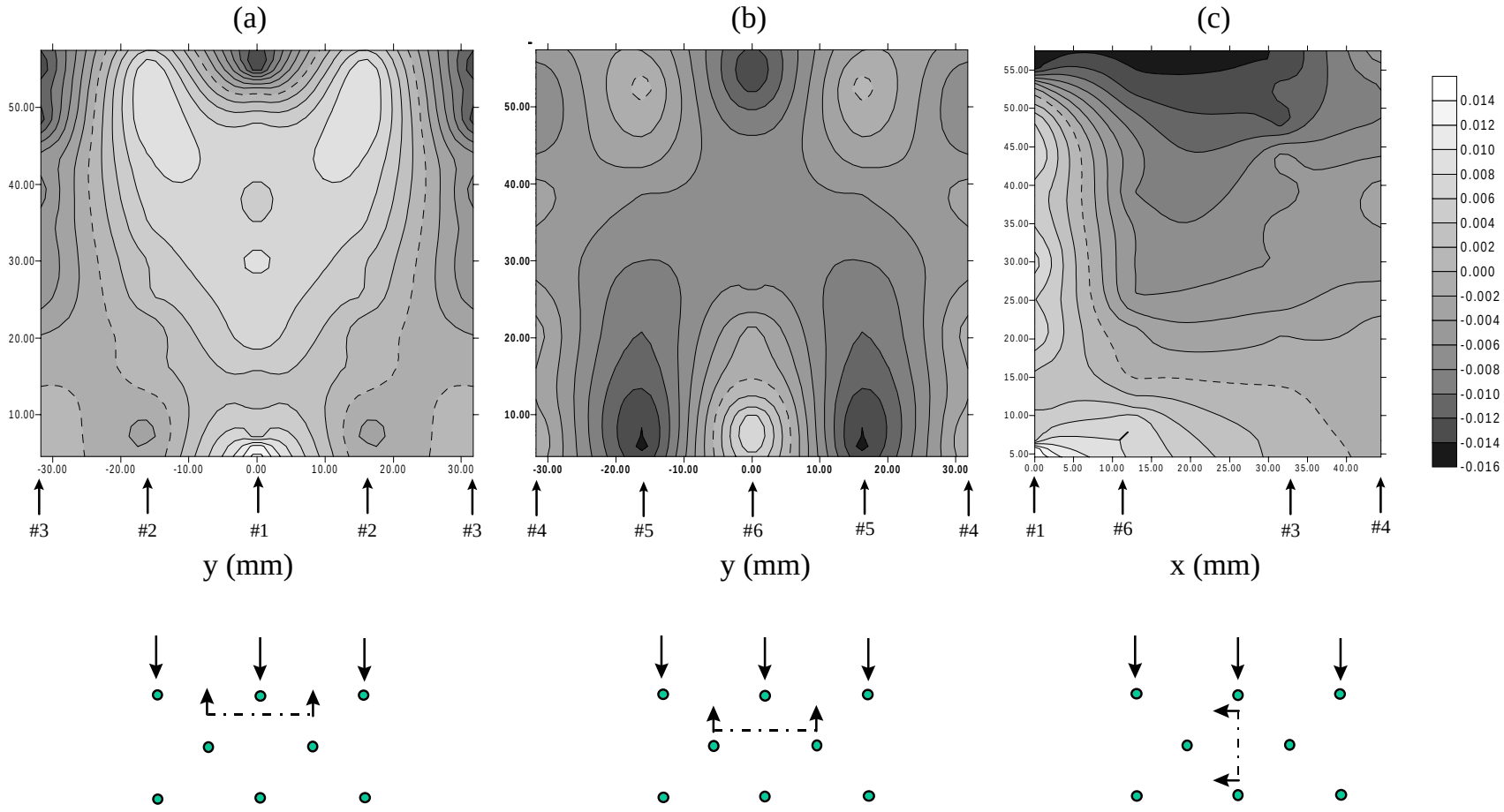

Figure 3.4 - Shaded Contour Images Showing Vertical Velocity in Partially Submerged Flow

3.2 Experiment with Bed Roughness and Smooth Dowels

An experiment was conducted with coarse sandpaper attached to the bed of the flume to determine how bed roughness affects the mean velocity and the turbulence characteristics in partially submerged flow. Measurements were taken only in the longitudinal direction for this roughness condition. The results presented below indicate that bed roughness alters the longitudinal velocity and turbulence intensity profiles. This is particularly true at Location #1, immediately downstream of a dowel.

3.2.1 Longitudinal Velocity

Figure 3.5 compares the smooth-bed and rough-bed longitudinal velocity profiles at the four locations in-line with dowels. The dotted lines represent the z-axes and the arrows below the bed show the position of the measurement locations.

When the bed is rough, the high-velocity spike becomes slightly more pronounced indicating that more momentum is drawn downward toward the bed. Possibly, the horseshoe vortex has a higher intensity when the bed is rough, causing more downward momentum transport. No research was found to support this hypothesis. Above the high-velocity spike, the secondary minimum is significantly more pronounced when the bed is rough. This is particularly evident at Location #1 where the mean velocity within the secondary minimum becomes negative.

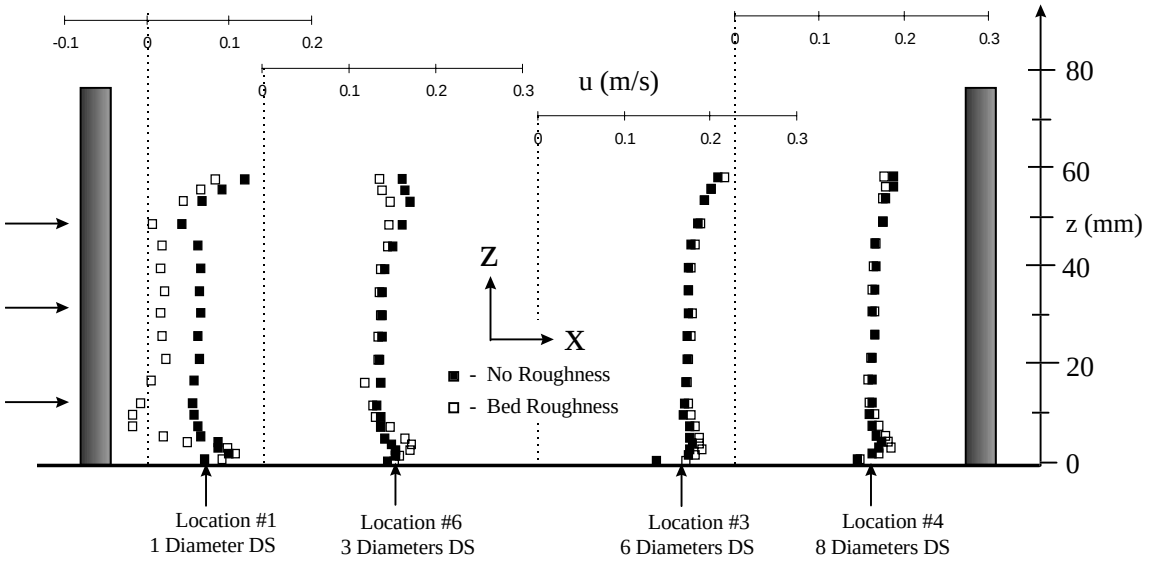

Figure 3.5 - Longitudinal Velocity Profiles Taken In-Line with Dowels (Smooth Dowels; Rough Bed)

The smooth-bed and rough-bed velocity profiles at locations #2 & #5 in the unobstructed flow region are shown in Figure 3.6. When the bed is rough, the mean velocity in the bed region tends to be slightly higher, further indicating that bed roughness may cause more momentum to be drawn downward toward the bed. Above the bed region, the profiles are similar for the two roughness conditions.

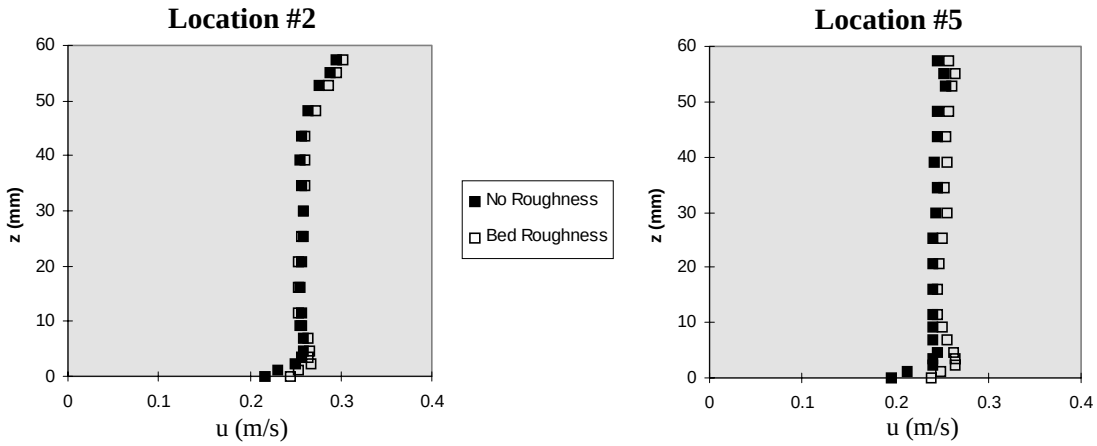

Figure 3.6 - Longitudinal Velocity Profiles in the Unobstructed Flow Region (Smooth Dowels; Rough Bed)

3.2.2 Vorticity

Lateral vorticity is a measure of the rotation about the y-axis:

$$\omega = \frac{\partial w}{\partial x} - \frac{\partial u}{\partial z} \qquad \text{(Eqn. 3.2)}$$

It was found that the term $\frac{\partial w}{\partial x}$ is very small in comparison to $\frac{\partial u}{\partial z}$ and therefore can be ignored. Positive vorticity indicates counter-clockwise rotation and negative vorticity indicates clockwise rotation. Figure 3.7 is a graph of the depth vs lateral vorticity at Location #1, immediately downstream of a dowel. This graph indicates that a counter-clockwise rotating vortex forms near the bed, above which a weaker clockwise rotating vortex forms. A wall jet causes similar vortices to form in the 'developing flow region' immediately downstream of the nozzle (Launder & Rodi 1983). The vorticity in both the clockwise and counter-clockwise rotating vortices increases when the bed is rough.

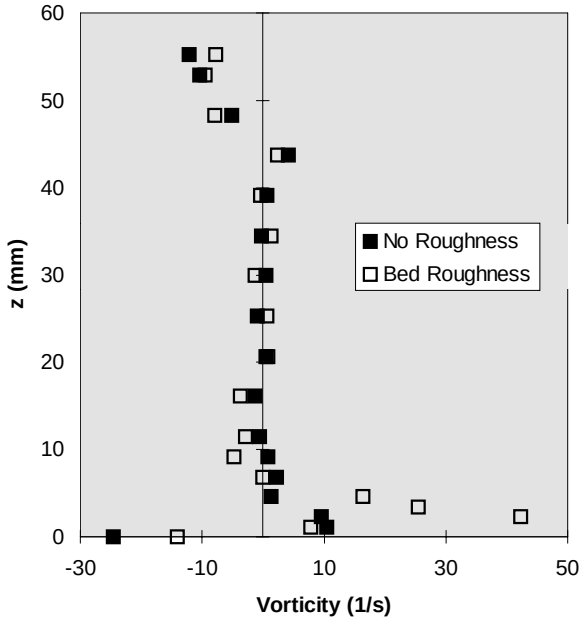

Figure 3.7 - Lateral Vorticity at Location #1 (Smooth Dowels; Rough Bed)

Above the bed region, the vorticity does not appear to be significantly influenced by bed roughness. For both roughness conditions, the vorticity is negligible in the intermediate region and negative in the free surface region.

3.2.3 Turbulence Intensity

The turbulence intensity profiles for the smooth-bed and rough-bed conditions differ most significantly at Location #1 (See Figure 3.8). At this location, the turbulence intensity is very high due to the wake turbulence in the vortex street. When the bed is rough, the turbulence intensity is considerably lower near the bed. This indicates that the bed roughness may influence the vortex shedding near the base of a dowel. Others have studied the vortex street near the base of a surface mounted cylinder. Dargahi (1989) found that the shedding frequency near the base of a cylinder is altered by the horseshoe vortex. Zavistoski (1994) found that the horseshoe vortex completely suppressed the vortex street near the bed.

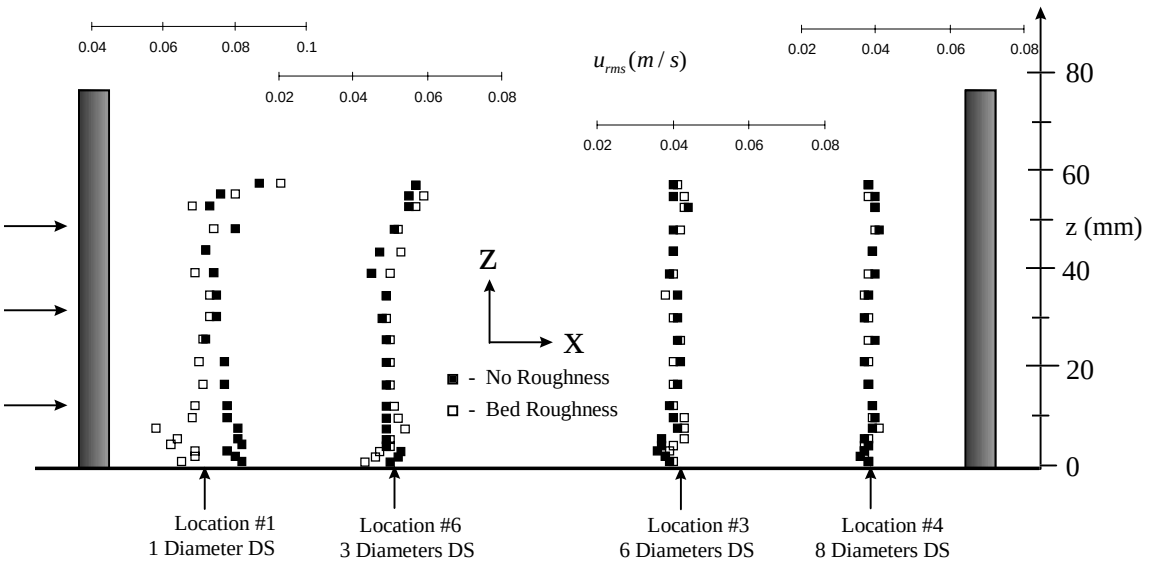

Figure 3.8 - Longitudinal Turbulence Intensity Profiles Taken In-Line with Dowels (Smooth Dowels; Rough Bed)

At the other three locations downstream of a dowel, the turbulence intensity profiles are similar for both roughness conditions. This is also true at the two locations in the unobstructed flow region (See Figure 3.9).

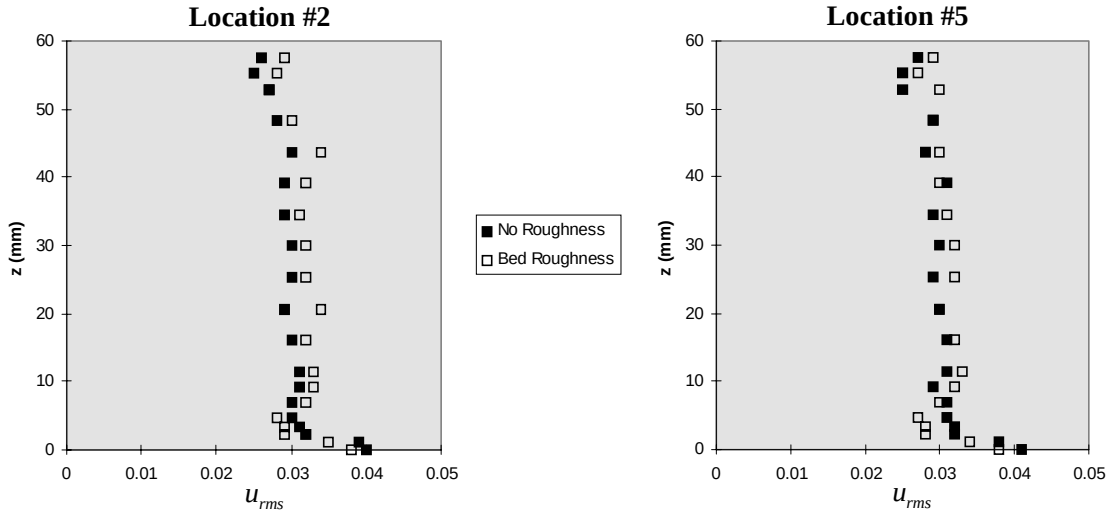

Figure 3.9 - Longitudinal Turbulence Intensity Profiles in the Unobstructed Flow Region (Smooth Dowels; Rough Bed)

3.3 Experiments with Bed Roughness and Dowels Roughness

Experiments were conducted with adhesive sandpaper wrapped around each dowel to simulate vegetative skin roughness. Fine and coarse sandpaper were tested to determine how different degrees of dowel roughness affect the flow characteristics. The bed was rough in each of these experiments.

The total flow resistance would be expected to increase when roughness is attached to the dowels. Higher overall resistance would cause the flow depth to increase and the depth-averaged velocity to decrease. An exception to this rule occurs when the dowel roughness triggers a turbulent boundary layer to form on the side of the dowels. The formation of a turbulent boundary layer shifts the separation point on the surface of the dowel downstream, causing the form drag on each individual dowel, as well as the total flow resistance, to decrease. According to Schlichting (1979), the minimum cylinder Reynolds number required to induce a turbulent boundary layer is approximately 30,000. As discussed in Section 3.1.2, the cylinder Reynolds number in each of the partially submerged experiments was approximately 1,000. Since the cylinder Reynolds number was not high enough to trigger the formation of a turbulent boundary layer, the total flow resistance increased when roughness was attached to the dowels. The results below support this discussion.

3.3.1 Longitudinal Velocity

Figures 3.10 and 3.11 show the longitudinal velocity profiles at the locations in-line with dowels and at locations in the unobstructed flow region. The vertical scale is normalized by the flow depth, Z, and the horizontal scale is normalized by the friction velocity, u_*. The friction velocity is given by Eqn. 1.3.

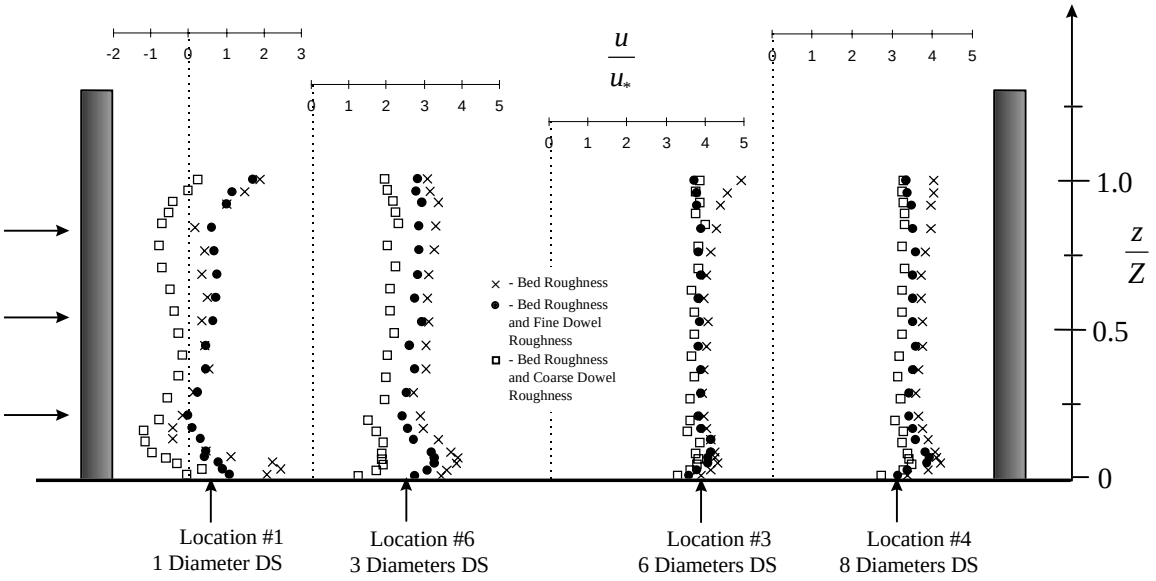

Figure 3.10 - Longitudinal Velocity Profiles for Different Roughness Conditions at Locations In-Line with Dowels

As seen in these figures, the depth averaged velocity decreases at each of the six measurement locations when the dowels are rough. As anticipated, the coarse dowel roughness lowers the mean velocity more than the fine dowel roughness. At Location #1, the mean velocity in the coarse roughness profile is negative throughout nearly the entire flow depth. This indicates that the pressure is low on the downstream side of a dowel, creating a strong suction in the upstream direction.

Dowel roughness also appears to influence the high-velocity spike. When roughness is attached to the dowels, the high-velocity spike becomes less pronounced.

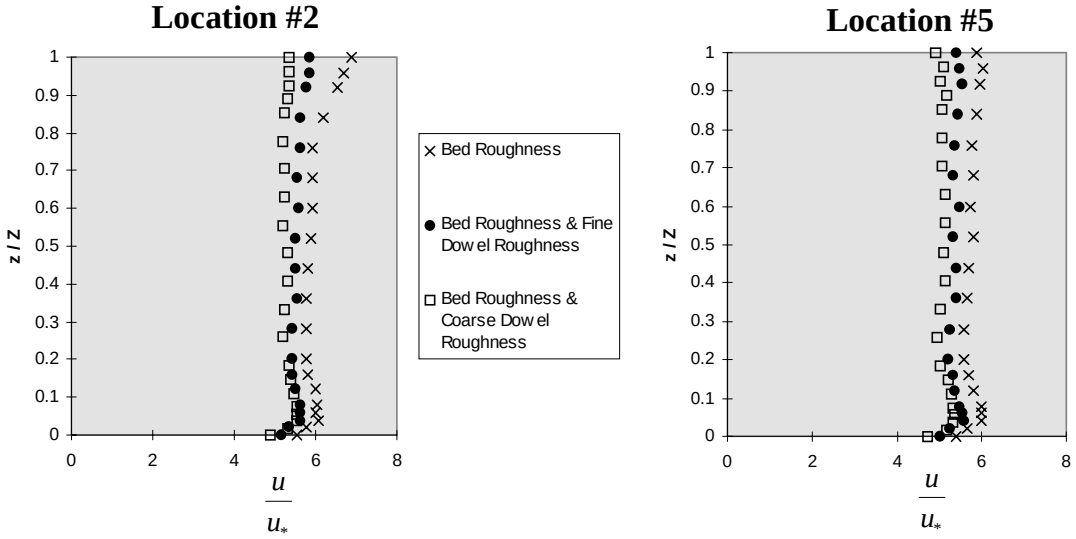

Figure 3.11 - Longitudinal Velocity Profiles for Different Roughness Conditions at Locations in the Unobstructed Flow Region

3.3.2 Turbulence Intensity

The longitudinal turbulence intensity tends to increase slightly when roughness is attached to the dowels. This is particularly evident at the two locations in the unobstructed flow region (See Figure 3.12). At locations in-line with dowels, the turbulence intensity profiles are fairly similar for the three roughness conditions shown (See Figure 3.13).

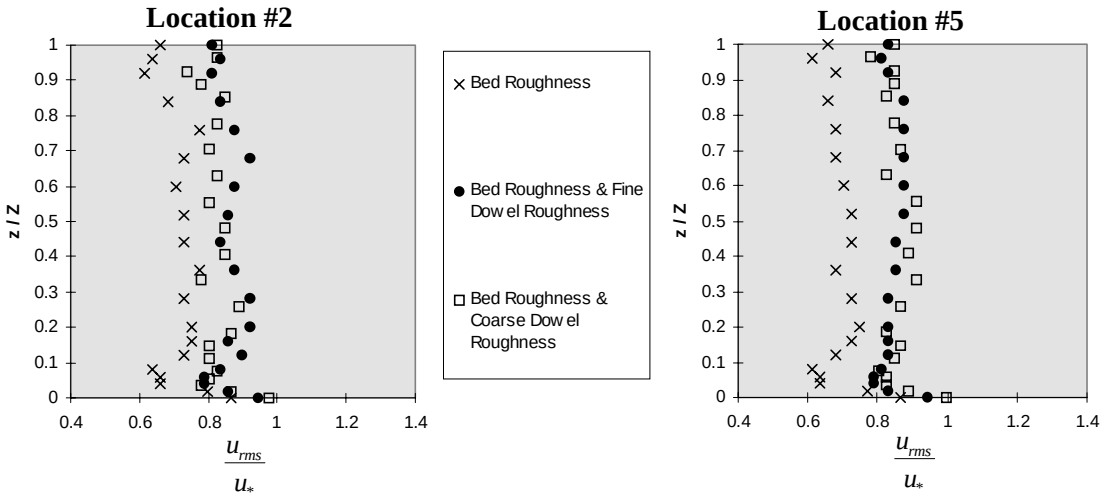

Figure 3.12 - Longitudinal Turbulence Profiles for Different Roughness Conditions at Locations in the Unobstructed Flow Region

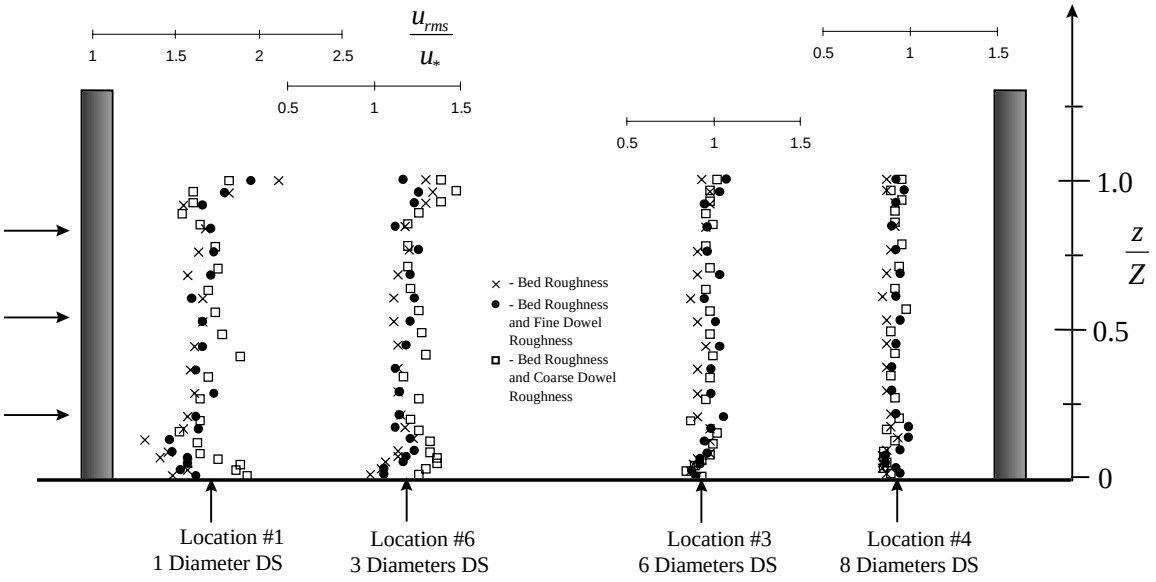

Figure 3.13 - Longitudinal Turbulence Intensity Profiles for Different Roughness Conditions at Locations In-Line with Dowels

3.3.3 Vertical Velocity

Vertical velocity profiles were taken with coarse roughness attached to the dowels. These measurements are compared in Figure 3.14 to the vertical velocity profiles when no roughness is present. Near the bed, both the upward flow on the downstream side of a dowel and the downward flow in upstream side of a dowel become more pronounced when the bed and dowels are rough. With roughness present, the upward velocity at Location #1 is magnified by nearly a factor of three. Also at Location #1, the downward motion near the free surface is more pronounced when there is roughness. Since no vertical velocity measurements are available for the smooth dowel/rough bed condition, it is unknown if these changes in vertical velocity are caused by the dowel roughness, the bed roughness or some combination of the two.

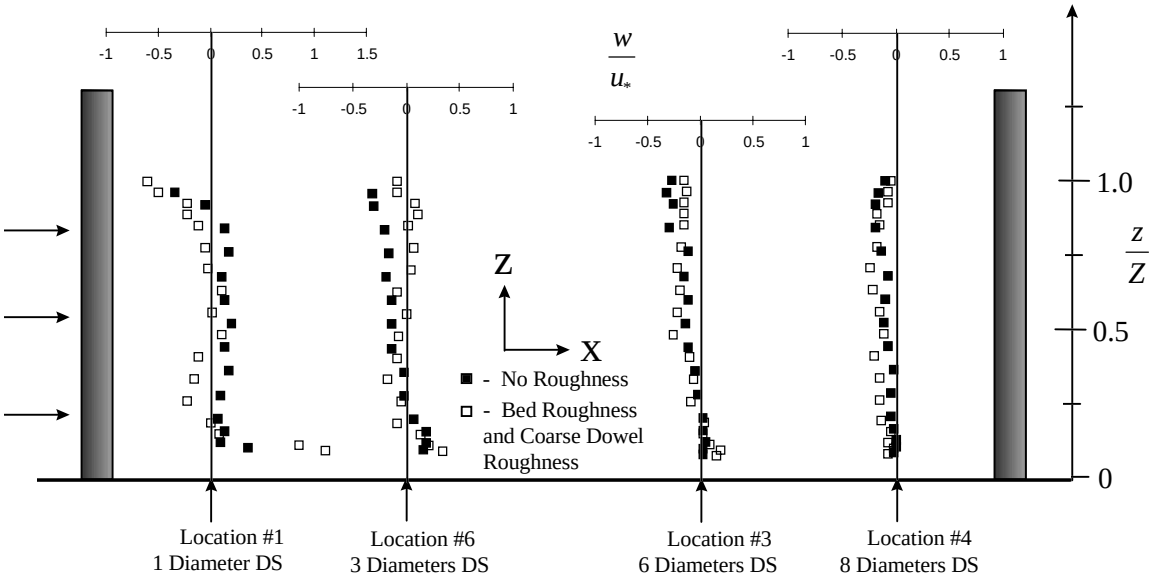

Figure 3.14 - Vertical Velocity Profiles for Different Roughness Conditions at Locations In-Line with Dowels

Chapter 4

Fully Submerged Flow

While turbulent flow above a rough wall has been studied extensively (See Raupach et al. 1991), much less research has been conducted to examine the flow characteristics within the roughness, particularly when the roughness elements occupy a significant portion of the flow depth. Although the flow within fully submerged vegetation is not spatially uniform, most studies have attempted to describe such flows by a single velocity or turbulence intensity profile. An example is the research by Tsujimoto et al (1992) in which measurements were only taken at the center of four model plants. Hodges (1997) is one of the few researchers to examine velocity and turbulence intensity profiles at various positions within fully submerged roughness.

Fully submerged experiments were initially conducted with the bed and the dowels smooth. Further experiments were then conducted with roughness attached to the bed and the dowels to determine how each would influence the mean velocity and turbulence characteristics. To achieve fully submerged conditions, the flow rate(Q) was increased to 0.0114 m^3/s. This is approximately 2.5 times larger than the flow rate used in the partially submerged experiments. The bed slope, dowel configuration and dowel density (λ) did not change from the partially submerged experiments. In each experiment, profiles were taken at the same six measurement locations shown in Figure 2.5.

4.1 Experiments with a Smooth Bed and Smooth Dowels

4.1.1 Flow Characteristics Above the Dowel Array

Figure 4.1 shows the longitudinal velocity profiles at the six measurement locations when the bed and the dowels are smooth. The dashed line represents the top of the dowels. All six profiles converge to a single logarithmic profile near the top of the dowels indicating that the dowels penetrate the fully turbulent logarithmic region.

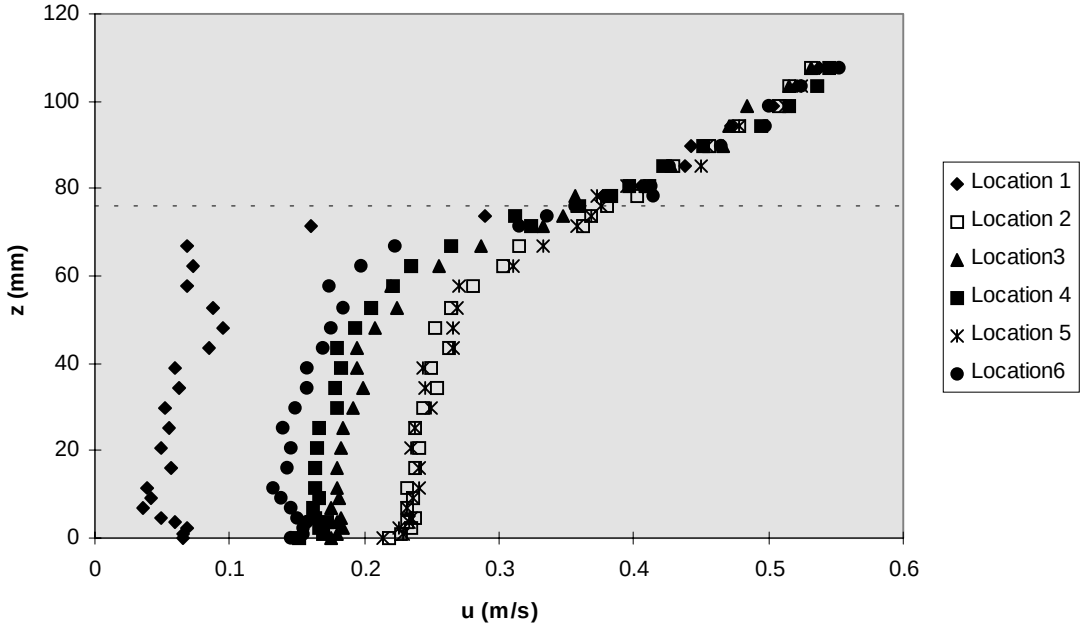

Figure 4.1 - Longitudinal Velocity Profiles in Fully Submerged Flow

The logarithmic profile extends from the top of the dowels to the free surface. The velocity profile above a rough wall can be described by:

$$\frac{u(z)}{u_*} = K^{-1} \ln \frac{(z - d_h)}{k_s} + 8.5 \qquad \text{(Eqn. 4.1)}$$

in which k = 0.4 = von Karman's constant, k_s = Nikuradse's equivalent sand grain roughness, and d_h = the zero-plane displacement height or simply the displaced height. The displaced height represents the distance above the bed at which the velocity in the logarithmic profile equals zero (See Figure 4.2).

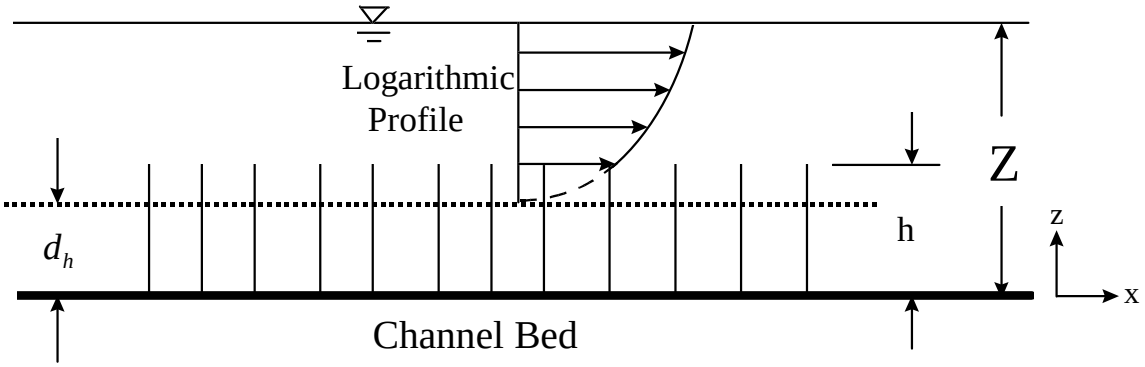

Figure 4.2 - Fully Turbulent Flow Above Rough Vegetation

Although many methods have been proposed to determine d_h, there is still no accepted standard. Nezu and Nakagawa (1993) suggest that the ratio of the displaced height to the roughness height, d_h/h, ranges from 0.7 to 0.85 for sand grain roughness. In other studies, Legg and Long (1975) measured $d_h/h=0.56$ in a wheat crop and Hicks et al.(1975) measured $d_h/h=0.89$ in a pine forest. The value of d_h is most commonly chosen so that the mean velocity profile above the roughness conforms to the logarithmic law (Raupach et al 1991). For flow over densely packed uniform sand, Nikuradse found that k_s equals the sand diameter. For different types of roughness, it is customary to adjust k_s so that the constant in Eqn.4.1 equals 8.5 (Sabersky et al. 1989).

All of the velocity data measured above the dowels closely fits the same logarithmic function, regardless of measurement location (See Figure 4.3). The dashed line in Figure 4.3 represents the top of the dowels. Below the top of the dowels, the velocity measurements diverge from a logarithmic profile. The d_h/h value for this experiment equals 0.82 which is the same value suggested by Grass (1971) for a fully rough boundary. The equivalent sand grain roughness was found to be 34mm or about 45% of the dowel height. Both the displaced height and the equivalent sand grain roughness were calculated by trial and error. Schlichting (1979) calculated k_s for staggered arrays of surface mounted spheres, hemispheres, and cones. He found that k_s/h can range from 0.12 to 3.6 depending on the density and the shape of the obstruction.

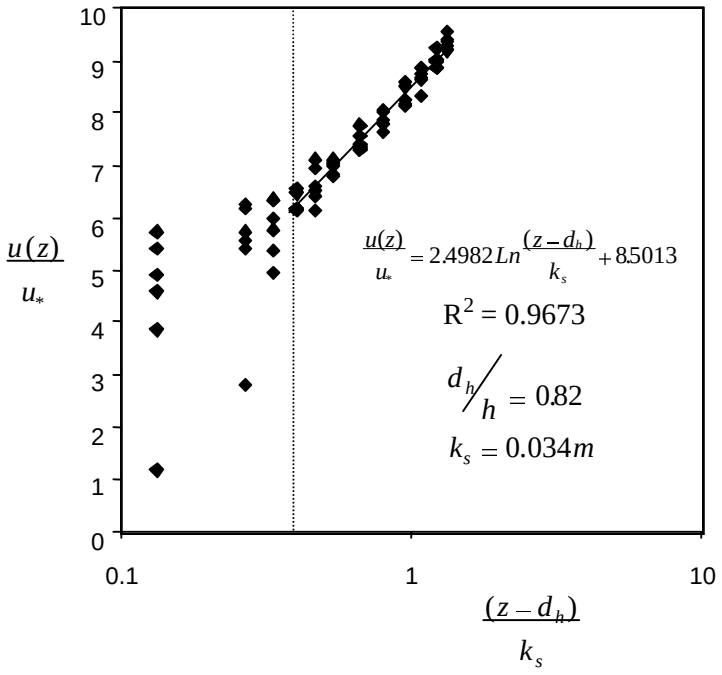

Figure 4.3 - Logarithmic Profile Above Fully Submerged Dowels

In meteorological applications, the logarithmic law is typically expressed as:

$$\frac{u(z)}{u_*} = \mathrm{K}^{-1} \ln \frac{z - d_h}{z_o} \qquad \text{(Eqn. 4.2)}$$

in which z_o = the roughness length. Both z_o and k_s are measures of the capacity of the rough surface to absorb momentum from the flow(Raupach et al. 1991). Through simple manipulation of Equations 4.1 & 4.2, it can be seen that the roughness length and the equivalent sand grain roughness are related by:

$$z_o = 0.03337 k_s \qquad \text{(Eqn. 4.3)}$$

Equation 4.3 is only valid when the boundary is fully rough.

Raupach et al. (1980) examined the relationship between roughness length and density for surfaces roughened by spheres, cubes, and cylinders. For three-dimensional roughness, the density (λ) can be defined as the frontal area of the roughness element per unit ground area that the element occupies (Raupach et al. 1991):

$$\lambda = \frac{dh}{s^2} \qquad \text{(Eqn. 4.4)}$$

where s = the mean separation between roughness elements. In both the partially and fully submerged experiments, the mean separation between roughness elements was 4.5 cm, which is the distance measured diagonally between the centers of two dowels. Raupach et al. (1991) found that the data for all three roughness shapes tends to follow the trendline shown in Figure 4.4. The normalized roughness length increases linearly with increased density to a point of maximum roughness at λ_{max}. Based on Eqn. 4.4, the mean separation between the dowels (7.62 cm tall; 0.635 cm diameter) would be 6.90 cm at λ_{max}. As the density increases above λ_{max}, each of the roughness elements become sheltered by upstream elements and a skimming flow eventually develops over the array (Shaw et al.1982). This *sheltering effect* causes the normalized roughness length to decrease when $\lambda > \lambda_m$.

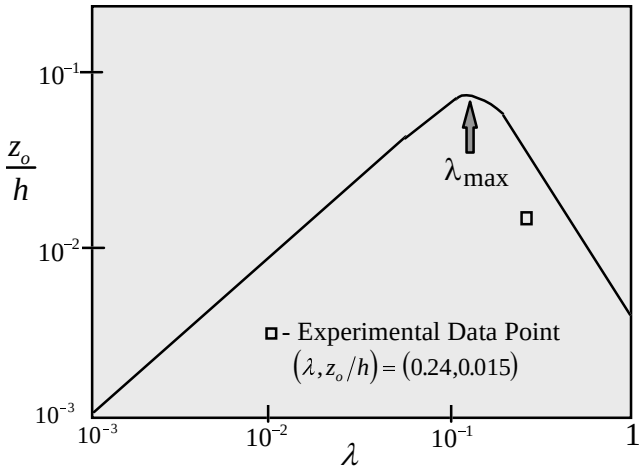

Figure 4.4 - Normalized Roughness Length as a Function of Roughness Density (Taken from Raupach et al. 1980)

The data point from the fully submerged experiments is plotted in Figure 4.4. The position of this point indicates that the density used in this study is higher than λ_{max}. Dirling (1973) suggested a similar method relating roughness density to the equivalent sand-grain roughness. He defined roughness density by:

$$\xi = \frac{s}{h}\left(\frac{A_s}{A_p}\right)^{4/3} \qquad \text{(Eqn. 4.5)}$$

where A_s = the roughness element frontal surface area, A_p = roughness element cross-sectional area, and s = roughness element spacing. This method for calculating density places more emphasis on the length scales of the individual roughness elements. The correlation curve suggested by Dirling (1973), seen in Figure 4.5, has a similar shape as the trendline suggested by Raupach et al. (1980). The data point from the fully submerged experiments falls almost directly on the correlation curve. This indicates that Dirling's method may be more appropriate when the diameter and height of the roughness elements vary considerably. Based on Eqn. 4.5, the mean separation between the dowels would be 6.40 cm at the point of maximum roughness. Both methods indicate that the array tested in the fully submerged experiments is dense enough that the dowels are mutually sheltered by one another.

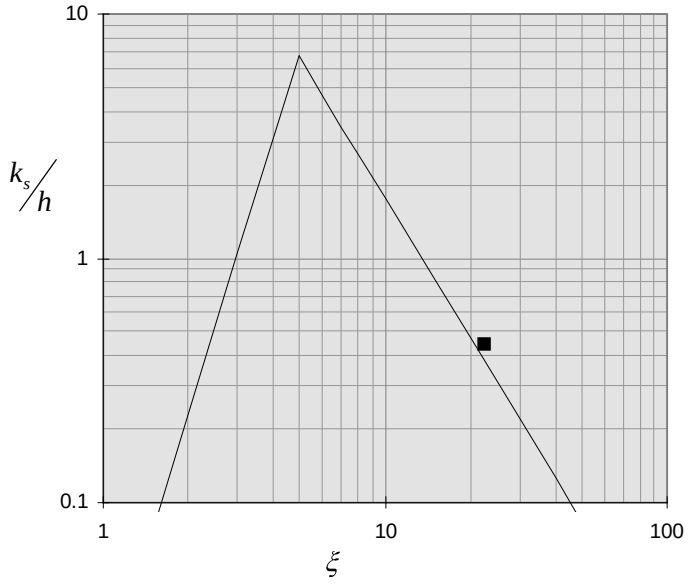

Recommended Correlation Curve:

$k_s/h = 0.0164\xi^{3.78}$ when $\xi \le 4.93$

$k_s/h = 139\xi^{-1.90}$ when $\xi \ge 4.93$

■ - Data Point $\left(\xi, k_s/h\right) = (22.34, 0.446)$

Figure 4.5 - Normalized Equivalent Sand-Grain Roughness as a Function of Density (Taken from Dirling, 1973)

Figure 4.6 shows that the longitudinal and vertical RMS profiles also tend to converge near the top of the dowels under fully submerged conditions. The longitudinal turbulence intensity is about 50% higher than the vertical turbulence intensity at z=h. A collection of measurements taken at the top of vegetation canopies supports this observation(Raupach et al 1991). Both the longitudinal and vertical components of turbulence intensity appear to decrease linearly between the top of the dowels and the free surface. Laboratory data from Ikeda et al.(1996) in flexible vegetation and Tsujimoto et al.(1992) in rigid vegetation also suggests a linear decrease in turbulence intensity above the vegetation layer.

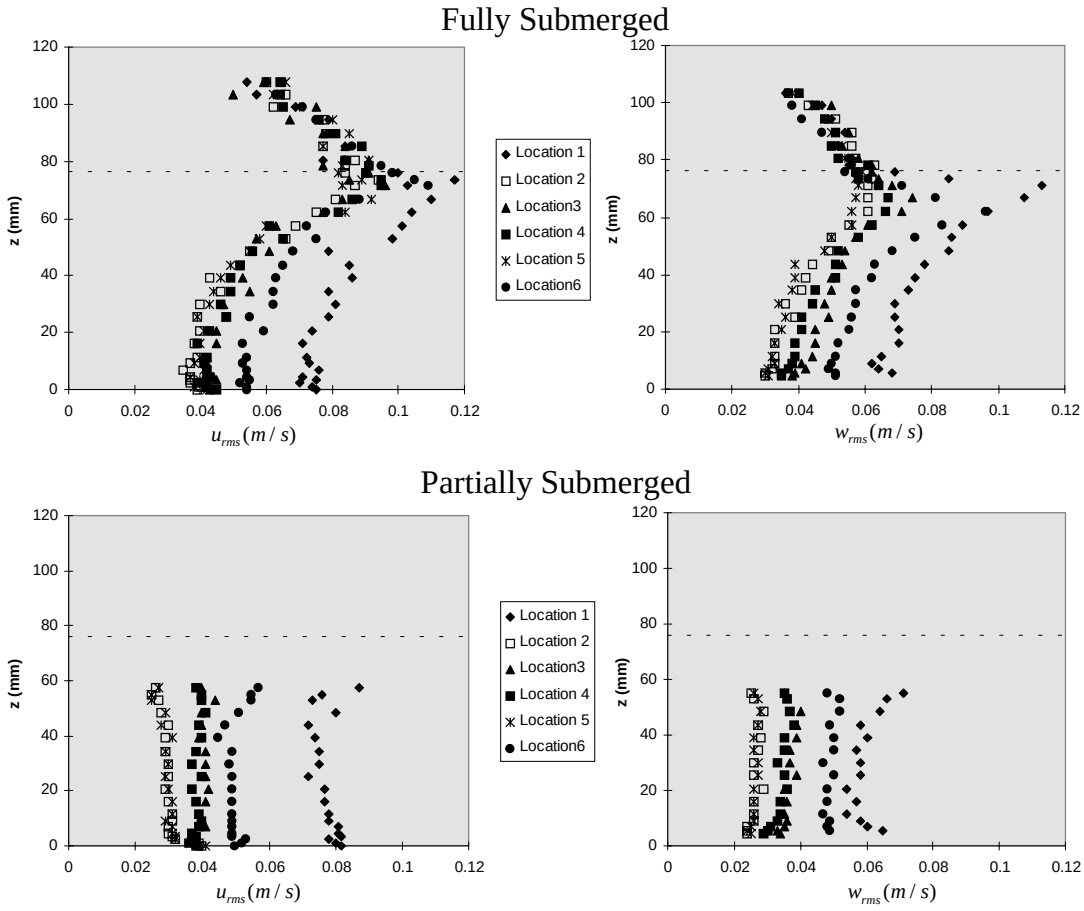

Figure 4.6 - Longitudinal and Vertical Turbulence Intensities

The flow above vegetation is similar to open channel flow over a rough boundary. As seen in Figure 4.3, the mean velocity data between the top of the dowels and the free surface closely fits the rough-wall logarithmic profile(Eqn. 4.1). Although shear stress was not measured in this study, researchers have found that the shear stress distribution above the vegetation layer is similar to the linear stress distribution found in open channel flow (See Figure 1.13). Ikeda et al. (1996) and Tsujimoto et al. (1992) both conclude that the shear stress increases linearly from zero at the free surface to its maximum value at the top of the vegetation layer.

4.1.2 Flow Characteristics Within the Dowel Array

Within the dowel array, many of the same trends were observed in both partially submerged and fully submerged experiments. The mean velocity and turbulence intensity profiles vary significantly at the different measurement locations (See Figures 4.1 & 4.6). The two components of turbulence intensity are much higher and the longitudinal velocity is much lower directly behind a dowel (Location#1). With increased distance downstream of a dowel, the turbulence intensities decrease and the longitudinal velocity

increases. The unobstructed flow region between dowels(Locations #2&#5) is characterized by the highest velocity and the lowest turbulence intensity.

Under fully submerged conditions, the interaction between the faster flow above the array and the slower flow within the array creates an inflection point in the mean velocity profile just below z=h. Figure 4.7 shows the longitudinal velocity profiles at the four measurement locations in-line with dowels. The horizontal scale is greatly exaggerated to show more detail. With increased distance downstream of a dowel, the inflection point is not as sharp and the flow near the top of the dowels becomes less sheared. As observed by Hodges (1997), the inflection point also moves deeper within the array with increased distance downstream of a dowel. In the vicinity of the bed, the high velocity spike was observed under fully submerged conditions indicating that a horseshoe vortex forms around each dowel. The high velocity spike appears to be less pronounced in fully submerged flow than in partially submerged flow (See Figure 3.1).

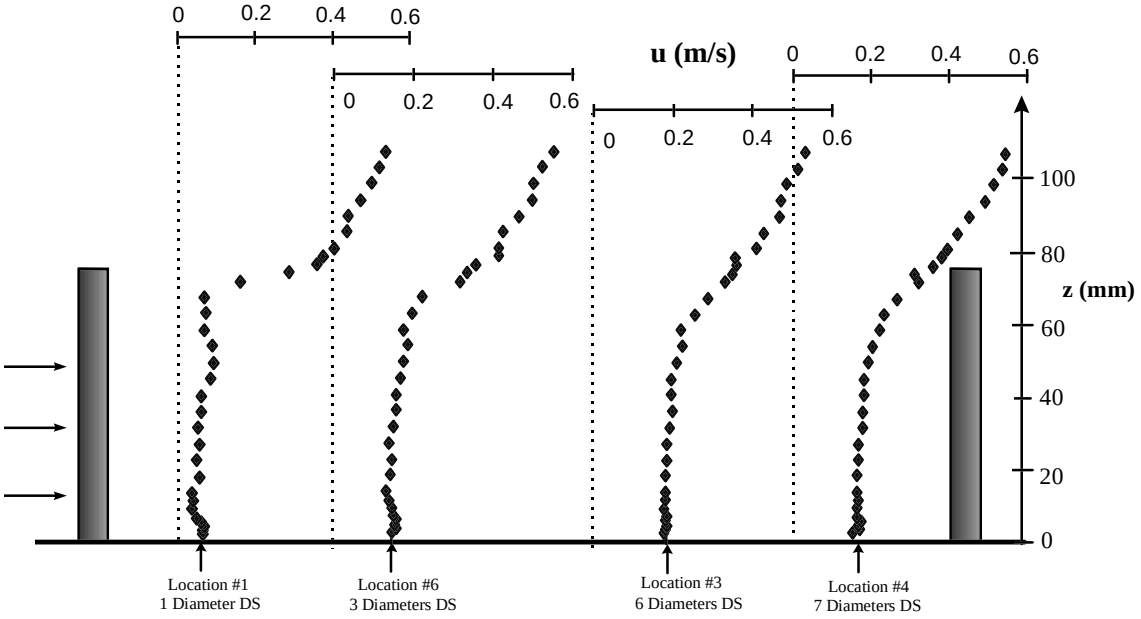

Figure 4.7 - Fully Submerged Longitudinal Velocity Profiles at Locations In-Line with Dowels

The highly sheared region near the top of the dowels appears to be where much of the turbulence is generated. Shear flows are a common source of energy for turbulent velocity fluctuations (Tennekes & Lumley 1972). The maximum u_{rms} and w_{rms} values at most of the measurement locations occur approximately where the shear $\left(\partial u/\partial z\right)$ is highest (See Figure 4.6). At Location #1, immediately downstream of a dowel, the turbulence intensities near z=h are higher because the flow is more sheared.

Recent studies indicate that instabilities cause the shear layer to roll up into discrete organized vortices (Ikeda et al. 1996, Gao et al. 1989). This phenomenon is characteristic of the plane mixing layer that develops between two co-flowing streams with different velocities (Raupach et al. 1996, Ho et al. 1984). Gao et al. (1989) found that the organized vortices at the top of a forest canopy consist of a weak ejection

$(u' < 0, w' > 0)$ from the top of the canopy followed by a strong sweep $(u' > 0, w' < 0)$ to the interior of the canopy. To properly quantify sweep and ejection motions, simultaneous u and w velocity measurements should be taken to determine the instantaneous Reynolds stress. Since this is not possible with a one-dimensional instrument, the skew of the u and w histograms were analyzed separately to detect asymmetry in the probability density functions(p.d.f.) of the turbulent fluctuations. The skew, which is used to detect bursting events, is given by the following:

$$\text{Skew u} = \left(\frac{u'^3}{u_{rms}^2} \right) \qquad \text{(Eqn. 4.6)}$$

Figure 4.8 shows the longitudinal and vertical skew profiles at measurement locations #2-6. The longitudinal skew profiles are virtually a mirror image of the vertical skew profiles. Below z=h, skew u is positive and skew w is negative indicating that the momentum transfer is dominated by sweeps. Above z=h, skew u is negative and skew w is positive indicating that the momentum transfer is dominated by ejections. The sweeps tend to have a higher intensity than the ejections as observed by Gao et al. (1989).

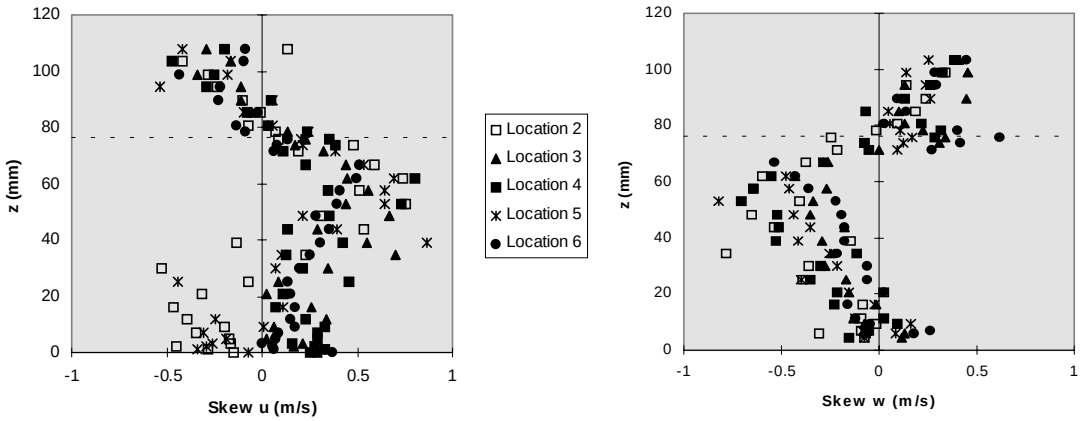

Figure 4.8 - Fully Submerged Longitudinal and Vertical Skew Profiles

Skewed histograms are typically found in flows with strong gradients of turbulence intensity; they occur where energy is transferred from regions of high intensity to regions of lower intensity (Townsend 1976). The ejection and sweep motions in Figure 4.8 indicate that energy is transferred upward and downward from the shear layer to regions of lower turbulence intensity. The downward sweeps increase the mean velocity and the turbulence intensities well below the top of the dowels. Gao et al. (1989) found that the organized vortices that develop in the shear layer are responsible for more than 75% of the momentum fluxes within a vegetation canopy.

The region below $z \cong 25mm$ does not appear to be significantly influenced by the shear flow near the top of the dowels. In this region, the u, u_{rms}, and w_{rms} profiles have a similar shape as the partially submerged profiles seen in Figures 3.1 & 3.2.

4.1.3 Vertical Velocity

Mean vertical velocity profiles were also taken under fully submerged conditions at the six measurement locations. Figure 4.9 shows the vertical velocity profiles at the four locations in-line with dowels. Unlike the longitudinal velocity, the vertical velocity above the dowels varies at the different measurement locations. In the surface flow region, there is upward motion as the fluid approaches a dowel and a strong downward motion on the lee-side of a dowel. Goncharov (1962) suggests that the streamlines are concave up as they approach a roughness element and then become concave down as they pass over the top of the roughness element. A similar flow pattern at the top of roughness elements has also been documented by other sources (Chow 1959, Vogel 1994).

The flow separates from the top of each roughness element (Chow 1959). Lateral vortices form in the separation region and are swept downward behind each roughness element (Goncharov 1962). A similar phenomenon has been observed behind ripples and dunes in streams (Vanoni 1977). The lateral vortices only appear to penetrate the upper 15mm of the array and are almost completely dissipated six diameters downstream of the dowel. The downward flow behind a dowel probably causes the inflection point in the longitudinal velocity profile to move deeper into the array with distance downstream of a dowel.

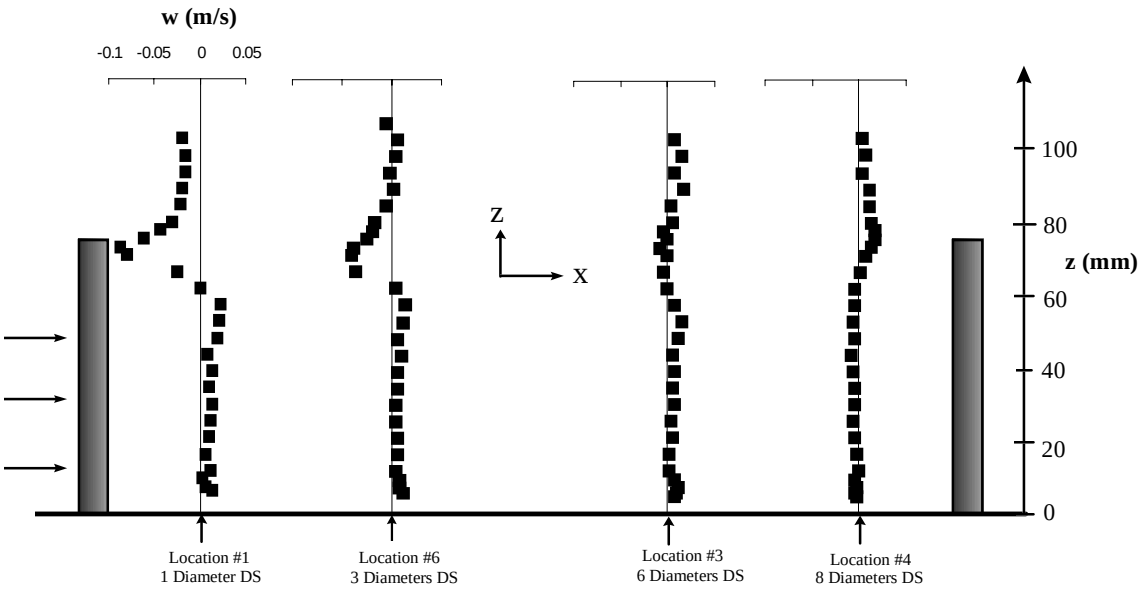

Figure 4.9 - Fully Submerged Vertical Velocity Profiles at Locations In-Line with Dowels

Within the dowel array, upward flow occurs on the downstream side of a dowel and a weak downward flow occurs on the upstream side of a dowel. A similar upward flow was also observed directly behind a dowel in the partially submerged experiments (See Figure 3.3). There is a slight tendency for the vertical velocity to increase in the vicinity of the bed at locations directly behind a dowel. The same phenomenon was

observed in partially submerged flow and is probably caused by vertical expansion of the high velocity spike (See Section 3.1.3). Since no vertical velocity measurements could be taken below z=5mm, it is unknown if the vertical velocity continues to increase closer to the bed.

SURFER (Surface Mapping Software) was used to generate the three images shown in Figure 4.10. The dashed line represents the zero velocity contour and the horizontal line represents the top of the dowels. The plan view below each image shows the location of the cross-section. Darker regions indicate downward motion and lighter regions indicate upward motion. All three images indicate that the downward thrust near the top of a dowel is very localized. The maximum vertical velocity in this region is about one-third of the longitudinal velocity. On either side of the downward thrust, upward flow occurs in the unobstructed flow region (See Images a & b in Figure 4.10).

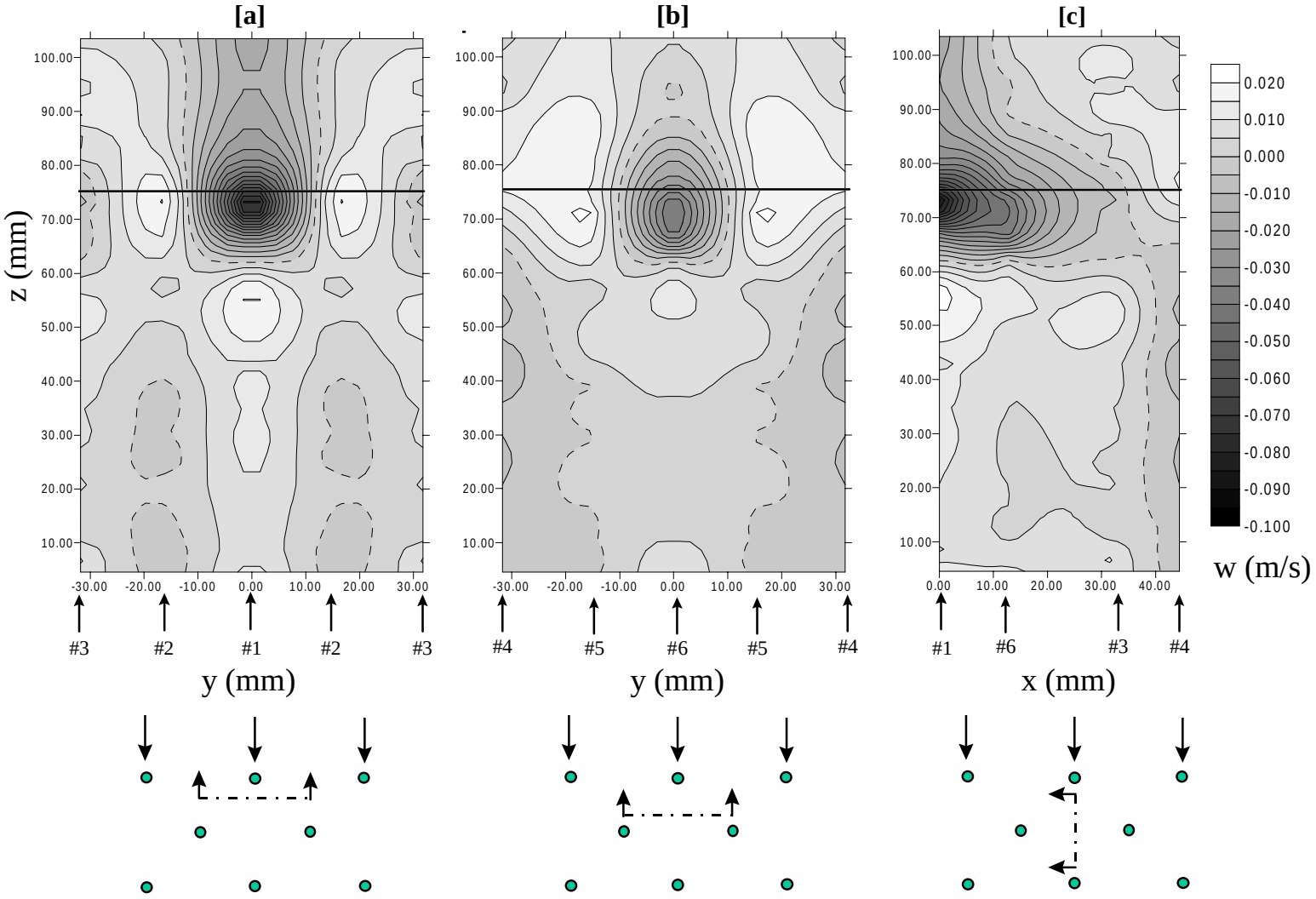

Figure 4.10 - Shaded Contour Images of Vertical Velocity in Fully Submerged Flow

4.1.4 Conveyance

The following analysis demonstrates how an array of obstructions affects the conveyance properties of a channel. The measured discharge in fully submerged flow was compared to the theoretical discharge when the flow depth is the same but no dowels are present. For both cases, the portion of the total discharge conveyed above z=h=0.0762m and the portion conveyed below z=h=0.0762m was calculated. Conveyance, (K), is a measure of the carrying capacity of a channel(Bedient and Huber 1992):

$$K = \frac{A_f U}{S^{1/2}} \qquad \text{(Eqn. 4.7)}$$

where A_f is the flow area and U is the bulk velocity in the cross-section. Since the channel slope remains constant at 0.003m/m, the conveyance in this analysis is proportional to the bulk discharge. The terms conveyance and bulk discharge will be used interchangeably in this section.

The bulk discharge was initially calculated for the fully submerged condition. All of the mean longitudinal velocity data from the six measurement locations was analyzed by SURFER to determine the bulk velocities above and below z=h. Above the dowels, the flow area was computed by A_f=(Z-h)/b where Z= 0.1141m = the flow depth and b = 0.3048m = the channel width. An effective flow area was computed within the array by assuming that the fraction of the cross-sectional area occupied by the dowels is equal to the fraction of the volume occupied by the dowels. Since the dowels make up only 1.47% of the total volume below z=h, the effective area was calculated by A_f=(1-0.0147)hb.

The theoretical discharge was then computed for the no-dowel condition, assuming that the flow depth (Z=0.1141m) does not change. Since no velocity measurements were taken for this flow condition, a velocity profile was developed using the equation for flow over a smooth wall (Sabersky et al. 1989):

$$\frac{u(z)}{u_*} = k^{-1} \ln \frac{u_* z}{\nu} + 5.5 \qquad \text{(Eqn. 4.8)}$$

where ν = the kinematic viscosity. Once again, SURFER was used to determine the bulk velocity in the two regions above and below z=h=0.0762m. The same effective flow areas were used for both the fully-submerged and the no-dowel conditions to ensure that the total flow area remained constant.

Figure 4.11 compares the conveyance for the fully-submerged and the no-dowel conditions. Below z=h, the conveyance for the two flow conditions differs most dramatically; the bulk discharge in this region is approximately 4.5 times higher when there are no dowels. For the entire flow area, the total conveyance increases by almost a factor of 3.5 when there are no dowels in the channel. This demonstrates that vegetation can significantly decrease the conveyance within a channel, even if the volume it

occupies is insignificant when compared to the total flow volume. Partially submerged flow was analyzed in a similar manner and the results are included in Figure 4.11.

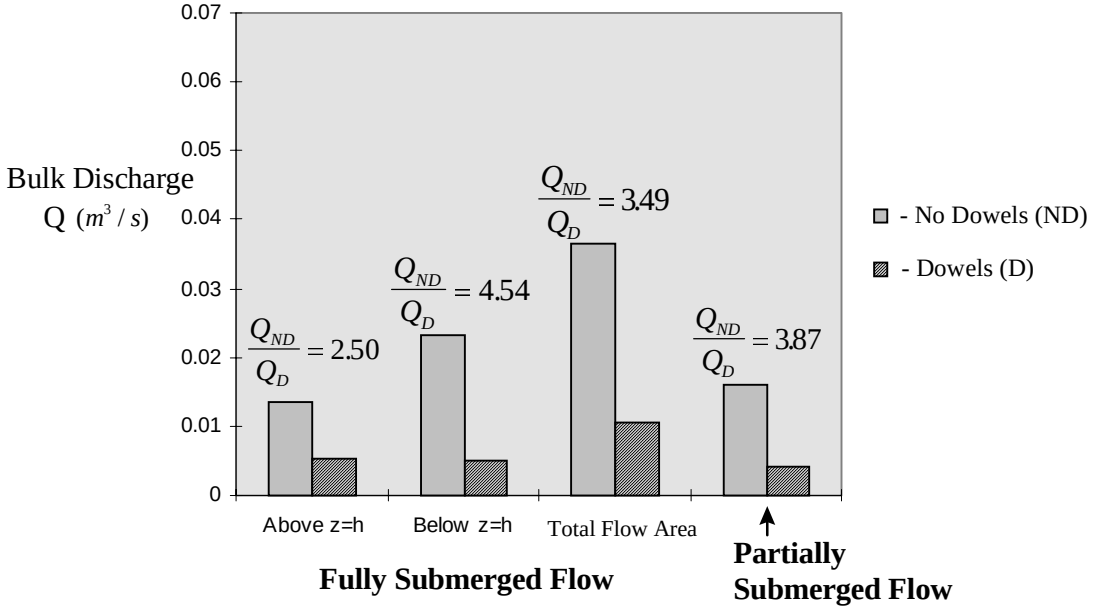

Figure 4.11 - Conveyance Properties of a Channel Containing an Array of Dowels

The bulk velocity in the partially submerged experiment was 0.2122 m/s while the bulk velocity below z=h in the fully submerged experiment was 0.2231 m/s. These two values are very similar considering that the total discharge in these experiments differed by a factor of 2.5. Hodges (1997) also found that the depth averaged velocity within a similar array of cylinders did not change significantly when the flow rate was doubled. This supports the results presented by Raupach and Thom (1981) in Figure 1.3. The slightly higher bulk velocity in fully submerged flow can be attributed primarily to the faster flow near the top of the dowels. As seen in Figure 4.12, the partially and fully submerged profiles have approximately the same magnitude within the lower portion of the array. This suggests that the conveyance within the array, and particularly in the lower portion of the array, may be somewhat independent of the total flow rate, assuming that the channel slope and dowel configuration remain constant.

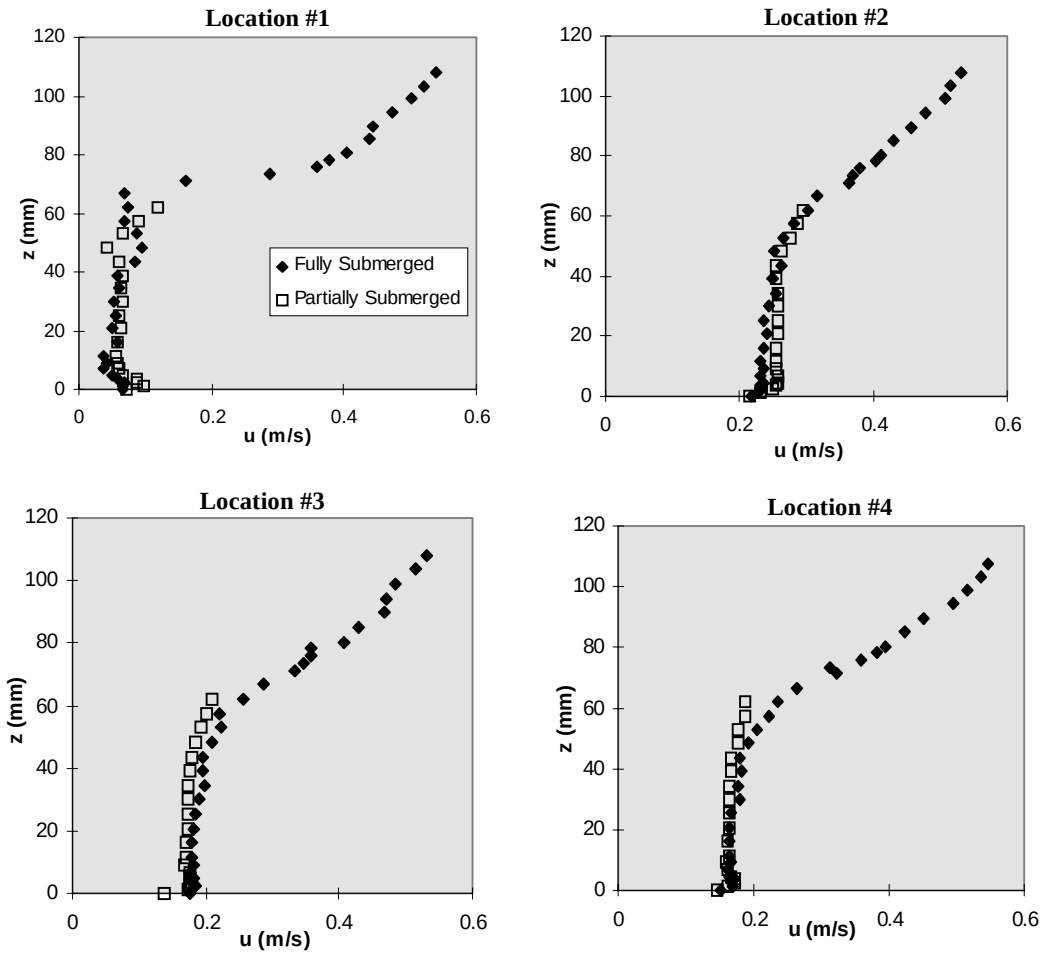

Figure 4.12 - Comparison Between Partially and Fully Submerged Velocity Profiles when the Bed and Dowels are Smooth

4.2 Experiment with Bed Roughness and Smooth Dowels

An experiment was conducted to determine how bed roughness influences the flow characteristics under fully submerged conditions. In this experiment, longitudinal velocity and turbulence intensity profiles were developed at the six measurement locations. Measurements were not taken in the vertical direction for this roughness configuration.

4.2.1 Longitudinal Velocity

Figure 4.13 shows a comparison between the smooth-bed and the rough-bed longitudinal velocity profiles at the four locations in-line with dowels. The smooth-bed

and the rough-bed profiles only differ significantly at Location #1, one-diameter downstream of a dowel. At this location, the high-velocity spike near the bed has a greater magnitude when the bed is rough. In addition, the longitudinal velocity in the secondary minimum is considerably lower. Similar observations were made in partially submerged flow when roughness was added to the bed (See Figure 3.5).

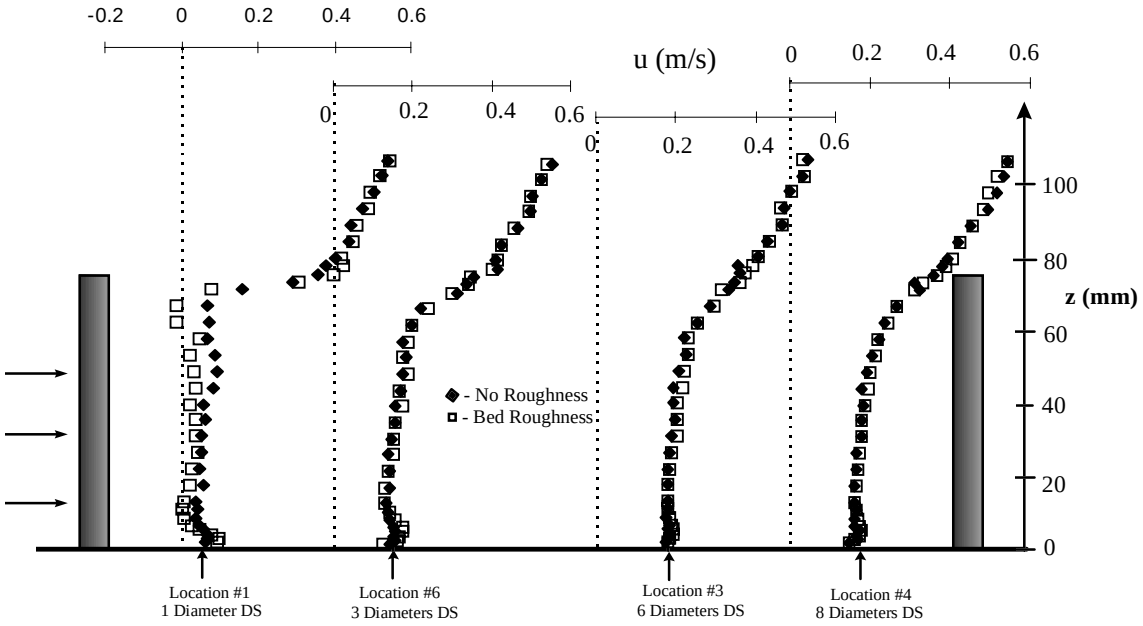

Figure 4.13 - Fully Submerged Longitudinal Velocity Profiles at Locations In-Line with Dowels (Smooth Dowels; Rough Bed)

The smooth-bed and rough-bed longitudinal velocity profiles are fairly similar at locations #3, #4, & #6 downstream of a dowel and at locations #2 & #5 in the unobstructed flow region (See Figure 4.14). There is, however, a tendency for the velocity to be slightly higher near the bed when the bed is rough. A similar phenomenon was also observed in the partially submerged experiments over a rough bed (See Figures 3.5 & 3.6). This indicates that the downward momentum transport caused by the horseshoe vortices may increase the mean velocity near the bed.

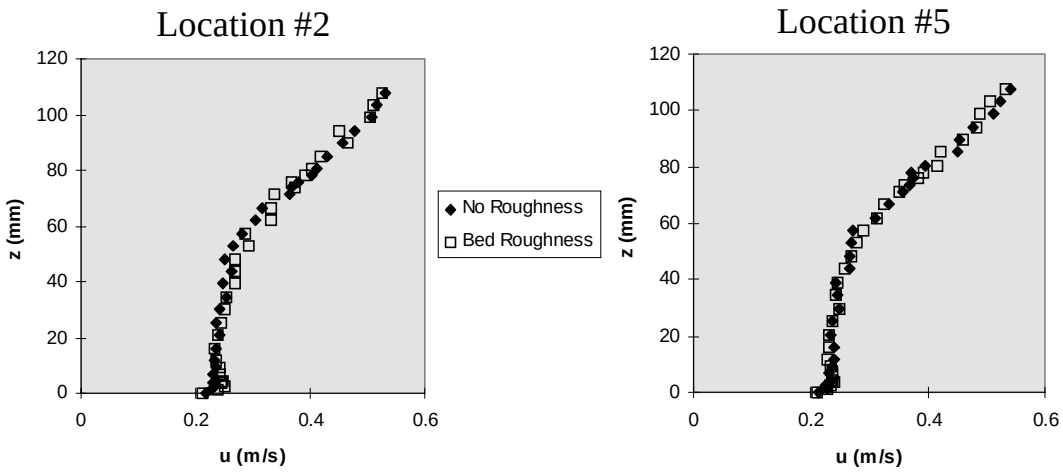

Figure 4.14 - Fully Submerged Longitudinal Velocity Profiles in the Unobstructed Flow Region (Smooth Dowels; Rough Bed)

4.2.2 Vorticity

Figure 4.15 shows the smooth-bed and the rough-bed lateral vorticity profiles at Location #1. The lateral vorticity is calculated by Eqn. 3.2, assuming that $\partial w/\partial x \cong 0$. At Location #1, there is counter-clockwise rotation just above the bed and clockwise rotation near the top of the dowels. When the bed is rough, the vorticity is magnified in each of these regions.

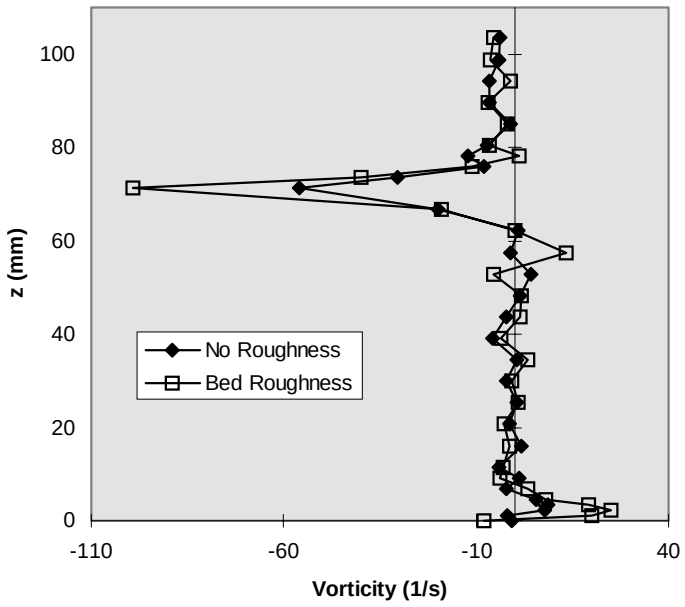

Figure 4.15 - Lateral Vorticity at Measurement Location #1 in Fully Submerged Flow

With the assumption that $\partial w/\partial x \cong 0$, the lateral vorticity is a measure of the shear in the longitudinal velocity profile. As seen in Figure 4.13, the velocity profile at Location #1 is more sheared near the top of the dowels when the bed is rough, causing the vorticity to be higher.

4.2.3 Turbulence Intensity

The rough-bed and smooth-bed turbulence intensity profiles at Locations #1 & #2 are shown in Figure 4.16. As discussed previously, regions that are more sheared tend to generate more turbulence. Near the top of the dowels, the turbulence intensity at Location #1 tends to be higher when the bed is rough because the flow is more sheared. The turbulence intensity profiles shown at location #2 are representative of the profiles at measurement locations #2-#6; the turbulence intensity does not change significantly at these locations when roughness is attached to the bed.

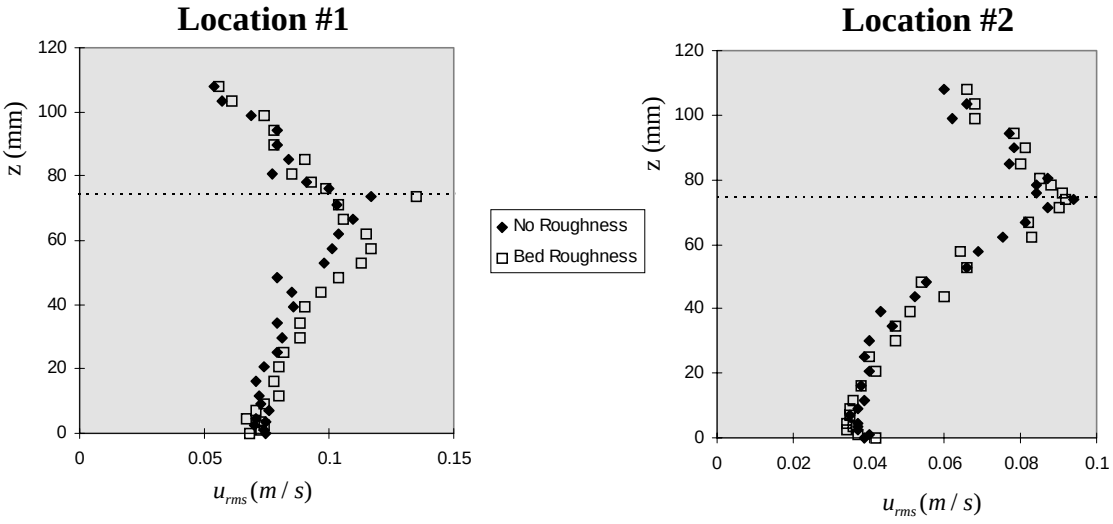

Figure 4.16 - Fully Submerged Turbulence Intensity Profiles (Smooth Dowels; Rough Bed)

4.3 Experiments with Bed Roughness and Dowel Roughness

Fully submerged experiments were conducted with sandpaper attached to the dowels to simulate vegetative skin roughness. The slope, discharge, and dowel density did not change from the previous fully submerged experiments. The two grades of sandpaper that were tested will be referred to throughout this section as fine and coarse

dowel roughness. When fine roughness was attached to the dowels, measurements were only taken in the longitudinal direction; measurements were taken in both the longitudinal and vertical directions when coarse roughness was attached to the dowels. In each of the following experiments, the bed was rough.

4.3.1 Longitudinal Velocity

In the fully submerged experiments, much like the partially submerged experiments, the cylinder Reynolds number was not high enough to trigger the formation of a turbulent boundary layer on the side of the dowels. Therefore, the total flow resistance increased slightly when roughness was attached to the dowels.

Figure 4.17 shows the longitudinal velocity profiles in the unobstructed flow region and Figure 4.18 shows the velocity profiles in-line with dowels. As expected, the mean velocity tends to be slightly lower when the dowels are rough. This is most apparent at Location #1, directly behind a dowel.

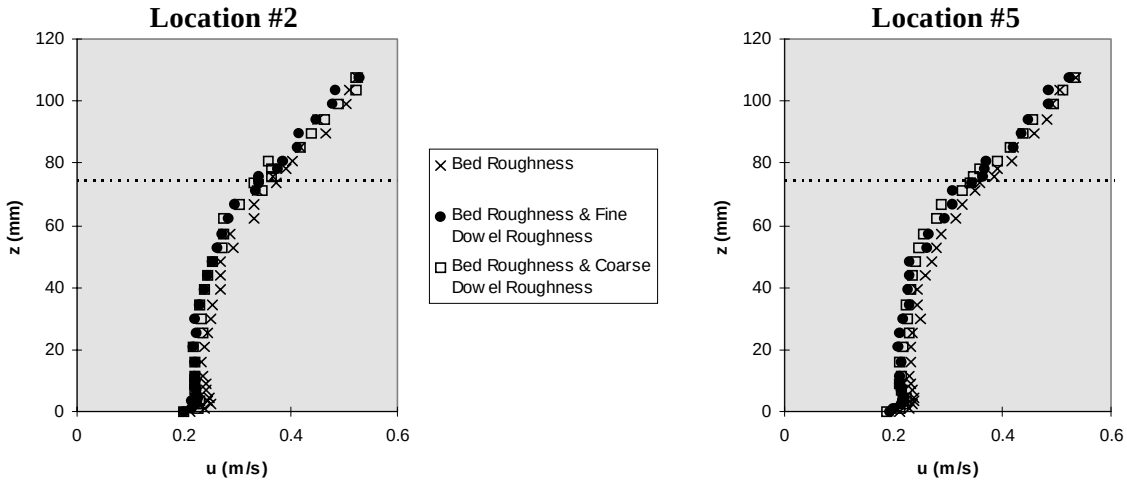

Figure 4.17 - Fully Submerged Longitudinal Velocity Profiles in the Unobstructed Flow Region for Different Roughness Conditions

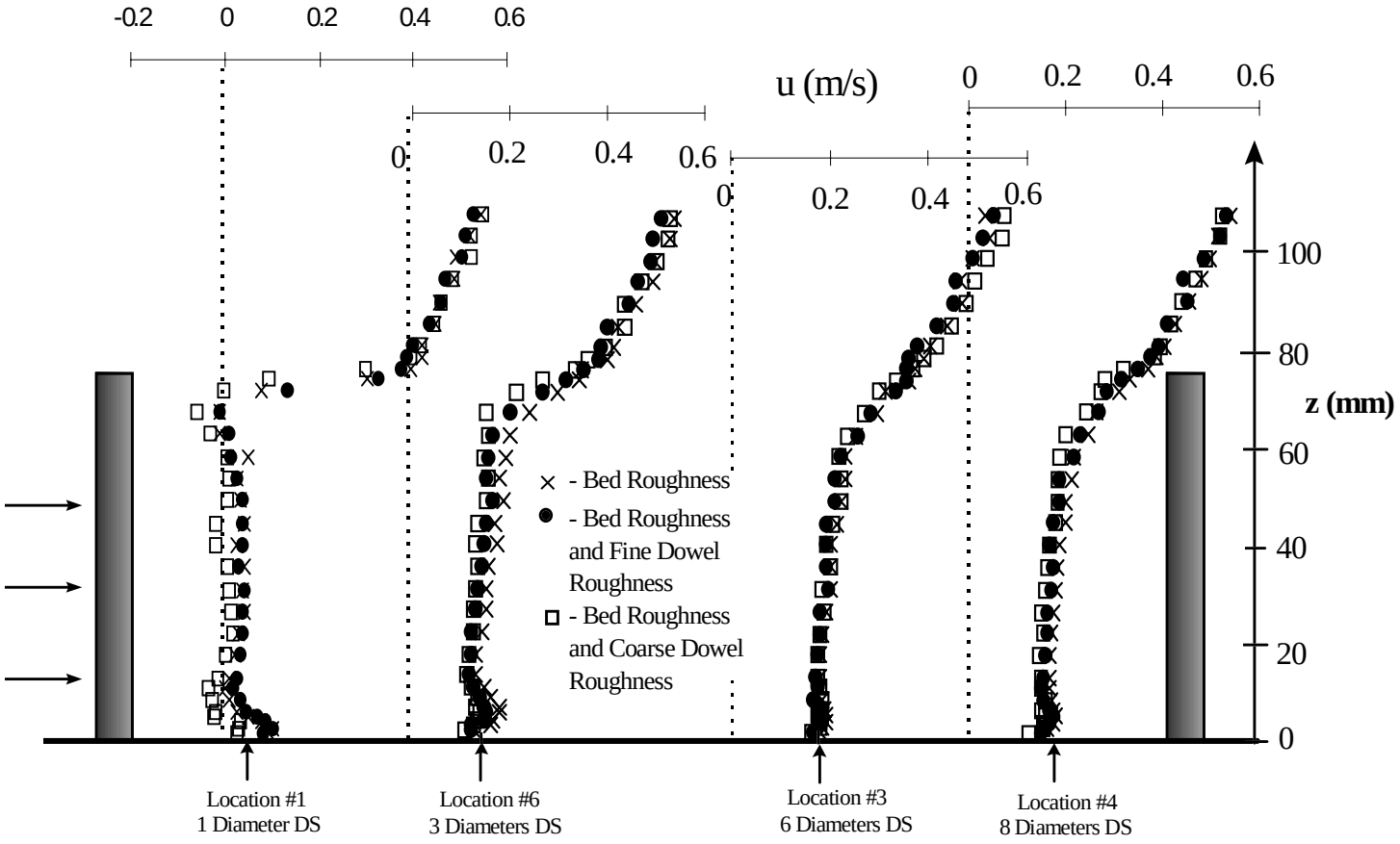

Figure 4.18 - Fully Submerged Longitudinal Velocity Profiles at Locations In-Line with Dowels for Different Roughness Conditions

4.3.2 Turbulence Intensity

Figures 4.19 & 4.20 show the longitudinal turbulence intensity profiles when roughness is attached to the dowels. The dowel roughness does not significantly influence the turbulence intensity at any of the measurement locations. This would be expected considering that the boundary layer separation on the side of the dowels was not altered by the dowel roughness.

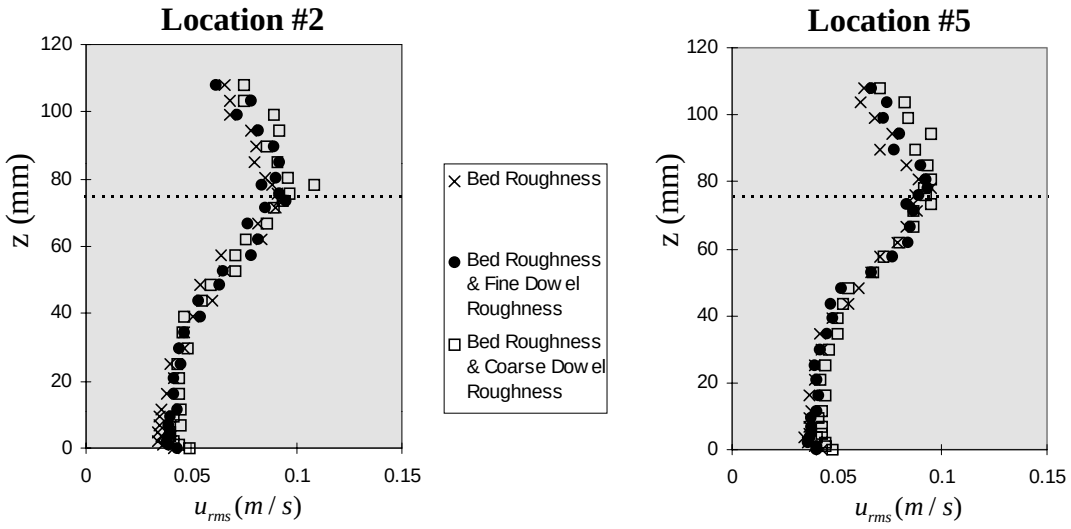

Figure 4.19 - Fully Submerged Longitudinal Turbulence Intensity Profiles at Locations in the Unobstructed Flow Region for Different Roughness Conditions

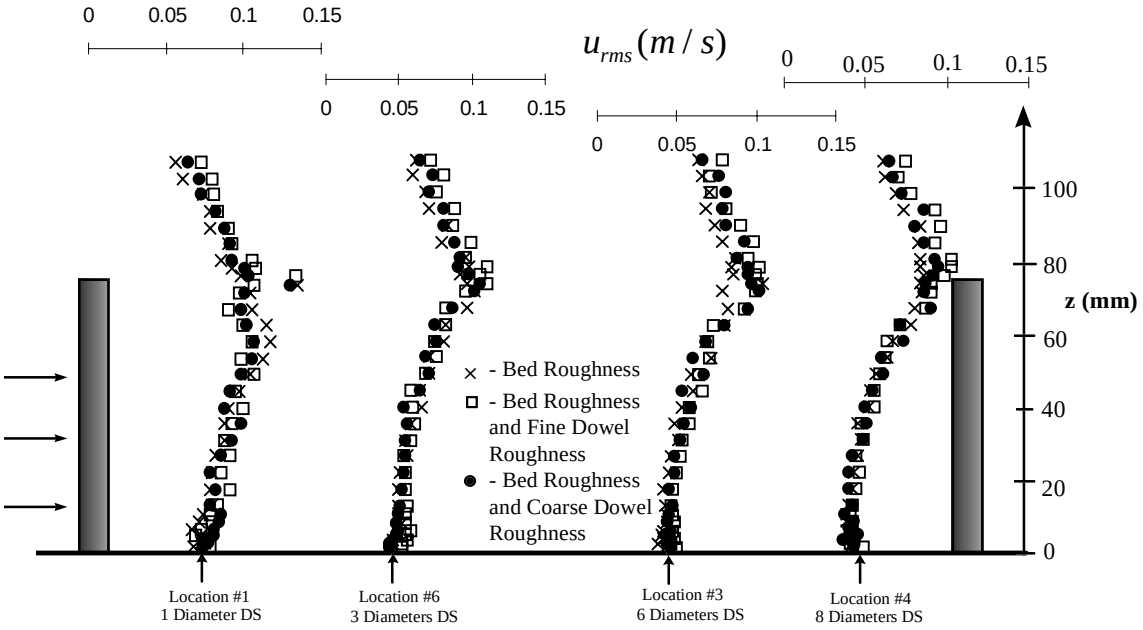

Figure 4.20 - Fully Submerged Longitudinal Turbulence Intensity Profiles at Locations In-Line with Dowels for Different Roughness Conditions

4.3.3 Vertical Velocity

Vertical velocity was only measured when coarse roughness was attached to the dowels. Figure 4.21 shows the vertical velocity profiles in the unobstructed flow region for the two roughness conditions tested. There tends to be more negative or downward flow in this region when the bed and the dowels are rough. Since no vertical velocity measurements were taken for the smooth dowel/rough bed condition, it is unknown if these changes are caused by the bed roughness or the dowel roughness.

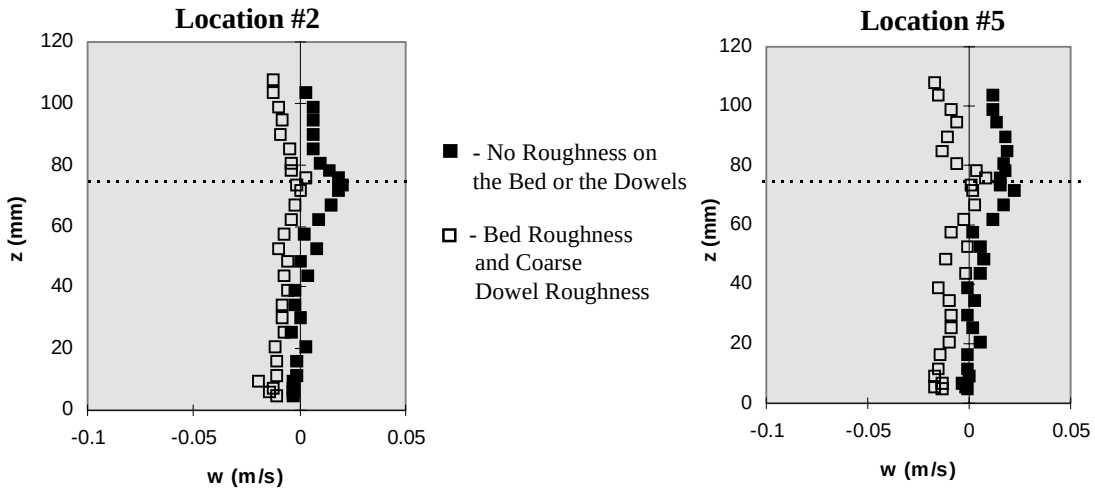

Figure 4.21 - Fully Submerged Vertical Velocity Profiles at Locations in the Unobstructed Flow Region for Different Roughness Conditions

Roughness also influences the vertical velocity at locations in-line with dowels as seen in Figure 4.22. There tends to be more secondary motion in the vicinity of a dowel when the bed and dowels are rough; the upward flow on the downstream side of a dowel and the downward flow on the upstream side of a dowel become more pronounced. The same phenomenon was observed under partially submerged conditions.

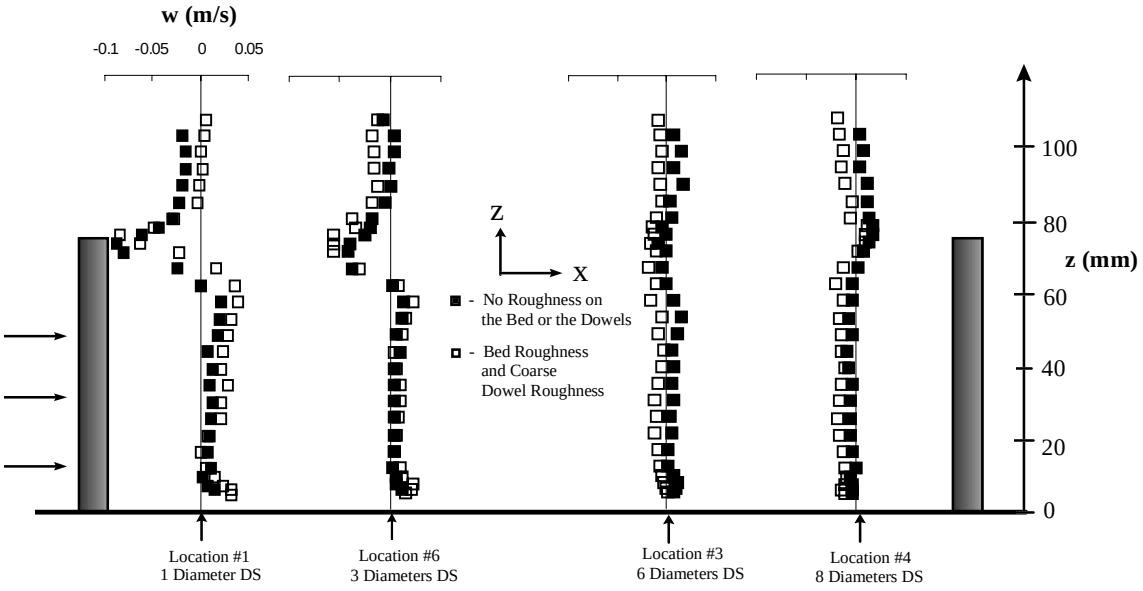

Figure 4.22 - Fully Submerged Vertical Velocity Profiles at Locations In-Line with Dowels for Different Roughness Conditions

Chapter 5

Double Layer Flow

The term double layer flow is used to describe flows that contain two different heights of vegetation. Double layer flows commonly occur in nature on floodplains and in certain wetland environments where trees and other tall vegetation grow among the denser low-lying shrubs and grasses. During high flow periods, the low-lying vegetation can become inundated while the tall vegetation remains partially submerged. Depending on the height and density of vegetation present, flows may periodically get high enough to completely submerge both the tall and short vegetation.

Experiments were conducted to examine the velocity and turbulence characteristics in flows containing double layer vegetation. Throughout this chapter, h_t=the height of the tall dowels and h_s=the height of the short dowels. In each of the double layer experiments, the dowels were arranged in the pattern shown in Figure 2.6. Longitudinal velocity profiles were taken at each of the 10 measurement locations shown in this Figure. It should be noted that the measurement locations used in the double layer experiments are not the same as the measurement locations used in the partially and fully submerged experiments.

The following three double layer roughness experiments were conducted:

1) h_t = 15.2cm = 5 inch; h_s = 7.6cm = 3 inch (Exp. DL#1)
2) h_t = 15.2cm = 6 inch; h_s = 5.1cm = 2 inch (Exp. DL#2)
3) h_t = 7.6cm = 3 inch; h_s = 5.1cm = 2 inch (Exp. DL#3)

The flow rate in each of the double layer experiments was the same as the flow rate in the fully submerged experiments (Q=0.0114 m^3/s). In experiments DL#1 & DL#2, the short dowels were fully submerged and the tall dowels were partially submerged. Both the tall and short dowels were fully submerged in experiment DL#3. The channel slope was kept constant at 0.3%, which is the same slope used throughout this research.

5.1 Double Layer Experiment #1 (DL#1) - h_t=15.2cm; h_s=7.6cm

The dowel configuration for experiment DL#1 was assembled by removing a portion of the 7.6 cm dowels from the fully submerged array and replacing them with 15.2cm dowels. The dowel density and configuration is the same below z=h_s(z=h) in both experiment DL#1 and the fully submerged experiment. Therefore, it is appropriate to compare the results from these two experiments. The dowel density (λ) above z=h_t is 0.04 while the dowel density below z=h_s is 0.24. Although the tall dowels in experiment DL#1 occupy only 0.4% of the total volume above z=h_s, they have a considerable influence on the overall flow characteristics. When tall dowels were introduced to the

fully submerged array, the bulk longitudinal velocity decreased by 9.8% and the flow depth increased by nearly 11% (See Table 5.1). Manning's n also increased from 0.0271 in the fully submerged experiment to 0.0312 in experiment DL#1. This demonstrates that tall vegetation can considerably increase the flow resistance, even when it occupies an insignificant portion of the total flow volume.

Table 5.1 - Flow and Resistance Characteristics for the Double Layer Experiments

Experiment	Bulk Velocity (m/s)	Flow Depth (m)	Manning's n
Double Layer #1	0.2950	0.1266	0.0312
Fully Submerged	0.3272	0.1141	0.0271
Double Layer #2	0.3082	0.1212	0.0294
Double Layer #3	0.3417	0.1093	0.0255

5.1.1 Longitudinal Mean Velocity

The longitudinal velocity profiles from experiment DL#1 are compared to the fully submerged velocity profiles in Figure 5.1. The dashed lines in each plot represent the top of the dowels. Below $z=h_s=7.6$cm, the velocity profiles from both experiments are fairly similar in shape and magnitude, considering that the measurement locations are not the same. In this region, all of the data points from experiment DL#1 follow one of three distinct profiles, representing three separate regions within the short dowel array. The lowest velocities occur at the three locations that are two dowel-diameters downstream of a dowel (Locations #1,#5, & #8), while the highest velocities occur at the four locations in the unobstructed flow region (Locations #2,#4,#7, & #9). The data points also line up on the same profile at the three locations that are two dowel-diameters upstream of a dowel (Locations #1,#5, & #8). As observed in both the partially and fully submerged experiments, a high velocity spike formed near the bed at locations in-line with a dowel.

Above $z=h_s$, the longitudinal velocities are higher because the dowels are less dense. Unlike the fully submerged profiles, the double layer profiles do not converge to a single logarithmic profile between the top of the short dowels and the free surface. Instead, the profiles vary in magnitude at the different measurement locations, much like the partially submerged profiles seen in Figure 3.1. The lower velocities occur at locations directly behind and in-line with dowels, while the higher velocities occur in the unobstructed flow region between dowels. In addition, each of the double layer profiles above $z=h_s$, with the exception of Location #1, can be divided into the same three regions observed in partially submerged flow (See Section 3.1.1). The sheared layer near the top of the short dowels can be viewed as the *bed region*. Directly above the bed region, an *intermediate region* exists in which the mean velocity remains nearly constant with height. This region is dominated by wake generated turbulence. Above the intermediate region lies a *free-surface* region in which the flow is sheared due to the higher velocities near the free-surface.

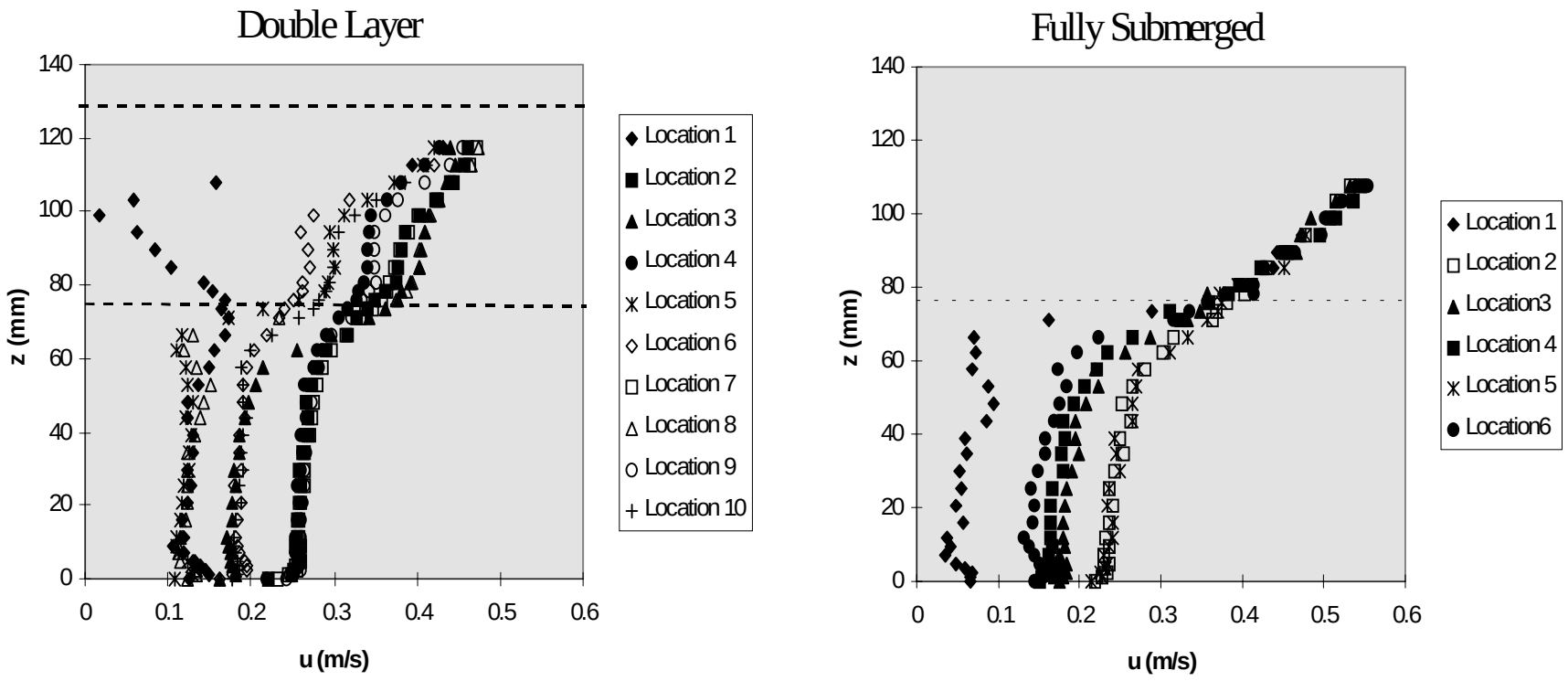

Figure 5.1 - Comparison Between Fully Submerged and Double Layer (h_t=15.2cm; h_s=7.6cm) Longitudinal Velocity Profiles

The double layer profile at Location #1 is quite different from the profiles at the other measurement locations. The velocity increases near the top of the short dowel array to a local maximum at $z=h_s$, above which the mean velocity decreases rapidly to a local minimum just below the free surface. A less pronounced local minimum was also observed slightly below the free-surface in partially submerged flow (See Location #1 profile in Figure 3.1). Possibly, the local minimum at Location #1 becomes more pronounced when the upstream approach velocity is higher.

5.1.2 Turbulence Intensity and Skew

As seen in Figure 5.1, the tall dowels in double layer flow reduce the velocity above $z=h_s$. Consequently, the double layer profiles in experiment DL#1 tend to be less sheared than the fully submerged profiles near $z=h_s(z=h)$. As discussed in Section 4.1.2, shear flows are a common source of energy for turbulent velocity fluctuations (Tennekes & Lumley 1972). The longitudinal turbulence intensity near $z=h_s(z=h)$ tends to be lower in experiment DL#1 than in the fully submerged experiment because the flow is less sheared (See Figure 5.2).

Unlike the fully submerged u_{rms} profiles, the u_{rms} profiles for experiment DL#1 do not converge to a single profile between $z=h_s$ and the free surface. In this region, the turbulence intensity varies depending on the position within the tall dowel array. As found in the partially and fully submerged experiments, the longitudinal turbulence intensity is higher at locations directly behind and downstream of a dowel where the wake turbulence is most pronounced. The turbulence intensity at Location #1, two-dowel diameters downstream of a tall dowel, is nearly twice as high above $z=h_s$ than below $z=h_s$. This indicates that the turbulence intensity behind a dowel increases as the upstream approach velocity increases. At Location #6, the upstream approach velocity is approximately 50% higher above $z=h_s$ than below $z=h_s$ (See Figure 5.1).

The double layer and fully submerged longitudinal skew profiles are compared in Figure 5.3. In fully submerged flow, the positive skew below z=h and the negative skew above z=h indicate that momentum transfer is dominated by sweep and ejection motions. As discussed in Section 4.1.2, the sweep and ejection motions are caused by organized vortices that form near the top of the dowels, where the faster flow above the array interacts with the slower flow within the array. The skew profiles for experiment DL#1 do not appear to follow a trend, indicating that organized vortices did not form in this experiment.

5.2 Double Layer Experiment #2 (DL2) - h_t=15.2cm; h_s=5.1cm

In this experiment, the height of the short dowels was reduced from 7.6 cm to 5.1 cm while the height of the tall dowels remained the same. The total volume occupied by the dowels in experiment DL#2 is approximately 6% less than the total volume occupied

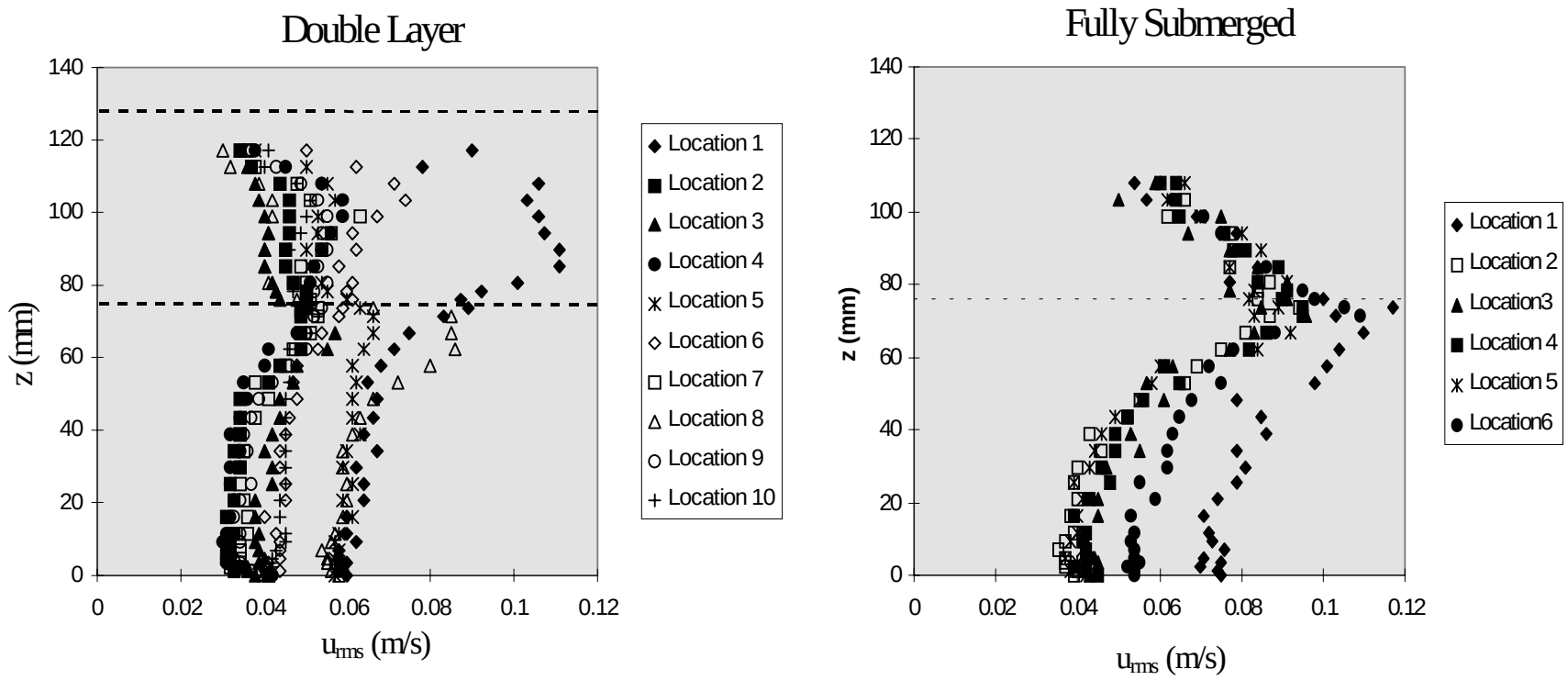

Figure 5.2 - Comparison Between Fully Submerged and Double Layer (h_t=15.2cm; h_s=7.6cm) Longitudinal Turbulence Intensity Profiles

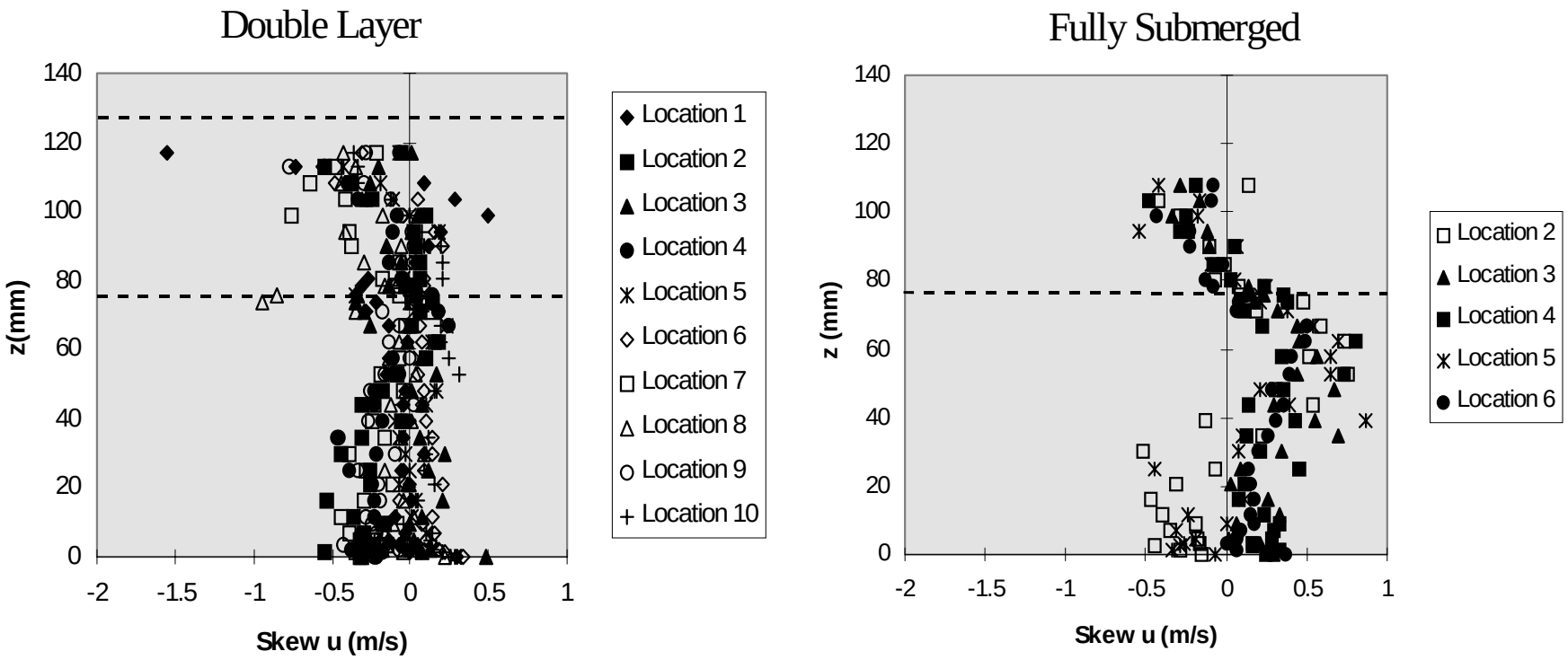

Figure 5.3 - Comparison Between Fully Submerged and Double Layer (h_t=15.2cm; h_s=7.6cm) Longitudinal Skew Profiles

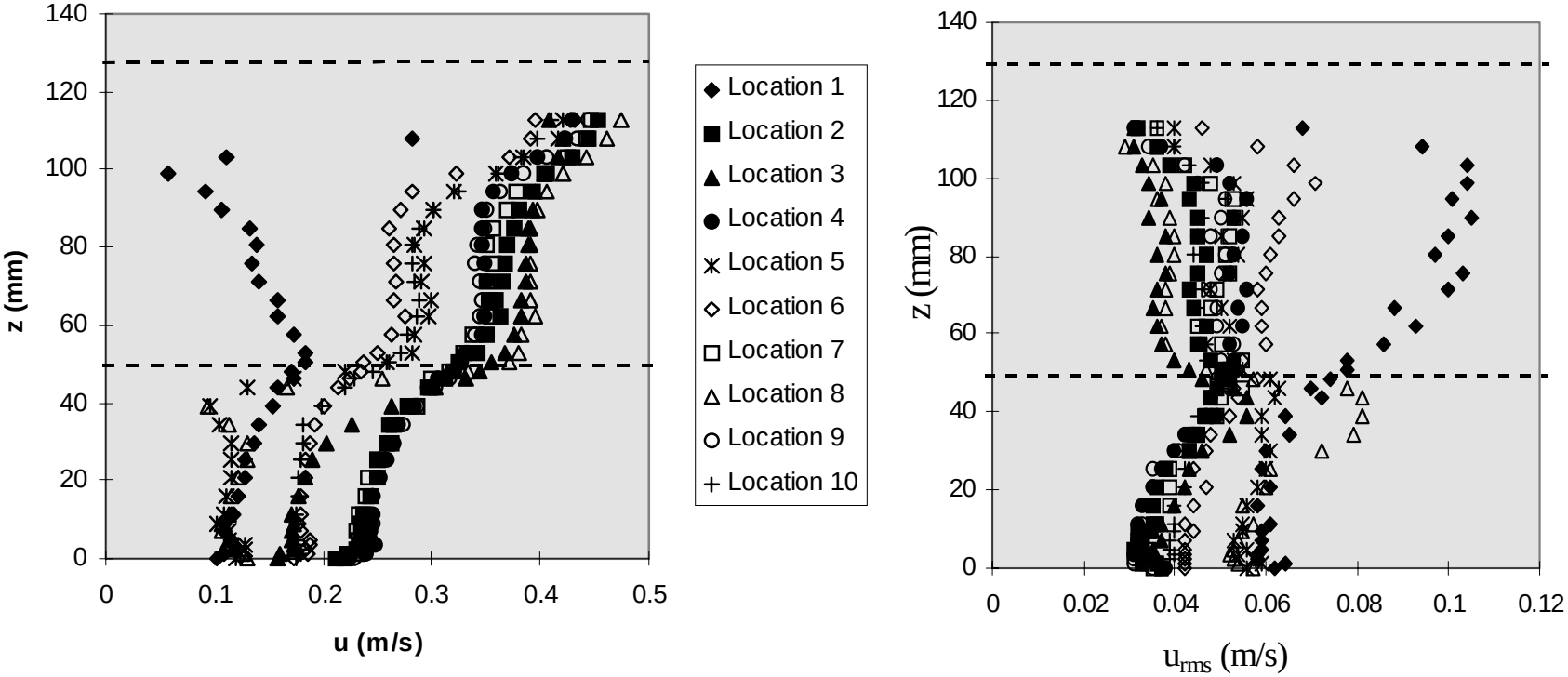

Figure 5.4 - Longitudinal Velocity and Turbulence Intensity Profiles for Experiment DL#2

by the dowels in the fully submerged single layer experiment; however, Manning's n is higher for experiment DL#2, indicating that the double layer configuration provides more flow resistance (See Table 5.1).

Although the tall dowels are fairly sparse, they are very effective at reducing the mean velocity and generating flow resistance. The drag on each individual dowel is proportional to the approach velocity squared and the projected area of the dowel normal to the flow (See Eqn 1.13). It was shown in the previous section that the approach velocity at Location #6 is nearly 50% higher above $z=h_s$ than below $z=h_s$. Assuming this is true, the dowels above $z=h_s$ provide approximately 2.25 more resistance than the dowels below $z=h_s$ per unit of projected area .

The results from experiment DL#2 are consistent with the results from DL#1. As seen in Figures 5.1, 5.2 & 5.4, the longitudinal velocity and turbulence intensity profiles from experiments DL#1 & DL#2 follow the same trends at each of the measurement locations.

The longitudinal velocity profiles from experiments DL#1 & DL#2 have been reduced to a non-dimensional form to provide a more generalized method to describe double layer flow. This method is only appropriate when the short dowels are fully submerged and the tall dowels are partially submerged. In this analysis, the regions above and below $z=h_s$ were analyzed separately. Below $z=h_s$, the longitudinal velocity was normalized by the friction velocity (u_*) and the vertical scale was normalized by the height of the short dowels (h_s). Above $z=h_s$, the longitudinal velocity was normalized by the friction velocity and the vertical scale was normalized by $(z-h_s)/(d-h_s)$. As seen in Figures 5.5 & 5.6, the normalized profiles for experiments DL#1 and DL #2 are similar to one another. The dimensionless profiles shown in these figures are representative of the profiles at each of the measurement locations.

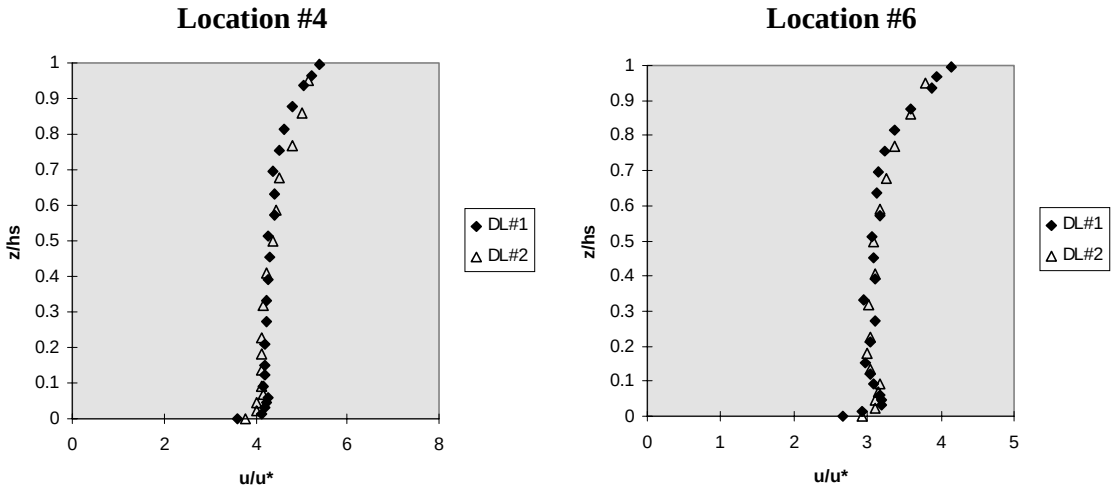

Figure 5.5 - Dimensionless Double Layer Velocity Profiles Below $z=h_s$

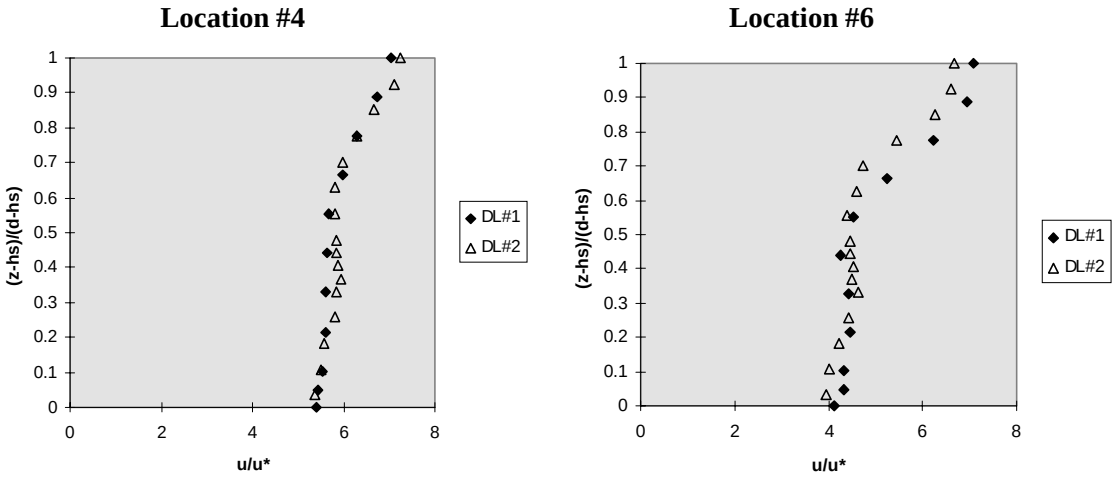

Figure 5.6 - Dimensionless Double Layer Velocity Profiles Above $z=h_s$

5.3 Double Layer Experiment #3 (DL#3) - h_t=7.6cm; h_s=5.1cm

Experiment DL#3 was the only experiment conducted in which both the tall and short dowels were fully submerged. Measurements were not taken at Locations #2 or #4 in this experiment. Below $z=h_s$=5.1cm, the longitudinal velocities are lower than in the other two double layer experiments (See Figure 5.7). This indicates that more of the flow is conveyed above $z=h_s$ where there is less resistance.

Between $h_s<z<h_t$, the flow is highly sheared. With the exception of Location #1, all of the velocity data points start to converge in this region. As seen in Figure 5.8, all of the velocity profiles converge to a single logarithmic profile slightly below $z=h_t$. Between $z=h_t$ and the free surface, all of the velocity data closely follows a single logarithmic profile.

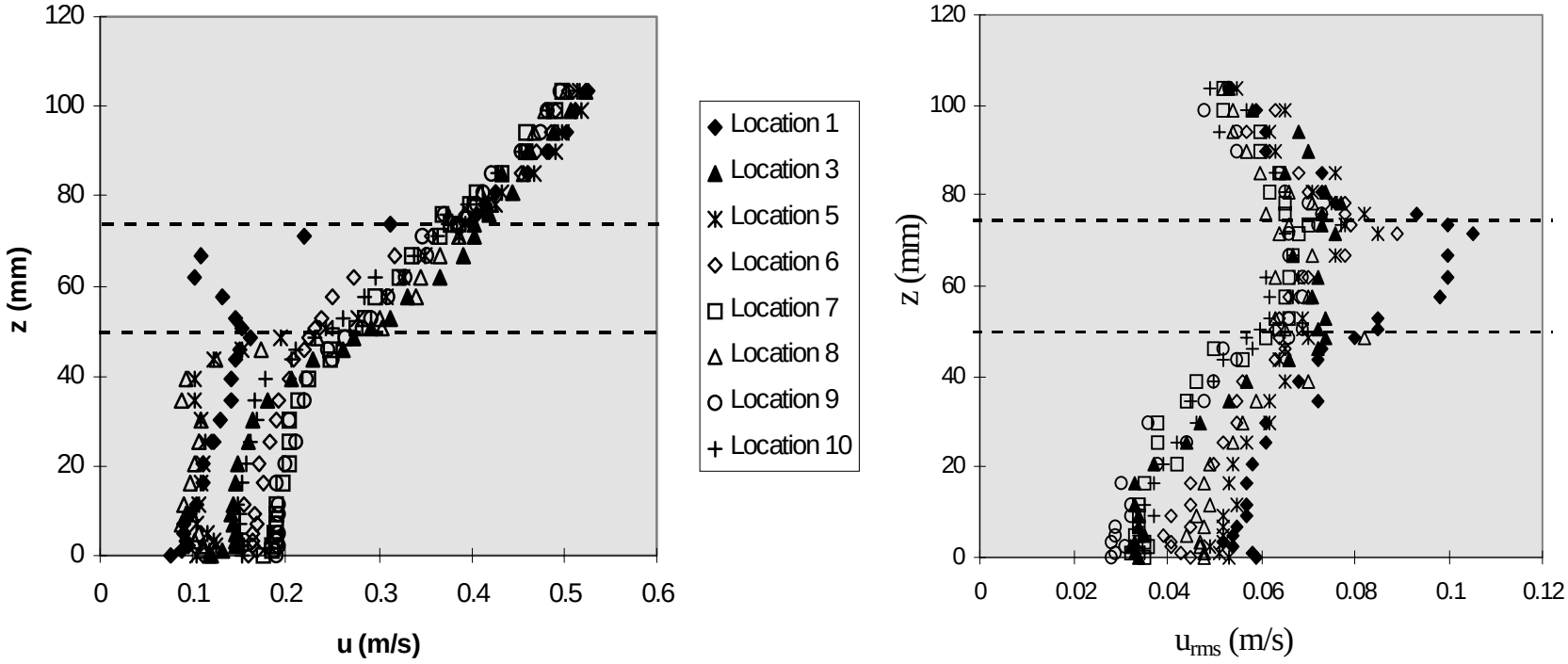

Figure 5.7 - Longitudinal Velocity and Turbulence Intensity Profiles for Experiment DL#3

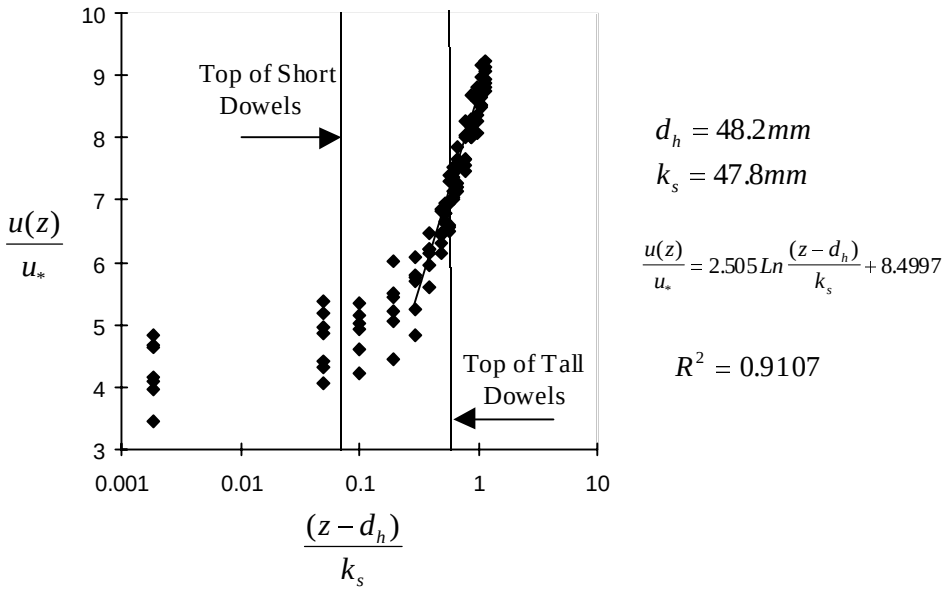

Figure 5.8 - Logarithmic Profile for Experiment DL#3

The longitudinal velocity profile at Location #1 has the same shape as the profiles observed in experiments DL#1 & DL#2. In experiment DL#3, however, the local minimum occurs slightly below h_t rather than slightly below the free surface.

As seen in the Figure 5.7, the longitudinal turbulence intensity increases between the bed and the top of the short dowels. Between $h_s<z<h_t$, the turbulence intensity remains fairly constant with height at most of the measurement locations. In this region, the turbulence intensity at Location #1 is significantly higher than elsewhere in the flow. Overall, the u_{rms} values from experiment DL#3 were higher than the u_{rms} values from the previous two double layer experiments, but lower than the u_{rms} values from the fully submerged experiment. All of the turbulence intensity profiles tend to converge near the $z=h_t$. As observed in fully submerged flow, the turbulence intensity decreases linearly between the top of the dowels and the free surface.

The longitudinal skew profiles for experiment DL#3 are shown in Figure 5.9. The profiles in this figure are similar to the fully submerged skew profiles shown in Figure 4.8. Below $z=h_t$, skew u is positive indicating that momentum transfer is dominated by sweeps; above $z=h_t$, skew u is negative indicating that momentum transfer is dominated by ejections. These results suggest that organized vortices form in the shear layer near the top of the tall dowels.

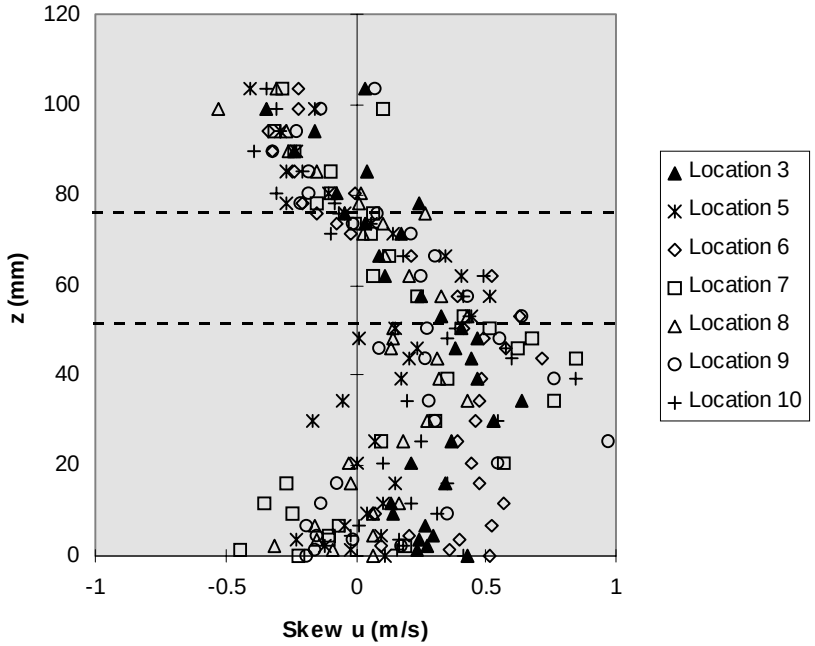

Figure 5.9 - Longitudinal Skew Profiles for Experiment DL#3

Chapter 6

Sediment Experiments

Sediment transport and deposition was examined under a variety of flow conditions. Although sediment movement has been studied extensively in open channel flow, much less research is available for flows containing vegetation. Experiments were conducted under partially submerged, fully submerged and double-layer flow conditions. A partially submerged experiment was also conducted with coarse roughness attached to the dowels. In each experiment, sediment was introduced to the flume at a constant rate of 140.89 g/min. over a period of 15 minutes. The total mass of material added to the flume in each experiment was slightly more than 2 kg. At the partially submerged flow rate ($0.0044\ m^3/\sec$), the sediment concentration was 0.5339 g/L; at the fully submerged flow rate ($0.0114\ m^3/\sec$), the sediment concentration was 0.2060 g/L. All of the sediment used in these experiments was sand, ranging in size from 0.075mm to 0.25mm. Sediment not deposited within the array was captured in a sediment trap at the end of the flume. The flow conditions, including channel slope, discharge, dowel arrangement and dowel density, were the same as the flow conditions described in Chapters 3, 4, & 5. In each experiment, the bed was smooth prior to the introduction of sediment.

6.1 Observations

Sediment was initially introduced to the flume when no dowels were present. At both the partially and fully submerged flow rates, none of the sediment was deposited on the bed; all of the sediment was transported as either bed load or suspended load. Table 6.1 shows the flow characteristics for the two sediment experiments when no dowels were present.

Table 6.1 – Sediment Experiments with no Dowels Present

Exp.	Q (m^3/s)	D_{50} (mm)	Fall Velocity, w (m/s)	Flow Depth, Z (m)	Rouse # ($z=w/Ku_*$)	τ^*, $ZS/(\gamma/\gamma_s - 1)D_{50}$
S#1	0.0044	0.138	0.0115	0.0231	1.10	0.31
S#2	0.0114	0.138	0.0115	0.0429	0.81	0.57

The Rouse # in each experiment indicates that the suspended concentration is relatively high near the bed and low near the free-surface. As anticipated, the dimensionless shear stress τ^*, is considerably higher than the critical dimensionless shear stress ($\tau_c^*=0.03$). This indicates that sediment motion occurs near the bed.

When dowels were attached to the bed, the mean velocity within the array was reduced, causing a portion of the sediment to fall out of suspension. In each of the experiments with dowels, some of the sediment was deposited on the bed, some was transported as bed load and some remained in suspension.

The horseshoe vortex at the base of each dowel significantly influences the transport of sediment near the bed. Increased fluid shear stresses associated with the horseshoe vortex caused a scour hole to form around each dowel (See Figure 6.1). Researchers have found that the shear stress beneath a horseshoe vortex can be as much as 12 times higher than the bottom shear stresses found elsewhere in the flow (Niedoroda et al., 1982). As observed by Niedoroda et al.(1982), the shape of each scour hole around the upstream half of each dowel is that of a half-frustrum of an inverted cone. They also found that the sediment in the scour hole is sloped at the angle of repose.

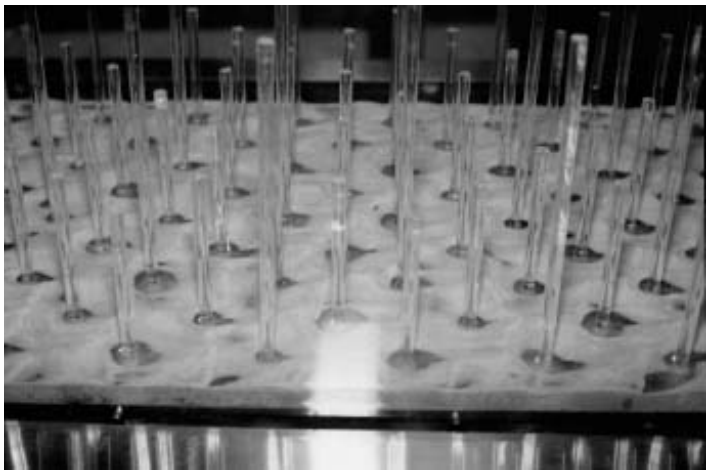

Figure 6.1 - Scour Holes at the Base of Each Dowel

A crest formed in the deposited sand just upstream of each scour hole. In each experiment, sediment appeared to slough off the crest into the scour hole at the same rate that additional material was deposited on the crest. The fine sediment used in these experiments served as an effective flow visualization tool. Sediment that sloughed into a scour hole was entrained by the horseshoe vortex and then rapidly transported around the sides of a dowel. As other researchers have observed (Simpson et al., 1990; Sumer et al. 1997), the horseshoe vortex rotates in the clockwise direction on the upstream face of a dowel. This rotation is transformed into longitudinal rotation as the horseshoe vortex wraps around the sides of a dowel. It could be seen from the entrained sediment that the two limbs of the horseshoe vortex rotate in opposite directions to one another.

Downstream of a dowel, the horseshoe vortex broke up. A trough formed in the sand in this region. Some of the sediment carried by the horseshoe vortex was lifted upward in the wake of a dowel and became part of the suspended load. As discussed in Chapters 3 & 4, upward flow was observed near the bed in the wake of a dowel. The rest of the sediment carried by the horseshoe vortex was deposited on the next downstream crest. This material eventually sloughed into the next downstream scour hole and became entrained by the horseshoe vortex. This process is illustrated in Figure 6.2.

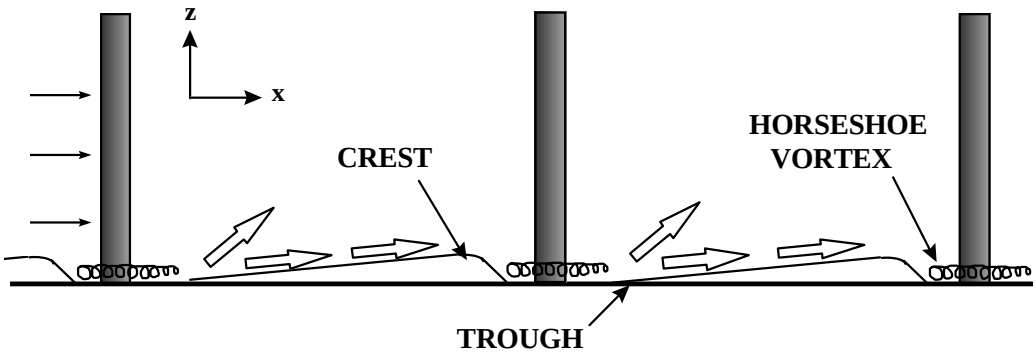

Figure 6.2 - Sediment Transport Within a Dowel Array

Very little sediment was deposited immediately downstream of a dowel. This region is located between the two limbs of the horseshoe vortex. Periodically, some sediment was swept into this region by the flow reversal. When this material moved, it was lifted vertically into suspension. This phenomenon was observed in each of the sediment experiments.

An experiment was conducted to determine how dowel roughness affects the scour processes at the base of a dowel. Figure 6.3 shows a comparison between the scour holes for the roughness and no-roughness conditions. In this figure, rough dowels were installed left of center and smooth dowels were installed right of center. When the dowels are rough, the scour holes are significantly larger and the troughs in the wake of the dowels are better defined, indicating that the horseshoe vortices may have a higher intensity.

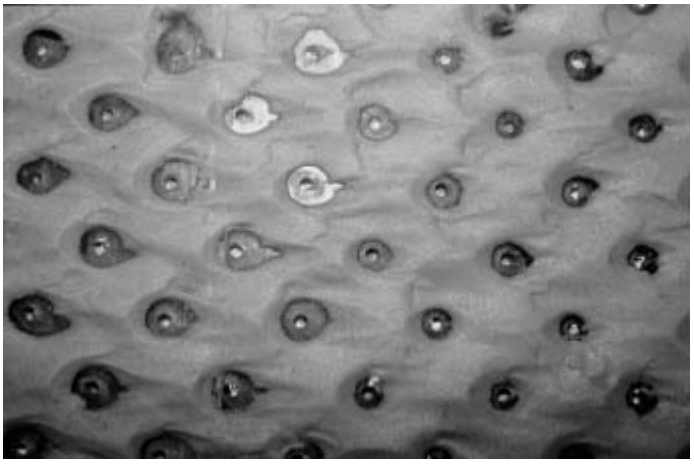

Figure 6.3 - Comparison Between Smooth Dowel and Rough Dowel Scour Holes

6.2 Sediment Analysis

After each experiment, the sediment captured in the sediment trap was baked to remove all moisture, weighed, and then sieved to determine the grain size distribution. The percentage of the sediment deposited within the array was calculated for each roughness configuration. The results are shown in Table 6.2.

Table 6.2 - Sediment Deposition in Each Experiment

Roughness Configuration	Flow Rate (m^3/s)	Mass In (g)	Mass Out (g)	Mass Deposited (g)	Percent Deposited
Partially Submerged	0.0044	2113.4	628.0	1485.4	**70.3**
Partially Submerged w/ Roughness	0.0044	2113.4	821.6	1291.8	**61.1**
No Dowels	0.0044	2113.4	2113.4	0	**0**
Fully Submerged	0.0114	2113.4	1006.4	1107.0	**52.4**
Double Layer	0.0114	2113.4	702.5	1410.9	**66.8**
No Dowels	0.0114	2113.4	2113.4	0	**0**

Two sediment experiments were conducted under partially submerged flow conditions - one with the dowels smooth and one with the dowels rough. Approximately 13% less sediment was deposited when the dowels were rough. The depth averaged velocity, however, was found to be considerably lower when the dowels were rough (See Section 3.3.1). These results appear to contradict one another; an increase in the resistance would generally reduce the depth averaged velocity and cause more deposition to occur. It is believed that the dowel roughness increases the intensity of the horseshoe vortices, causing more sediment to be scoured around each dowel and thus increasing the amount of sediment in suspension. This hypothesis is consistent with the photograph in Figure 6.3, showing larger scour holes around the rough dowels.

The amount of sediment deposited in the fully submerged experiment was approximately 25% lower than the amount deposited in the partially submerged experiment (smooth dowels). This difference was less than anticipated considering that the fully submerged flow rate is over 2.5 times higher than the partially submerged flow rate. As discussed in Section 4.1.4, the longitudinal velocities within the array are similar for both the partially submerged and fully submerged flow conditions, despite the difference in the flow rate. The slower flows within the array promote deposition. At the same time, the faster flows that occur above the array under fully submerged conditions, tend to increase the amount of sediment in suspension.

In the double layer flow experiment, a portion of the dowels were partially submerged and a portion were fully submerged. This roughness condition was assembled

by removing approximately 25% of the 7.6 cm(3 inch) dowels from the fully submerged array and replacing them with 15.2 cm(6 inch) dowels. The discharge was the same for the double layer and fully submerged experiments. The dowel arrangement for the double layer flow condition is shown in Figure 2.6.

Above the top of the short dowels ($z=h_s$), the fraction of the total volume occupied by dowels is only 0.4%. Although the tall dowels account for only a small portion of the total volume above $z=h_s$, they have a significant impact on the flow characteristics. Double layer roughness effectively reduces the longitudinal velocity above $z=h_s$ (See Figures 5.2 & 5.4), allowing far more sediment deposition to occur. In the double layer experiment, 66.8% of the sediment introduced to the flume was deposited, when compared to 52.4% in the fully submerged experiment. As seen in Table 6.2, the amount of sediment deposited in the double layer experiment was nearly as high as the amount deposited in the partially submerged experiment, although the flow rates differ by a factor of approximately 2.5.

Double layer roughness would be effective in a sediment retention basin or a wetland environment to induce sediment and contaminant deposition. During low flow periods, both the short and tall vegetation would be partially submerged. When flooding occurs, the shorter vegetation would be fully submerged and the tall vegetation would be partially submerged. This research indicates that the tall vegetation can be fairly sparse, when compared to the density of the short vegetation, and still be effective at reducing the mean velocity and promoting deposition.

The grain size distributions for the sediment collected in the trap are shown in Figures 6.4 & 6.5. In each of the experiments, the sediment collected in the trap is finer than the sediment that was introduced to the flume. This occurs because the larger sand particles tend to settle out, while the smaller sand particles tend to remain in suspension. As seen in Figure 6.4, the sediment collected in the trap under partially submerged conditions is somewhat coarser when the dowels are rough. This probably occurs because the horseshoe vortices have a higher intensity when the dowels are rough. As discussed in Section 6.1, the horseshoe vortex scours the bed material at the base of each dowel and lifts a portion of the scoured material into suspension. The bed sediment entrained by the horseshoe vortices tends to be some of the coarser sediment since it has fallen out of suspension and been deposited on the bed. As the intensity of the horseshoe vortices increase, more of the coarse bed material is scoured around each dowel and transported downstream toward the sediment trap.

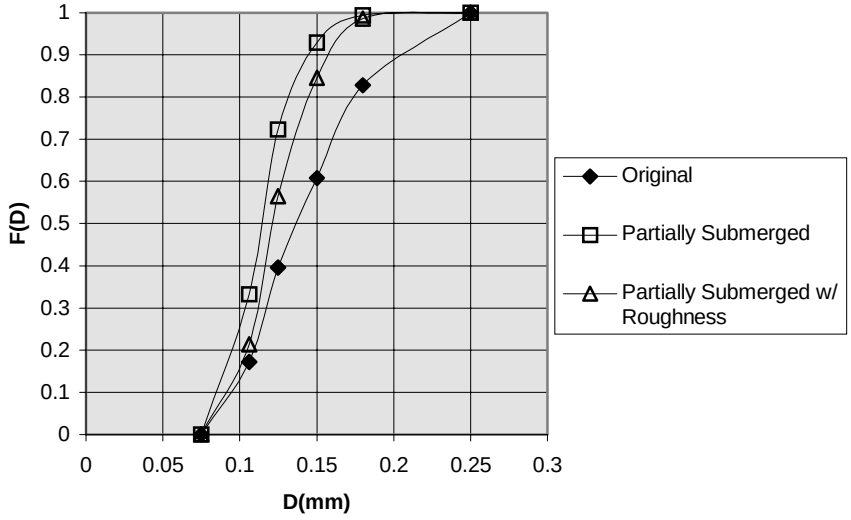

Figure 6.4 - Grain Size Distributions for Sediment Collected in Trap (Q=0.0044m^3/s)

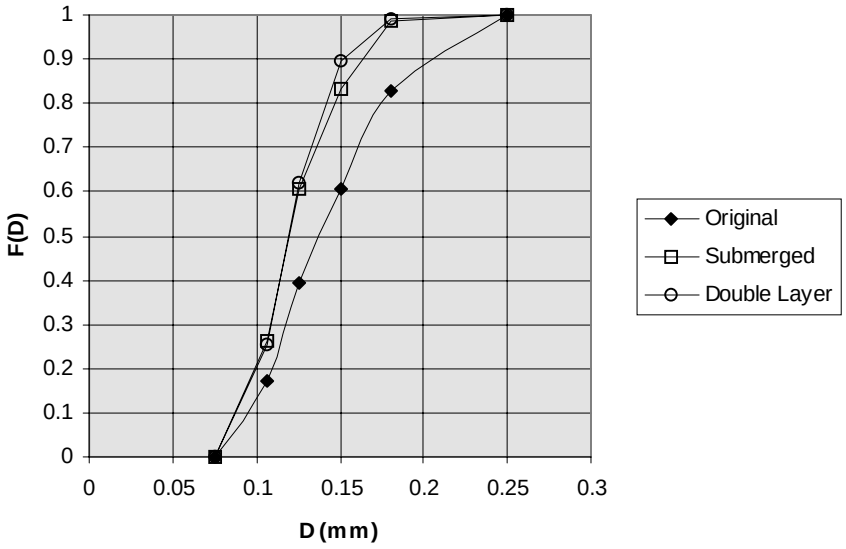

Figure 6.5 - Grain Size Distributions for Sediment Collected in Trap (Q=0.0114m^3/s)

As seen in Figure 6.5, the sediment collected in the fully submerged experiment was slightly coarser than the sediment collected in the double layer experiment. When the dowels are fully submerged, the faster flow above the dowels keeps more of the finer sediment in suspension; in double layer flow, the tall dowels significantly reduce the velocity above $z=h_s$, allowing more of the finer sediment to fall out of suspension.

Chapter 7

Conclusions and Recommendations

Flows through vegetation were studied for a wide range of flow conditions. This chapter discusses some of the similarities and differences between the different experiments. In addition, this chapter highlights some of the more interesting observations and provides recommendations for future research.

Under fully submerged conditions, the flow is highly sheared near the top of the dowels. In each of the experiments, the maximum turbulence intensities occur where the flow is most sheared. The fully submerged longitudinal and vertical skew profiles indicate that organized vortices develop in the shear layer near the top of the dowels. Below the top of the dowels, momentum transfer is dominated by sweeps; above the top of the dowels, momentum transfer is dominated by ejections. The skew profiles indicate that the sweeps have a higher intensity than the ejections.

Between the top of the dowels and the free-surface, all of the longitudinal velocity data closely follows the same logarithmic profile. The vertical velocity data, however, is not spatially uniform between the top of the dowels and the free-surface, indicating that secondary motion occurs. Just below the top of the dowels, the velocity data diverges from a logarithmic profile.

Within the vegetation the partially submerged and fully submerged velocity profiles are similar in shape and magnitude, although the fully submerged flow rate is higher by a factor of 2.5. In this region, the mean velocity and turbulence intensity varies considerably depending on the measurement location with respect to the dowels. The mean velocity and turbulence intensity tend to have an inverse relationship within the array; the highest turbulence intensities occur at positions where the mean velocity is lowest, and vice-versa. In each experiment, the highest turbulence intensity and the lowest mean velocity occur at locations immediately downstream of a dowel. Similarly, the highest mean velocity the lowest turbulence intensity occur at locations in the unobstructed flow region between dowels

A horseshoe vortex formed at the base of each dowel. In the sediment experiments, the horseshoe vortex created a scour hole around each dowel. At locations downstream of a dowel, a high-velocity spike formed near the bed. In addition a less pronounced low velocity region (secondary minimum) formed just above the high-velocity spike. It is believed that the horseshoe vortex transports momentum to the central wake region behind a dowel, causing a high velocity spike to form in this region. It was observed that the high-velocity spike behaves much like a wall jet in quiescent fluid.

The experiments with bed and vegetative roughness did not provide any conclusive results; however, certain trends were observed in these experiments. The bed roughness tends to increase the longitudinal velocity in the vicinity of the bed. In addition, both the high velocity spike and the secondary minimum were more pronounced when the bed was rough. This may indicate that the horseshoe vortex has a higher

intensity when the bed is rough. The size of the scour holes increased considerably when the dowels were rough, suggesting that vegetative skin roughness may also increase the intensity of the horseshoe vortex. Both the bed roughness and the dowel roughness increased the flow depth and reduced the depth averaged velocity at each measurement location.

The double layer vegetation experiments demonstrated that vegetation can considerably increase the flow resistance even when it occupies an insignificant portion of the total flow volume. Double layer vegetation effectively reduced the mean velocity and promoted sediment deposition when the tall dowels were partially submerged. When both the tall and short dowels were fully submerged, the flow behaved much like single layer fully submerged flow.

To develop a better overall understanding of fluid flow through vegetation, additional research needs to be conducted. Since vegetation can vary considerably in shape and size, more research is necessary to understand how the vegetative length scales influence the flow and resistance characteristics. Flow through vegetation is highly three-dimensional in nature. Therefore, more research is needed in which the velocity and turbulence characteristics are examined in all three flow directions. The structure of the horseshoe vortex and the scour processes caused by the horseshoe vortex are not well understood and should be examined in more detail. Finally, further research should be conducted to examine the resistance characteristics of double layer vegetation. Today there is a growing interest in erosion and sediment control practices. Double layer vegetation could be used in a sediment retention basin or wetland environment to effectively reduce the mean velocity and induce sediment and contaminant deposition.

Reference List

Bedient, P.B. and Huber, W.C. Hydrology and Floodplain Analysis. Addison-Wesley Publishing Company: Reading, Massachusetts, 1992.

Chow, V.T. Open Channel Hydraulics. McGraw Hill: New York, 1959.

Cionco, R.M. (1972). Intensity of Turbulence within Canopies with Simple and Complex Roughness Elements. *Boundary Layer Meteorology* **2**, 453-465.

Cowan, I.R. (1968). Mass, Heat and Momentum Exchange Between Stands of Plants and their Atmospheric Environment. *Q. J. R. Meteorological Society* **94**, 318-332.

Daugherty, R.L., Franzini, J.B. and Finnemore, J.E. Fluid Mechanics with Engineering Applications. McGraw Hill, Inc: New York, 1985.

Dargahi, B (1989). The Turbulent Flow Field Around a Circular Cylinder. *Exps. Fluids* **8**, 1-12.

Devenport, W.J. and Simpson, R.L. (1990). Time-Dependent and Time-Averaged Turbulence Structure Near the Nose of a Wing Body Junction. *Journal of Fluid Mechanics* **210**, 23-55.

Gao, W., Shaw, R.H. and Paw UKT (1989). Observation of Organized Structure in Turbulent Flow Within and Above a Forest Canopy. *Boundary Layer Meteorology* **47**, 349-377.

Goncharov, V.N. Dynamics of Channel Flow. Israel Program for Scientific Translations: Jerusalem, 1964.

Grass, A.J. (1971). Structural Features of Turbulent Flow Over Smooth and Rough Boundaries. *Journal of Fluid Mechanics* **50**, 233-255.

Hartley, David M. "Resistance to Shallow Flow Through Vegetation." Thesis, Colorado State University, 1980.

Hodges, C.C. "Resistance to Flow Through Riparian Wetlands." Master's Thesis, Virginia Polytechnic Institute & State University, 1997.

Ikeda, S. and Kanazawa, M. (1996). Three-Dimensional Organized Vortices Above Flexible Water Plants. *Journal of Hydraulic Engineering* **122**, 634-640.

Inoue, E. (1955). Studies of the Phenomena of Waving Plants (Honami) Caused by Wind. Part I. Mechanism and Characteristics of Waving Plants Phenomena. *Journal of Agricultural Meteorology Japan* **11**, 18-22.

Janna,W.S. Introduction to Fluid Mechanics. PWS Publishers: Boston, 1987.

Kouwen, N., Unny, T.E., and Hill (1969). Flow Retardance in Vegetated Channels. *Journal of Irrigation and Drainage* **95**, 329-342.

Launder, B.E. and Rodi, W. (1983). The Turbulent Wall Jet – Measurements and Modelling. *Annual Review Fluid Mechanics* **15**, 429-459.

Li, R.M., Shen, H.W. (1973). Effects of Tall Vegetation on Flow and Sediment. *Journal of the Hydraulics Division* **99**, 793-814.

Liu, C.K., Kline, S.J. and Johnson, J (1966). An Experimental Study of Turbulent Boundary Layers on Rough Walls. Report MD-15, Dept. of Mechanical Engineering, Stanford University.

Marshall, J.K (1971). Drag Measurements in Roughness Arrays of Varying Density and Distribution. *Agricultural Meteorology* **8**, 269-292.

Nezu, I. And Nakagawa, H. Turbulence in Open Channel Flows. A.A. Balkema: Rotterdam, 1993.

Niedoroda, A.W. and Dalton, C. (1982). A Review of the Fluid Mechanics of Ocean Scour. *Ocean Engineering* **9,** 159-170.

Palmer, V.J. (1945). A Method for Designing Vegetated Waterways. *Agricultural Engineering* **26**, 516-520.

Petryk, S. “Drag on cylinders in Open Channel Flow” thesis presented to Colorado State University at Fort Collins, Colorado, 1969.

Petryk, S. and Bosmajian,G (1975). Analysis of Flow Through Vegetation. *Journal of the Hydraulics Division* **101**, 871-884.

Raupach, M.R., Finnigan, J.J. and Brunet, Y. (1996). Coherent Eddies and Turbulence in Vegetation Canopies: The Mixing Layer Analogy. *Boundary-layer Meteorology* **78**, 351-382.

Raupach, M.R. (1992). Drag and Drag Partition on Rough Surfaces. *Boundary-layer Meteorology* **60**, 375-396.

Raupach, M.R., Antonia, R.A. and Rajogopalan, S. (1991). Rough-Wall Turbulent Boundary Layers. *Applied Mechanics Review* **44**, 1-25.

Raupach, M.R. and Thom, A.S. (1981). Turbulence in and Above Plant Canopies. *Ann. Rev. Fluid Mechanics* **13**, 97-129.

Raupach, M.R., Thom, A.S. and Edwards, I. (1980). A Wind-Tunnel Study of Turbulent Flow Close to Regularly Arrayed Rough Surfaces. *Boundary-Layer Meteorology* **18**, 373-397.

Sabersky, R.H. Acosta, A.J. and Hauptmann, E.G. Fluid Flow - A First Course in Fluid Mechanics. Macmillan Publishing Co.: New York, 1989.

Schlichting, H. Boundary Layer Theory 6th edition. McGraw Hill: New York, 1968.

Seigner, I., Mulhearn, P.J., Bradley, E.F. and Finnigan, J.J (1976). Turbulent Flow in a Model Plant Canopy. *Boundary Layer Meteorology* **10**, 423-453

Shaw, R.H., den Hartog, G, King, K.M. and Thurtell, G.W. (1974). Measurements of Mean Wind Flow and Three-Dimensional Turbulence intensity within a mature corn canopy. *Agricultural Meteorology* **13**, 419-425.

Shaw, R.H. (1977). Secondary wind speed maxima inside plant canopies. *Journal of Applied Meteorology* **16**, 514-521.

Shaw, R.H. and Pereira, A.R. (1982). Aerodynamic Roughness of a Plant Canopy: A Numerical Experiment. *Agricultural Meteorology* **26**, 51-65.

Shaw, R.H., Silversides, R.H. and Thurtell, G.W. (1982). Some Observations of Turbulence and Turbulent Transport Within and Above Plant Canopies. *Boundary Layer Meteorology* **5**, 429-449.

Sumer, B.M., Christiansen, N. and Fredsoe, J. (1997) The Horseshoe Vortex and Vortex Shedding Around a Vertical Wall-Mounted Cylinder Exposed to Waves. *Journal of Fluid Mechanics* **332**, 41-70.

Tennekes, H and Lumley, J.L. A First Course in Turbulence. MIT Press: Cambridge, 1972.

Thom, A.S. (1971). Momentum Absorption by Vegetation. *Q. J. R. Meteorological Society* **97**, 414-428.

Thomson, G.T, and Roberson, J.A. (1976). A Theory of Flow Resistance for Vegetated Channels. *Trans. ASAE* **19**, 288-293.

Townsend, A.A. The Structure of Turbulent Shear Flow. Cambridge University Press: Cambridge, 1976.

Tsujimoto, Shimizu, Kitamura, and Okada. (1992). Turbulent Open Channel Flow Over a Bed Covered by Rigid Vegetation. *Journal of Hydoscience and Hydraulic Engineering* **10**, 13-25.

Vanoni, V.A. editor. Sedimentation Engineering. American Society of Civil Engineers: New York, 1975.

Vennard, J.K. and Street, R.L. Elementary Fluid Mechanics. John Wiley and Sons: New York, 1982.

Vogel, S. Life in Moving Fluids. Princeton University Press: Princeton, 1994.

Wilson, N.R. and Shaw, R.H. (1977). A Higher Order Closure Model for Canopy Flow. *Journal of Applied Meteorology* **16**, 1198-1205.

Zavistoski, R.A. and Nepf, H.M. "Hydrodynamic Effects of Surface Piercing Plants." Thesis, Mass. Institute of Technology, 1994.

APPENDIX

List of Experiments

Partially Submerged Experiments

Exp. #	Description	Upstream Depth (m)	Downstream Depth (m)
PS#1	No Roughness; Longitudinal Velocity	0.0649	0.0649
PS#2	No Roughness; Vertical Velocity	0.0649	0.0649
PS#3	Bed Roughness and Fine Dowel Roughness; Longitudinal Velocity	0.0697	0.0672
PS#4	Bed Roughness and Coarse Dowel Roughness; Longitudinal Velocity	0.0762	0.0722
PS#5	Bed Roughness and Coarse Dowel Roughness; Vertical Velocity	0.0762	0.0722
PS#6	Bed Roughness and No Dowel Roughness; Longitudinal Velocity	0.0664	0.0657

Fully Submerged Experiments

Exp. #	Description	Upstream Depth (m)	Downstream Depth (m)
FS#1	No Roughness; Longitudinal Velocity	0.1141	0.1141
FS#2	No Roughness; Vertical Velocity	0.1141	0.1141
FS#3	Bed Roughness and Fine Dowel Roughness; Longitudinal Velocity	0.1192	0.1169
FS#4	Bed Roughness and Coarse Dowel Roughness; Longitudinal Velocity	0.1215	0.1173
FS#5	Bed Roughness and Coarse Dowel Roughness; Vertical Velocity	0.1215	0.1173
FS#6	Bed Roughness and No Dowel Roughness; Longitudinal Velocity	0.1156	0.1136

Double Layer Experiments

Exp. #	Description	Upstream Depth (m)	Downstream Depth (m)
DL#1	h_t = 15.2cm (Partially Submerged) h_s = 7.6 cm (Fully Submerged); Longitudinal Velocity	0.1278	0.1253
DL#2	h_t = 15.2 cm (Partially Submerged) h_s = 5.1 cm (Fully Submerged); Longitudinal Velocity	0.1224	0.1199
DL#3	h_t = 7.6 cm (Fully Submerged) h_s = 5.1 cm (Fully Submerged); Longitudinal Velocity	0.1095	0.1090

Experiment PS#1

Location #1

Z	U Mean	U RMS	U Skew	U Flat	U Turb
(mm)	(m/s)	(m/s)	(m/s)	(m/s)	(%)
0	0.071	0.082	0.032	2.417	116.511
1.14	0.099	0.08	-0.219	2.655	80.415
2.29	0.087	0.078	-0.144	2.645	89.898
3.45	0.087	0.082	-0.137	2.65	94.476
4.59	0.065	0.081	0.003	2.558	124.224
6.9	0.062	0.081	0.039	2.541	129.079
9.19	0.057	0.078	-0.082	2.54	136.846
11.5	0.055	0.078	-0.12	2.612	142.65
16.1	0.058	0.077	-0.075	2.657	133.089
20.7	0.064	0.077	-0.055	2.642	121.382
25.29	0.062	0.072	-0.074	2.658	116.733
29.89	0.066	0.075	-0.112	2.634	112.617
34.5	0.064	0.075	-0.111	2.758	116.482
39.09	0.065	0.074	-0.112	2.685	113.429
43.7	0.062	0.072	-0.098	2.7	116.956
48.29	0.043	0.08	0.035	2.46	188.543
52.9	0.067	0.073	0.029	2.786	109.739
55.2	0.091	0.076	-0.016	2.677	83.67
57.5	0.119	0.087	-0.03	2.461	73.516

Location #2

Z	U Mean	U RMS	U Skew	U Flat	U Turb
(mm)	(m/s)	(m/s)	(m/s)	(m/s)	(%)
0	0.216	0.04	-0.203	2.846	18.69
1.14	0.23	0.039	-0.22	2.783	16.726
2.29	0.249	0.032	-0.29	3.183	12.747
3.45	0.256	0.031	-0.298	3.551	12.034
4.59	0.258	0.03	-0.409	3.467	11.535
6.9	0.258	0.03	-0.252	3.296	11.807
9.19	0.256	0.031	-0.222	3.36	12.079
11.5	0.256	0.031	-0.22	3.282	12
16.1	0.255	0.03	-0.121	3.438	11.64
20.7	0.257	0.029	-0.195	3.497	11.481
25.29	0.258	0.03	-0.132	3.072	11.564
29.89	0.258	0.03	-0.144	3.231	11.66
34.5	0.257	0.029	-0.111	3.226	11.204
39.09	0.255	0.029	-0.066	3.436	11.465
43.7	0.256	0.03	-0.073	3.069	11.622
48.29	0.263	0.028	-0.127	2.822	10.763
52.9	0.276	0.027	-0.128	3.322	9.788
55.2	0.288	0.025	-0.136	3.123	8.751
57.5	0.296	0.026	-0.301	3.845	8.9

Experiment PS#1

Location #3

Z	U Mean	U RMS	U Skew	U Flat	U Turb
(mm)	(m/s)	(m/s)	(m/s)	(m/s)	(%)
0	0.137	0.039	0.277	2.899	28.721
1.14	0.174	0.038	0.138	3.234	21.644
2.29	0.176	0.036	-0.11	2.768	20.316
3.45	0.179	0.037	0.115	2.777	20.528
4.59	0.176	0.037	-0.072	2.783	20.834
6.9	0.176	0.041	-0.036	2.618	23.375
9.19	0.169	0.04	0.025	2.798	23.794
11.5	0.17	0.039	0.038	2.783	23.193
16.1	0.171	0.041	-0.094	2.694	23.889
20.7	0.173	0.042	0.022	2.782	24.191
25.29	0.173	0.041	0.077	2.895	23.705
29.89	0.174	0.041	0.026	2.976	23.442
34.5	0.174	0.041	0.124	2.823	23.544
39.09	0.175	0.039	0.21	3.126	22.122
43.7	0.178	0.04	0.104	2.753	22.568
48.29	0.185	0.04	-0.086	2.927	21.793
52.9	0.193	0.044	0.012	2.842	22.697
55.2	0.201	0.04	-0.011	2.789	19.958
57.5	0.209	0.04	-0.155	2.847	19.177

Location #4

Z	U Mean	U RMS	U Skew	U Flat	U Turb
(mm)	(m/s)	(m/s)	(m/s)	(m/s)	(%)
0	0.145	0.038	-0.043	2.941	26.016
1.14	0.162	0.036	0.095	3.011	22.431
2.29	0.171	0.037	-0.002	3.069	21.505
3.45	0.173	0.038	0.069	2.841	21.741
4.59	0.167	0.037	0.145	2.791	21.97
6.9	0.162	0.039	0.024	3.047	23.948
9.19	0.16	0.04	0.143	2.837	24.755
11.5	0.163	0.039	0.146	2.785	23.981
16.1	0.162	0.038	-0.023	2.848	23.599
20.7	0.163	0.037	-0.117	2.859	22.42
25.29	0.165	0.04	0.062	2.699	24.173
29.89	0.163	0.037	0.058	2.813	22.994
34.5	0.165	0.038	0.106	2.953	23.204
39.09	0.167	0.04	-0.145	3.068	24.13
43.7	0.166	0.039	0.137	2.895	23.33
48.29	0.176	0.041	-0.126	2.877	23.111
52.9	0.178	0.04	-0.091	2.906	22.294
55.2	0.188	0.04	-0.265	3.008	21.441
57.5	0.188	0.038	-0.244	3.146	20.156

Experiment PS#1

Location #5

Z	U Mean	U RMS	U Skew	U Flat	U Turb
(mm)	(m/s)	(m/s)	(m/s)	(m/s)	(%)
0	0.196	0.041	-0.129	2.72	20.712
1.14	0.213	0.038	-0.1	2.803	17.928
2.29	0.24	0.032	-0.056	3	13.506
3.45	0.241	0.032	-0.223	3.126	13.254
4.59	0.245	0.031	-0.241	3.401	12.705
6.9	0.241	0.031	-0.302	3.3	12.977
9.19	0.24	0.029	-0.31	3.087	12.193
11.5	0.241	0.031	-0.161	3.083	12.874
16.1	0.241	0.031	-0.267	3.124	12.715
20.7	0.241	0.03	-0.445	3.561	12.644
25.29	0.24	0.029	-0.198	3.232	12.259
29.89	0.244	0.03	-0.275	3.408	12.24
34.5	0.245	0.029	-0.266	3.16	11.981
39.09	0.242	0.031	-0.213	3.258	12.589
43.7	0.245	0.028	-0.222	3.449	11.603
48.29	0.246	0.029	-0.212	3.371	11.833
52.9	0.254	0.025	-0.126	3.392	9.911
55.2	0.253	0.025	-0.289	3.517	10.019
57.5	0.246	0.027	-0.607	6.461	11.08

Location #6

Z	U Mean	U RMS	U Skew	U Flat	U Turb
(mm)	(m/s)	(m/s)	(m/s)	(m/s)	(%)
0	0.144	0.05	0.407	3.78	34.665
1.14	0.154	0.052	0.059	2.857	33.641
2.29	0.154	0.053	-0.254	3.147	34.578
3.45	0.149	0.049	-0.039	2.762	33.089
4.59	0.141	0.049	0.042	2.504	34.968
6.9	0.137	0.049	0.112	2.817	35.642
9.19	0.137	0.049	0.176	2.933	35.379
11.5	0.133	0.049	0.321	3.137	36.602
16.1	0.137	0.049	0.036	2.7	35.83
20.7	0.136	0.049	0.029	3.12	36.117
25.29	0.139	0.049	-0.03	2.778	35.001
29.89	0.139	0.048	0.039	2.808	34.569
34.5	0.138	0.049	0.06	2.892	35.143
39.09	0.141	0.045	0.081	2.971	32.017
43.7	0.15	0.047	-0.099	2.75	31.527
48.29	0.161	0.051	-0.267	2.704	31.783
52.9	0.171	0.055	-0.235	3.009	31.982
55.2	0.164	0.055	-0.126	2.707	33.649
57.5	0.162	0.057	-0.195	2.762	34.982

Experiment PS#2

Location #1

Z	U Mean	U RMS	U Skew	U Flat	U Turb
(mm)	(m/s)	(m/s)	(m/s)	(m/s)	(%)
5.75	0.016	0.065	0.21	3.632	393.602
6.9	0.004	0.06	0.049	3.56	1369.092
9.19	0.006	0.058	0.014	3.667	990.594
11.5	0.003	0.054	0.113	3.949	1678.952
16.1	0.004	0.057	0.058	3.804	1269.684
20.7	0.008	0.054	0.108	3.883	716.963
25.29	0.006	0.058	0.032	3.416	1052.374
29.89	0.009	0.058	-0.006	3.568	629.593
34.5	0.006	0.057	-0.234	3.91	917.215
39.09	0.005	0.06	-0.154	3.637	1097.195
43.7	0.008	0.058	-0.289	3.881	732.064
48.29	0.006	0.064	-0.144	3.462	1153.541
52.9	-0.002	0.066	0.04	3.041	3456.276
55.2	-0.015	0.071	0.151	3.243	478.191

Location #2

Z	U Mean	U RMS	U Skew	U Flat	U Turb
(mm)	(m/s)	(m/s)	(m/s)	(m/s)	(%)
4.59	-0.002	0.024	-0.292	4.619	1040.257
5.75	-0.001	0.024	0.011	3.837	1748.494
6.9	-0.003	0.024	-0.072	3.801	955.264
9.19	-0.002	0.026	-0.022	3.61	1191.178
11.5	-0.001	0.026	0.109	3.537	4546.514
16.1	0.002	0.026	0.079	3.665	1603.35
20.7	0	0.029	0.038	4.043	103630.4
25.29	0.004	0.026	0.21	4.458	671.013
29.89	0.004	0.026	-0.107	3.222	632.636
34.5	0.006	0.027	-0.02	3.277	413.722
39.09	0.007	0.028	-0.157	3.793	433.546
43.7	0.008	0.027	-0.173	3.772	338.856
48.29	0.01	0.029	-0.125	3.987	297.48
52.9	0.01	0.026	-0.062	3.489	259.886
55.2	0.01	0.025	0.105	3.495	241.573

Experiment PS#2

Location #3

Z	U Mean	U RMS	U Skew	U Flat	U Turb
(mm)	(m/s)	(m/s)	(m/s)	(m/s)	(%)
4.59	0.001	0.034	0.206	3.561	4770.318
5.75	0.001	0.033	0.317	3.494	5809.237
6.9	0.002	0.035	0.067	3.164	2248.636
9.19	0.001	0.036	-0.003	3.398	2415.32
11.5	0.001	0.035	0.037	3.19	2577.145
16.1	-0.001	0.036	-0.008	2.898	2762.037
20.7	-0.002	0.035	-0.169	3.213	1616.665
25.29	-0.005	0.039	-0.066	2.949	749.871
29.89	-0.006	0.037	-0.075	3.229	614.029
34.5	-0.005	0.037	-0.076	3.179	790.19
39.09	-0.007	0.039	-0.102	3.137	544.653
43.7	-0.005	0.039	-0.175	3.188	759.316
48.29	-0.013	0.04	-0.011	3.157	299.641
52.9	-0.011	0.036	-0.021	2.968	320.7
55.2	-0.014	0.035	0.062	3.054	258.317
57.5	-0.012	0.037	0.022	3.123	307.352

Location #4

Z	U Mean	U RMS	U Skew	U Flat	U Turb
(mm)	(m/s)	(m/s)	(m/s)	(m/s)	(%)
4.59	-0.001	0.029	-0.09	3.459	3376.509
5.75	0	0.03	-0.098	3.305	6309.966
6.9	0	0.031	0.038	3.228	6688.821
9.19	-0.001	0.033	0.052	3.474	2309.373
11.5	-0.002	0.034	0.135	3.308	1465.317
16.1	-0.002	0.034	0.13	3.259	1387.313
20.7	-0.001	0.036	0.027	2.938	2448.374
25.29	-0.003	0.035	-0.061	3.295	1039.023
29.89	-0.005	0.033	0.022	2.906	694.426
34.5	-0.004	0.035	-0.114	3.353	1006.983
39.09	-0.003	0.035	-0.109	3.142	1058.915
43.7	-0.006	0.038	-0.133	3.017	578.279
48.29	-0.008	0.037	-0.238	2.933	446.297
52.9	-0.008	0.036	0.079	2.905	438.833
55.2	-0.007	0.035	0.098	3.073	467.89
57.5	-0.004	0.033	-0.054	2.969	799.214

Experiment PS#2

Location #5

Z	U Mean	U RMS	U Skew	U Flat	U Turb
(mm)	(m/s)	(m/s)	(m/s)	(m/s)	(%)
4.59	-0.013	0.025	0.138	3.604	192.158
5.75	-0.015	0.024	0.04	3.459	160.12
6.9	-0.014	0.025	-0.122	3.498	172.046
9.19	-0.014	0.026	0.008	3.327	188.889
11.5	-0.013	0.026	0.078	3.486	206.504
16.1	-0.011	0.026	0.018	3.286	243.09
20.7	-0.01	0.026	-0.003	3.375	262.103
25.29	-0.01	0.027	0.112	3.677	271.297
29.89	-0.008	0.027	-0.068	3.278	322.757
34.5	-0.007	0.026	0.18	3.434	364.669
39.09	-0.006	0.026	-0.056	3.53	472.239
43.7	-0.003	0.027	-0.161	3.152	1068.568
48.29	-0.001	0.028	-0.05	3.383	2313.415
52.9	0.001	0.027	0.033	3.868	3167.748
55.2	-0.001	0.026	0.102	3.257	3866.115

Location #6

Z	U Mean	U RMS	U Skew	U Flat	U Turb
(mm)	(m/s)	(m/s)	(m/s)	(m/s)	(%)
5.75	0.007	0.049	0.332	3.709	750.415
6.9	0.008	0.048	0.145	3.203	619.124
9.19	0.008	0.049	0.157	3.211	627.017
11.5	0.003	0.047	0.093	3.387	1434.524
16.1	-0.001	0.048	0.008	3.476	4371.585
20.7	-0.001	0.048	0.162	3.623	7843.851
25.29	-0.006	0.05	-0.145	3.76	904.891
29.89	-0.006	0.047	0.096	2.97	840.478
34.5	-0.006	0.05	-0.201	3.564	885.05
39.09	-0.008	0.05	-0.141	3.293	657.155
43.7	-0.007	0.049	-0.192	3.437	695.113
48.29	-0.009	0.052	-0.183	3.333	559.118
52.9	-0.013	0.052	-0.035	3.269	396.738
55.2	-0.014	0.048	-0.007	3.148	343.53

Experiment PS#3

Location #1

Z	U Mean	U RMS	U Skew	U Flat	U Turb
(mm)	(m/s)	(m/s)	(m/s)	(m/s)	(%)
0	0.049	0.072	0.047	2.763	145.625
1.14	0.04	0.068	0.041	2.909	167.959
2.29	0.036	0.07	0.048	2.96	192.647
3.45	0.019	0.07	0.045	2.711	374.155
4.59	0.02	0.066	0.167	2.834	321.211
6.9	0.014	0.065	0.099	2.662	459.302
9.19	0.004	0.073	0.154	2.695	2092.85
11.5	0	0.072	0.164	2.639	74530.56
16.1	0.01	0.077	0.161	2.73	784.206
20.7	0.021	0.072	-0.019	2.721	346.331
25.29	0.021	0.074	-0.075	2.877	349.432
29.89	0.028	0.074	-0.1	2.723	259.211
34.5	0.032	0.071	0.024	3.068	218.143
39.09	0.034	0.076	0.037	2.649	221.283
43.7	0.03	0.077	0.068	2.611	255.116
48.29	0.027	0.076	0.262	2.991	284.238
52.9	0.045	0.074	0.108	2.686	164.564
55.2	0.052	0.08	0.271	2.916	152.719
57.5	0.076	0.087	0.274	2.99	115.041

Location #2

Z	U Mean	U RMS	U Skew	U Flat	U Turb
(mm)	(m/s)	(m/s)	(m/s)	(m/s)	(%)
0	0.23	0.042	-0.215	2.832	18.221
1.14	0.238	0.038	-0.214	3.259	15.932
2.29	0.25	0.035	-0.28	3.504	14.148
3.45	0.249	0.035	-0.015	2.971	14.047
4.59	0.249	0.037	-0.297	3.338	14.867
6.9	0.244	0.04	-0.251	3.67	16.383
9.19	0.241	0.038	-0.111	3.162	15.708
11.5	0.241	0.041	-0.022	2.922	16.998
16.1	0.241	0.041	-0.471	3.52	16.885
20.7	0.246	0.039	-0.014	3.253	15.735
25.29	0.244	0.037	-0.121	3.053	15.311
29.89	0.245	0.038	-0.203	3.719	15.541
34.5	0.248	0.039	-0.182	3.141	15.802
39.09	0.246	0.041	-0.322	3.082	16.663
43.7	0.249	0.039	-0.21	3.185	15.546
48.29	0.249	0.037	-0.194	3.309	15.009
52.9	0.256	0.036	-0.23	2.824	14.229
55.2	0.26	0.037	-0.192	2.946	14.271
57.5	0.26	0.036	-0.162	3.193	13.845
59.79	0.264	0.041	0.038	3.74	15.559

Experiment PS#3

Location #3

Z	U Mean	U RMS	U Skew	U Flat	U Turb
(mm)	(m/s)	(m/s)	(m/s)	(m/s)	(%)
0	0.159	0.04	0.131	3.192	25.069
1.14	0.169	0.039	0.144	3.202	23.31
2.29	0.181	0.041	0.09	2.805	22.826
3.45	0.182	0.041	-0.134	3.025	22.293
4.59	0.185	0.043	0.004	3.04	23.201
6.9	0.185	0.042	0.051	3.123	22.837
9.19	0.174	0.044	0.103	2.735	25.191
11.5	0.171	0.047	-0.037	2.77	27.496
16.1	0.173	0.044	0.163	2.821	25.515
20.7	0.173	0.044	0.128	2.798	25.59
25.29	0.171	0.046	0.164	3.042	27.125
29.89	0.172	0.045	0.107	3.083	26.345
34.5	0.17	0.042	0.112	2.86	24.842
39.09	0.173	0.046	0.052	2.907	26.382
43.7	0.17	0.043	0.077	2.892	25.156
48.29	0.173	0.043	-0.044	2.69	24.851
52.9	0.168	0.042	0.149	2.863	24.96
55.2	0.169	0.046	0.029	2.758	27.108
57.5	0.165	0.048	0.118	2.952	28.947
59.79	0.174	0.046	0.154	3.242	26.425

Location #4

Z	U Mean	U RMS	U Skew	U Flat	U Turb
(mm)	(m/s)	(m/s)	(m/s)	(m/s)	(%)
0	0.14	0.042	-0.071	3.021	29.761
1.14	0.15	0.041	0.031	3.009	27.267
2.29	0.172	0.038	0.157	2.93	21.908
3.45	0.175	0.038	-0.092	3.17	21.732
4.59	0.17	0.042	0.09	3.183	24.536
6.9	0.159	0.044	0.073	2.573	27.555
9.19	0.157	0.044	-0.002	2.967	28.3
11.5	0.152	0.041	0.154	2.842	27.034
16.1	0.152	0.04	-0.059	3.168	26.501
20.7	0.157	0.04	0.212	3.047	25.41
25.29	0.16	0.041	0.066	2.872	25.66
29.89	0.157	0.042	0.012	2.86	26.77
34.5	0.156	0.041	0.171	2.699	26.377
39.09	0.157	0.042	-0.029	2.936	26.733
43.7	0.16	0.041	0.038	2.87	25.479
48.29	0.156	0.04	0.008	2.934	25.978
52.9	0.155	0.041	0.025	2.894	26.439
55.2	0.15	0.043	0.021	2.65	28.318
57.5	0.149	0.041	0.155	2.845	27.842
59.79	0.153	0.043	0.264	2.987	28.436

Experiment PS#3

Location #5

Z	U Mean	U RMS	U Skew	U Flat	U Turb
(mm)	(m/s)	(m/s)	(m/s)	(m/s)	(%)
0	0.223	0.042	-0.325	3.067	18.94
1.14	0.233	0.037	-0.059	3.189	16.038
2.29	0.248	0.035	-0.159	3.11	14.156
3.45	0.247	0.035	-0.206	3.068	14.14
4.59	0.243	0.036	-0.165	3.301	14.731
6.9	0.238	0.037	-0.126	3.154	15.387
9.19	0.237	0.037	-0.329	3.342	15.54
11.5	0.231	0.037	-0.244	3.213	15.845
16.1	0.234	0.037	-0.147	3.044	15.818
20.7	0.24	0.038	-0.298	3.11	15.729
25.29	0.24	0.038	-0.306	3.235	15.638
29.89	0.236	0.039	-0.381	3.524	16.543
34.5	0.244	0.039	-0.253	3.122	15.992
39.09	0.237	0.039	-0.1	3.097	16.307
43.7	0.238	0.039	-0.352	3.343	16.256
48.29	0.242	0.039	-0.208	3.45	16.106
52.9	0.247	0.037	-0.256	3.233	14.989
55.2	0.243	0.036	-0.311	3.239	15.017
57.5	0.24	0.037	-0.294	3.335	15.405
59.79	0.236	0.037	-0.29	3.346	15.612

Location #6

Z	U Mean	U RMS	U Skew	U Flat	U Turb
(mm)	(m/s)	(m/s)	(m/s)	(m/s)	(%)
0	0.123	0.047	-0.132	3.536	37.747
1.14	0.138	0.047	0.075	3.166	33.961
2.29	0.145	0.052	0.063	2.788	36.042
3.45	0.145	0.053	-0.042	2.843	36.441
4.59	0.142	0.055	0.02	2.937	38.459
6.9	0.121	0.054	0.083	2.746	44.593
9.19	0.114	0.05	0.119	2.835	43.635
11.5	0.108	0.051	0.188	3.113	46.836
16.1	0.113	0.051	0.036	3.194	44.734
20.7	0.122	0.05	-0.07	3.064	40.989
25.29	0.116	0.053	0.213	2.931	45.86
29.89	0.131	0.054	0.164	2.772	41.456
34.5	0.123	0.055	0.275	3.453	44.513
39.09	0.126	0.054	0.065	2.706	43.121
43.7	0.127	0.056	0.06	2.787	44.406
48.29	0.127	0.05	0.069	2.648	39.621
52.9	0.13	0.055	0.184	3.037	42.147
55.2	0.124	0.056	0.112	2.866	45.133
57.5	0.126	0.052	0.05	2.695	41.158
59.79	0.122	0.055	0.248	2.975	45.095

Experiment PS#4

Location #1

Z	U Mean	U RMS	U Skew	U Flat	U Turb
(mm)	(m/s)	(m/s)	(m/s)	(m/s)	(%)
0	-0.002	0.089	0.162	2.476	5257.779
1.14	0.017	0.086	0.067	2.492	500.433
2.29	-0.015	0.087	0.074	2.652	591.511
3.45	-0.027	0.081	0.244	2.766	303.163
4.59	-0.044	0.076	0.478	2.956	173.253
6.9	-0.054	0.075	0.595	3.227	138.33
9.19	-0.055	0.07	0.45	2.958	127.464
11.5	-0.037	0.076	0.441	2.79	204.334
16.1	-0.026	0.076	0.49	3.014	296.481
20.7	-0.012	0.078	0.18	2.561	637.799
25.29	-0.007	0.087	0.285	2.496	1245.393
29.89	-0.013	0.082	0.381	2.679	632.242
34.5	-0.017	0.08	0.317	2.659	462.475
39.09	-0.023	0.078	0.398	2.713	333.344
43.7	-0.033	0.081	0.157	2.51	242.905
48.29	-0.036	0.08	0.432	2.888	220.811
52.9	-0.033	0.076	0.311	2.766	230.371
55.2	-0.025	0.071	0.199	2.771	288.916
57.5	-0.02	0.074	0.203	2.682	376.064
59.79	-0.001	0.074	0.049	2.669	6989.125
62.09	0.011	0.084	0.329	2.954	776.597

Location #2

Z	U Mean	U RMS	U Skew	U Flat	U Turb
(mm)	(m/s)	(m/s)	(m/s)	(m/s)	(%)
0	0.226	0.045	-0.178	2.713	19.741
1.14	0.245	0.04	-0.292	3.303	16.158
2.29	0.255	0.036	-0.193	3.024	14.273
3.45	0.256	0.037	-0.175	2.875	14.491
4.59	0.255	0.038	-0.261	2.96	14.773
6.9	0.252	0.037	-0.404	3.514	14.497
9.19	0.248	0.037	-0.257	3.029	14.743
11.5	0.246	0.04	-0.286	3.179	16.428
16.1	0.239	0.041	-0.318	3.354	17.278
20.7	0.241	0.036	-0.169	3.414	14.944
25.29	0.244	0.039	-0.014	3.075	15.849
29.89	0.244	0.039	-0.145	2.876	15.886
34.5	0.24	0.037	-0.008	3.282	15.519
39.09	0.242	0.038	-0.196	3.224	15.817
43.7	0.242	0.037	-0.209	3.217	15.293
48.29	0.24	0.038	-0.197	3.149	16.033
52.9	0.242	0.039	-0.13	2.977	15.922
55.2	0.245	0.036	-0.192	3.198	14.503
57.5	0.246	0.034	-0.16	3.016	14.029
59.79	0.247	0.038	-0.119	3.133	15.183
62.09	0.247	0.038	-0.152	2.88	15.565

Experiment PS#4

Location #3

Z	U Mean	U RMS	U Skew	U Flat	U Turb
(mm)	(m/s)	(m/s)	(m/s)	(m/s)	(%)
0	0.152	0.043	0.104	2.937	28.462
1.14	0.166	0.039	0.062	3.195	23.739
2.29	0.175	0.041	0.094	3.026	23.569
3.45	0.176	0.043	0.094	2.916	24.68
4.59	0.174	0.045	-0.084	2.762	25.726
6.9	0.178	0.046	-0.037	2.967	25.853
9.19	0.163	0.047	0.3	3.208	28.827
11.5	0.166	0.04	-0.199	3.028	24.121
16.1	0.166	0.044	0.12	3.27	26.469
20.7	0.171	0.045	0.086	2.983	26.574
25.29	0.168	0.046	0.177	2.96	27.522
29.89	0.171	0.045	0.097	2.795	26.223
34.5	0.172	0.045	0.013	3.187	25.987
39.09	0.169	0.044	0.058	2.888	26.198
43.7	0.177	0.045	0.087	3.119	25.632
48.29	0.177	0.044	0.009	2.935	24.732
52.9	0.185	0.046	0.041	2.776	25.035
55.2	0.174	0.044	0.124	2.93	25.455
57.5	0.178	0.045	0.048	2.887	25.152
59.79	0.173	0.045	0.149	2.818	26.194
62.09	0.178	0.047	-0.035	3.207	26.343

Location #4

Z	U Mean	U RMS	U Skew	U Flat	U Turb
(mm)	(m/s)	(m/s)	(m/s)	(m/s)	(%)
0	0.126	0.041	0.034	3.226	32.562
1.14	0.151	0.039	0.098	2.902	25.883
2.29	0.161	0.04	0.113	3.125	24.712
3.45	0.157	0.039	-0.021	3.352	24.665
4.59	0.156	0.039	0.098	2.986	25.364
6.9	0.15	0.042	0.067	3.035	27.789
9.19	0.151	0.04	-0.11	3.081	26.698
11.5	0.142	0.043	-0.006	3.304	29.93
16.1	0.148	0.042	0.152	3.254	28.344
20.7	0.145	0.041	0.22	2.993	28.401
25.29	0.147	0.042	0.023	2.969	28.348
29.89	0.149	0.041	0.063	2.847	27.51
34.5	0.15	0.045	0.055	3.061	29.726
39.09	0.15	0.042	0.059	2.963	27.737
43.7	0.152	0.043	0.09	2.846	28.189
48.29	0.15	0.044	-0.153	3.075	29.106
52.9	0.152	0.042	0.063	3.236	27.901
55.2	0.152	0.042	-0.005	2.814	27.893
57.5	0.151	0.044	-0.011	2.908	28.772
59.79	0.149	0.041	-0.009	3.107	27.456
62.09	0.151	0.044	0.17	3.205	28.886

Experiment PS#4

Location #5

Z	U Mean	U RMS	U Skew	U Flat	U Turb
(mm)	(m/s)	(m/s)	(m/s)	(m/s)	(%)
0	0.217	0.046	-0.306	2.928	21.023
1.14	0.239	0.041	-0.198	2.922	17.016
2.29	0.245	0.038	-0.295	3.011	15.384
3.45	0.247	0.038	-0.306	3.194	15.331
4.59	0.245	0.037	-0.313	3.218	15.064
6.9	0.243	0.039	-0.275	3.12	15.87
9.19	0.24	0.04	-0.299	2.926	16.545
11.5	0.232	0.038	-0.037	3.096	16.417
16.1	0.228	0.04	-0.307	2.876	17.514
20.7	0.232	0.042	-0.262	3.378	18.266
25.29	0.237	0.041	-0.402	3.304	17.288
29.89	0.235	0.042	-0.062	3.04	17.7
34.5	0.236	0.042	-0.098	2.92	17.675
39.09	0.236	0.038	-0.199	2.936	15.899
43.7	0.233	0.04	-0.182	2.909	17.084
48.29	0.234	0.039	-0.169	2.975	16.607
52.9	0.234	0.038	-0.12	3.161	16.288
55.2	0.238	0.039	-0.345	3.529	16.181
57.5	0.231	0.039	-0.126	3.515	16.976
59.79	0.235	0.036	-0.222	3.107	15.529
62.09	0.227	0.039	-0.164	3.168	16.97

Location #6

Z	U Mean	U RMS	U Skew	U Flat	U Turb
(mm)	(m/s)	(m/s)	(m/s)	(m/s)	(%)
0	0.058	0.058	0.118	2.729	99.199
1.14	0.079	0.06	-0.013	2.903	75.816
2.29	0.088	0.063	0.044	2.779	72.14
3.45	0.087	0.063	0.012	2.841	72.508
4.59	0.087	0.061	0.154	2.759	69.953
6.9	0.088	0.061	0.078	2.665	68.822
9.19	0.08	0.058	0.235	3.546	72.263
11.5	0.07	0.056	0.004	3.103	80.759
16.1	0.09	0.058	-0.01	2.811	64.411
20.7	0.092	0.054	0.162	2.977	58.385
25.29	0.093	0.06	-0.064	2.667	64.599
29.89	0.101	0.059	0.051	2.724	58.653
34.5	0.097	0.058	0.104	2.865	59.252
39.09	0.097	0.056	-0.072	3.032	58.494
43.7	0.103	0.055	0.078	2.931	53.611
48.29	0.093	0.055	0.084	2.78	59.014
52.9	0.106	0.055	0.016	2.814	52.021
55.2	0.104	0.058	0.036	2.67	55.461
57.5	0.1	0.064	-0.052	2.885	63.722
59.79	0.094	0.068	-0.012	2.727	71.794
62.09	0.09	0.064	-0.001	2.966	70.847

Experiment PS#5

Location #1

Z	U Mean	U RMS	U Skew	U Flat	U Turb
(mm)	(m/s)	(m/s)	(m/s)	(m/s)	(%)
5.75	0.051	0.08	0.018	2.91	157.149
6.9	0.039	0.072	-0.142	3.021	183.921
9.19	0.004	0.067	-0.14	3.123	1663.385
11.5	0	0.071	-0.187	3.402	43259.43
16.1	-0.01	0.067	-0.021	3.01	652.138
20.7	-0.007	0.066	-0.028	3.212	975.442
25.29	-0.005	0.069	0.017	2.94	1264.314
29.89	0.005	0.066	-0.139	3.269	1347.333
34.5	0.001	0.068	0.006	3.31	7080.224
39.09	0.005	0.069	-0.341	3.383	1466.9
43.7	-0.001	0.07	0.099	3.143	5141.406
48.29	-0.002	0.073	-0.074	2.78	3882.645
52.9	-0.005	0.069	0.019	3.203	1303.998
55.2	-0.01	0.07	0.126	3.363	703.509
57.5	-0.01	0.07	0.091	3.288	714.136
59.79	-0.023	0.074	-0.054	2.901	320.538
62.09	-0.028	0.067	0.063	3.305	239.211

Location #2

Z	U Mean	U RMS	U Skew	U Flat	U Turb
(mm)	(m/s)	(m/s)	(m/s)	(m/s)	(%)
4.59	-0.005	0.033	-0.167	3.794	600.43
5.75	-0.008	0.032	-0.256	3.808	398.281
6.9	-0.008	0.035	0.001	3.407	449.026
9.19	-0.01	0.036	-0.245	3.444	356.739
11.5	-0.009	0.038	-0.125	3.441	433.285
16.1	-0.007	0.038	0.035	3.638	573.356
20.7	-0.002	0.04	0.118	3.536	1700.204
25.29	-0.002	0.038	0.062	3.823	1605.929
29.89	0.002	0.034	0	3.261	1890.345
34.5	0.002	0.036	-0.085	3.151	1554.938
39.09	0.004	0.036	-0.102	3.304	897.131
43.7	0.001	0.036	-0.09	3.068	3140.827
48.29	0.002	0.039	-0.156	3.115	2169.446
52.9	0.003	0.036	-0.04	2.932	1367.591
55.2	0.003	0.039	0.056	3.154	1471.822
57.5	0	0.035	-0.043	3.252	11101.09
59.79	0	0.038	-0.135	3.267	12785.11
62.09	-0.001	0.037	0.027	3.205	6390.053

Experiment PS#5

Location #3

Z	U Mean	U RMS	U Skew	U Flat	U Turb
(mm)	(m/s)	(m/s)	(m/s)	(m/s)	(%)
4.59	0.007	0.039	0.112	3.573	526.696
5.75	0.009	0.041	0.173	3.416	438.269
6.9	0.004	0.046	0.136	3.501	1084.711
9.19	0.001	0.045	0.165	3.361	5088.2
11.5	0.002	0.044	0.002	3.21	1973.247
16.1	-0.004	0.045	0.002	3.328	1026.798
20.7	-0.003	0.045	0.098	3.223	1510.986
25.29	-0.005	0.044	0.084	3.268	947.904
29.89	-0.012	0.047	-0.152	3.343	386.605
34.5	-0.01	0.046	-0.001	3.511	459.514
39.09	-0.009	0.043	-0.171	3.262	488.898
43.7	-0.01	0.044	-0.113	3.086	434.132
48.29	-0.008	0.045	-0.152	3.224	549.825
52.9	-0.007	0.043	-0.167	3.424	620.788
55.2	-0.007	0.044	-0.049	3.241	670.426
57.5	-0.007	0.042	-0.053	3.33	588.305
59.79	-0.006	0.042	0.094	3.424	671.035
62.09	-0.007	0.043	0.13	3.413	656.601

Location #4

Z	U Mean	U RMS	U Skew	U Flat	U Turb
(mm)	(m/s)	(m/s)	(m/s)	(m/s)	(%)
4.59	-0.003	0.037	-0.061	3.522	1336.58
5.75	-0.001	0.038	0.111	3.162	3014.372
6.9	-0.003	0.039	0.006	3.313	1216.681
9.19	-0.002	0.039	0.074	3.036	2445.57
11.5	-0.006	0.04	0.043	3.169	626.515
16.1	-0.007	0.043	-0.084	3.099	657.178
20.7	-0.007	0.04	0.025	3.469	596.994
25.29	-0.009	0.042	-0.08	3.616	448.399
29.89	-0.005	0.041	-0.095	3.341	851.672
34.5	-0.007	0.041	-0.066	3.475	581.738
39.09	-0.01	0.044	0.008	3.473	418.596
43.7	-0.011	0.042	-0.099	3.19	380.661
48.29	-0.008	0.041	-0.061	2.848	512.146
52.9	-0.007	0.042	-0.102	3.649	583.323
55.2	-0.008	0.041	-0.095	3.17	491.359
57.5	-0.003	0.04	-0.028	3.113	1546.209
59.79	-0.003	0.04	0.037	3.21	1372.326
62.09	-0.002	0.039	0.072	3.233	1840.896

Experiment PS#5

Location #5

Z	U Mean	U RMS	U Skew	U Flat	U Turb
(mm)	(m/s)	(m/s)	(m/s)	(m/s)	(%)
4.59	-0.01	0.031	-0.09	3.183	300.48
5.75	-0.011	0.033	-0.091	3.312	294.023
6.9	-0.011	0.034	0.06	3.313	312.187
9.19	-0.011	0.035	-0.199	3.459	317.891
11.5	-0.012	0.038	0.162	3.29	316.324
16.1	-0.007	0.035	-0.047	3.249	530.965
20.7	-0.006	0.035	-0.027	3.28	576.18
25.29	-0.005	0.037	-0.059	3.447	766.553
29.89	0	0.037	-0.004	3.8	102305.8
34.5	-0.003	0.035	-0.188	3.075	1369.211
39.09	0	0.036	-0.015	3.272	17681.77
43.7	0	0.035	-0.033	3.383	8739.219
48.29	0.002	0.037	-0.147	3.367	2248.303
52.9	-0.002	0.037	0.158	3.404	1609.409
55.2	-0.002	0.036	0.004	3.698	1564.314
57.5	-0.001	0.034	-0.125	3.105	5538.621
59.79	-0.001	0.035	0.084	3.436	2856.899
62.09	-0.003	0.034	0.074	3.243	1118.648

Location #6

Z	U Mean	U RMS	U Skew	U Flat	U Turb
(mm)	(m/s)	(m/s)	(m/s)	(m/s)	(%)
5.75	0.016	0.06	0.292	3.408	383.15
6.9	0.01	0.062	0.207	3.553	624.7
9.19	0.006	0.063	0.048	3.504	990.625
11.5	-0.004	0.06	0.179	3.43	1572.607
16.1	-0.002	0.057	0.028	3.39	2739.182
20.7	-0.008	0.059	0.127	3.531	704.066
25.29	-0.004	0.057	-0.053	3.24	1362.344
29.89	-0.003	0.056	-0.061	3.69	2172.493
34.5	0	0.059	0.032	3.322	41989.8
39.09	-0.004	0.058	-0.106	3.283	1309.297
43.7	0.002	0.062	0.025	3.515	3114.949
48.29	0.003	0.06	-0.059	3.899	2265.735
52.9	0.001	0.059	-0.136	3.33	7832.165
55.2	0.005	0.059	-0.076	3.115	1094.387
57.5	0.004	0.057	-0.009	3.253	1450.777
59.79	-0.004	0.059	-0.109	3.402	1365.67
62.09	-0.004	0.058	-0.144	3.549	1454.969

Experiment PS#6

Location #1

Z	U Mean	U RMS	U Skew	U Flat	U Turb
(mm)	(m/s)	(m/s)	(m/s)	(m/s)	(%)
0	0.091	0.065	0.186	2.664	70.931
1.14	0.107	0.069	-0.079	2.763	64.637
2.29	0.098	0.069	-0.146	2.878	70.735
3.45	0.049	0.062	0.044	2.968	126.862
4.59	0.02	0.064	0.168	2.758	313.065
6.9	-0.018	0.058	0.226	3.076	326.728
9.19	-0.018	0.068	0.514	3.194	385.455
11.5	-0.007	0.069	0.304	2.863	1016.074
16.1	0.006	0.071	0.063	2.604	1143.03
20.7	0.023	0.07	0.114	2.669	297.849
25.29	0.019	0.071	0.09	2.635	369.354
29.89	0.016	0.073	0.137	2.703	460.278
34.5	0.022	0.073	0.141	2.486	331.488
39.09	0.016	0.069	0.102	2.656	437.364
43.7	0.018	0.072	0.05	2.761	398.261
48.29	0.007	0.074	0.187	2.7	1062.565
52.9	0.044	0.068	0.17	2.588	155.852
55.2	0.066	0.08	0.329	2.712	122.112
57.5	0.084	0.093	0.37	2.665	111.415

Location #2

Z	U Mean	U RMS	U Skew	U Flat	U Turb
(mm)	(m/s)	(m/s)	(m/s)	(m/s)	(%)
0	0.244	0.038	-0.338	2.829	15.483
1.14	0.254	0.035	-0.4	3.506	13.614
2.29	0.268	0.029	-0.401	3.194	10.872
3.45	0.264	0.029	-0.324	3.792	11.013
4.59	0.265	0.028	-0.481	4.062	10.712
6.9	0.263	0.032	-0.337	3.714	12.153
9.19	0.255	0.033	-0.331	3.479	12.775
11.5	0.254	0.033	-0.578	3.828	12.882
16.1	0.253	0.032	-0.331	3.203	12.724
20.7	0.253	0.034	-0.254	2.887	13.245
25.29	0.256	0.032	-0.164	3.111	12.387
29.89	0.258	0.032	-0.368	3.281	12.25
34.5	0.26	0.031	-0.376	3.475	11.931
39.09	0.261	0.032	-0.189	3.133	12.404
43.7	0.26	0.034	-0.448	3.594	13.069
48.29	0.273	0.03	-0.081	2.941	10.837
52.9	0.287	0.027	-0.368	3.487	9.33
55.2	0.295	0.028	-0.527	4.02	9.631
57.5	0.302	0.029	-0.224	3.337	9.673

Experiment PS#6

Location #3

Z	U Mean	U RMS	U Skew	U Flat	U Turb
(mm)	(m/s)	(m/s)	(m/s)	(m/s)	(%)
0	0.171	0.04	0.077	2.865	23.358
1.14	0.183	0.038	0.109	2.998	20.883
2.29	0.19	0.039	-0.08	2.925	20.783
3.45	0.187	0.04	0.081	2.857	21.129
4.59	0.187	0.043	-0.074	2.835	23.048
6.9	0.183	0.043	-0.094	2.888	23.775
9.19	0.178	0.043	-0.008	2.766	23.936
11.5	0.175	0.04	0.112	2.801	22.935
16.1	0.173	0.04	0.065	2.765	22.981
20.7	0.175	0.04	0.104	2.846	22.967
25.29	0.178	0.042	0.053	2.872	23.739
29.89	0.179	0.04	0.187	3.115	22.446
34.5	0.174	0.038	0.055	2.512	21.614
39.09	0.178	0.04	0.057	2.974	22.567
43.7	0.182	0.04	-0.025	3.054	21.97
48.29	0.189	0.042	0.136	2.753	22.441
52.9	0.194	0.043	-0.056	2.943	22.302
55.2	0.201	0.043	0.129	2.797	21.146
57.5	0.216	0.041	-0.081	3.071	18.858

Location #4

Z	U Mean	U RMS	U Skew	U Flat	U Turb
(mm)	(m/s)	(m/s)	(m/s)	(m/s)	(%)
0	0.149	0.038	0.09	2.996	25.639
1.14	0.171	0.037	0.005	2.979	21.402
2.29	0.185	0.037	0.002	2.707	19.775
3.45	0.181	0.037	-0.087	3.009	20.182
4.59	0.179	0.038	-0.07	2.805	21.361
6.9	0.171	0.041	0.156	2.917	23.751
9.19	0.165	0.039	0.257	3.061	23.379
11.5	0.16	0.039	-0.067	3.083	24.687
16.1	0.158	0.038	0.089	2.97	23.97
20.7	0.161	0.038	0.258	3.061	23.656
25.29	0.166	0.038	-0.079	2.979	22.62
29.89	0.166	0.038	0.127	2.935	22.683
34.5	0.163	0.037	0.223	3.212	22.967
39.09	0.164	0.038	0.111	3.05	23.204
43.7	0.168	0.039	-0.024	3.007	23.4
48.29	0.175	0.04	-0.032	3.033	23.156
52.9	0.175	0.04	-0.023	2.858	23.094
55.2	0.178	0.038	0.062	3.094	21.652
57.5	0.177	0.038	-0.095	2.634	21.795

Experiment PS#6

Location #5

Z	U Mean	U RMS	U Skew	U Flat	U Turb
(mm)	(m/s)	(m/s)	(m/s)	(m/s)	(%)
0	0.238	0.038	-0.39	3.073	15.912
1.14	0.249	0.034	-0.397	3.394	13.718
2.29	0.264	0.028	-0.425	3.467	10.655
3.45	0.264	0.028	-0.218	3.258	10.672
4.59	0.263	0.027	-0.458	3.706	10.422
6.9	0.256	0.03	-0.339	3.386	11.569
9.19	0.25	0.032	-0.375	3.55	12.814
11.5	0.246	0.033	-0.611	4.622	13.394
16.1	0.245	0.032	-0.358	3.572	13.04
20.7	0.248	0.03	-0.416	3.256	12.241
25.29	0.25	0.032	-0.284	2.888	12.938
29.89	0.255	0.032	-0.345	3.154	12.368
34.5	0.252	0.031	-0.241	3.142	12.15
39.09	0.255	0.03	-0.414	3.362	11.711
43.7	0.254	0.03	-0.346	3.343	11.854
48.29	0.258	0.029	-0.277	3.28	11.381
52.9	0.261	0.03	-0.508	3.988	11.524
55.2	0.265	0.027	-0.244	3.375	10.118
57.5	0.258	0.029	-0.29	3.556	11.417

Location #6

Z	U Mean	U RMS	U Skew	U Flat	U Turb
(mm)	(m/s)	(m/s)	(m/s)	(m/s)	(%)
0	0.152	0.043	0.284	3.387	28.115
1.14	0.158	0.046	0.109	3.182	28.92
2.29	0.17	0.047	-0.054	3.038	27.647
3.45	0.172	0.05	-0.104	2.814	29.102
4.59	0.164	0.05	-0.224	3.215	30.492
6.9	0.148	0.054	-0.014	2.532	36.118
9.19	0.131	0.052	-0.069	2.817	39.628
11.5	0.127	0.051	-0.001	2.883	40.274
16.1	0.119	0.05	0.212	3.181	42.226
20.7	0.134	0.05	0.01	2.995	36.93
25.29	0.134	0.05	0.13	2.728	37.442
29.89	0.137	0.049	0.113	2.851	35.378
34.5	0.136	0.049	0.097	2.87	36.045
39.09	0.137	0.05	0.056	2.921	36.876
43.7	0.144	0.053	-0.015	2.9	36.849
48.29	0.146	0.052	0.022	2.944	35.897
52.9	0.148	0.057	0	2.732	38.593
55.2	0.139	0.059	0.133	3	42.333
57.5	0.135	0.057	0.084	2.798	42.438

Experiment FS#1

Location #1

Z	U Mean	U RMS	U Skew	U Flat	U Turb
(mm)	(m/s)	(m/s)	(m/s)	(m/s)	(%)
0	0.065	0.075	0.101	2.876	114.346
1.14	0.066	0.074	-0.197	2.934	113.237
2.29	0.068	0.07	-0.118	2.909	102.426
3.45	0.059	0.075	-0.015	3.13	125.989
4.59	0.049	0.071	-0.11	2.955	145.844
6.9	0.036	0.076	0.042	2.779	210.814
9.19	0.041	0.073	-0.137	2.817	177.529
11.5	0.038	0.072	0.072	2.863	191.585
16.1	0.057	0.071	-0.099	2.985	124.01
20.7	0.049	0.074	0.051	2.916	152.376
25.29	0.055	0.079	-0.062	2.962	143.434
29.89	0.052	0.081	0.082	2.634	154.666
34.5	0.062	0.079	-0.043	3.3	127.274
39.09	0.059	0.086	0.327	3.192	147.06
43.7	0.085	0.085	0.036	3.183	100.132
48.29	0.095	0.079	0.118	3.307	84.016
52.9	0.088	0.098	0.108	2.872	111.749
57.5	0.068	0.101	0.15	3.045	148.086
62.09	0.073	0.104	0.287	3.252	143.138
66.69	0.069	0.11	0.341	2.996	159.919
71.3	0.161	0.103	0.092	2.916	63.949
73.59	0.289	0.117	-0.078	2.579	40.576
75.9	0.359	0.1	-0.197	2.91	27.716
78.19	0.377	0.091	-0.116	2.687	24.157
80.5	0.405	0.077	-0.122	2.601	19.011
85.09	0.438	0.084	-0.125	2.698	19.104
89.69	0.443	0.079	-0.125	2.607	17.821
94.3	0.473	0.079	-0.093	2.442	16.631
98.9	0.503	0.069	-0.183	2.78	13.629
103.5	0.522	0.057	-0.092	2.966	11.001
107.8	0.538	0.054	-0.045	3.58	10.065

Experiment FS#1

Location #2

Z	U Mean	U RMS	U Skew	U Flat	U Turb
(mm)	(m/s)	(m/s)	(m/s)	(m/s)	(%)
0	0.218	0.039	-0.153	3.103	17.743
1.14	0.227	0.04	-0.285	3.229	17.487
2.29	0.234	0.037	-0.45	3.511	15.976
3.45	0.231	0.037	-0.162	3.052	16.069
4.59	0.237	0.037	-0.174	3.144	15.585
6.9	0.231	0.035	-0.349	3.344	15.254
9.19	0.236	0.037	-0.196	3.254	15.692
11.5	0.232	0.039	-0.395	3.462	16.948
16.1	0.237	0.038	-0.465	4.377	16.054
20.7	0.241	0.04	-0.316	3.58	16.598
25.29	0.237	0.039	-0.069	3.306	16.499
29.89	0.243	0.04	-0.524	3.965	16.465
34.5	0.254	0.046	0.228	3.423	17.991
39.09	0.249	0.043	-0.135	3.518	17.29
43.7	0.263	0.052	0.537	3.882	19.852
48.29	0.252	0.055	0.31	3.328	21.958
52.9	0.265	0.066	0.759	3.946	24.925
57.5	0.281	0.069	0.511	3.5	24.447
62.09	0.303	0.075	0.737	3.916	24.73
66.69	0.315	0.081	0.589	3.323	25.788
71.3	0.363	0.087	0.192	2.636	24.024
73.59	0.368	0.094	0.481	2.764	25.613
75.9	0.38	0.084	0.083	2.672	22.022
78.19	0.403	0.084	0.073	2.76	20.84
80.5	0.411	0.087	-0.073	2.248	21.028
85.09	0.429	0.077	-0.006	2.421	17.993
89.69	0.456	0.078	-0.1	2.702	17.192
94.3	0.478	0.077	-0.238	2.779	16.065
98.9	0.508	0.062	-0.285	3.285	12.126
103.5	0.515	0.066	-0.42	3.048	12.736
107.8	0.532	0.06	0.132	2.851	11.246

Experiment FS#1

Location #3

Z	U Mean	U RMS	U Skew	U Flat	U Turb
(mm)	(m/s)	(m/s)	(m/s)	(m/s)	(%)
0	0.175	0.043	0.293	3.222	24.771
1.14	0.18	0.042	0.318	3.397	23.262
2.29	0.184	0.042	0.168	3.452	22.781
3.45	0.18	0.045	0.212	3.871	25.071
4.59	0.183	0.044	0.022	2.921	24.131
6.9	0.175	0.042	0.067	2.82	23.711
9.19	0.181	0.042	0.066	2.907	23.368
11.5	0.179	0.042	0.338	3.394	23.709
16.1	0.18	0.045	0.259	3.172	25.087
20.7	0.182	0.045	0.025	3.144	24.545
25.29	0.184	0.048	0.087	2.912	25.887
29.89	0.191	0.047	0.343	3.615	24.634
34.5	0.199	0.055	0.7	4.303	27.645
39.09	0.195	0.053	0.55	4.227	27.11
43.7	0.195	0.052	0.293	3.014	26.592
48.29	0.208	0.061	0.669	4.611	29.131
52.9	0.224	0.057	0.444	4.311	25.357
57.5	0.22	0.063	0.558	3.536	28.643
62.09	0.256	0.077	0.448	3.394	29.872
66.69	0.286	0.083	0.441	2.962	29.195
71.3	0.332	0.096	0.319	2.64	28.829
73.59	0.348	0.085	0.17	2.537	24.346
75.9	0.358	0.091	0.229	2.796	25.495
78.19	0.357	0.077	0.132	2.6	21.622
80.5	0.408	0.091	0.034	2.55	22.393
85.09	0.428	0.084	-0.056	2.328	19.561
89.69	0.467	0.077	-0.109	2.403	16.501
94.3	0.471	0.067	-0.113	2.387	14.328
98.9	0.484	0.075	-0.34	2.814	15.447
103.5	0.515	0.05	-0.164	3.045	9.721
107.8	0.532	0.059	-0.288	3.338	11.002

Experiment FS#1

Location #4

Z	U Mean	U RMS	U Skew	U Flat	U Turb
(mm)	(m/s)	(m/s)	(m/s)	(m/s)	(%)
0	0.151	0.045	0.252	3.175	29.601
1.14	0.169	0.042	0.33	3.364	24.689
2.29	0.167	0.039	0.279	3.531	23.254
3.45	0.173	0.042	0.159	3.159	24.48
4.59	0.164	0.043	0.289	3.231	26.441
6.9	0.162	0.042	0.29	2.787	26.063
9.19	0.167	0.041	0.329	3.317	24.788
11.5	0.164	0.042	0.23	2.877	25.558
16.1	0.164	0.039	0.074	3.057	24.138
20.7	0.165	0.043	0.109	2.595	26.123
25.29	0.167	0.048	0.454	3.478	28.711
29.89	0.179	0.046	0.214	2.85	25.466
34.5	0.178	0.049	0.124	3.123	27.356
39.09	0.182	0.049	0.425	3.587	26.877
43.7	0.18	0.052	0.134	2.902	28.845
48.29	0.193	0.056	0.352	3.184	29.237
52.9	0.205	0.065	0.734	3.892	31.684
57.5	0.222	0.061	0.348	3.251	27.656
62.09	0.235	0.082	0.805	3.729	34.791
66.69	0.265	0.086	0.228	2.616	32.631
71.3	0.324	0.095	0.11	2.595	29.298
73.59	0.312	0.095	0.384	2.402	30.387
75.9	0.359	0.09	0.356	2.657	24.96
78.19	0.383	0.091	0.236	2.756	23.905
80.5	0.396	0.084	0.034	2.604	21.282
85.09	0.422	0.089	-0.079	2.207	21.105
89.69	0.452	0.081	0.05	2.832	17.989
94.3	0.494	0.076	-0.293	2.895	15.442
98.9	0.515	0.065	-0.254	2.794	12.665
103.5	0.536	0.064	-0.476	3.228	12.009
107.8	0.545	0.064	-0.193	3.23	11.718

Experiment FS#1

Location #5

Z	U Mean	U RMS	U Skew	U Flat	U Turb
(mm)	(m/s)	(m/s)	(m/s)	(m/s)	(%)
0	0.214	0.042	-0.074	2.645	19.381
1.14	0.228	0.038	-0.339	3.479	16.695
2.29	0.226	0.039	-0.288	3.303	17.342
3.45	0.233	0.04	-0.259	2.937	17.225
4.59	0.234	0.037	-0.187	3.176	15.621
6.9	0.231	0.041	-0.307	3.516	17.564
9.19	0.236	0.038	0.009	3.251	16.144
11.5	0.241	0.04	-0.241	3.669	16.494
16.1	0.241	0.04	0.11	3.653	16.53
20.7	0.234	0.041	0.113	3.639	17.695
25.29	0.237	0.039	-0.442	3.58	16.372
29.89	0.25	0.043	0.072	3.278	17.181
34.5	0.245	0.044	0.104	3.147	17.872
39.09	0.244	0.046	0.867	6.08	19.056
43.7	0.266	0.049	0.39	3.804	18.347
48.29	0.266	0.055	0.209	3.517	20.663
52.9	0.269	0.058	0.642	3.771	21.551
57.5	0.271	0.06	0.648	4.624	22.263
62.09	0.311	0.084	0.696	3.736	27.119
66.69	0.333	0.092	0.536	2.814	27.639
71.3	0.358	0.083	0.386	2.945	23.23
73.59	0.369	0.089	0.216	2.291	24.048
75.9	0.375	0.082	0.205	2.697	21.743
78.19	0.373	0.083	0.244	2.854	22.146
80.5	0.395	0.091	0.052	2.362	23.05
85.09	0.45	0.077	-0.094	2.548	17.155
89.69	0.454	0.085	0.059	2.631	18.73
94.3	0.478	0.08	-0.537	2.823	16.766
98.9	0.513	0.07	-0.178	2.989	13.568
103.5	0.524	0.062	-0.167	2.788	11.752
107.8	0.542	0.066	-0.419	4.106	12.26

Experiment FS#1

Location #6

Z	U Mean	U RMS	U Skew	U Flat	U Turb
(mm)	(m/s)	(m/s)	(m/s)	(m/s)	(%)
0	0.145	0.054	0.368	3.872	37.434
1.14	0.155	0.054	0.065	2.883	34.967
2.29	0.154	0.052	0.058	2.961	33.944
3.45	0.157	0.055	0.003	2.974	35.152
4.59	0.15	0.054	0.067	2.907	35.886
6.9	0.145	0.054	0.086	2.889	37.145
9.19	0.138	0.053	0.173	3.081	38.329
11.5	0.132	0.054	0.151	2.9	40.945
16.1	0.143	0.053	0.174	3.22	37.259
20.7	0.145	0.059	0.152	3.138	40.818
25.29	0.14	0.055	0.135	3.136	38.981
29.89	0.149	0.062	0.195	3.083	41.307
34.5	0.157	0.062	0.255	3.169	39.714
39.09	0.158	0.063	0.307	3.565	40.235
43.7	0.169	0.065	0.353	3.576	38.296
48.29	0.175	0.068	0.283	3.38	38.872
52.9	0.184	0.075	0.395	3.61	40.467
57.5	0.174	0.072	0.409	3.507	41.192
62.09	0.197	0.078	0.494	3.309	39.592
66.69	0.223	0.088	0.508	3.156	39.44
71.3	0.315	0.109	0.06	2.371	34.54
73.59	0.335	0.105	0.081	2.524	31.358
75.9	0.356	0.098	0.133	2.636	27.586
78.19	0.414	0.095	-0.087	2.653	22.979
80.5	0.413	0.084	-0.132	2.917	20.406
85.09	0.426	0.086	-0.025	2.454	20.17
89.69	0.465	0.079	-0.226	2.667	16.98
94.3	0.497	0.075	-0.223	2.825	15.153
98.9	0.501	0.071	-0.431	3.01	14.161
103.5	0.524	0.063	-0.091	2.96	11.982
107.8	0.553	0.06	-0.083	3.15	10.807

Experiment FS#2

Location #1

Z	U Mean	U RMS	U Skew	U Flat	U Turb
(mm)	(m/s)	(m/s)	(m/s)	(m/s)	(%)
5.75	0.014	0.068	0.201	3.806	488.622
6.9	0.007	0.064	0.266	3.923	948.275
9.19	0.003	0.062	-0.001	3.478	2379.185
11.5	0.011	0.065	-0.02	4.22	580.466
16.1	0.007	0.07	-0.179	3.82	1030.991
20.7	0.01	0.07	-0.12	3.368	706.091
25.29	0.011	0.069	0.101	3.89	628.809
29.89	0.013	0.069	0.011	3.68	527.725
34.5	0.01	0.073	-0.123	3.753	751.298
39.09	0.013	0.075	-0.031	3.68	569.889
43.7	0.008	0.078	0.106	3.957	943.703
48.29	0.018	0.085	-0.099	3.814	471.49
52.9	0.02	0.086	-0.021	4.031	437.527
57.5	0.022	0.089	0.116	4.285	405.076
62.09	0	0.097	-0.396	4.567	27659.71
66.69	-0.025	0.108	-0.393	3.677	425.805
71.3	-0.08	0.113	0.046	3.333	141.827
73.59	-0.087	0.085	0.455	3.099	97.515
75.9	-0.061	0.069	0.507	3.8	113.616
78.19	-0.043	0.055	0.244	3.196	128.318
80.5	-0.03	0.056	0.014	2.87	183.579
85.09	-0.022	0.052	0.205	3.039	237.313
89.69	-0.019	0.054	0.224	3.675	277.643
94.3	-0.015	0.05	0.266	3.563	329.878
98.9	-0.016	0.047	0.221	3.167	287.115
103.5	-0.019	0.036	0.431	4.022	192.671

Experiment FS#2

Location #2

Z	U Mean	U RMS	U Skew	U Flat	U Turb
(mm)	(m/s)	(m/s)	(m/s)	(m/s)	(%)
4.59	-0.003	0.03	-0.076	3.447	1118.677
5.75	-0.003	0.03	-0.305	3.893	998.688
6.9	-0.003	0.032	-0.089	3.744	1092.585
9.19	-0.003	0.033	-0.013	3.794	974.973
11.5	-0.001	0.033	-0.093	3.374	2461.668
16.1	-0.001	0.033	-0.082	3.525	3233.865
20.7	0.003	0.033	0.024	3.259	1214.106
25.29	-0.004	0.039	-0.391	3.98	894.018
29.89	0	0.036	-0.359	3.675	8414.073
34.5	-0.002	0.041	-0.786	4.893	1820.529
39.09	-0.002	0.042	-0.146	3.502	2111.663
43.7	0.004	0.044	-0.542	4.164	1216.414
48.29	0	0.049	-0.652	4.181	9997.133
52.9	0.008	0.05	-0.407	3.508	609.346
57.5	0.002	0.055	-0.644	3.681	3025.646
62.09	0.009	0.061	-0.602	3.837	647.743
66.69	0.015	0.061	-0.38	2.928	410.429
71.3	0.018	0.061	-0.218	2.989	340.414
73.59	0.02	0.062	-0.076	2.976	307.349
75.9	0.018	0.06	-0.248	3.014	339.038
78.19	0.014	0.063	-0.016	3.171	462.147
80.5	0.01	0.057	0.094	2.9	571.935
85.09	0.006	0.056	0.182	2.961	941.435
89.69	0.006	0.056	0.241	2.879	992.068
94.3	0.006	0.051	0.141	3.136	922.387
98.9	0.006	0.043	0.336	3.216	680.734
103.5	0.003	0.037	0.389	3.655	1094.961

Experiment FS#2

Location #3

Z	U Mean	U RMS	U Skew	U Flat	U Turb
(mm)	(m/s)	(m/s)	(m/s)	(m/s)	(%)
4.59	0.008	0.038	0.113	3.482	495.465
5.75	0.009	0.039	0.132	3.939	444.686
6.9	0.011	0.042	-0.065	3.628	396.355
9.19	0.008	0.041	-0.074	3.468	516.354
11.5	0.002	0.044	-0.133	3.543	1949.112
16.1	0.002	0.045	-0.016	3.323	2274.379
20.7	0.006	0.045	-0.156	3.331	775.881
25.29	0.003	0.049	-0.166	3.166	1905.269
29.89	0.007	0.048	-0.277	3.298	683.498
34.5	0.005	0.05	-0.247	3.6	1059.996
39.09	0.008	0.05	-0.292	3.713	661.194
43.7	0.006	0.053	-0.175	3.276	831.673
48.29	0.011	0.054	-0.351	3.565	486.393
52.9	0.015	0.057	-0.342	3.594	392.542
57.5	0.008	0.061	-0.268	3.164	730.552
62.09	0	0.071	-0.431	2.946	19013.46
66.69	-0.004	0.074	-0.264	2.974	1887.384
71.3	-0.001	0.068	0.003	2.877	8213.503
73.59	-0.009	0.064	0.311	3.047	740.08
75.9	-0.001	0.062	0.335	3.176	10818.71
78.19	-0.005	0.062	0.224	3.2	1240.281
80.5	0.006	0.058	0.127	3.019	926.086
85.09	0.004	0.053	0.099	3.252	1408.098
89.69	0.016	0.055	0.443	4.142	337.166
94.3	0.007	0.049	0.133	3.349	670.281
98.9	0.015	0.05	0.45	3.836	329.986
103.5	0.007	0.04	0.405	3.871	585.534

Experiment FS#2

Location #4

Z	U Mean	U RMS	U Skew	U Flat	U Turb
(mm)	(m/s)	(m/s)	(m/s)	(m/s)	(%)
4.59	-0.003	0.035	-0.152	3.428	1142.529
5.75	-0.004	0.035	-0.066	3.498	901.815
6.9	-0.003	0.037	-0.055	3.891	1339.66
9.19	-0.005	0.038	0.09	3.389	712.711
11.5	0	0.039	0.023	3.212	12061.85
16.1	-0.003	0.039	-0.228	3.576	1563.911
20.7	-0.005	0.041	-0.212	3.008	791.909
25.29	-0.006	0.041	-0.356	3.688	728.268
29.89	-0.005	0.044	-0.302	3.772	911.33
34.5	-0.004	0.045	-0.118	3.525	1182.538
39.09	-0.007	0.051	-0.53	3.464	759.379
43.7	-0.009	0.051	-0.512	3.969	537.235
48.29	-0.004	0.052	-0.523	3.859	1402.767
52.9	-0.007	0.058	-0.71	4.316	866.738
57.5	-0.004	0.062	-0.644	3.879	1525.495
62.09	-0.004	0.066	-0.55	3.699	1770.613
66.69	0.002	0.067	-0.284	3.323	3160.642
71.3	0.008	0.064	-0.057	2.81	836.901
73.59	0.013	0.058	-0.079	2.881	431.023
75.9	0.016	0.057	0.285	2.846	347.386
78.19	0.016	0.061	0.318	3.155	370.566
80.5	0.013	0.052	0.213	3.453	391.425
85.09	0.011	0.05	-0.072	3.625	447.524
89.69	0.011	0.051	0.13	3.301	475.299
94.3	0.003	0.048	0.264	3.246	1914.454
98.9	0.007	0.045	0.326	3.183	636.5
103.5	0.003	0.04	0.382	4.434	1402.804

Experiment FS#2

Location #5

Z	U Mean	U RMS	U Skew	U Flat	U Turb
(mm)	(m/s)	(m/s)	(m/s)	(m/s)	(%)
4.59	-0.001	0.031	-0.074	3.776	3084.364
5.75	-0.002	0.03	0.082	3.392	1748.461
6.9	-0.004	0.031	-0.087	4.071	833.617
9.19	0	0.033	0.161	3.699	8561.589
11.5	-0.001	0.032	-0.125	3.441	3456.073
16.1	-0.001	0.033	-0.021	4.012	2221.918
20.7	0.005	0.035	-0.153	3.463	685.997
25.29	0.002	0.036	-0.403	3.226	1985.505
29.89	-0.001	0.034	-0.218	3.381	4873.642
34.5	0.003	0.038	-0.251	4.108	1177.328
39.09	-0.001	0.039	-0.417	3.653	4452.272
43.7	0.005	0.039	-0.355	3.867	713.349
48.29	0.007	0.048	-0.441	3.673	719.107
52.9	0.005	0.05	-0.822	5.141	927.934
57.5	0.002	0.056	-0.458	3.558	2287.554
62.09	0.012	0.056	-0.474	3.591	466.848
66.69	0.017	0.057	-0.285	3.05	341.103
71.3	0.022	0.058	0.095	3.381	265.331
73.59	0.015	0.057	0.124	2.912	373.615
75.9	0.015	0.059	0.172	2.997	401.653
78.19	0.018	0.056	0.107	2.968	318.109
80.5	0.017	0.054	0.054	3.027	312.323
85.09	0.019	0.053	0.047	3.196	278.553
89.69	0.018	0.05	0.26	3.373	282.094
94.3	0.013	0.048	0.24	3.492	371.106
98.9	0.012	0.044	0.142	3.449	368.285
103.5	0.012	0.038	0.252	3.07	313.86

Experiment FS#2

Location #6

Z	U Mean	U RMS	U Skew	U Flat	U Turb
(mm)	(m/s)	(m/s)	(m/s)	(m/s)	(%)
5.75	0.011	0.051	0.178	3.847	481.129
6.9	0.007	0.051	0.26	3.708	689.448
9.19	0.007	0.049	-0.045	3.436	702.468
11.5	0.003	0.05	-0.123	3.636	1676.755
16.1	0.005	0.051	-0.165	4.029	1000.794
20.7	0.005	0.052	0.026	3.445	977.247
25.29	0.004	0.055	-0.064	3.665	1446.622
29.89	0.004	0.056	-0.063	3.454	1556.314
34.5	0.005	0.057	-0.218	3.546	1063.842
39.09	0.005	0.057	-0.179	3.609	1226.879
43.7	0.009	0.062	-0.177	3.636	700.727
48.29	0.006	0.063	-0.191	3.618	1093.172
52.9	0.012	0.068	-0.224	3.964	569.257
57.5	0.013	0.075	-0.363	4.03	582.861
62.09	0.003	0.083	-0.431	4.511	2656.718
66.69	-0.037	0.096	-0.536	3.57	258.782
71.3	-0.041	0.081	0.268	3.049	199.665
73.59	-0.039	0.071	0.412	3.225	182.225
75.9	-0.025	0.061	0.619	3.882	247.888
78.19	-0.019	0.054	0.397	3.766	286.808
80.5	-0.017	0.056	0.021	3.126	330.267
85.09	-0.005	0.055	0.137	3.556	1096.831
89.69	0.001	0.052	0.09	3.161	4401.3
94.3	-0.002	0.047	0.295	3.328	2467.719
98.9	0.004	0.041	0.288	4.136	1018.586
103.5	0.005	0.038	0.447	4.088	731.567
107.8	-0.006	0.037	1.057	4.231	660.178

Experiment FS#3

Location #1

Z	U Mean	U RMS	U Skew	U Flat	U Turb
(mm)	(m/s)	(m/s)	(m/s)	(m/s)	(%)
0	0.083	0.074	-0.116	2.593	88.445
1.14	0.1	0.077	-0.298	2.839	76.519
2.29	0.084	0.074	-0.137	2.68	87.898
3.45	0.068	0.081	-0.022	2.476	118.91
4.59	0.044	0.081	-0.045	2.524	183.725
6.9	0.032	0.084	0.24	2.504	265.272
9.19	0.018	0.085	0.215	2.433	477.026
11.5	0.025	0.079	0.151	2.597	317.578
16.1	0.035	0.082	-0.02	2.549	235.364
20.7	0.039	0.079	0.016	2.552	201.522
25.29	0.039	0.086	0.035	2.696	219.278
29.89	0.04	0.093	0.05	2.694	234.174
34.5	0.03	0.098	0.259	3.164	331.495
39.09	0.038	0.088	0.102	2.95	230.623
43.7	0.036	0.091	0.043	2.711	255.55
48.29	0.039	0.098	0.028	2.76	251.688
52.9	0.024	0.106	0.376	3.163	437.518
57.5	0.014	0.107	0.273	3.055	770.292
62.09	0.009	0.102	0.169	2.894	1095.134
66.69	-0.012	0.099	0.597	3.713	864.832
71.3	0.132	0.101	0.242	3.304	77.026
73.59	0.327	0.13	0.102	2.633	39.754
75.9	0.374	0.103	0.28	2.669	27.581
78.19	0.387	0.101	0.148	2.877	26.214
80.5	0.4	0.092	0.233	2.653	22.866
85.09	0.435	0.091	-0.041	2.623	21.032
89.69	0.459	0.088	-0.003	2.481	19.242
94.3	0.467	0.082	-0.036	2.715	17.508
98.9	0.503	0.073	-0.186	2.828	14.554
103.5	0.512	0.071	-0.296	3.185	13.927
107.8	0.529	0.064	-0.102	2.781	12.053

Experiment FS#3

Location #2

Z	U Mean	U RMS	U Skew	U Flat	U Turb
(mm)	(m/s)	(m/s)	(m/s)	(m/s)	(%)
0	0.2	0.043	0.042	2.877	21.49
1.14	0.216	0.039	-0.248	3.366	18.13
2.29	0.224	0.038	-0.169	3.204	16.927
3.45	0.216	0.039	-0.117	3.5	17.874
4.59	0.228	0.04	-0.042	3.213	17.487
6.9	0.225	0.039	-0.059	3.716	17.428
9.19	0.221	0.04	-0.284	2.971	18.087
11.5	0.22	0.043	-0.039	3.646	19.661
16.1	0.222	0.042	-0.086	3.083	19.102
20.7	0.219	0.042	-0.275	3.631	19.301
25.29	0.223	0.045	-0.086	2.942	20.238
29.89	0.22	0.044	-0.108	3.861	20.104
34.5	0.229	0.047	0.271	3.702	20.683
39.09	0.239	0.054	0.633	4.51	22.421
43.7	0.245	0.053	0.03	3.311	21.813
48.29	0.255	0.063	0.513	3.987	24.877
52.9	0.262	0.065	0.413	3.587	24.902
57.5	0.271	0.078	0.803	4.476	28.807
62.09	0.284	0.082	0.667	3.44	28.872
66.69	0.295	0.077	0.421	2.898	26.092
71.3	0.335	0.085	0.294	2.967	25.463
73.59	0.341	0.095	0.346	2.388	27.983
75.9	0.341	0.092	0.393	2.692	26.909
78.19	0.377	0.083	0.156	2.632	21.946
80.5	0.385	0.09	0.142	2.451	23.289
85.09	0.412	0.092	0.056	2.659	22.374
89.69	0.415	0.089	0.072	2.441	21.502
94.3	0.447	0.082	-0.137	2.519	18.243
98.9	0.477	0.072	-0.169	2.737	15.008
103.5	0.484	0.078	-0.276	2.735	16.092
107.8	0.527	0.062	0.069	3.825	11.826

Experiment FS#3

Location #3

Z	U Mean	U RMS	U Skew	U Flat	U Turb
(mm)	(m/s)	(m/s)	(m/s)	(m/s)	(%)
0	0.166	0.046	0.27	2.997	27.746
1.14	0.176	0.044	0.283	3.419	24.922
2.29	0.183	0.045	0.236	3.187	24.411
3.45	0.18	0.043	0.044	2.953	23.79
4.59	0.183	0.046	0.33	4.202	25.122
6.9	0.169	0.044	-0.029	2.738	26.16
9.19	0.176	0.045	0.048	3.02	25.359
11.5	0.171	0.047	0.28	3.373	27.7
16.1	0.175	0.045	0.21	2.86	25.518
20.7	0.178	0.048	0.369	3.314	27.011
25.29	0.18	0.049	0.181	3.295	27.242
29.89	0.198	0.052	0.335	3.546	26.542
34.5	0.194	0.054	0.445	3.526	27.801
39.09	0.195	0.059	0.466	3.519	30.066
43.7	0.191	0.053	0.383	3.489	27.523
48.29	0.208	0.067	0.714	4.119	32.155
52.9	0.209	0.06	0.313	3.362	28.935
57.5	0.224	0.068	0.645	3.368	30.512
62.09	0.258	0.08	0.528	3.134	31.227
66.69	0.281	0.095	0.687	3.105	33.841
71.3	0.334	0.101	0.143	2.408	30.16
73.59	0.354	0.097	0.09	2.348	27.469
75.9	0.355	0.095	0.243	2.493	26.793
78.19	0.362	0.095	0.218	2.554	26.244
80.5	0.376	0.088	0.063	2.426	23.28
85.09	0.414	0.092	-0.038	2.641	22.221
89.69	0.449	0.081	-0.14	2.522	17.951
94.3	0.456	0.079	0.054	2.514	17.414
98.9	0.489	0.081	-0.336	2.791	16.469
103.5	0.509	0.076	-0.339	3.204	14.925
107.8	0.53	0.066	-0.103	2.919	12.445

Experiment FS#3

Location #4

Z	U Mean	U RMS	U Skew	U Flat	U Turb
(mm)	(m/s)	(m/s)	(m/s)	(m/s)	(%)
0	0.148	0.043	0.231	3.117	29.205
1.14	0.157	0.043	0.163	3.323	27.178
2.29	0.166	0.036	0.161	2.949	21.88
3.45	0.173	0.045	0.095	3.225	25.718
4.59	0.165	0.041	-0.105	3.188	24.693
6.9	0.154	0.043	0.009	3.337	27.75
9.19	0.15	0.037	0.005	3.2	24.424
11.5	0.155	0.042	0.006	3.191	26.844
16.1	0.156	0.04	-0.078	2.871	25.635
20.7	0.163	0.04	0.393	4.109	24.748
25.29	0.161	0.042	0.18	3.065	26.086
29.89	0.171	0.049	0.285	3.473	28.6
34.5	0.173	0.051	0.334	3.277	29.319
39.09	0.167	0.05	0.19	3.228	29.96
43.7	0.176	0.054	0.487	3.843	30.857
48.29	0.189	0.061	0.52	3.721	32.225
52.9	0.188	0.06	0.259	3.232	31.81
57.5	0.216	0.073	0.816	3.743	33.672
62.09	0.23	0.071	0.611	3.358	30.765
66.69	0.267	0.09	0.434	2.88	33.781
71.3	0.284	0.086	0.269	2.625	30.14
73.59	0.313	0.087	0.401	2.655	27.691
75.9	0.35	0.091	0.069	2.569	25.915
78.19	0.373	0.095	0.102	2.438	25.465
80.5	0.392	0.093	0.136	2.47	23.782
85.09	0.407	0.086	0.037	2.707	21.231
89.69	0.452	0.08	0.094	2.611	17.589
94.3	0.441	0.086	-0.003	2.605	19.544
98.9	0.484	0.072	-0.241	2.965	14.781
103.5	0.519	0.066	-0.37	2.958	12.777
107.8	0.53	0.064	-0.363	3.386	12.132

Experiment FS#3

Location #5

Z	U Mean	U RMS	U Skew	U Flat	U Turb
(mm)	(m/s)	(m/s)	(m/s)	(m/s)	(%)
0	0.194	0.04	-0.121	3.072	20.915
1.14	0.201	0.04	0.006	3.206	19.696
2.29	0.216	0.036	0.065	3.205	16.595
3.45	0.218	0.037	0.006	3.196	16.975
4.59	0.221	0.038	-0.264	2.964	17.208
6.9	0.216	0.038	-0.062	3.151	17.458
9.19	0.213	0.038	-0.127	3.292	17.826
11.5	0.212	0.04	-0.091	2.866	18.627
16.1	0.214	0.041	-0.054	2.986	19.128
20.7	0.208	0.04	-0.321	3.248	19.273
25.29	0.213	0.039	-0.007	3.182	18.533
29.89	0.219	0.042	0.103	3.673	19.231
34.5	0.23	0.045	0.55	4.951	19.686
39.09	0.227	0.048	0.257	3.983	20.979
43.7	0.229	0.047	0.192	3.43	20.598
48.29	0.229	0.052	0.416	3.867	22.836
52.9	0.261	0.066	0.602	3.81	25.119
57.5	0.266	0.076	0.63	3.755	28.398
62.09	0.293	0.084	0.473	3.166	28.734
66.69	0.308	0.085	0.416	2.722	27.489
71.3	0.31	0.086	0.586	3.208	27.758
73.59	0.344	0.083	0.226	2.546	24.241
75.9	0.366	0.089	0.162	2.389	24.326
78.19	0.367	0.093	0.306	2.398	25.227
80.5	0.371	0.092	0.362	2.598	24.764
85.09	0.421	0.09	-0.082	2.687	21.471
89.69	0.436	0.077	-0.062	2.66	17.674
94.3	0.447	0.08	0.126	3	17.911
98.9	0.484	0.072	0.187	2.477	14.969
103.5	0.486	0.074	-0.127	2.951	15.329
107.8	0.524	0.066	-0.252	2.993	12.585

Experiment FS#3

Location #6

Z	U Mean	U RMS	U Skew	U Flat	U Turb
(mm)	(m/s)	(m/s)	(m/s)	(m/s)	(%)
0	0.121	0.044	0.324	3.429	36.15
1.14	0.122	0.043	0.129	2.925	35.008
2.29	0.147	0.046	0.119	3.163	31.345
3.45	0.153	0.048	-0.072	2.967	31.371
4.59	0.145	0.05	-0.167	3.277	34.85
6.9	0.139	0.048	0.059	3.096	34.404
9.19	0.123	0.049	-0.025	2.996	40.015
11.5	0.117	0.051	0.285	3.148	43.664
16.1	0.118	0.052	0.248	3.275	43.848
20.7	0.122	0.053	0.085	3.145	43.311
25.29	0.131	0.055	0.19	3.033	41.838
29.89	0.135	0.055	0.109	3.315	40.373
34.5	0.143	0.056	-0.049	3.146	39.123
39.09	0.147	0.053	0.104	3.073	36.287
43.7	0.153	0.064	0.388	3.906	41.513
48.29	0.163	0.071	0.548	4.009	43.751
52.9	0.152	0.068	0.337	4.025	44.926
57.5	0.155	0.075	0.215	3.226	48.226
62.09	0.165	0.074	0.481	3.786	45.077
66.69	0.198	0.087	0.477	3.427	44.15
71.3	0.266	0.102	0.317	2.773	38.372
73.59	0.314	0.105	0.134	2.743	33.394
75.9	0.353	0.098	-0.016	2.633	27.69
78.19	0.382	0.091	-0.17	2.709	23.736
80.5	0.388	0.092	0.17	2.636	23.579
85.09	0.4	0.088	0.067	2.418	21.919
89.69	0.445	0.08	-0.174	2.614	17.962
94.3	0.46	0.08	-0.157	2.641	17.401
98.9	0.488	0.071	-0.062	2.757	14.614
103.5	0.495	0.073	-0.265	3.101	14.778
107.8	0.512	0.065	-0.325	2.938	12.738

Experiment FS#4

Location #1

Z	U Mean	U RMS	U Skew	U Flat	U Turb
(mm)	(m/s)	(m/s)	(m/s)	(m/s)	(%)
0	0.027	0.079	0.229	2.577	289.507
1.14	0.03	0.075	0.117	3.029	248.252
2.29	0.033	0.075	0.234	2.981	223.78
3.45	-0.022	0.069	0.185	2.91	308.699
4.59	-0.019	0.073	0.272	2.815	374.705
6.9	-0.028	0.08	0.47	3.184	280.783
9.19	-0.037	0.078	0.521	3.121	209.347
11.5	-0.017	0.083	0.286	2.54	483.571
16.1	-0.001	0.091	0.15	2.433	8387.24
20.7	0.016	0.085	0.086	2.575	521.817
25.29	0.013	0.091	0.029	2.562	693.066
29.89	0.009	0.088	0.01	2.558	966.214
34.5	0.007	0.092	0.022	2.804	1379.65
39.09	-0.021	0.1	0.16	2.742	484.692
43.7	-0.018	0.095	0.239	2.706	532.581
48.29	0.006	0.107	0.319	2.906	1847.375
52.9	0.011	0.099	0.233	2.832	937.872
57.5	0.006	0.105	0.163	2.777	1630.703
62.09	-0.033	0.1	0.244	2.789	300.094
66.69	-0.06	0.09	0.414	3.499	148.327
71.3	-0.002	0.097	0.103	2.782	4717.485
73.59	0.093	0.107	0.277	3.212	114.732
75.9	0.298	0.134	0.033	2.573	44.916
78.19	0.393	0.108	-0.133	2.606	27.597
80.5	0.415	0.106	-0.122	3.007	25.62
85.09	0.442	0.093	0.01	2.501	21.035
89.69	0.459	0.09	-0.209	2.767	19.676
94.3	0.484	0.083	-0.03	2.893	17.104
98.9	0.524	0.081	0.052	2.928	15.432
103.5	0.522	0.08	-0.324	2.723	15.266
107.8	0.546	0.073	-0.273	2.961	13.353

Experiment FS#4

Location #2

Z	U Mean	U RMS	U Skew	U Flat	U Turb
(mm)	(m/s)	(m/s)	(m/s)	(m/s)	(%)
0	0.2	0.049	0.026	2.879	24.269
1.14	0.227	0.044	0.019	3.134	19.199
2.29	0.223	0.042	0.004	3.102	19.068
3.45	0.229	0.04	-0.254	3.569	17.538
4.59	0.225	0.04	-0.34	3.635	17.757
6.9	0.222	0.045	-0.256	3.155	20.419
9.19	0.22	0.042	-0.394	3.965	18.914
11.5	0.22	0.045	0.045	3.472	20.49
16.1	0.222	0.044	0.007	3.098	19.637
20.7	0.218	0.044	-0.263	3.453	20.232
25.29	0.235	0.043	0.071	3.205	18.338
29.89	0.233	0.048	-0.145	4.258	20.404
34.5	0.229	0.046	-0.046	3.715	20.179
39.09	0.239	0.047	0.316	3.936	19.642
43.7	0.245	0.055	0.262	3.747	22.627
48.29	0.253	0.059	0.367	3.791	23.297
52.9	0.272	0.071	0.578	4.16	25.946
57.5	0.274	0.071	0.558	3.889	25.894
62.09	0.275	0.076	0.769	3.94	27.642
66.69	0.303	0.086	0.667	3.407	28.232
71.3	0.346	0.089	0.398	2.549	25.757
73.59	0.33	0.093	0.413	2.695	28.085
75.9	0.364	0.097	0.335	2.799	26.725
78.19	0.364	0.108	0.35	2.619	29.617
80.5	0.357	0.096	0.186	2.484	26.935
85.09	0.417	0.091	0.062	2.604	21.792
89.69	0.438	0.086	0.023	2.821	19.567
94.3	0.462	0.092	-0.108	2.769	19.868
98.9	0.491	0.089	-0.248	2.597	18.093
103.5	0.521	0.075	-0.208	2.991	14.463
107.8	0.523	0.075	-0.297	2.927	14.387

Experiment FS#4

Location #3

Z	U Mean	U RMS	U Skew	U Flat	U Turb
(mm)	(m/s)	(m/s)	(m/s)	(m/s)	(%)
0	0.161	0.05	0.255	3.097	31.275
1.14	0.18	0.046	0.44	3.948	25.841
2.29	0.18	0.048	0.374	3.527	26.819
3.45	0.177	0.045	0.285	3.4	25.651
4.59	0.18	0.047	0.109	2.912	25.902
6.9	0.183	0.049	-0.079	2.884	26.616
9.19	0.18	0.047	0.095	3.119	26.157
11.5	0.176	0.046	0.169	3.212	26.323
16.1	0.176	0.047	0.044	2.833	26.726
20.7	0.182	0.05	0.113	3.077	27.291
25.29	0.189	0.052	0.158	3.003	27.363
29.89	0.185	0.053	0.25	3.321	28.551
34.5	0.201	0.058	0.096	3.153	28.905
39.09	0.195	0.058	0.258	2.907	29.961
43.7	0.206	0.066	0.232	3.078	32.152
48.29	0.225	0.064	0.411	3.692	28.494
52.9	0.221	0.07	0.586	4.201	31.946
57.5	0.22	0.069	0.621	3.842	31.191
62.09	0.236	0.073	0.553	3.314	31.154
66.69	0.272	0.092	0.618	2.939	33.909
71.3	0.3	0.099	0.555	2.924	32.95
73.59	0.333	0.1	0.331	2.575	29.933
75.9	0.37	0.099	0.415	2.819	26.757
78.19	0.389	0.102	0.087	2.4	26.121
80.5	0.416	0.095	0.104	2.691	22.806
85.09	0.447	0.098	-0.015	2.285	21.875
89.69	0.475	0.09	0.065	2.585	18.911
94.3	0.494	0.081	-0.473	3.104	16.311
98.9	0.519	0.072	-0.174	2.981	13.837
103.5	0.547	0.07	-0.352	2.924	12.735
107.8	0.551	0.078	-0.383	3.228	14.107

Experiment FS#4

Location #4

Z	U Mean	U RMS	U Skew	U Flat	U Turb
(mm)	(m/s)	(m/s)	(m/s)	(m/s)	(%)
0	0.124	0.048	0.22	3.511	38.451
1.14	0.154	0.041	0.208	2.919	26.992
2.29	0.155	0.043	0.178	2.914	27.461
3.45	0.158	0.042	0.104	3.196	26.545
4.59	0.149	0.041	0.117	2.927	27.168
6.9	0.156	0.042	0.117	3.499	27.025
9.19	0.15	0.041	0.082	2.952	27.57
11.5	0.148	0.042	-0.055	2.991	28.445
16.1	0.146	0.044	0.087	3.295	30.25
20.7	0.155	0.046	0.047	3.275	29.374
25.29	0.147	0.044	0.063	3.161	29.977
29.89	0.158	0.048	0.162	3.689	30.141
34.5	0.16	0.047	0.118	3.659	29.682
39.09	0.166	0.055	0.071	3.359	33.241
43.7	0.177	0.055	0.421	4.068	30.955
48.29	0.183	0.059	0.189	3.219	32.256
52.9	0.182	0.062	0.287	3.569	34.395
57.5	0.187	0.063	0.427	3.709	33.894
62.09	0.202	0.071	0.551	3.656	35.38
66.69	0.243	0.087	0.474	3.196	35.881
71.3	0.272	0.09	0.47	2.87	33.179
73.59	0.282	0.09	0.433	2.918	31.836
75.9	0.321	0.098	0.185	2.472	30.374
78.19	0.381	0.103	0.224	2.252	27.085
80.5	0.395	0.103	0.123	2.381	26.094
85.09	0.419	0.092	-0.014	2.289	22.029
89.69	0.439	0.096	-0.173	2.476	21.745
94.3	0.469	0.092	-0.117	2.537	19.665
98.9	0.491	0.078	-0.297	2.787	15.864
103.5	0.521	0.07	0.065	2.743	13.426
107.8	0.522	0.074	-0.276	3.063	14.247

Experiment FS#4

Location #5

Z	U Mean	U RMS	U Skew	U Flat	U Turb
(mm)	(m/s)	(m/s)	(m/s)	(m/s)	(%)
0	0.188	0.048	0.124	2.8	25.669
1.14	0.211	0.044	-0.075	3.051	20.744
2.29	0.218	0.044	0.016	3.278	20.104
3.45	0.219	0.04	-0.112	3.087	18.084
4.59	0.223	0.043	-0.182	3.289	19.134
6.9	0.216	0.043	-0.185	3.055	19.977
9.19	0.212	0.041	-0.061	2.991	19.178
11.5	0.216	0.043	-0.272	3.335	20.059
16.1	0.211	0.044	-0.19	2.888	21.025
20.7	0.218	0.042	-0.157	3.123	19.414
25.29	0.228	0.044	0.099	3.41	19.138
29.89	0.226	0.046	-0.255	3.482	20.525
34.5	0.223	0.05	0	4.501	22.185
39.09	0.233	0.05	-0.148	3.225	21.456
43.7	0.235	0.053	0.415	4.144	22.518
48.29	0.241	0.055	0.491	4.752	22.88
52.9	0.246	0.067	0.517	3.835	27.223
57.5	0.256	0.072	0.784	4.585	28.299
62.09	0.279	0.08	0.492	3.7	28.585
66.69	0.289	0.086	0.702	3.483	29.646
71.3	0.326	0.086	0.37	2.875	26.465
73.59	0.34	0.095	0.243	2.453	28.049
75.9	0.347	0.092	0.212	2.657	26.583
78.19	0.358	0.091	0.145	2.724	25.364
80.5	0.391	0.095	-0.159	2.4	24.278
85.09	0.415	0.093	-0.004	2.612	22.365
89.69	0.439	0.087	0.051	2.853	19.918
94.3	0.456	0.095	-0.1	2.475	20.779
98.9	0.493	0.084	-0.134	2.734	17.004
103.5	0.512	0.082	-0.338	3.207	15.961
107.8	0.531	0.07	-0.398	3.383	13.148

Experiment FS#4

Location #6

Z	U Mean	U RMS	U Skew	U Flat	U Turb
(mm)	(m/s)	(m/s)	(m/s)	(m/s)	(%)
0	0.106	0.052	0.078	3.469	49.14
1.14	0.126	0.052	0.01	3.333	41.639
2.29	0.135	0.056	0.046	3.215	41.107
3.45	0.138	0.055	-0.126	3.011	39.533
4.59	0.131	0.058	-0.298	3.077	44
6.9	0.133	0.055	-0.073	3.021	41.595
9.19	0.12	0.054	-0.155	3.365	44.665
11.5	0.112	0.056	0.162	3.105	50.23
16.1	0.114	0.055	0.015	3.188	48.121
20.7	0.124	0.054	0.118	2.922	43.768
25.29	0.123	0.053	0.098	3.292	42.656
29.89	0.127	0.058	0.121	3.324	45.251
34.5	0.132	0.061	0.295	4.085	45.952
39.09	0.13	0.06	0.198	3.472	46.003
43.7	0.135	0.058	-0.059	3.626	43.236
48.29	0.149	0.068	0.243	3.15	45.744
52.9	0.154	0.076	0.373	3.891	49.051
57.5	0.146	0.074	0.217	3.698	50.574
62.09	0.154	0.082	0.563	3.967	53.043
66.69	0.153	0.082	0.204	2.924	53.68
71.3	0.212	0.096	0.692	3.417	45.243
73.59	0.266	0.11	0.233	2.45	41.546
75.9	0.334	0.105	-0.141	2.76	31.293
78.19	0.361	0.11	0.025	2.56	30.515
80.5	0.396	0.096	-0.11	2.658	24.351
85.09	0.434	0.099	0.001	2.471	22.692
89.69	0.437	0.087	0.294	2.81	20.008
94.3	0.469	0.088	-0.264	2.689	18.847
98.9	0.501	0.076	-0.135	2.739	15.263
103.5	0.523	0.08	-0.372	2.641	15.249
107.8	0.528	0.072	-0.095	2.973	13.567

Experiment FS#5

Location #1

Z	U Mean	U RMS	U Skew	U Flat	U Turb
(mm)	(m/s)	(m/s)	(m/s)	(m/s)	(%)
4.59	0.032	0.072	-0.044	3.37	228.385
5.75	0.032	0.073	-0.074	3.118	230.175
6.9	0.023	0.069	-0.171	2.887	305.825
9.19	0.015	0.069	-0.075	2.975	472.599
11.5	0.006	0.068	0.016	3.096	1163.194
16.1	0.001	0.067	-0.041	3.045	10587.99
20.7	0.007	0.068	-0.109	3.182	1034.879
25.29	0.021	0.071	0.013	3.359	338.255
29.89	0.021	0.071	-0.1	3.199	342.327
34.5	0.028	0.074	-0.103	3.275	266.71
39.09	0.022	0.079	-0.087	3.181	362.715
43.7	0.023	0.079	0.134	3.16	342.695
48.29	0.029	0.081	0.016	3.362	280.897
52.9	0.032	0.084	0.122	3.49	263.776
57.5	0.039	0.083	0.247	3.414	212.063
62.09	0.036	0.09	0.332	3.789	254.252
66.69	0.016	0.089	0.018	3.36	561.691
71.3	-0.022	0.1	-0.165	3.306	466.162
73.59	-0.063	0.103	0.002	3.041	163.275
75.9	-0.085	0.088	0.522	3.223	103.726
78.19	-0.049	0.057	0.667	4.892	116.066
80.5	-0.028	0.056	0.051	3.153	200.704
85.09	-0.003	0.06	-0.146	3.266	2270.587
89.69	-0.002	0.058	0.261	3.119	2443.768
94.3	0.002	0.057	0.26	3.463	3023.515
98.9	0	0.053	0.224	3.244	22415.47
103.5	0.004	0.045	0.318	3.56	1038.515
107.8	0.006	0.042	0.505	4	720.664

Experiment FS#5

Location #2

Z	U Mean	U RMS	U Skew	U Flat	U Turb
(mm)	(m/s)	(m/s)	(m/s)	(m/s)	(%)
4.59	-0.011	0.032	-0.112	3.922	282.517
5.75	-0.014	0.037	-0.208	3.945	269.506
6.9	-0.013	0.037	-0.127	4.352	282.002
9.19	-0.019	0.04	-0.204	3.477	213.449
11.5	-0.011	0.038	-0.046	3.579	350.922
16.1	-0.011	0.039	-0.085	3.353	358.022
20.7	-0.012	0.039	0.033	3.986	337.82
25.29	-0.007	0.04	-0.063	3.116	585.846
29.89	-0.008	0.04	-0.008	3.472	489.681
34.5	-0.008	0.045	-0.498	4.116	570.583
39.09	-0.006	0.049	-0.506	4.239	803.957
43.7	-0.007	0.051	-0.425	4.056	712.516
48.29	-0.006	0.055	-0.576	3.851	938.296
52.9	-0.01	0.058	-0.377	3.275	584.251
57.5	-0.007	0.059	-0.427	3.851	866.074
62.09	-0.004	0.063	-0.405	3.538	1643.766
66.69	-0.002	0.066	-0.542	3.567	3334.647
71.3	0	0.069	-0.112	2.871	34311.79
73.59	-0.001	0.069	-0.102	2.896	8792.704
75.9	0.003	0.068	0.09	3.273	2360.728
78.19	-0.004	0.069	0.013	3.042	1927.076
80.5	-0.004	0.067	0.112	2.943	1621.377
85.09	-0.005	0.063	0.06	2.795	1235.071
89.69	-0.009	0.062	0.163	3.054	686.993
94.3	-0.008	0.057	0.235	3.631	716.615
98.9	-0.01	0.055	0.298	3.152	568.597
103.5	-0.013	0.049	0.37	3.409	366.204
107.8	-0.013	0.041	0.364	4.134	321.966

Experiment FS#5

Location #3

Z	U Mean	U RMS	U Skew	U Flat	U Turb
(mm)	(m/s)	(m/s)	(m/s)	(m/s)	(%)
4.59	0.002	0.041	-0.031	3.396	2627.719
5.75	-0.001	0.041	-0.036	3.185	7694.345
6.9	-0.002	0.044	0.026	3.457	2472.774
9.19	-0.005	0.044	-0.09	3.458	815.278
11.5	-0.007	0.044	-0.221	4.402	654.383
16.1	-0.008	0.047	-0.05	3.296	627.2
20.7	-0.012	0.048	-0.269	3.39	412.775
25.29	-0.011	0.05	-0.291	3.41	445.469
29.89	-0.013	0.055	-0.221	3.218	405.503
34.5	-0.008	0.053	-0.394	3.416	628.678
39.09	-0.004	0.058	-0.29	3.634	1436.316
43.7	-0.002	0.057	-0.18	3.491	3121.997
48.29	-0.008	0.062	-0.373	3.425	813.935
52.9	-0.005	0.064	-0.371	3.944	1262.612
57.5	-0.017	0.073	-0.711	4.322	438.328
62.09	-0.01	0.075	-0.693	3.802	789.319
66.69	-0.018	0.081	-0.339	3.07	443.242
71.3	-0.011	0.078	0.129	2.701	732.275
73.59	-0.016	0.077	0.033	2.959	487.466
75.9	-0.013	0.07	0.125	2.816	550.089
78.19	-0.014	0.065	0.058	2.879	450.528
80.5	-0.011	0.066	0.328	3.873	602.453
85.09	-0.005	0.065	0.118	3.126	1316.968
89.69	-0.007	0.058	0.113	3.07	786.009
94.3	-0.009	0.053	0.015	2.931	564.672
98.9	-0.005	0.056	0.511	3.742	1075.809
103.5	-0.006	0.047	0.294	3.786	816.023
107.8	-0.008	0.038	0.397	3.833	451.162

Experiment FS#5

Location #4

Z	U Mean	U RMS	U Skew	U Flat	U Turb
(mm)	(m/s)	(m/s)	(m/s)	(m/s)	(%)
4.59	-0.011	0.037	-0.181	3.505	349.728
5.75	-0.014	0.038	0.104	3.252	277.968
6.9	-0.011	0.039	-0.234	3.128	365.6
9.19	-0.01	0.038	-0.09	3.247	369.508
11.5	-0.011	0.041	-0.177	4.073	384.401
16.1	-0.013	0.045	-0.078	3.273	358.826
20.7	-0.016	0.047	-0.197	2.964	289.556
25.29	-0.019	0.049	-0.28	3.268	251.005
29.89	-0.016	0.051	-0.502	3.932	316.777
34.5	-0.015	0.052	-0.34	3.253	340.353
39.09	-0.011	0.054	-0.315	3.552	493.658
43.7	-0.015	0.054	-0.576	3.748	365.007
48.29	-0.015	0.061	-0.455	3.382	394.316
52.9	-0.016	0.064	-0.499	3.738	409.569
57.5	-0.013	0.068	-0.573	3.667	509.39
62.09	-0.021	0.073	-0.512	3.091	341.367
66.69	-0.013	0.076	-0.234	2.892	593.177
71.3	0.001	0.072	-0.187	2.804	5518.399
73.59	0.009	0.068	0.081	2.856	788.438
75.9	0.009	0.068	0.052	3.221	744.083
78.19	0.012	0.066	0.043	2.892	535.509
80.5	-0.005	0.065	0.155	3.016	1397.657
85.09	-0.003	0.061	0.008	2.938	1811.331
89.69	-0.011	0.06	0.061	3.083	535.932
94.3	-0.015	0.059	0.172	3.374	390.058
98.9	-0.013	0.051	0.259	3.286	380.886
103.5	-0.017	0.051	0.31	3.473	305.215
107.8	-0.019	0.04	0.438	3.427	209.116

Experiment FS#5

Location #5

Z	U Mean	U RMS	U Skew	U Flat	U Turb
(mm)	(m/s)	(m/s)	(m/s)	(m/s)	(%)
4.59	-0.013	0.034	-0.217	3.917	263.619
5.75	-0.017	0.034	-0.149	3.691	198.444
6.9	-0.013	0.036	-0.123	3.136	275.108
9.19	-0.017	0.038	-0.025	3.002	227.739
11.5	-0.015	0.035	0.18	3.539	230.777
16.1	-0.014	0.04	0.1	3.732	286.892
20.7	-0.01	0.04	-0.227	3.286	396.062
25.29	-0.009	0.041	-0.111	3.073	437.051
29.89	-0.009	0.04	-0.566	3.991	428.751
34.5	-0.01	0.042	-0.253	3.362	435.503
39.09	-0.015	0.05	-0.561	3.889	339.142
43.7	-0.002	0.046	-0.61	3.673	2603.213
48.29	-0.012	0.055	-0.617	4.194	452.918
52.9	-0.001	0.056	-0.668	3.995	4284.987
57.5	-0.009	0.057	-0.688	5.031	607.508
62.09	-0.003	0.06	-0.374	3.543	1786.781
66.69	0.003	0.064	-0.458	3.234	2449.269
71.3	0.002	0.062	-0.115	2.925	2885.837
73.59	0.001	0.067	-0.357	2.928	7573.879
75.9	0.008	0.067	-0.109	3.059	809.369
78.19	0.004	0.071	0.069	2.742	1919.881
80.5	-0.006	0.064	-0.056	2.764	1149.676
85.09	-0.013	0.063	0.069	3.087	487.1
89.69	-0.011	0.06	0.098	2.844	540.873
94.3	-0.006	0.058	0.236	3.164	998.008
98.9	-0.009	0.054	0.261	3.395	583.757
103.5	-0.015	0.049	0.467	3.698	331.761
107.8	-0.017	0.042	0.451	4.28	247.7

Experiment FS#5

Location #6

Z	U Mean	U RMS	U Skew	U Flat	U Turb
(mm)	(m/s)	(m/s)	(m/s)	(m/s)	(%)
4.59	0.016	0.061	0.102	4.248	376.803
5.75	0.02	0.06	0.036	3.545	305.214
6.9	0.022	0.061	0.172	3.613	271.972
9.19	0.011	0.058	0.183	3.597	525.3
11.5	0.009	0.06	0.316	3.783	670.114
16.1	0.005	0.058	0.311	4.476	1225.559
20.7	0.006	0.054	-0.018	3.076	883.571
25.29	0.008	0.057	0.063	3.354	673.479
29.89	0.01	0.058	-0.007	4	611.25
34.5	0.009	0.064	-0.028	3.459	743.785
39.09	0.007	0.063	-0.148	3.839	870.691
43.7	0.004	0.065	-0.194	3.271	1452.908
48.29	0.011	0.068	-0.273	3.748	592.704
52.9	0.015	0.073	0.036	3.861	478.836
57.5	0.022	0.078	-0.004	3.808	353.565
62.09	0.008	0.089	-0.579	4.118	1125.45
66.69	-0.03	0.11	-0.612	3.668	371.768
71.3	-0.056	0.107	0	2.764	190.722
73.59	-0.057	0.096	0.369	3.091	167.185
75.9	-0.056	0.074	0.425	3.339	131.68
78.19	-0.035	0.071	0.613	3.862	199.161
80.5	-0.037	0.064	0.262	3.611	176.078
85.09	-0.017	0.063	0.036	3.459	380.677
89.69	-0.013	0.062	0.135	3.195	469.039
94.3	-0.016	0.058	0.266	3.496	367.009
98.9	-0.016	0.053	0.271	3.28	319.555
103.5	-0.018	0.052	0.685	5.159	291.316
107.8	-0.012	0.041	0.449	3.361	331.556

Experiment FS#6

Location #1

Z	U Mean	U RMS	U Skew	U Flat	U Turb
(mm)	(m/s)	(m/s)	(m/s)	(m/s)	(%)
0	0.092	0.068	0.001	2.647	74.139
1.14	0.101	0.073	-0.096	2.864	72.888
2.29	0.078	0.074	-0.135	2.722	96.053
3.45	0.049	0.073	-0.081	2.87	150.604
4.59	0.027	0.067	0.211	3.166	251.249
6.9	0.008	0.071	0.239	2.681	858.729
9.19	0	0.074	0.304	2.844	39507.89
11.5	0.009	0.08	0.117	2.714	848.6
16.1	0.023	0.078	0.119	2.977	335.089
20.7	0.029	0.08	-0.119	2.69	273.344
25.29	0.041	0.082	-0.173	2.931	197.551
29.89	0.037	0.088	0.084	2.988	236.255
34.5	0.04	0.088	-0.009	2.791	220.316
39.09	0.024	0.09	0.078	2.75	373.997
43.7	0.04	0.097	-0.002	2.994	244.173
48.29	0.033	0.104	0.244	2.827	310.703
52.9	0.025	0.113	0.198	2.999	447.551
57.5	0.05	0.117	0.129	2.987	234.953
62.09	-0.011	0.115	0.559	3.461	1043.395
66.69	-0.011	0.106	0.673	3.908	921.745
71.3	0.077	0.104	0.211	3.336	134.769
73.59	0.304	0.135	-0.114	2.856	44.34
75.9	0.396	0.099	0.025	2.592	25.118
78.19	0.421	0.093	0.051	2.524	22.17
80.5	0.418	0.085	0.285	2.594	20.262
85.09	0.448	0.09	-0.079	2.378	20.03
89.69	0.456	0.078	0.101	2.559	17.137
94.3	0.487	0.078	-0.289	2.628	16.037
98.9	0.492	0.074	-0.381	2.913	15.009
103.5	0.521	0.061	-0.292	3.363	11.707
107.8	0.545	0.056	-0.124	2.99	10.361

Experiment FS#6

Location #2

Z	U Mean	U RMS	U Skew	U Flat	U Turb
(mm)	(m/s)	(m/s)	(m/s)	(m/s)	(%)
0	0.213	0.042	-0.088	2.83	19.693
1.14	0.239	0.037	-0.171	3.413	15.414
2.29	0.25	0.034	0.096	3.975	13.46
3.45	0.246	0.036	-0.127	3.598	14.519
4.59	0.248	0.034	-0.181	3.755	13.773
6.9	0.241	0.035	-0.07	3.578	14.47
9.19	0.241	0.035	-0.446	4.132	14.487
11.5	0.236	0.036	-0.311	3.413	15.46
16.1	0.234	0.038	-0.153	3.57	16.377
20.7	0.239	0.042	0.299	4.184	17.407
25.29	0.244	0.04	0.046	3.383	16.335
29.89	0.251	0.047	0.566	5.139	18.871
34.5	0.254	0.047	0.402	4.039	18.389
39.09	0.269	0.051	0.244	3.654	18.843
43.7	0.269	0.06	0.502	3.749	22.429
48.29	0.269	0.054	0.421	3.904	20.167
52.9	0.294	0.066	0.516	3.392	22.362
57.5	0.288	0.064	0.418	4.291	22.115
62.09	0.331	0.083	0.661	3.286	25.132
66.69	0.33	0.082	0.322	2.602	24.949
71.3	0.338	0.09	0.35	2.761	26.597
73.59	0.374	0.092	0.212	2.795	24.521
75.9	0.367	0.091	0.181	2.401	24.823
78.19	0.391	0.088	0.218	2.434	22.574
80.5	0.402	0.085	0.039	2.594	21.258
85.09	0.418	0.08	0.076	2.527	19.176
89.69	0.466	0.081	-0.131	2.604	17.34
94.3	0.451	0.078	-0.04	2.55	17.206
98.9	0.503	0.068	-0.273	2.835	13.556
103.5	0.509	0.068	-0.27	3.03	13.351
107.8	0.525	0.066	-0.196	2.972	12.546

Experiment FS#6

Location #3

Z	U Mean	U RMS	U Skew	U Flat	U Turb
(mm)	(m/s)	(m/s)	(m/s)	(m/s)	(%)
0	0.18	0.043	0.229	3.301	23.709
1.14	0.185	0.038	0.17	3.278	20.709
2.29	0.194	0.042	0.243	3.593	21.74
3.45	0.194	0.04	0.269	3.431	20.453
4.59	0.19	0.042	0.029	3.1	22.121
6.9	0.186	0.044	0.078	3.083	23.836
9.19	0.181	0.044	0.248	3.164	24.396
11.5	0.179	0.043	0.05	3.108	23.807
16.1	0.178	0.042	0.206	3.638	23.823
20.7	0.185	0.045	0.15	3.112	24.544
25.29	0.191	0.046	0.271	3.091	24.148
29.89	0.202	0.051	0.301	3.132	25.272
34.5	0.201	0.048	0.336	3.499	23.933
39.09	0.201	0.053	0.573	4.291	26.304
43.7	0.215	0.06	0.582	3.849	28.032
48.29	0.221	0.059	0.452	3.711	26.721
52.9	0.231	0.072	0.695	3.821	31.204
57.5	0.233	0.068	0.42	3.261	29.282
62.09	0.254	0.08	0.739	3.706	31.482
66.69	0.295	0.082	0.418	3.216	27.803
71.3	0.313	0.079	0.068	2.793	25.096
73.59	0.358	0.104	0.097	2.304	29.077
75.9	0.373	0.085	0.033	2.464	22.91
78.19	0.392	0.084	0.022	2.507	21.374
80.5	0.405	0.086	-0.189	2.439	21.164
85.09	0.436	0.078	-0.23	2.829	17.807
89.69	0.468	0.074	-0.033	2.58	15.81
94.3	0.461	0.068	-0.141	2.69	14.759
98.9	0.489	0.07	-0.242	2.714	14.273
103.5	0.521	0.066	-0.404	3.058	12.597
107.8	0.516	0.063	-0.236	3.142	12.285

Experiment FS#6

Location #4

Z	U Mean	U RMS	U Skew	U Flat	U Turb
(mm)	(m/s)	(m/s)	(m/s)	(m/s)	(%)
0	0.15	0.041	0.176	3.674	27.556
1.14	0.163	0.042	0.138	3.145	25.422
2.29	0.174	0.041	0.238	3.242	23.345
3.45	0.178	0.04	0.267	3.333	22.674
4.59	0.175	0.038	-0.08	3.009	21.931
6.9	0.17	0.038	0.108	3.321	22.505
9.19	0.166	0.038	-0.066	2.84	23.126
11.5	0.164	0.04	0.1	3.513	24.464
16.1	0.166	0.042	0.307	3.083	25.379
20.7	0.171	0.043	0.292	3.392	25.237
25.29	0.175	0.045	0.225	3.159	26.046
29.89	0.178	0.047	0.447	3.656	26.456
34.5	0.181	0.045	0.175	3.145	25.048
39.09	0.188	0.052	0.294	3.334	27.576
43.7	0.198	0.053	0.605	3.798	26.8
48.29	0.2	0.056	0.404	3.62	27.85
52.9	0.214	0.063	0.458	3.571	29.197
57.5	0.218	0.067	0.427	3.272	30.826
62.09	0.247	0.078	0.703	3.312	31.508
66.69	0.265	0.08	0.605	3.168	30.16
71.3	0.31	0.085	0.269	2.615	27.451
73.59	0.333	0.084	0.133	2.486	25.266
75.9	0.37	0.086	0.081	2.371	23.225
78.19	0.389	0.083	0.009	2.594	21.439
80.5	0.406	0.083	-0.001	2.549	20.382
85.09	0.425	0.082	-0.106	2.373	19.191
89.69	0.454	0.084	-0.289	2.708	18.453
94.3	0.481	0.073	0.02	2.527	15.198
98.9	0.496	0.069	-0.329	3.041	13.847
103.5	0.515	0.062	-0.272	2.738	11.941
107.8	0.541	0.061	-0.118	3.112	11.36

Experiment FS#6

Location #5

Z	U Mean	U RMS	U Skew	U Flat	U Turb
(mm)	(m/s)	(m/s)	(m/s)	(m/s)	(%)
0	0.211	0.043	-0.071	3.01	20.363
1.14	0.228	0.039	-0.239	3.073	17.132
2.29	0.234	0.036	-0.174	3.127	15.424
3.45	0.239	0.034	-0.275	3.405	14.229
4.59	0.237	0.037	-0.061	3.628	15.422
6.9	0.236	0.037	-0.249	3.24	15.582
9.19	0.233	0.037	-0.162	3.348	15.809
11.5	0.228	0.038	-0.303	3.631	16.546
16.1	0.232	0.037	0.021	3.358	16.182
20.7	0.232	0.039	-0.127	3.385	16.797
25.29	0.236	0.039	-0.102	3.164	16.689
29.89	0.249	0.043	0.175	3.634	17.338
34.5	0.244	0.042	0.271	3.598	17.323
39.09	0.245	0.048	0.4	3.732	19.726
43.7	0.258	0.055	0.384	4.145	21.468
48.29	0.27	0.06	0.551	3.611	22.253
52.9	0.279	0.066	0.634	3.895	23.769
57.5	0.289	0.07	0.392	2.919	24.297
62.09	0.314	0.079	0.425	3.152	24.988
66.69	0.326	0.083	0.488	2.938	25.434
71.3	0.35	0.088	0.384	2.634	25.113
73.59	0.359	0.086	0.359	2.771	24.057
75.9	0.384	0.087	0.057	2.392	22.556
78.19	0.391	0.095	0.2	2.36	24.213
80.5	0.417	0.089	-0.006	2.566	21.304
85.09	0.422	0.083	0.063	2.42	19.566
89.69	0.459	0.07	-0.158	2.608	15.175
94.3	0.482	0.076	-0.27	3.224	15.723
98.9	0.49	0.068	-0.127	2.737	13.829
103.5	0.506	0.061	-0.532	3.503	12.007
107.8	0.534	0.063	-0.116	3.178	11.826

Experiment FS#6

Location #6

Z	U Mean	U RMS	U Skew	U Flat	U Turb
(mm)	(m/s)	(m/s)	(m/s)	(m/s)	(%)
0	0.123	0.045	0.235	2.952	36.239
1.14	0.16	0.046	-0.016	2.849	28.894
2.29	0.165	0.046	0.002	2.961	27.832
3.45	0.176	0.049	-0.136	3.193	27.982
4.59	0.176	0.048	-0.142	3.53	27.574
6.9	0.158	0.052	-0.276	3.668	33.191
9.19	0.145	0.05	-0.081	3.137	34.64
11.5	0.129	0.049	0.14	3.063	37.737
16.1	0.131	0.05	0.099	3.026	38.583
20.7	0.14	0.051	0.12	3.008	36.717
25.29	0.153	0.056	0.25	3.281	36.262
29.89	0.152	0.055	0.217	3.742	35.773
34.5	0.155	0.058	0.401	3.938	37.66
39.09	0.175	0.066	0.084	3.211	37.676
43.7	0.167	0.065	0.203	3.359	39.021
48.29	0.188	0.071	0.25	3.399	37.826
52.9	0.176	0.071	-0.026	3.071	40.093
57.5	0.189	0.081	0.323	3.49	42.559
62.09	0.198	0.082	0.312	3.227	41.324
66.69	0.24	0.097	0.297	2.993	40.616
71.3	0.299	0.102	0.177	2.606	34.208
73.59	0.34	0.097	-0.17	2.791	28.423
75.9	0.346	0.092	0.146	2.727	26.456
78.19	0.4	0.098	-0.077	2.458	24.529
80.5	0.414	0.095	0.254	2.739	22.838
85.09	0.424	0.079	0.142	2.661	18.698
89.69	0.457	0.083	-0.011	2.358	18.222
94.3	0.495	0.071	-0.21	2.777	14.435
98.9	0.497	0.068	-0.068	2.803	13.577
103.5	0.528	0.059	-0.522	3.286	11.074
107.8	0.538	0.062	-0.031	3.159	11.491

Experiment DL#1

Location #1

Z	U Mean	U RMS	U Skew	U Flat	U Turb
(mm)	(m/s)	(m/s)	(m/s)	(m/s)	(%)
0	0.126	0.06	0.299	4.402	47.526
1.14	0.149	0.058	-0.009	3.424	38.821
2.29	0.145	0.059	-0.031	3.213	40.973
3.45	0.138	0.06	-0.056	3.548	43.422
4.59	0.133	0.058	-0.13	3.183	43.921
6.9	0.119	0.058	-0.036	2.817	49.117
9.19	0.106	0.062	-0.144	2.943	58.11
11.5	0.119	0.06	-0.092	3.143	50.422
16.1	0.117	0.06	0.014	2.895	51.219
20.7	0.123	0.064	-0.002	2.819	52.082
25.29	0.127	0.064	-0.062	3.005	50.263
29.89	0.124	0.062	0.09	3.674	50.079
34.5	0.129	0.067	-0.045	3.107	52.261
39.09	0.131	0.064	-0.005	3.246	48.967
43.7	0.124	0.066	-0.05	3.256	53.206
48.29	0.124	0.067	-0.032	3.028	54.125
52.9	0.136	0.065	-0.156	3.074	48.125
57.5	0.149	0.068	-0.135	3.057	45.491
62.09	0.156	0.071	-0.021	2.995	45.303
66.69	0.168	0.075	-0.141	3.485	44.819
71.3	0.173	0.083	-0.284	3.519	47.807
73.59	0.164	0.089	-0.215	3.171	54.336
75.9	0.169	0.087	-0.347	3.264	51.252
78.19	0.154	0.092	-0.306	3.241	60.05
80.5	0.144	0.101	-0.268	3.068	69.777
85.09	0.104	0.111	0.03	2.719	107.136
89.69	0.084	0.111	0.114	2.929	132.373
94.3	0.063	0.107	0.198	2.807	169.501
98.9	0.018	0.106	0.493	3.248	589.04
103.5	0.058	0.103	0.289	3.308	178.259
108.09	0.158	0.106	0.09	3.105	66.954
112.69	0.394	0.078	-0.728	5.012	19.817
117.3	0.43	0.09	-1.554	13.46	20.839

Experiment DL#1

Location #2

Z	U Mean	U RMS	U Skew	U Flat	U Turb
(mm)	(m/s)	(m/s)	(m/s)	(m/s)	(%)
0	0.221	0.041	-0.31	2.878	18.592
1.14	0.25	0.033	-0.55	3.323	13.18
2.29	0.251	0.034	-0.334	3.419	13.345
3.45	0.256	0.032	-0.253	3.138	12.69
4.59	0.257	0.031	-0.323	3.297	12.057
6.9	0.257	0.032	-0.299	3.472	12.575
9.19	0.253	0.032	-0.161	2.851	12.694
11.5	0.255	0.033	-0.36	3.238	12.834
16.1	0.258	0.031	-0.527	4.241	12.091
20.7	0.259	0.033	-0.256	3.482	12.824
25.29	0.26	0.032	-0.261	3.31	12.199
29.89	0.258	0.034	-0.446	3.538	13.166
34.5	0.264	0.033	-0.314	3.562	12.641
39.09	0.268	0.034	-0.051	3.197	12.64
43.7	0.269	0.034	-0.309	3.747	12.734
48.29	0.266	0.034	-0.174	3.098	12.949
52.9	0.273	0.041	-0.078	3.281	14.848
57.5	0.28	0.044	0.096	3.197	15.881
62.09	0.29	0.049	0.176	2.992	16.75
66.69	0.317	0.049	0.006	3.102	15.569
71.3	0.326	0.049	0.066	3.08	14.964
73.59	0.341	0.049	0.144	2.78	14.244
75.9	0.348	0.05	0.031	3.076	14.225
78.19	0.361	0.05	-0.033	2.57	13.718
80.5	0.374	0.047	0.063	2.793	12.446
85.09	0.377	0.045	0.063	2.678	11.933
89.69	0.381	0.045	0.04	2.421	11.806
94.3	0.385	0.046	0.019	2.567	12.064
98.9	0.403	0.046	0.106	2.873	11.396
103.5	0.422	0.046	-0.239	2.951	11.006
108.09	0.443	0.044	-0.377	3.046	9.958
112.69	0.457	0.037	-0.549	3.828	7.983
117.3	0.462	0.034	-0.051	3.133	7.4

Experiment DL#1

Location #3

Z	U Mean	U RMS	U Skew	U Flat	U Turb
(mm)	(m/s)	(m/s)	(m/s)	(m/s)	(%)
0	0.163	0.038	0.48	3.752	23.031
1.14	0.183	0.036	0.081	3.076	19.536
2.29	0.182	0.036	0.124	3.354	19.809
3.45	0.177	0.039	0.046	2.849	21.828
4.59	0.176	0.04	0.024	2.947	22.684
6.9	0.175	0.039	-0.034	2.93	22.313
9.19	0.174	0.038	0	3.013	22.058
11.5	0.172	0.039	0.081	3.178	22.891
16.1	0.177	0.038	0.207	3.063	21.271
20.7	0.178	0.038	-0.013	3.309	21.444
25.29	0.181	0.042	0.11	2.933	23.185
29.89	0.18	0.042	0.217	3.063	23.577
34.5	0.186	0.04	0.068	2.924	21.353
39.09	0.186	0.042	-0.062	2.996	22.536
43.7	0.193	0.044	0.078	2.851	23.037
48.29	0.198	0.044	0.015	2.753	22.324
52.9	0.206	0.047	0.163	3.162	22.687
57.5	0.215	0.048	0.077	2.975	22.565
62.09	0.255	0.055	-0.013	2.979	21.635
66.69	0.297	0.057	-0.251	2.793	19.334
71.3	0.343	0.049	-0.295	3.455	14.311
73.59	0.362	0.05	-0.353	3.357	13.934
75.9	0.376	0.044	-0.336	3.215	11.813
78.19	0.381	0.043	-0.134	2.915	11.272
80.5	0.392	0.042	0.067	2.765	10.638
85.09	0.402	0.04	-0.055	2.803	10.037
89.69	0.406	0.04	-0.146	3.193	9.795
94.3	0.41	0.041	0.006	3.131	9.962
98.9	0.414	0.04	0.048	2.866	9.706
103.5	0.427	0.039	-0.281	2.878	9.173
108.09	0.435	0.038	-0.261	3.174	8.659
112.69	0.447	0.036	-0.203	2.982	7.958
117.3	0.44	0.034	0.005	3.217	7.683

Experiment DL#1

Location #4

Z	U Mean	U RMS	U Skew	U Flat	U Turb
(mm)	(m/s)	(m/s)	(m/s)	(m/s)	(%)
0	0.219	0.042	-0.22	2.781	19.137
1.14	0.251	0.033	-0.181	2.894	13.13
2.29	0.254	0.034	-0.381	3.012	13.554
3.45	0.256	0.031	-0.31	3.348	11.921
4.59	0.258	0.031	-0.287	3.291	12.002
6.9	0.253	0.031	-0.313	3.426	12.128
9.19	0.255	0.03	-0.183	3.181	11.813
11.5	0.254	0.031	-0.23	3.154	12.361
16.1	0.255	0.032	-0.226	3.059	12.553
20.7	0.257	0.033	-0.244	3.336	12.768
25.29	0.256	0.032	-0.386	3.872	12.662
29.89	0.26	0.032	-0.22	2.889	12.254
34.5	0.262	0.034	-0.465	3.982	13.078
39.09	0.259	0.032	-0.176	3.087	12.32
43.7	0.268	0.034	-0.223	3.349	12.813
48.29	0.267	0.036	-0.227	3.213	13.283
52.9	0.265	0.035	-0.074	3.629	13.271
57.5	0.275	0.04	-0.111	3.503	14.424
62.09	0.28	0.041	0.153	3.276	14.741
66.69	0.291	0.048	0.252	3.165	16.455
71.3	0.305	0.049	0.182	3.087	15.974
73.59	0.316	0.05	0.146	2.756	15.799
75.9	0.327	0.05	0.147	2.688	15.19
78.19	0.33	0.05	0.007	2.796	15.083
80.5	0.336	0.051	-0.038	2.88	15.236
85.09	0.34	0.052	-0.131	3.006	15.169
89.69	0.34	0.054	0.029	2.828	15.873
94.3	0.343	0.056	-0.105	2.833	16.362
98.9	0.345	0.059	-0.085	2.645	17.248
103.5	0.363	0.059	-0.338	3.003	16.168
108.09	0.382	0.054	-0.402	3.094	14.154
112.69	0.409	0.045	-0.545	3.757	11.08
117.3	0.427	0.038	-0.075	3.426	8.834

Experiment DL#1

Location #5

Z	U Mean	U RMS	U Skew	U Flat	U Turb
(mm)	(m/s)	(m/s)	(m/s)	(m/s)	(%)
0	0.108	0.057	0.281	3.491	52.834
1.14	0.129	0.057	0.029	3.125	44.057
2.29	0.132	0.059	0.131	3.257	44.546
3.45	0.128	0.057	-0.107	3.013	44.904
4.59	0.123	0.057	-0.223	2.989	46.505
6.9	0.113	0.058	0.099	3.199	51.149
9.19	0.11	0.057	-0.166	3.27	51.642
11.5	0.11	0.058	0.008	2.872	53.175
16.1	0.115	0.061	0.033	3.097	52.72
20.7	0.117	0.059	-0.073	2.867	50.391
25.29	0.12	0.061	-0.008	3.102	50.714
29.89	0.125	0.059	-0.036	3.03	47.335
34.5	0.126	0.06	-0.067	3.019	47.949
39.09	0.127	0.063	-0.091	2.954	49.188
43.7	0.121	0.061	0.098	3.448	50.566
48.29	0.129	0.061	0.171	3.208	47.494
52.9	0.124	0.062	-0.138	3.277	49.989
57.5	0.121	0.061	0.064	3.663	49.95
62.09	0.11	0.064	0.139	2.911	58.148
66.69	0.118	0.066	0.24	3.159	56.116
71.3	0.173	0.066	0.02	3.1	38.222
73.59	0.214	0.063	-0.004	3.254	29.412
75.9	0.258	0.06	-0.343	3.222	23.098
78.19	0.288	0.055	-0.001	3.042	18.954
80.5	0.292	0.054	-0.04	2.993	18.575
85.09	0.3	0.051	0.031	2.951	16.861
89.69	0.299	0.05	0.092	2.843	16.673
94.3	0.294	0.053	0.183	2.638	18.113
98.9	0.312	0.053	-0.007	2.688	17.053
103.5	0.339	0.057	-0.113	2.617	16.694
108.09	0.372	0.055	-0.185	2.899	14.779
112.69	0.407	0.05	-0.433	3.252	12.361
117.3	0.42	0.038	-0.075	3.223	9.021

Experiment DL#1

Location #6

Z	U Mean	U RMS	U Skew	U Flat	U Turb
(mm)	(m/s)	(m/s)	(m/s)	(m/s)	(%)
0	0.162	0.041	0.342	3.448	25.45
1.14	0.178	0.044	0.217	3.111	24.828
2.29	0.194	0.04	0.178	3.023	20.551
3.45	0.194	0.041	0.146	3.177	21.21
4.59	0.192	0.044	0.096	2.701	22.707
6.9	0.187	0.044	0.159	3.044	23.794
9.19	0.185	0.044	0.076	2.968	23.97
11.5	0.181	0.043	0.14	2.936	23.792
16.1	0.185	0.04	-0.074	2.577	21.919
20.7	0.188	0.045	0.212	3.121	23.977
25.29	0.179	0.045	0.083	2.696	25.038
29.89	0.189	0.044	0.139	2.954	23.012
34.5	0.187	0.044	0.144	2.937	23.333
39.09	0.186	0.045	0.102	3.129	24.115
43.7	0.192	0.046	0.07	3.034	24.05
48.29	0.19	0.048	0.089	3.073	25.006
52.9	0.191	0.047	0.044	2.865	24.368
57.5	0.196	0.048	0.084	2.944	24.357
62.09	0.204	0.053	0.076	2.825	26.135
66.69	0.218	0.054	0.06	2.883	24.661
71.3	0.235	0.058	0.187	3.309	24.732
73.59	0.24	0.059	0.072	2.849	24.635
75.9	0.251	0.061	0.062	2.939	24.23
78.19	0.263	0.06	0.084	2.968	22.924
80.5	0.263	0.061	0.092	3.073	23.017
85.09	0.271	0.058	0.005	3.12	21.51
89.69	0.268	0.062	0.212	3.124	23.225
94.3	0.259	0.061	0.148	3.208	23.501
98.9	0.275	0.067	0.09	2.931	24.379
103.5	0.319	0.074	0.042	2.645	23.338
108.09	0.379	0.071	-0.483	3.537	18.719
112.69	0.421	0.062	-0.562	3.696	14.782
117.3	0.43	0.05	-0.306	3.737	11.618

Experiment DL#1

Location #7

Z	U Mean	U RMS	U Skew	U Flat	U Turb
(mm)	(m/s)	(m/s)	(m/s)	(m/s)	(%)
0	0.231	0.041	-0.324	3.021	17.87
1.14	0.244	0.038	-0.35	3.069	15.697
2.29	0.256	0.032	-0.294	3.251	12.423
3.45	0.254	0.033	-0.146	3.136	12.9
4.59	0.26	0.034	-0.237	3.405	13.172
6.9	0.258	0.034	-0.39	3.286	13.193
9.19	0.259	0.032	-0.176	3.134	12.169
11.5	0.257	0.036	-0.435	3.674	13.992
16.1	0.256	0.036	-0.29	3.109	13.866
20.7	0.258	0.035	-0.106	3.269	13.669
25.29	0.265	0.034	-0.284	3.825	12.777
29.89	0.265	0.034	-0.387	3.145	12.872
34.5	0.263	0.035	-0.16	3.234	13.37
39.09	0.27	0.034	-0.242	3.135	12.602
43.7	0.273	0.038	-0.228	3.041	14.083
48.29	0.275	0.041	-0.043	3.783	14.746
52.9	0.28	0.038	-0.183	3.21	13.629
57.5	0.286	0.045	-0.071	3.26	15.778
62.09	0.297	0.047	0.158	3.02	15.763
66.69	0.315	0.051	-0.032	3.203	16.274
71.3	0.332	0.053	0.136	2.945	15.933
73.59	0.346	0.053	0.003	2.716	15.462
75.9	0.358	0.051	-0.064	2.796	14.365
78.19	0.363	0.05	-0.078	2.771	13.769
80.5	0.366	0.05	-0.178	3.045	13.67
85.09	0.373	0.049	-0.066	2.771	13.148
89.69	0.379	0.054	-0.377	3.329	14.355
94.3	0.39	0.056	-0.391	3.338	14.275
98.9	0.401	0.063	-0.759	3.914	15.757
103.5	0.425	0.051	-0.412	3.475	11.954
108.09	0.44	0.048	-0.642	4.153	10.809
112.69	0.464	0.038	-0.48	3.431	8.115
117.3	0.473	0.036	-0.212	3.226	7.682

Experiment DL#1

Location #8

Z	U Mean	U RMS	U Skew	U Flat	U Turb
(mm)	(m/s)	(m/s)	(m/s)	(m/s)	(%)
0	0.124	0.058	0.214	3.309	47.023
1.14	0.134	0.056	-0.049	3.055	42.153
2.29	0.134	0.058	-0.181	3.244	43.054
3.45	0.134	0.055	-0.144	3.27	41.124
4.59	0.115	0.055	-0.187	2.9	48.099
6.9	0.113	0.054	-0.166	2.907	47.887
9.19	0.112	0.056	-0.116	2.944	49.491
11.5	0.114	0.057	0.026	3.132	50.222
16.1	0.121	0.059	-0.041	3.059	49.003
20.7	0.123	0.06	-0.007	3.416	48.987
25.29	0.123	0.06	-0.161	3.233	49.083
29.89	0.124	0.059	0.094	3.203	47.194
34.5	0.124	0.059	-0.055	2.946	47.62
39.09	0.132	0.061	0.006	3.109	45.99
43.7	0.138	0.063	-0.122	3.384	46.065
48.29	0.144	0.066	-0.033	3.295	45.942
52.9	0.152	0.072	0.032	3.265	47.149
57.5	0.135	0.08	-0.141	3.103	59.507
62.09	0.119	0.086	-0.074	3.054	71.685
66.69	0.129	0.085	0	2.877	66.048
71.3	0.233	0.085	-0.347	3.051	36.339
73.59	0.314	0.066	-0.938	4.713	20.979
75.9	0.374	0.048	-0.848	5.978	12.785
78.19	0.388	0.043	-0.161	3.042	11.115
80.5	0.395	0.041	-0.069	2.922	10.287
85.09	0.403	0.04	-0.294	2.843	9.921
89.69	0.403	0.04	-0.062	2.994	9.977
94.3	0.409	0.041	-0.412	3.387	9.93
98.9	0.416	0.042	-0.182	3.086	9.983
103.5	0.424	0.042	-0.314	3.045	9.986
108.09	0.444	0.039	-0.444	3.287	8.803
112.69	0.465	0.032	-0.346	3.283	6.88
117.3	0.475	0.03	-0.433	4.019	6.233

Experiment DL#1

Location #9

Z	U Mean	U RMS	U Skew	U Flat	U Turb
(mm)	(m/s)	(m/s)	(m/s)	(m/s)	(%)
0	0.243	0.039	-0.233	3.039	16.074
1.14	0.247	0.037	-0.279	2.899	15.154
2.29	0.26	0.033	-0.077	3.156	12.777
3.45	0.258	0.034	-0.422	3.297	13.08
4.59	0.261	0.033	-0.228	3.695	12.741
6.9	0.258	0.032	-0.216	3.012	12.202
9.19	0.258	0.034	-0.237	3.344	13.278
11.5	0.259	0.034	-0.288	3.245	13.179
16.1	0.259	0.033	-0.195	3.239	12.944
20.7	0.262	0.034	-0.208	3.228	12.806
25.29	0.264	0.037	-0.34	3.268	14.197
29.89	0.265	0.034	-0.099	3.633	12.99
34.5	0.267	0.036	-0.451	4.553	13.401
39.09	0.266	0.035	-0.263	3.15	13.356
43.7	0.267	0.037	0.021	3.05	13.724
48.29	0.273	0.039	-0.259	3.57	14.155
52.9	0.273	0.042	-0.16	3.263	15.461
57.5	0.281	0.046	-0.004	3.332	16.34
62.09	0.285	0.05	-0.139	3.13	17.585
66.69	0.296	0.05	-0.073	3.289	16.964
71.3	0.32	0.052	-0.176	3.224	16.334
73.59	0.325	0.054	0.01	2.753	16.612
75.9	0.333	0.05	0.01	2.836	15.009
78.19	0.343	0.052	-0.09	2.69	15.297
80.5	0.35	0.055	-0.061	2.613	15.57
85.09	0.348	0.053	-0.051	2.767	15.127
89.69	0.349	0.055	0.02	2.577	15.851
94.3	0.348	0.054	0.01	2.598	15.366
98.9	0.362	0.055	-0.053	2.413	15.312
103.5	0.376	0.053	-0.121	2.499	14.191
108.09	0.41	0.049	-0.299	2.891	11.965
112.69	0.439	0.043	-0.777	4.459	9.849
117.3	0.455	0.037	-0.276	3.175	8.06

Experiment DL#1

Location #10

Z	U Mean	U RMS	U Skew	U Flat	U Turb
(mm)	(m/s)	(m/s)	(m/s)	(m/s)	(%)
0	0.177	0.04	0.257	3.552	22.622
1.14	0.184	0.04	0.207	2.91	21.663
2.29	0.186	0.042	0.136	3.375	22.556
3.45	0.185	0.042	-0.019	3.021	22.641
4.59	0.185	0.042	0.126	2.725	22.922
6.9	0.183	0.043	0.14	2.988	23.481
9.19	0.179	0.045	-0.046	2.681	25.131
11.5	0.179	0.045	-0.09	3.903	24.865
16.1	0.182	0.044	0.053	3.243	24.297
20.7	0.188	0.044	0.151	2.773	23.548
25.29	0.186	0.045	0.083	2.636	24.184
29.89	0.19	0.045	0.099	2.976	23.806
34.5	0.189	0.045	0.111	2.773	23.929
39.09	0.191	0.045	-0.036	2.978	23.645
43.7	0.195	0.045	-0.06	2.892	23.059
48.29	0.19	0.045	0.148	2.969	23.651
52.9	0.191	0.046	0.31	3.136	24.326
57.5	0.189	0.048	0.252	3.155	25.435
62.09	0.199	0.046	0.192	3.277	23.126
66.69	0.226	0.051	0.192	3.109	22.421
71.3	0.258	0.053	0.069	2.891	20.576
73.59	0.275	0.051	-0.018	2.899	18.405
75.9	0.282	0.05	0.063	2.851	17.755
78.19	0.291	0.047	0.063	2.901	16.097
80.5	0.294	0.047	0.21	2.968	15.862
85.09	0.299	0.045	0.211	3.079	14.95
89.69	0.299	0.046	0.192	2.912	15.345
94.3	0.305	0.049	0.079	2.898	15.928
98.9	0.325	0.05	-0.011	2.934	15.329
103.5	0.351	0.051	-0.12	2.746	14.487
108.09	0.386	0.048	-0.341	3.137	12.533
112.69	0.412	0.04	-0.341	3.108	9.816
117.3	0.432	0.041	-0.366	3.7	9.524

Experiment DL#2

Location #1

Z	U Mean	U RMS	U Skew	U Flat	U Turb
(mm)	(m/s)	(m/s)	(m/s)	(m/s)	(%)
0	0.102	0.062	0.083	2.943	60.513
1.14	0.108	0.064	0.063	3.069	58.737
2.29	0.12	0.058	-0.047	3.058	48.209
3.45	0.117	0.058	-0.019	3.275	50.045
4.59	0.115	0.059	-0.148	3.186	51.095
6.9	0.108	0.059	-0.197	3.033	53.983
9.19	0.108	0.059	-0.056	3.104	54.578
11.5	0.118	0.061	-0.173	3.63	51.274
16.1	0.121	0.058	-0.15	3.061	47.973
20.7	0.128	0.061	-0.036	3.377	47.148
25.29	0.129	0.059	0.071	3.006	45.673
29.89	0.137	0.06	0.096	3.379	43.518
34.5	0.141	0.065	-0.085	3.212	45.911
39.09	0.154	0.064	-0.046	3.02	41.72
43.7	0.159	0.072	-0.155	3.49	45.279
46	0.173	0.07	-0.095	3.034	40.317
48.29	0.172	0.074	-0.087	3.46	42.735
50.59	0.184	0.078	-0.209	3.475	42.478
52.9	0.183	0.078	-0.254	3.48	42.492
57.5	0.173	0.086	-0.313	3.689	49.798
62.09	0.158	0.093	-0.401	3.692	58.521
66.69	0.159	0.088	-0.377	3.278	55.39
71.3	0.142	0.1	-0.346	3.247	70.224
75.9	0.135	0.103	-0.305	2.917	76.584
80.5	0.139	0.097	-0.173	2.856	69.895
85.09	0.133	0.1	-0.153	3.018	75.071
89.69	0.107	0.105	-0.01	2.715	97.307
94.3	0.091	0.101	-0.015	2.752	111.179
98.9	0.057	0.104	0.251	2.896	182.638
103.5	0.111	0.104	-0.01	3.124	93.596
108.09	0.283	0.094	-0.209	3.15	33.267
112.69	0.432	0.068	-0.389	5.206	15.623

Experiment DL#2

Location #2

Z	U Mean	U RMS	U Skew	U Flat	U Turb
(mm)	(m/s)	(m/s)	(m/s)	(m/s)	(%)
0	0.211	0.037	-0.264	2.851	17.741
1.14	0.223	0.036	-0.181	2.998	15.976
2.29	0.231	0.033	-0.315	3.156	14.16
3.45	0.235	0.033	-0.19	3.086	14.139
4.59	0.234	0.031	-0.136	3.25	13.165
6.9	0.237	0.033	-0.343	3.489	14.002
9.19	0.237	0.032	-0.177	3.568	13.455
11.5	0.238	0.035	-0.169	3.135	14.699
16.1	0.243	0.035	-0.151	3.287	14.362
20.7	0.25	0.036	-0.091	3.286	14.465
25.29	0.251	0.038	-0.067	3.022	15.123
29.89	0.258	0.043	0.09	3.414	16.78
34.5	0.261	0.045	-0.039	3.253	17.329
39.09	0.278	0.047	-0.187	3.072	16.856
43.7	0.297	0.048	-0.094	3.283	16.075
46	0.313	0.049	-0.001	2.658	15.765
48.29	0.321	0.052	0.086	2.408	16.175
50.59	0.325	0.05	0.066	2.761	15.47
52.9	0.342	0.048	-0.15	2.702	13.991
57.5	0.351	0.045	-0.072	2.797	12.85
62.09	0.363	0.047	-0.123	2.607	12.935
66.69	0.358	0.044	-0.003	2.738	12.321
71.3	0.365	0.043	-0.004	2.653	11.901
75.9	0.367	0.045	-0.003	2.661	12.266
80.5	0.37	0.047	0.069	2.595	12.67
85.09	0.375	0.045	0.014	2.938	11.955
89.69	0.38	0.045	0.002	2.887	11.817
94.3	0.393	0.043	-0.052	2.816	11.004
98.9	0.406	0.044	-0.23	2.622	10.93
103.5	0.429	0.039	-0.455	3.149	9.146
108.09	0.445	0.036	-0.503	3.328	8.118
112.69	0.454	0.032	-0.23	3.677	7.082

Experiment DL#2

Location #3

Z	U Mean	U RMS	U Skew	U Flat	U Turb
(mm)	(m/s)	(m/s)	(m/s)	(m/s)	(%)
0	0.158	0.037	0.306	3.55	23.122
1.14	0.16	0.037	0.231	3.059	23.104
2.29	0.173	0.035	0.079	2.93	20.16
3.45	0.173	0.035	-0.01	3.102	20.407
4.59	0.171	0.035	-0.001	2.895	20.592
6.9	0.172	0.037	0.098	2.912	21.613
9.19	0.174	0.035	0.06	2.897	20.191
11.5	0.171	0.037	0.042	2.89	21.505
16.1	0.177	0.04	0.116	3.093	22.606
20.7	0.183	0.042	-0.064	3.138	23.143
25.29	0.19	0.043	0.148	3.027	22.821
29.89	0.202	0.046	0.075	2.861	22.918
34.5	0.226	0.052	0.186	2.897	22.845
39.09	0.262	0.056	-0.077	2.749	21.37
43.7	0.304	0.056	-0.367	3.078	18.37
46	0.331	0.053	-0.336	3.161	16.049
48.29	0.343	0.046	-0.491	3.321	13.396
50.59	0.355	0.043	-0.333	3.315	12.187
52.9	0.368	0.04	-0.233	2.954	10.964
57.5	0.376	0.037	-0.221	2.813	9.917
62.09	0.383	0.036	-0.095	3.113	9.395
66.69	0.382	0.035	-0.093	2.857	9.28
71.3	0.387	0.036	-0.16	2.869	9.31
75.9	0.386	0.038	-0.068	2.712	9.95
80.5	0.389	0.036	-0.289	2.867	9.272
85.09	0.391	0.038	-0.024	2.883	9.695
89.69	0.394	0.034	-0.154	3.064	8.723
94.3	0.395	0.037	-0.176	2.998	9.296
98.9	0.404	0.034	-0.331	3.178	8.41
103.5	0.416	0.033	-0.328	3.369	7.895
108.09	0.42	0.031	-0.124	3.373	7.367
112.69	0.409	0.032	-0.068	3.214	7.753

Experiment DL#2

Location #4

Z	U Mean	U RMS	U Skew	U Flat	U Turb
(mm)	(m/s)	(m/s)	(m/s)	(m/s)	(%)
0	0.224	0.038	-0.227	2.84	16.853
1.14	0.239	0.033	-0.359	3.28	13.878
2.29	0.238	0.034	-0.413	3.418	14.119
3.45	0.247	0.031	-0.182	3.035	12.547
4.59	0.244	0.033	-0.143	3.193	13.503
6.9	0.244	0.032	-0.311	3.443	12.952
9.19	0.244	0.034	-0.207	3.16	13.784
11.5	0.245	0.032	-0.302	3.496	13.157
16.1	0.246	0.033	-0.23	3.464	13.35
20.7	0.251	0.035	-0.032	3.482	14.011
25.29	0.259	0.037	0.184	3.322	14.296
29.89	0.264	0.04	-0.23	4.09	15.252
34.5	0.269	0.042	-0.068	3.615	15.451
39.09	0.284	0.049	-0.211	3.571	17.262
43.7	0.298	0.048	0.076	2.734	16.258
46	0.306	0.049	0.067	2.747	15.98
48.29	0.318	0.051	-0.092	2.659	16.136
50.59	0.326	0.053	-0.26	2.795	16.274
52.9	0.332	0.053	-0.111	2.537	16.032
57.5	0.346	0.052	-0.237	2.829	15.002
62.09	0.348	0.055	-0.384	3.047	15.849
66.69	0.353	0.054	-0.395	3.003	15.353
71.3	0.35	0.056	-0.383	3.171	15.893
75.9	0.348	0.052	-0.293	3.199	14.837
80.5	0.347	0.053	-0.34	2.942	15.385
85.09	0.346	0.055	-0.216	2.689	15.946
89.69	0.346	0.053	-0.225	2.854	15.334
94.3	0.356	0.056	-0.285	2.852	15.637
98.9	0.374	0.052	-0.487	3.633	13.927
103.5	0.397	0.049	-0.589	3.58	12.44
108.09	0.423	0.037	-0.485	3.875	8.843
112.69	0.43	0.031	-0.191	3.359	7.261

Experiment DL#2

Location #5

Z	U Mean	U RMS	U Skew	U Flat	U Turb
(mm)	(m/s)	(m/s)	(m/s)	(m/s)	(%)
0	0.12	0.056	0.255	3.278	46.161
1.14	0.123	0.059	0.169	3.166	48.297
2.29	0.128	0.057	-0.148	3.2	44.67
3.45	0.129	0.054	0.072	3.485	42.048
4.59	0.114	0.056	0.048	2.965	48.853
6.9	0.113	0.053	-0.108	3.379	47.276
9.19	0.102	0.055	-0.024	3.498	54.134
11.5	0.11	0.055	-0.083	2.97	50.065
16.1	0.112	0.056	0.086	2.895	50.241
20.7	0.115	0.058	-0.087	2.842	50.027
25.29	0.116	0.06	-0.008	3.062	51.872
29.89	0.115	0.061	0.12	2.929	53.017
34.5	0.104	0.059	0.204	3.028	56.424
39.09	0.097	0.059	0.09	2.853	61.104
43.7	0.131	0.062	0.144	2.824	47.286
46	0.173	0.063	-0.201	3.172	36.481
48.29	0.221	0.061	0.042	3.396	27.746
50.59	0.258	0.055	-0.063	3.374	21.152
52.9	0.281	0.053	0.075	3.127	18.973
57.5	0.285	0.047	0.147	3.095	16.593
62.09	0.296	0.052	0.144	2.977	17.457
66.69	0.299	0.05	-0.05	2.898	16.805
71.3	0.291	0.048	0.176	3.106	16.517
75.9	0.293	0.051	0.067	2.836	17.523
80.5	0.285	0.054	0.054	2.818	18.791
85.09	0.293	0.05	0.032	2.817	17.031
89.69	0.302	0.055	0.009	2.709	18.08
94.3	0.321	0.056	0.025	2.543	17.373
98.9	0.36	0.053	-0.143	2.904	14.593
103.5	0.385	0.048	-0.245	3.16	12.498
108.09	0.416	0.04	-0.48	3.27	9.677
112.69	0.421	0.04	-0.234	2.872	9.426

Experiment DL#2

Location #6

Z	U Mean	U RMS	U Skew	U Flat	U Turb
(mm)	(m/s)	(m/s)	(m/s)	(m/s)	(%)
0	0.174	0.042	0.119	3.046	24.239
1.14	0.185	0.042	0.135	3.193	22.546
2.29	0.184	0.042	0.096	3.043	22.511
3.45	0.187	0.042	-0.006	2.89	22.73
4.59	0.189	0.042	0.06	3.33	22.298
6.9	0.18	0.042	0.205	3.105	23.548
9.19	0.178	0.044	0.175	2.758	24.632
11.5	0.18	0.042	0.045	2.97	23.401
16.1	0.179	0.044	0.132	2.917	24.421
20.7	0.184	0.047	0.153	2.812	25.398
25.29	0.183	0.044	0.123	2.929	23.917
29.89	0.189	0.047	0.202	2.768	24.871
34.5	0.193	0.048	0.079	3.105	24.78
39.09	0.2	0.052	0.274	3.089	26.096
43.7	0.213	0.054	0.179	2.882	25.18
46	0.225	0.053	0.153	3.405	23.381
48.29	0.234	0.058	0.112	2.78	24.91
50.59	0.238	0.054	0.073	3.103	22.747
52.9	0.25	0.055	-0.024	3.045	21.992
57.5	0.263	0.06	-0.045	2.96	22.625
62.09	0.275	0.059	0.036	3.15	21.423
66.69	0.266	0.059	0.153	2.775	22.241
71.3	0.268	0.058	-0.017	2.965	21.817
75.9	0.264	0.06	-0.04	2.902	22.891
80.5	0.265	0.061	0.025	3.047	23.137
85.09	0.26	0.063	-0.006	2.814	24.206
89.69	0.272	0.063	0.127	2.773	23.184
94.3	0.282	0.066	0.09	3.077	23.368
98.9	0.323	0.071	-0.053	2.732	21.996
103.5	0.372	0.066	-0.369	3.427	17.651
108.09	0.392	0.058	-0.442	3.713	14.724
112.69	0.396	0.046	-0.409	3.74	11.697

Experiment DL#2

Location #7

Z	U Mean	U RMS	U Skew	U Flat	U Turb
(mm)	(m/s)	(m/s)	(m/s)	(m/s)	(%)
0	0.22	0.035	-0.149	3.122	15.806
1.14	0.231	0.033	-0.23	2.978	14.439
2.29	0.232	0.034	-0.29	3.363	14.633
3.45	0.235	0.033	-0.102	2.97	14.066
4.59	0.233	0.034	-0.457	3.81	14.424
6.9	0.231	0.032	-0.133	3.338	14.03
9.19	0.234	0.034	-0.352	3.841	14.489
11.5	0.233	0.036	-0.218	3.255	15.499
16.1	0.24	0.039	-0.303	3.44	16.107
20.7	0.241	0.039	0.069	3.12	16.26
25.29	0.249	0.039	0.169	3.723	15.649
29.89	0.263	0.043	0.184	3.074	16.256
34.5	0.265	0.044	0.179	3.126	16.639
39.09	0.286	0.049	0.167	3.184	17.262
43.7	0.299	0.05	0.054	2.807	16.734
46	0.3	0.055	0.124	3.317	18.245
48.29	0.316	0.05	-0.082	3.008	15.67
50.59	0.324	0.052	-0.214	3.226	15.986
52.9	0.329	0.055	-0.34	3.348	16.763
57.5	0.338	0.05	-0.318	3.239	14.954
62.09	0.354	0.045	-0.167	3.242	12.839
66.69	0.353	0.048	-0.285	3.047	13.627
71.3	0.351	0.049	-0.338	3.172	14.04
75.9	0.357	0.052	-0.396	3.389	14.687
80.5	0.351	0.051	-0.27	3.23	14.428
85.09	0.357	0.052	-0.501	3.838	14.654
89.69	0.369	0.053	-0.59	4.113	14.315
94.3	0.378	0.053	-0.508	3.298	14.157
98.9	0.403	0.048	-0.698	5.024	11.858
103.5	0.425	0.042	-0.655	3.939	9.842
108.09	0.443	0.036	-0.296	4.111	8.049
112.69	0.446	0.036	-0.138	4.806	8.174

Experiment DL#2

Location #8

Z	U Mean	U RMS	U Skew	U Flat	U Turb
(mm)	(m/s)	(m/s)	(m/s)	(m/s)	(%)
0	0.13	0.057	-0.343	3.74	43.896
1.14	0.126	0.054	-0.351	3.119	42.695
2.29	0.12	0.053	-0.179	3.139	44.464
3.45	0.112	0.052	-0.18	2.963	46.62
4.59	0.116	0.053	-0.064	3.007	45.387
6.9	0.107	0.054	-0.104	3.098	50.328
9.19	0.107	0.055	0.174	3.329	51.432
11.5	0.113	0.057	-0.072	3.329	49.905
16.1	0.116	0.055	0.06	2.965	47.179
20.7	0.122	0.06	-0.119	2.91	49.397
25.29	0.13	0.061	-0.026	2.919	46.984
29.89	0.13	0.072	-0.23	3.172	55.326
34.5	0.114	0.079	0.095	3.127	69.411
39.09	0.095	0.081	0.327	2.868	85.706
43.7	0.166	0.081	-0.062	2.757	48.962
46	0.255	0.078	-0.686	3.48	30.584
48.29	0.334	0.057	-0.895	4.066	17.107
50.59	0.372	0.047	-0.518	3.892	12.62
52.9	0.38	0.04	-0.213	3.016	10.61
57.5	0.383	0.038	-0.2	2.985	9.82
62.09	0.396	0.037	-0.161	2.958	9.392
66.69	0.39	0.038	-0.258	2.787	9.635
71.3	0.391	0.038	-0.137	2.93	9.7
75.9	0.392	0.039	-0.254	3.047	9.842
80.5	0.392	0.04	-0.319	3.11	10.131
85.09	0.389	0.04	-0.164	2.893	10.247
89.69	0.397	0.039	-0.182	2.983	9.791
94.3	0.405	0.036	-0.115	2.694	8.916
98.9	0.42	0.038	-0.262	2.763	8.928
103.5	0.443	0.035	-0.327	2.985	7.955
108.09	0.462	0.029	-0.322	3.606	6.237
112.69	0.475	0.031	0.165	7.512	6.519

Experiment DL#2

Location #9

Z	U Mean	U RMS	U Skew	U Flat	U Turb
(mm)	(m/s)	(m/s)	(m/s)	(m/s)	(%)
0	0.229	0.035	-0.341	3.193	15.206
1.14	0.24	0.031	-0.134	3.117	13.027
2.29	0.238	0.031	-0.145	2.946	12.811
3.45	0.241	0.032	-0.121	3.173	13.3
4.59	0.24	0.033	-0.127	3.48	13.928
6.9	0.241	0.032	-0.043	3.105	13.439
9.19	0.245	0.033	-0.137	3.017	13.598
11.5	0.242	0.033	-0.165	2.824	13.586
16.1	0.245	0.034	-0.093	3.205	13.926
20.7	0.253	0.035	-0.092	3.253	13.872
25.29	0.253	0.035	-0.083	3.019	13.935
29.89	0.262	0.041	-0.015	3.347	15.503
34.5	0.274	0.044	-0.059	3.163	16.078
39.09	0.286	0.047	-0.195	3.454	16.397
43.7	0.303	0.048	0.01	3.117	15.791
46	0.317	0.052	-0.041	2.717	16.569
48.29	0.321	0.049	-0.004	2.82	15.364
50.59	0.327	0.052	0.017	2.726	15.841
52.9	0.334	0.05	-0.22	2.596	15.104
57.5	0.34	0.053	-0.204	2.805	15.466
62.09	0.345	0.049	-0.226	2.673	14.301
66.69	0.347	0.049	-0.181	2.822	14.109
71.3	0.344	0.048	-0.049	2.722	14.004
75.9	0.34	0.05	-0.157	2.584	14.779
80.5	0.341	0.051	-0.123	2.792	14.835
85.09	0.348	0.048	-0.108	2.844	13.887
89.69	0.35	0.05	-0.105	2.625	14.232
94.3	0.364	0.051	-0.378	2.868	13.943
98.9	0.384	0.045	-0.281	3.32	11.776
103.5	0.407	0.042	-0.482	3.006	10.25
108.09	0.434	0.034	-0.678	3.994	7.871
112.69	0.444	0.032	-0.419	3.45	7.134

Experiment DL#2

Location #10

Z	U Mean	U RMS	U Skew	U Flat	U Turb
(mm)	(m/s)	(m/s)	(m/s)	(m/s)	(%)
0	0.175	0.037	0.366	3.433	21.163
1.14	0.179	0.037	0.082	3.21	20.425
2.29	0.178	0.039	0.1	2.867	21.62
3.45	0.178	0.04	0.258	3.099	22.394
4.59	0.176	0.039	0.053	2.872	22.38
6.9	0.174	0.039	0.096	3.029	22.484
9.19	0.176	0.04	0.059	2.849	22.992
11.5	0.176	0.04	-0.008	3.192	22.575
16.1	0.178	0.04	0.148	2.901	22.637
20.7	0.178	0.042	0.062	2.814	23.394
25.29	0.179	0.042	0.333	3.331	23.434
29.89	0.181	0.042	0.075	3.118	23.261
34.5	0.182	0.043	0.273	3.154	23.715
39.09	0.199	0.045	0.137	3.021	22.632
43.7	0.22	0.048	0.019	2.899	21.646
46	0.228	0.05	0.159	2.867	22.097
48.29	0.245	0.049	0.151	2.997	19.862
50.59	0.261	0.052	0.058	2.821	19.885
52.9	0.272	0.047	0.156	3.47	17.435
57.5	0.277	0.047	0.11	2.896	17.095
62.09	0.287	0.046	-0.101	2.74	16.11
66.69	0.289	0.045	0.113	2.916	15.411
71.3	0.285	0.046	0.027	2.743	16.086
75.9	0.283	0.045	0.088	2.906	15.886
80.5	0.282	0.044	0.196	2.846	15.718
85.09	0.289	0.045	0.09	2.869	15.667
89.69	0.301	0.046	-0.005	2.868	15.137
94.3	0.324	0.051	-0.097	2.778	15.72
98.9	0.361	0.046	-0.2	3.027	12.802
103.5	0.382	0.043	-0.298	3.16	11.269
108.09	0.397	0.04	-0.307	3.509	10.198
112.69	0.41	0.036	-0.061	3.03	8.883

Experiment DL#3

Location #1

Z	U Mean	U RMS	U Skew	U Flat	U Turb
(mm)	(m/s)	(m/s)	(m/s)	(m/s)	(%)
0	0.076	0.059	-0.015	3.547	77.319
1.14	0.088	0.058	-0.019	3.431	65.86
2.29	0.094	0.054	0.006	3.281	56.894
3.45	0.092	0.052	0.136	3.295	55.896
4.59	0.091	0.054	0.121	3.386	59.209
6.9	0.09	0.055	0.075	3.64	61.452
9.19	0.098	0.057	0.143	3.287	58.219
11.5	0.105	0.057	0.295	3.468	54.733
16.1	0.112	0.057	0.328	3.607	50.794
20.7	0.112	0.058	0.316	3.307	52.097
25.29	0.122	0.061	0.397	4.575	50.504
29.89	0.129	0.061	0.209	3.667	47.434
34.5	0.142	0.072	0.359	4.141	50.76
39.09	0.141	0.068	-0.016	4.11	48.309
43.7	0.146	0.072	0.073	3.492	49.346
46	0.15	0.073	0.091	3.225	48.445
48.29	0.163	0.08	0.149	3.281	49.175
50.59	0.152	0.085	-0.147	3.058	56.284
52.9	0.147	0.085	-0.088	3.361	57.733
57.5	0.133	0.098	-0.002	3.261	73.462
62.09	0.102	0.1	0.133	2.956	98.514
66.69	0.108	0.1	0.211	2.969	92.636
71.3	0.22	0.105	-0.086	2.902	47.802
73.59	0.313	0.1	-0.188	2.59	31.995
75.9	0.405	0.093	-0.309	3.141	23.002
78.19	0.415	0.076	-0.223	3.167	18.298
80.5	0.427	0.073	-0.086	2.751	16.989
85.09	0.46	0.073	0.028	2.354	15.804
89.69	0.483	0.061	-0.188	2.87	12.612
94.3	0.502	0.061	-0.429	3.038	12.145
98.9	0.512	0.059	-0.128	2.734	11.433
103.5	0.527	0.053	-0.228	3.148	10.134

Experiment DL#3

Location #3

Z	U Mean	U RMS	U Skew	U Flat	U Turb
(mm)	(m/s)	(m/s)	(m/s)	(m/s)	(%)
0	0.121	0.034	0.43	3.331	27.734
1.14	0.133	0.033	0.235	3.339	24.59
2.29	0.146	0.032	0.272	3.36	21.87
3.45	0.147	0.033	0.241	3.1	22.274
4.59	0.147	0.035	0.295	3.157	23.65
6.9	0.143	0.034	0.265	3.113	23.855
9.19	0.142	0.034	0.139	2.945	23.977
11.5	0.144	0.033	0.137	3.235	22.959
16.1	0.145	0.033	0.342	3.359	23.003
20.7	0.148	0.037	0.209	2.992	25.286
25.29	0.161	0.044	0.368	3.345	27.229
29.89	0.164	0.047	0.53	3.776	28.573
34.5	0.181	0.053	0.634	4.042	29.254
39.09	0.207	0.057	0.471	3.052	27.534
43.7	0.229	0.066	0.447	3.202	28.934
46	0.261	0.072	0.385	3.149	27.54
48.29	0.273	0.074	0.469	3.024	27.031
50.59	0.293	0.072	0.405	2.978	24.442
52.9	0.313	0.074	0.326	2.866	23.542
57.5	0.332	0.071	0.248	2.768	21.399
62.09	0.367	0.072	0.113	2.438	19.676
66.69	0.391	0.067	0.085	2.539	17.087
71.3	0.402	0.076	0.17	2.489	19.044
73.59	0.403	0.073	0.033	2.609	18.065
75.9	0.419	0.073	-0.043	2.6	17.486
78.19	0.418	0.077	0.244	2.496	18.501
80.5	0.444	0.074	-0.073	2.568	16.551
85.09	0.434	0.065	0.039	2.534	15.049
89.69	0.461	0.07	-0.234	2.64	15.106
94.3	0.488	0.068	-0.16	2.895	13.861
98.9	0.508	0.058	-0.343	2.815	11.461
103.5	0.523	0.053	0.031	3.687	10.211

Experiment DL#3

Location #5

Z	U Mean	U RMS	U Skew	U Flat	U Turb
(mm)	(m/s)	(m/s)	(m/s)	(m/s)	(%)
0	0.105	0.053	0.112	3.601	49.983
1.14	0.117	0.051	-0.021	3.139	43.764
2.29	0.125	0.049	-0.123	3.555	39.452
3.45	0.123	0.052	-0.224	3.605	42.493
4.59	0.115	0.052	0.093	3.329	44.767
6.9	0.104	0.052	-0.039	3.2	50.252
9.19	0.099	0.052	0.039	3.102	52.776
11.5	0.107	0.055	0.105	3.264	51.675
16.1	0.109	0.053	0.15	3.074	48.324
20.7	0.112	0.054	0.004	3.402	48.143
25.29	0.114	0.057	0.077	3.236	50.483
29.89	0.109	0.062	-0.167	3.378	56.901
34.5	0.102	0.062	-0.049	3.561	61.24
39.09	0.103	0.065	0.173	3.595	63.186
43.7	0.123	0.064	0.203	3.102	52.203
46	0.154	0.065	0.237	3.396	42.525
48.29	0.195	0.07	0.009	3.396	35.713
50.59	0.244	0.069	0.151	3.532	28.206
52.9	0.279	0.069	0.446	3.501	24.688
57.5	0.308	0.067	0.511	3.395	21.631
62.09	0.326	0.068	0.408	2.872	20.823
66.69	0.349	0.076	0.343	2.951	21.687
71.3	0.388	0.085	0.146	2.514	21.923
73.59	0.394	0.078	0.06	2.538	19.682
75.9	0.413	0.082	-0.043	2.386	19.777
78.19	0.426	0.075	-0.267	2.769	17.633
80.5	0.433	0.071	-0.102	2.723	16.371
85.09	0.468	0.076	-0.266	2.362	16.191
89.69	0.491	0.063	-0.23	3.343	12.907
94.3	0.499	0.062	-0.291	2.831	12.474
98.9	0.519	0.065	-0.159	3.21	12.51
103.5	0.517	0.055	-0.409	3.318	10.645

Experiment DL#3

Location #6

Z	U Mean	U RMS	U Skew	U Flat	U Turb
(mm)	(m/s)	(m/s)	(m/s)	(m/s)	(%)
0	0.16	0.045	0.511	3.476	28.245
1.14	0.169	0.043	0.36	3.417	25.227
2.29	0.165	0.041	0.099	3.019	25.063
3.45	0.164	0.041	0.399	3.363	25.206
4.59	0.164	0.039	0.202	3.151	23.58
6.9	0.17	0.045	0.525	3.848	26.405
9.19	0.167	0.041	0.073	2.87	24.824
11.5	0.156	0.045	0.57	3.464	28.795
16.1	0.176	0.045	0.473	3.424	25.818
20.7	0.171	0.05	0.443	3.363	28.99
25.29	0.182	0.052	0.388	3.425	28.834
29.89	0.191	0.055	0.459	3.465	28.8
34.5	0.192	0.055	0.478	3.418	28.65
39.09	0.204	0.056	0.479	3.218	27.562
43.7	0.209	0.063	0.713	3.769	29.902
46	0.219	0.065	0.577	3.615	29.653
48.29	0.224	0.064	0.488	3.581	28.353
50.59	0.231	0.063	0.413	3.149	27.362
52.9	0.239	0.064	0.628	3.805	26.916
57.5	0.251	0.066	0.389	3.045	26.357
62.09	0.274	0.07	0.519	3.489	25.403
66.69	0.318	0.078	0.215	2.763	24.532
71.3	0.357	0.089	-0.019	2.554	24.997
73.59	0.384	0.079	-0.077	2.682	20.463
75.9	0.393	0.078	-0.153	2.672	19.916
78.19	0.414	0.078	-0.201	2.719	18.849
80.5	0.427	0.07	-0.002	2.829	16.372
85.09	0.453	0.068	-0.239	2.625	14.966
89.69	0.47	0.062	-0.319	3.024	13.267
94.3	0.487	0.057	-0.337	3.173	11.606
98.9	0.492	0.063	-0.221	2.918	12.748
103.5	0.506	0.053	-0.223	2.963	10.477

Experiment DL#3

Location #7

Z	U Mean	U RMS	U Skew	U Flat	U Turb
(mm)	(m/s)	(m/s)	(m/s)	(m/s)	(%)
0	0.176	0.035	-0.223	2.773	19.612
1.14	0.186	0.032	-0.445	3.561	17.086
2.29	0.186	0.036	0.193	4.368	19.069
3.45	0.191	0.035	-0.106	3.453	18.155
4.59	0.188	0.033	-0.102	3.458	17.498
6.9	0.191	0.034	-0.066	3.673	17.965
9.19	0.191	0.034	-0.246	3.977	17.908
11.5	0.19	0.034	-0.355	3.415	17.607
16.1	0.197	0.035	-0.263	3.146	17.861
20.7	0.204	0.042	0.566	4.251	20.624
25.29	0.203	0.038	0.094	3.647	18.6
29.89	0.203	0.038	0.304	3.731	18.781
34.5	0.212	0.044	0.764	4.858	20.853
39.09	0.224	0.046	0.351	4.123	20.656
43.7	0.247	0.056	0.847	4.134	22.73
46	0.247	0.05	0.623	3.822	20.208
48.29	0.263	0.061	0.676	3.687	23.041
50.59	0.276	0.064	0.517	3.656	23.161
52.9	0.284	0.066	0.415	3.189	23.327
57.5	0.296	0.065	0.239	3.163	21.868
62.09	0.322	0.066	0.065	2.913	20.549
66.69	0.337	0.067	0.127	2.872	19.802
71.3	0.366	0.068	0.059	3.022	18.701
73.59	0.378	0.07	-0.005	2.764	18.367
75.9	0.369	0.065	0.063	2.789	17.581
78.19	0.399	0.065	-0.15	2.902	16.318
80.5	0.405	0.062	-0.098	2.79	15.335
85.09	0.434	0.064	-0.096	2.845	14.802
89.69	0.459	0.06	-0.239	2.522	13.027
94.3	0.458	0.06	-0.313	2.928	13.012
98.9	0.49	0.052	0.108	2.794	10.554
103.5	0.499	0.052	-0.279	3.024	10.442

Experiment DL#3

Location #8

Z	U Mean	U RMS	U Skew	U Flat	U Turb
(mm)	(m/s)	(m/s)	(m/s)	(m/s)	(%)
0	0.117	0.048	0.065	3.239	41.247
1.14	0.112	0.048	-0.088	3.185	42.681
2.29	0.112	0.047	-0.315	3.435	41.664
3.45	0.101	0.047	-0.149	3.14	46.717
4.59	0.106	0.044	0.064	3.099	41.162
6.9	0.089	0.048	-0.155	3.067	54.569
9.19	0.093	0.046	0.063	3.327	49.336
11.5	0.091	0.049	0.164	3.216	53.799
16.1	0.097	0.048	-0.022	2.987	49.518
20.7	0.103	0.049	-0.024	2.982	47.382
25.29	0.107	0.054	0.185	3.49	50.604
29.89	0.109	0.056	0.271	3.282	51.525
34.5	0.088	0.059	0.428	3.961	66.883
39.09	0.093	0.07	0.32	3.425	75.215
43.7	0.126	0.066	0.314	3.529	52.144
46	0.173	0.072	0.137	2.908	41.698
48.29	0.235	0.082	0.141	2.978	34.968
50.59	0.304	0.065	0.14	3.306	21.449
52.9	0.302	0.063	0.43	3.314	20.868
57.5	0.34	0.07	0.329	2.52	20.521
62.09	0.345	0.063	0.203	2.509	18.203
66.69	0.367	0.071	0.11	2.494	19.282
71.3	0.387	0.064	0.026	2.534	16.594
73.59	0.385	0.066	0.108	2.587	17.148
75.9	0.394	0.061	0.27	2.974	15.474
78.19	0.421	0.071	0.008	2.5	16.88
80.5	0.409	0.066	0.019	2.531	16.175
85.09	0.456	0.06	-0.148	2.681	13.197
89.69	0.463	0.057	-0.261	3.007	12.37
94.3	0.468	0.054	-0.265	2.958	11.472
98.9	0.48	0.054	-0.526	3.264	11.317
103.5	0.502	0.052	-0.306	3.242	10.447

Experiment DL#3

Location #9

Z	U Mean	U RMS	U Skew	U Flat	U Turb
(mm)	(m/s)	(m/s)	(m/s)	(m/s)	(%)
0	0.19	0.028	-0.186	3.083	14.593
1.14	0.187	0.029	-0.155	3.049	15.432
2.29	0.192	0.031	0.173	3.355	16.281
3.45	0.19	0.028	-0.011	3.25	14.901
4.59	0.192	0.029	-0.153	3.161	15.119
6.9	0.189	0.029	-0.189	3.374	15.178
9.19	0.193	0.032	0.353	3.643	16.57
11.5	0.193	0.032	-0.138	3.15	16.334
16.1	0.191	0.03	-0.072	3.756	15.892
20.7	0.199	0.038	0.544	4.022	19.182
25.29	0.21	0.044	0.968	5.497	21.106
29.89	0.204	0.036	0.305	4.196	17.734
34.5	0.22	0.048	0.283	3.405	21.68
39.09	0.223	0.05	0.76	3.814	22.593
43.7	0.251	0.055	0.27	2.719	21.836
46	0.246	0.052	0.092	2.948	21.138
48.29	0.264	0.066	0.554	3.193	25.101
50.59	0.282	0.069	0.271	2.859	24.595
52.9	0.292	0.066	0.64	3.137	22.731
57.5	0.311	0.069	0.429	2.912	22.242
62.09	0.328	0.069	0.254	2.559	21.179
66.69	0.351	0.066	0.303	2.682	18.845
71.3	0.348	0.066	0.216	2.669	18.874
73.59	0.385	0.072	-0.011	2.566	18.766
75.9	0.371	0.073	0.08	2.315	19.683
78.19	0.405	0.07	-0.212	2.383	17.273
80.5	0.412	0.065	-0.178	2.84	15.722
85.09	0.422	0.064	-0.183	2.683	15.11
89.69	0.453	0.055	-0.322	2.698	12.137
94.3	0.474	0.055	-0.227	2.5	11.549
98.9	0.483	0.048	-0.138	2.936	10.043
103.5	0.495	0.053	0.076	3.415	10.758

Experiment DL#3

Location #10

Z	U Mean	U RMS	U Skew	U Flat	U Turb
(mm)	(m/s)	(m/s)	(m/s)	(m/s)	(%)
0	0.152	0.034	0.415	3.714	22.402
1.14	0.155	0.035	0.159	2.915	22.651
2.29	0.155	0.034	0.184	3.129	22.124
3.45	0.152	0.034	0.163	2.959	22.191
4.59	0.151	0.034	-0.016	2.857	22.572
6.9	0.15	0.034	0.015	3.04	22.439
9.19	0.151	0.037	0.314	3.441	24.218
11.5	0.148	0.035	0.215	3.208	23.667
16.1	0.154	0.037	0.351	3.15	23.912
20.7	0.158	0.039	0.104	3.086	24.493
25.29	0.162	0.042	0.25	3.495	25.667
29.89	0.169	0.046	0.547	3.459	26.954
34.5	0.166	0.045	0.194	3.014	26.914
39.09	0.179	0.05	0.845	5.56	27.689
43.7	0.206	0.052	0.596	3.87	25.001
46	0.21	0.058	0.572	4.05	27.725
48.29	0.232	0.057	0.348	2.77	24.566
50.59	0.251	0.06	0.381	3.034	23.784
52.9	0.261	0.062	0.434	3.085	23.69
57.5	0.286	0.062	0.412	2.864	21.721
62.09	0.297	0.061	0.489	3.057	20.552
66.69	0.339	0.067	0.18	2.66	19.684
71.3	0.364	0.065	-0.094	2.704	17.908
73.59	0.376	0.077	0.055	2.35	20.481
75.9	0.373	0.073	-0.065	2.439	19.591
78.19	0.397	0.076	-0.08	2.548	19.021
80.5	0.426	0.065	-0.307	2.815	15.169
85.09	0.428	0.063	-0.208	2.838	14.68
89.69	0.453	0.061	-0.389	2.758	13.463
94.3	0.493	0.051	-0.289	2.864	10.39
98.9	0.483	0.057	-0.304	2.893	11.85
103.5	0.514	0.049	-0.341	3.153	9.605

Vita

Jonathan D. Fairbanks was born on May 7, 1973 in Baltimore, Maryland. Jonathan received his high school diploma from Baltimore Polytechnic Institute in 1991. In 1995, he received his Bachelor of Science in Civil Engineering from Virginia Tech. After completing his undergraduate studies, Jonathan enrolled in the Hydrosystems Division of the Civil Engineering Department at Virginia Tech to pursue a Master of Science degree. Jonathan has worked as an Assistant Hydrologist at the National Weather Service in Blacksburg, Virginia and a lab instructor in the Civil Engineering Hydraulics Lab at Virginia Tech. Currently, Jonathan is employed as a Project Engineer at Anderson & Associates, Inc. in Blacksburg, Virginia.